A THESIS ENTITLED

IMPROVED PERFORMANCE OF INDUCTIVELY COUPLED PLASMA ATOMIC EMISSION SPECTROMETRY IN GEOCHEMICAL ANALYSIS

Submitted for the degree of

DOCTOR OF PHILOSOPHY

in the

FACULTY OF SCIENCE OF THE UNIVERSITY OF LONDON

by

Michael Henry Ramsey

Applied Geochemistry Research Group
Department of Geology
Royal School of Mines
Imperial College of Science and Technology
London

October 1986

ABSTRACT

In applied geochemistry there is an increasing emphasis on the interpretation of inter-element relationships, within multielement data, produced by techniques such as Inductively Coupled Plasma Atomic Emission Spectrometry (ICPAES). However, analytical errors in ICPAES show a high degree of inter-element correlation which can lead to erroneous geochemical interpretation. Sources of apparently random and systematic analytical errors were therefore examined in the multielement dimension.

More than 90% of instrumental variance in routine ICPAES analysis was shown to be multielement correlated and therefore potentially correctable. Variation in ten operating parameters was found to produce either of two multi-analyte patterns of variation, each related to the excitation potentials of the analyte lines measured. A new correction procedure (PRISM) based on this finding was devised, which reduced instrumental variance by 70%.

Matrix effects were established as a major potential cause of inaccuracy in ICPAES. For example, a calcium matrix caused biases of between -30% and +6%, depending on the excitation potential of the analyte line. A hypothesis was postulated that matrix effects were due to a lowering of the excitation temperature of the plasma by the matrix. Temperature drops of up to 100K (at ~7500K) were observed. The effect of 18 different matrix elements on 16 different analyte lines supported this theory. A predictive model was constructed for matrix effects based on fundamental properties of the matrix element and the analyte line.

A new cause of calibration curvature in ICPAES is proposed, self-matrix effects. A series of calcium lines showed curvature that was consistent with that predicted by the fall in excitation temperature measured from other elements.

New methods for the correction of bias due to matrix effects were devised and tested. Some of the methods were computational whilst others were based on a novel principle involving computer-controlled physical intervention in the analysis.

ACKNOWLEDGEMENTS

The research described in this thesis was undertaken in the Applied Geochemistry Research Group (AGRG) at Imperial College, London University.

I am deeply indebted to Dr Michael Thompson for his inspired supervision of this research and many helpful suggestions on its clear exposition.

This investigation could not have proceeded without the positive support of all the technical staff of AGRG. Mrs Eva Banerjee was particularly helpful, as was Mr Barry Coles in respect of electronics and computation. Thanks are due to Mr Stephen J. Walton (Applied Research Laboratories, Luton) who facilitated the operation of the sequential ICP, Dr R.J. Howarth (B.P., Sunbury) for advice on multivariate statistics, Dr R.D. Snook (Chelsea Instruments) for assistance with spectrochemical theory and Mrs Gloria Bello for her typing skills.

Finally, I would like to thank my wife and daughter for their help and encouragement during the five years of part-time study which produced this thesis.

CONTENTS

	Page
Abstract	2
Acknowledgements	3
Contents	4
List of Figures	11
List of Tables	16
CHAPTER 1	
Introduction	19
1.1 Aims and Intentions	19
1.2 Pseudorandom Errors	20
1.3 Systematic Errors	22
1.4 Calibration Line Curvature	24
CHAPTER 2	
ICPAES in Geochemical Analysis	
2.1 Introduction	26
2.2 Development of Atomic Emission Spectrometry	26
2.3 Operating Principles of ICPAES	27
2.4 Sources of Analytical Error in ICPAES	31
2.4.1 Random Error	31
2.4.2 Systematic Error	33
2.5 Advantages of ICPAES for Geochemical Analysis	37
2.6 Current Limitations of ICPAES for Geochemical Analysis	38
2.7 The Selection of the Research Objectives	40
2.7.1 The Feasibility of the Possible Research Objectives	40
2.7.2 The Need for Improved Data Quality in ICPAES	43

2.8 Summary 45

CHAPTER 3
General Experimental Design and Equipment

3.1 Introduction 46
3.2 ICPAES Instrumentation 46
3.3 Solution Preparation Techniques 49
3.3.1 Purity of Chemicals 49
3.3.2 Volumetric Procedures 49
3.4 The Determination of Relative Sensitivity 52
3.4.1 The Experimental Method 52
3.4.2 The Volumetric Precision 53
3.5 Computation of Results 55

CHAPTER 4
Sources of Imprecision

4.1 Introduction 57
4.2 Terminology of Precision 58
4.3 Established Sources of Imprecision 59
4.4 Target for Investigation 59
4.5 Experimental Design for Investigation of 'Quasi-Routine Analysis' 61
4.6 Experimental Design to Establish Possible Causes of Imprecision 63
4.7 Results and Discussion 65
4.7.1 Quasi-Routine Analysis 65
4.7.2 Calculation of Multielement Parameter Signatures (MPS) 71
4.7.3 The Significance of the Multielement Parameter Signatures 80
4.8 Correlation Structure of the Background Intensities 87
4.9 Summary 87

CHAPTER 5

Methods of Improving Precision

5.1	Introduction	89
5.2	Review of Internal Standard Methods for Emission Spectrometry	91
5.3	The Parameter Related Internal Standard Method (PRISM)	95
5.4	Testing the PRISM Model	103
5.5	Some Practical Observations on the use of PRISM	110
5.6	Comparison of PRISM and the Myers-Tracy Method	111
5.7	Comparison of PRISM and GIRM	113
5.8	Variability in Spectral Background	114
5.9	Summary and Discussion	114

CHAPTER 6

Matrix Effects as a Source of Inaccuracy

6.1	Introduction	116
6.2	Previous Work on Matrix Effects	117
6.3	Matrix Effects from Calcium	121
6.3.1	Experimental Design for the Study of Matrix Effects due to Calcium	121
6.3.2	Results for the Matrix Effects due to Calcium under Standard Operating Conditions	123
6.3.3	Comparison of Pumped and Free-uptake Nebulisation	125
6.3.4	Dual Nebulisers for the Separate Introduction of Analytes and Interferent	127
6.3.5	The Stability of the Matrix Effect	130
6.3.6	Interim Conclusions from Investigation of Matrix Effects from Calcium	131
6.4	Proposed Mechanism of Matrix Effects due to Calcium	134

6.4.1 The Effect of Temperature on Spectral Intensity 134
6.4.2 Determination of Excitation Temperature 137
6.4.3 Determination of Change in Excitation Temperature 139
6.5 The Multi-matrix Domain 141
6.5.1 Experimental Design 143
6.5.2 Results 145
6.5.3 The Mechanism of Plasma Matrix Effects 153
6.6 Summary 156

CHAPTER 7
Methods of Correcting Matrix Effects

7.1 Introduction 158
7.2 Current Methods of Correcting Matrix Effects 159
7.3 The 'MED-Model' Method 163
7.4 The 'Variable Concentration (VC) Model' Method 165
7.5 The Parameter Related Internal Standard Method (PRISM) 171
7.5.1 Introduction 171
7.5.2 The Application 173
7.5.3 Discussion 174
7.5.4 Limitations 175
7.6 Interactive Matrix Matching (IMM) 176
7.6.1 Introduction 176
7.6.2 General Operation of IMM 177
7.6.3 Hardware 180
7.6.4 Software 181
7.6.5 The Experimental Trial of IMM 184
7.6.6 Possible Improvements to IMM 187
7.7 Other Methods of Correction 189
7.7.1 Matrix Swamping 189
7.7.2 Interactive Power Adjustment (IPA) 191
7.8 Comparison Between Methods for Correcting Matrix Effects 193

CHAPTER 8

Self-Matrix Effects as a Cause of Calibration Curvature

8.1	Introduction	197
8.2	Established Causes of Calibration Curvature in ICPAES	199
8.3	Initial Investigations	203
8.4	Experimental Design	207
8.5	A New Curve Fitting Equation	209
8.6	Results and Discussion	211
8.6.1	Estimation of Relative Sensitivity	215
8.6.2	Lines Showing Anomalous Curvature	219
8.6.3	Comparison of Self-matrix Effects with Matrix Effects on Other Elements	221
8.6.4	Conventional Views of ICPAES Calibration Curvature Refuted	222
8.7	Conclusions and Recommendations for Future Work	223

CHAPTER 9

Conclusions and Recommendations for Future Work

9.1	The Precision of ICPAES	228
9.1.1	Identification of the Problem	228
9.1.2	The Structure of Multielement Variations	229
9.1.3	The Improvement of Precision	230
9.1.4	Future Work on Precision Improvement	232
9.1.4.1	Fundamental studies	232
9.1.4.2	Improved methods of precision correction	233
9.1.4.3	Broader application of PRISM for precision improvement	234
9.2	Inaccuracy Caused by Matrix Effects	235
9.2.1	The Investigation and Modelling of Matrix Effects	235
9.2.2	Methods of Correcting Matrix Effects	236

9.2.3 The Theory of Matrix Effect Correction 238
9.2.4 Future Work on Improving Accuracy 239
9.2.4.1 Plasma investigations 239
9.2.4.2 Nebuliser based matrix effects 240
9.2.4.3 Variable concentrations of matrix element 240
9.2.4.4 The effects of multiple matrix elements 241
9.2.4.5 The spatial dimension 242
9.2.4.6 Improved methods for the correction of bias 242
9.3.1 Self-matrix Effects and Calibration Curvature 243
9.3.2 Future Work on Self-matrix Effects 244
9.4 General Conclusions 244
9.5 Priorities for Future Work 246

REFERENCES 249

APPENDICES 253

Appendix A Quasi-routine Analysis Data Set 253
Appendix B MINITAB macro for Principal Component Analysis 256
Appendix C Matrix Effects from Calcium on 14 Analytes - Set 1 used for VC-model correction 257
Appendix D Matrix Effects of 18 Elements on 16 Analytes 258
Appendix E Matrix Effects of Calcium on 14 Analytes - Set 2 Used for PRISM correction 259
Appendix F Program listing for Interactive Matrix Matching (IMM) 260
Appendix G Operating Procedure for Interactive Matrix Matching (IMM) 263
Appendix H Matrix Effects of Calcium on 14 Analytes - Set 3 Used for IMM Correction 266

Appendix I Calibration and Fitting Data for 14 Calcium Emission Lines 267
Appendix J Symbols and Abbreviations 270
Appendix K List of Publications 273

LIST OF FIGURES

Page

Fig. 2.1 28
Schematic diagram for an ICPAES used for simultaneous multielement analysis.

Fig. 2.2 32
Schematic representation of the variation of precision with analyte concentration when expressed as;
(a) standard deviation; a value s_o is approached at low concentrations,
(b) precision (100s /$\bar{x}$), a constant value of precision (P') is approached at high concentrations.

Fig. 2.3 34
Schematic calibration graphs illustrating the effects of (a) the translational interference: B, no interferent; A, interferent present at concentration c_1; producing a constant bias x; (b) the rotational interference produced by an interfering element of concentration c_1: C, no interferent; D, interferent present at concentration c_1, producing a relative change in sensitivity y.

Fig. 4.1 64
Fluctuations in the response of five elements showing multielement correlation. All responses are scaled to their respective standard deviations.

Fig. 4.2 68
Percentage of the total variance accounted for by the first six principal components in the PCA of the quasi-routine analysis data. The values above the scree line are considered significant and account for 93.4% of the total variance.

Fig. 4.3 70
Different effects on the responses of three elements on changing the forward power. Lithium shows no significant change. For regression statistics on all elements see Table 4.5.

Fig. 4.4 74
Multielement parameter signatures (MPS) for four instrumental and environmental parameters that correlate strongly with the forward power MPS. The data used are given in Table 4.6 and are arranged in order of descending susceptibility to forward power for all four parameters.

Fig. 4.5 75
Multielement parameter signatures (MPS) for four instrumental and environmental parameters that correlate strongly with the sample uptake rate MPS. The data used are given in Table 4.7 and are arranged as in Fig. 4.4, that is, in order of descending susceptibility to forward power for all four parameters.

Fig. 4.6 84
Susceptibility to forward power of 36 elements compared with their excitation potential (E) for atom lines and excitation plus ionisation potential ($E+V_1$) for ion lines (bold type).

Fig. 4.7 85
Susceptibility to sample uptake rate of 36 elements compared with their excitation potential (E) for atom lines and excitation plus ionisation potential ($E+V_1$) for ion lines (bold type).

Fig. 5.1 104
Effect of using PRISM on the variation in response of sodium for discrete integration on a single solution. Both traces are plotted using the same ordinate scale, i.e., the percentage change in response from the initial value. Other elements generally show improvement to a similar degree (see Table 5.1).

Fig. 5.2 106
Effect of using PRISM on the variance of the principal components shown in Fig. 4.2. The variance of the PRISM corrected data is expressed as a fraction of the residual variance calculated from the data given in Table 5.1 (i.e. 30%).

Fig. 5.3 106
Apportionment of the total variance within the quasi-routine analysis data. The variance typical of contiguous integration is shown for comparison.

Fig. 6.1 122
Effect of concomitant calcium concentration on the sensitivity of a selection of analytes.

Fig. 6.2 122
Comparison of the effects of concomitant calcium (at 10000 $\mu g\ ml^{-1}$) and of a reduction in forward power to 91.5% of the normal levels on the relative sensitivities of several analyte lines. The two factors produce very similar effects, suggesting a common mechanism.

Fig. 6.3 124
Relationship between the effect of concomitant calcium (at 10000 $\mu g\ ml^{-1}$) on analyte line sensitivities and the excitation potentials of the lines, indicating that the effects are related to a plasma process.

Fig. 6.4 124
Comparison of the matrix effect of concomitant calcium (at 10000 $\mu g\ ml^{-1}$) on several analyte lines, with pumped and free-uptake nebulisers running under identical flow conditions.

Fig. 6.5 126
Dual nebuliser equipment for the separate introduction of analyte and interferent solutions into the plasma. The nebulisers were matched, and the mixed aerosol was split equally to obtain realistic conditions.

Fig. 6.6 126
Flow spoiler, constructed from titanium foil, used to mix the aerosol streams from the two nebulisers.

Fig. 6.7 128
Comparison of the effects of equal calcium concentrations on analyte line sensitivities when the calcium is added either as a concomitant element (i.e., in the same solution) or through a separate nebuliser.

Fig. 6.8 132
Change in matrix effect in two nominally identical experiments separated in time by about 3 years. The differences are due to small variations in operating conditions (e.g., different plasma torches and nebulisers).

Fig. 6.9 136
(a) Relative sensitivities of 14 analytes in 10000 μg ml^{-1} calcium plotted against the total excitation potential of each analyte line. These linear relationships are consistent with a fall in excitation temperature in the plasma of 130 ± 14K caused by the calcium. (b) Relative sensitivity data adjusted for the change in the numbers of atoms and ions caused by the change in temperature. The ion lines lie on a linear trend consistent with a fall in excitation temperature in the plasma of 94 ± 17K caused by the calcium. The atom lines, in parentheses, were not used in the regression.

Fig. 6.10 138
Determination of excitation temperature using pairs of calcium atom lines. The modified intensity ratio varies as a function of the difference in excitation potential with a slope yielding an excitation temperature of 7460 ± 500K.

Fig. 6.11 142
Fall in excitation temperature calculated from relative sensitivity measurements, for a range of analyte in matrices of calcium at various concentrations.

Fig. 6.12 144
Matrix effect on a single analyte, zinc, expressed as relative sensitivity, for a range of 17 matrix elements at 0.05 M expressed as a function of various properties of the matrix element. (a) First ionisation potential. No overall trend is evident (r = -0.14) although elements from Groups I and II of the Periodic Table lie on their own 'pseudo trends' (broken lines). (b) "Total ionisation energy" including first and second ionisation potentials and degrees of ionisation. Again, no overall trend is evident (r = -0.47). (c) "Dissociation energy" derived from lattice energy without caution ionisation potentials. A discernable trend is evident but with a large amount of variability (r = -0.86). (d) "Matrix energy demand" (MED) as summation of "total ionisation energy" and "dissociation energy" gives a linear relationship with a high degree of correlation (r = -0.97). MED can therefore be used as a predictive property.

Fig. 6.13 148
Variation in matrix effects on ten representative analytes as from a range of matrix elements expressed as a function of their MED. Regression coefficients are given in Table 6.5

Fig. 6.14 150
(a) Slopes and (b) intercepts of the regression lines shown in Fig. 6.13 (and listed in Table 6.5) as a function of the total excitation potential of the analyte line. Both trends are linear and enable a predictive model of matrix effects to be considered.

Fig. 6.15 150
Contour map of predicted matrix effects generated with equation (6.15) annotated with selected analyte and matrix elements. The contour lines are for values of equal relative sensitivity. To predict a relative sensitivity of any analyte - matrix combination, locate the coordinates of the excitation potential of the analyte line and the MED of the matrix element. Biases of >10% occur only in the top right-hand corner of the diagram.

Fig. 6.16 152
Calculated fall in excitation temperature caused by a range of matrix elements using the zinc analyte as a thermometer. The trend is clearly linear and supports the hypothesis that matrix elements remove energy from the plasma in proportion to their MED.

Fig. 7.1 164
Closeness of fit of the predictive model and the experimental relative sensitivities from which it was generated. A method of matrix effect correction based on the current model would be expected to reduce most matrix effects (-30 to +5%) to within a few per cent.

Fig. 7.2 166
Relative sensitivity of cobalt (s) as a function of calcium concentration (c), with the data points fitted to an exponential decay curve $S = 1 + A(1 - e^{-Bc})$.

Fig. 7.3 167
Effectiveness of three methods of correcting the calcium matrix effect: black bars represent raw data; grey bars show the same data corrected by the method designated in the column heading. Relative sensitivities for each analyte are given on a scale from 0.5 to 1.0 in each instance. Zinc is not corrected in the PRISM column as it is used as a parameter-related internal standard. In the IMM column, the raw data contain both matrix effects and spectral interferences, which were corrected simultaneously by IMM. The calcium concentrations given are those for the test solution before analysis. In the IMM technique the solutions are diluted to 4000 $\mu g\ ml^{-1}$ during the procedure.

Fig. 7.4 178
Schematic diagram of the interactive matrix matching (IMM) system. The variable-speed pump (and thence the dilution of the test solution) are controlled by the computer, in response to the initial determination of the matrix element. The dilution of the test solution is adjusted so that the matrix element concentration moves to a reference level used in the calibration solutions.

Fig. 7.5 178
Circuit diagram of electronic interface between ICP and IMM.

Fig. 7.6 183
Simplified Flow Chart for Interactive Matrix Matching (IMM).

Fig. 8.1 202
A schematic calibration graph. The relative sensitivity at concentration c is the slope of the cord A divided by the slope of the tangent at zero concentration B (i.e. the reference sensitivity).

Fig. 8.2 205
The effect of increasing calcium concentration on (i) the relative sensitivities of concomitant analytes and (ii) the Ca II 317.9nm emission line. The similarity in curve shape suggests a common cause.

Fig. 8.3 212
The calibration graphs of the fourteen calcium lines between their detection limit and concentration at which 5% curvature occurs. Also marked are background equivalent, concentration (•), and concentration at which 1% curvature (.) is apparent. Non linearity is not apparent on the log/log scale.

Fig. 8.4 218
(a) Relative sensitivities of calcium lines at 5000 µg ml Ca plotted against total excitation potential, with the regression line. Points 2 and 10 are not included in the regression. (b) Relative sensitivities of lines of other elements in 5000 µg ml^{-1} Ca with regression line. The overall trends of the two data sets are indistinguishable by regression, suggesting the common origin of reduced excitation temperature. Deviations of individual points from the regressions, where greater than the experimental error (ca 1%), are presumably due to factors affecting specific lines.

Fig. 8.5 220
Wavelength scan of Ca line #2 (Ca I 272.2 nm) showing suggestion of a complex structure.

Fig. 8.6 226
An example of the reduction of calibration curvature using the PRISM correction (e.g. Ca II 317.93nm).

LIST OF TABLES

Page

Table 3.1 47
Description of ICPAES instrumentation and operating conditions.

Table 4.1 60
Data for lines used and concentrations in the test solution for quasi-routine analysis.

Table 4.2 62
Instrumental parameters variation scheme.

Table 4.3 66
Correlation matrix for the quasi-routine analysis data after drift correction, showing the generally high level of correlation and particularly strong correlation between certain sets of elements. For example, zinc and cadmium are highly correlated with each other but not with lithium or sodium.

Table 4.4 70
Principal component loadings for the principal components analysis of the quasi-routine analysis data after drift correction. The high values indicate strong correlation between the element and the component.

Table 4.5 72
Linear coefficients describing the susceptabilities of 24 elements to nine parameters. All values are % changes in the element response for the various units stated at the top of each column. For example %/% signifies that a 1% increase in forward power will result in a 4.442% increase in the zinc response. t-ratios are given for the parameter coefficients estimated by regression.

Table 4.6 74
Four multielement parameter signatures, normalised to zinc as the highest value. These data are shown in Fig. 4.4 where the overall similarities to forward power MPS can be discerned.

Table 4.7 75
Four multielement parameter signatures, normalised to lithium as the highest value. These data are shown in Fig. 4.5 where the overall similarities to the sample uptake rate MPS can be discerned.

Table 4.8 76
Correlation coefficients between the independently determined MPSs given in Tables 4.6 and 4.7. These values are all highly significant (i.e., >0.61 using $P = 0.001$).

Table 4.9 82
Correlation coefficients between MPS values and properties of the analyte element and emission line.

Table 5.1 102
Effect of PRISM correction on the precision and accuracy of the quasi-routine analysis data.

Table 5.2 104
Varying contributions of the two internal standards within the PRISM correction to the precision of three elements.

Table 6.1 120
Information on analyte elements.

Table 6.2 128
Experimental design for the comparison of matrix effects with equal calcium concentration added either concomitantly or by separate nebuliser.

Table 6.3 136
Nine calcium lines used for the determination of excitation temperature.

Table 6.4 142
Information on matrix elements.

Table 6.5 148
Regression coefficients of analyte relative sensitivity against matrix energy demand (MED).

Table 7.1 166
Matrix effect of calcium on various element lines, expressed as parameters of the empirical function $S_r = 1 + A (1 - e^{-Bc})$, where c is the calcium concentration (µg ml^{-1}) and S_r is the analyte sensitivity relative to c = 0.

Table 7.2 168
Comparison of the improvements in accuracy by three techniques. Values are the average absolute bias of 14 analytes before ("Raw") and after ("Corr") correction (except for PRISM Corr., which is on 13 analytes).

Table 7.3 172
Forward power multielement parameter signature used for PRISM correction of matrix effects shown in Figure 7.3

Table 7.4 179
Equipment and instrumental conditions used in interactive matrix matching (IMM) experiment.

Table 7.5 182
Calibration scheme for IMM experiment.

Table 7.6 185
Calcium concentration values determined by IMM compared with actual values.

Table 7.7 190
Correction of matrix effects from 8000 µg ml^{-1} Ca by interactive power adjustment (IPA).

Table 7.8 194
Comparison of ten methods of correcting bias due to matrix effects.

Table 8.1 204
A comparison of self-matrix effects and matrix effects on other elements. The calibration data for calcium (Ca II 317.93 nm) expressed as relative sensitivity shows similarity to the relative sensitivity of concomitant cadmium and berylium.

Table 8.2 208
Description of 14 calcium lines studied.

Table 8.3 213
Example of goodness of fit between experimental data from Ca I 370.6nm and equation 8.9. The scaling factor for the residuals was 0.008 of the gross intensity.

Table 8.4 214
Parameters for equation 7 fitted to the calibration data of the calcium lines.

Table 8.5 216
Curvature data for the calcium lines.

CHAPTER 1

INTRODUCTION

1.1 Aims and Intentions

The greater part of the work described in this thesis was directed towards improvements in the quality of data produced by inductively coupled plasma atomic emission spectrometry (ICPAES).

ICPAES has been applied to the analysis of geological materials since its inception in 1964, and is now probably the most intensively-used multielement method in this field. The benefits of the method are quite clear and have been documented in considerable detail. However, the many strengths of the method are somewhat offset by limitations which have become apparent only for the more stringent application needs recently encountered.

The precision and accuracy that can be achieved by ICPAES were quickly identified as factors that are currently limiting the application of ICPAES. They were chosen as the main topics of this thesis because there was both a clear requirement for improvements and reasonable scope for success. There was potential for the greater utilisation of computer power in routine analysis, for the improvement of data quality. The detailed context of these considerations is described in Chapter 2.

The instrumentation and operating conditions used for the study are discussed in Chapter 3. Generally conditions were selected to be typical of those used for routine simultaneous multielement analysis. This ensured that the conclusions drawn concerning the causes of imprecision and inaccuracy, and methods

devised for their correction, have the widest applicability.

A special experimental design was constructed to study these problems. Without such a design, many of the effects could not have been estimated, as they are themselves at the limits of quantification. This attention to detail allowed important generalisation to be discovered.

The availability of computer software packages for the flexible manipulation of large data sets, was also crucial to the investigation. Various chemometric techniques were thereby evaluated for their usefulness in both the understanding and the correction of multielement data.

1.2 Pseudorandom Errors

There were two important factors which emerged during this study of the precision in routine analysis by ICPAES. Firstly the timescale used in the measurement of precision is crucial to its realistic evaluation. The reproducibility which is normally measured during less than one minute is not representative of that experienced over several hours of routine analysis. It was the improvement of the latter which was considered the most feasible.

The second perhaps more important realisation was that the variations in the emission at a single wavelength, although apparently random, were correlated to a large extent with the variations of all other lines simultaneously recorded. Principal component analysis (PCA) revealed that over 90% of all the variance of the emissions in routine polychromator analysis was multielement correlated and therefore not random. The identity of the causes of the correlated variance was sought. Two independent causes were found to account for ca. 70% of the

variance. Eight of ten controllable operating parameters which were investigated produced effects which conformed to these two causes. The identification was based on effects in the multielement dimension. One group of effects could be caused by variations in forward power to the plasma and the other by variations in sample uptake rate on individual spectral lines. Both of these causes gave effects related to the total excitation potential of the line.

The high level of multielement correlation shown to be present suggested that substantial improvements in the precision could be made by a specifically designed correction procedure. Chapter 5 describes such a procedure, named the parameter related internal standard method (PRISM). This was based on a mathematical model which describes the routine analytical variations. In PRISM the intensity of each analyte line was corrected twice, once each for the variations caused by the two identified factors. Two internal standard elements were added to each sample solution and used separately to monitor variations in each of the causal factors. The PRISM mathematical model was used to 'predict' what the combined effect of the two causes would be for each analyte line. This information was then used to correct the analyte intensity.

This method of precision improvement was compared with other methods both in terms of resultant precision and the practicability of the method. The fact that PRISM correction removed ca. 70% of the variance in routine analysis confirmed that the model successfully described the majority of the variation.

1.3 Systematic Errors

Systematic errors in analysis by ICPAES caused by the matrix effects are examined in Chapter 6. Matrix effects are biases caused by changes in the sensitivity of the analytes. Although generally small in ICPAES (<5%) biases greater than 36% occur for certain combinations of matrix and analyte element. No method existed, prior to the work described in this thesis, which enabled a prediction to be made as to which element combinations would produce serious bias.

Calcium was selected as the matrix element for intensive study in the multi-analyte dimension. A pattern was discerned in which susceptibilities of different analyte lines were related to their total excitation potentials (E'). This finding suggested the causal hypothesis that matrix effects were a consequence of the matrix element reducing the excitation temperature of the ICP.

This hypothesis was then tested by extending the study to effects of a large range of matrix elements at equimolar concentrations. The initial hypothesis was broadly supported by the common multi-analyte signatures found. However no obvious property of the matrix element was able to predict the extent of the fall in excitation temperature. Detailed investigations in the multi-matrix dimension revealed an appropriate property termed 'matrix energy demand' (MED), which was derived from lattice energy corrected to include the ionisation energy for the appropriate degree of ionisation. These findings enabled the construction of a predictive mathematical model for matrix effects in ICPAES.

In the 'MED-Model' the fundamental properties of the matrix element (MED) and analyte line (E') were used to calculate the expected matrix effect. Although limited at present to one concentration of matrix element, the model can be used for quantitative predictions at that concentration, and qualitative predictions at other concentrations. It identified the relatively small fraction (~25%) of matrix-analyte pairs which are prone to serious interference effects (>10% bias). The model was compatible with the mechanism of reduced excitation temperature and values in the range 0-100K were estimated from various matrix elements.

The efficient correction of matrix effects in ICPAES, addressed in Chapter 7, drew in part, on the conclusion of the previous chapter. Eleven methods of correction were assessed against a list of suitable criteria at various levels of detail. All of the seven methods devised for this study were computer-based either in a passive chemometric role (e.g. PRISM) or else in an interactive role where feedback from the computer brought about a physical intervention in the process of the analysis (e.g. interactive matrix matching (IMM)). The various methods are at different levels of development but it is evident that each method will have certain strengths and weaknesses. For example IMM achieved the most accurate removal of matrix effects but was relatively slow and somewhat limited in its range of applications. PRISM was less accurate although more flexible, being capable potentially of correcting any analyte-matrix combination.

1.4 Calibration Line Curvature

Chapter 8 reports on investigations of an apparently unrelated aspect of ICPAES; the curvature of calibration graphs of instrument response on analyte concentration. This work is related however to the rest of the thesis in two ways. The causes of the curvature in the calibration of ICPAES are generally not well understood, and no theory is available to predict the linear working range to be expected for any given line. A conjecture tested in this thesis is that a major unsuspected cause of curvature is a self-matrix effect. In the above mentioned work on matrix effects the progressive addition of some matrix elements was shown to reduce the excitation temperature of the plasma and alter the sensitivity of the analyte emission lines. This temperature fall would also be expected to reduce the spectral intensity of emission lines of the matrix element. This would be evident as curvature of the calibration towards the concentration axis. The inspection of existing data supported this hypothesis for one calcium line and new experimentation on fourteen calcium lines showed that the curvature of eleven of them also conformed to the hypothesis.

In the course of this work a new curve fitting equation was devised, which was based on an empirical description of matrix effects. This equation showed very good correspondence with the fundamental shape of the calibration line, unlike the current equations used in ICPAES calibration, which are not based on any spectrochemical considerations. The accuracy of ICPAES analysis is affected by fitting errors in calibration. These errors are poorly perceived by users, but are undoubtedly a significant cause of bias. A more appropriate curve fitting equation should

help to reduce errors from this source.

The conclusions of this thesis are drawn together in Chapter 9. The summaries of each chapter are considered and the wider significance of the results are assessed. The many possibilities for future work suggested by the findings are discussed.

Several aspects of the research carried out for this thesis have already been published and are listed in Appendix K.

CHAPTER 2

ICPAES IN GEOCHEMICAL ANALYSIS

2.1 Introduction

The objective of this chapter is to outline the context into which the work of this thesis was set and to explain why this topic of research was chosen from the many possibilities presented by the rapidly developing area of ICPAES.

A comprehensive review of the method in geochemical analysis has been given by Thompson and Walsh (1983). Only papers with a direct relevance to the work of this thesis will be discussed.

2.2 Development of Atomic Emission Spectrometry

Atomic emission spectrometry (AES) is one of the oldest instrumental techniques of chemical analysis. It was first described in a qualitative form by Bunsen and Kirchoff in 1859 and its quantitative capability was realised by Gerlach in 1925 using the technique of internal standardisation. Refinement of this technique can further improve the accuracy and precision of analysis and this forms a major part of the present research. With a DC-arc as the excitation source commercial AES instruments were widely used for geochemical analysis from the 1950's onwards, but fell into relative unpopularity from the mid 1960's owing to the superior precision, accuracy and detection limits of atomic absorption spectrophotometry (AAS). It was the development of a new more stable emission source, the inductively coupled plasma (ICP) primarily by Greenfield et al (1964) and later by Wendt and Fassel (1965), which progressively rejuvenated atomic

emission spectrometry. The first commercial ICPAES instruments appeared in the mid 1970's, with geochemical analysis being one of their main areas of application. Ten years of routine analysis have firmly established the role of ICPAES as one of the three main multielement techniques for geochemical analysis, together with X-Ray Fluorescence (XRF) and Neutron Activation Analysis (NAA). Each of these techniques have their strengths and weaknesses but often only one technique can be economically justified by a single laboratory. There is a requirement therefore to extend the abilities of each technique to cover the largest range of analytical tasks. High precision of analysis, for example, has been possible previously by only XRF. If this ability could be added to the many other strengths of ICPAES for geochemical analysis (section 2.5) then this one technique could accomplish the vast majority of analytical requirements for geological materials.

2.3 Operating Principles of ICPAES

Detailed descriptions of inductively coupled plasma atomic emission spectrometry (ICPAES) are available from the literature (Greenfield et al., (1964), Thompson and Walsh (1983)). A brief description of the main component parts of ICPAES and the basic principles of operation are given here to introduce the terminology and analytical characteristics which will be referred to subsequently. An explanation of the symbols and abbreviations is given in Appendix J.

A schematic diagram of a typical ICPAES system used for simultaneous multielement analysis is shown in Figure 2.1. The sample is conventionally in the form of a liquid, so that most

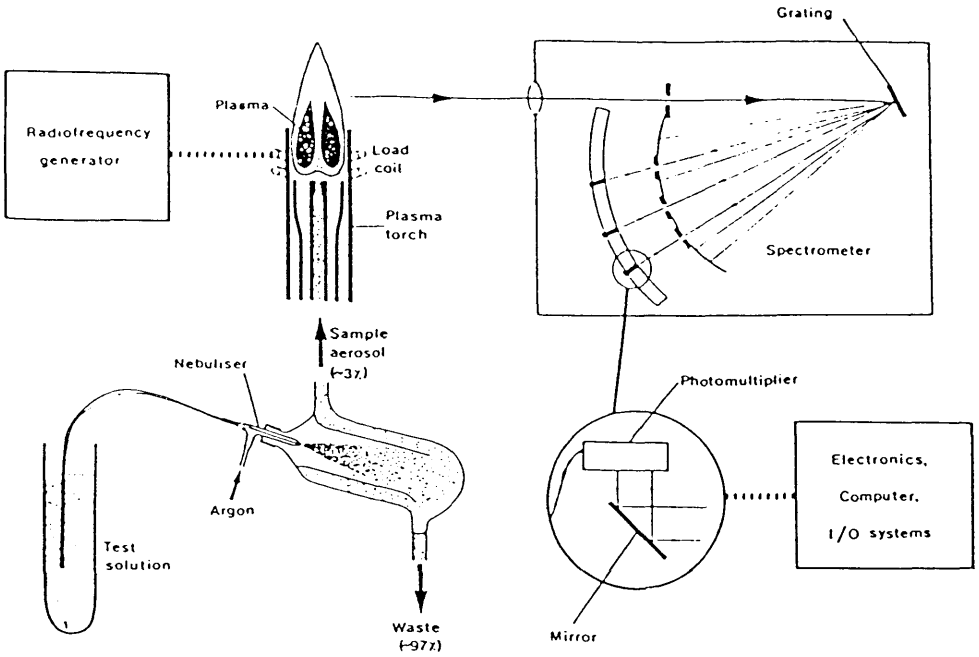


Fig. 2.1
Schematic diagram for an ICPAES used for simultaneous multielement analysis.

geological materials must first be decomposed and solubilised by one of a range of techniques such as those described by Thompson and Walsh (1983 p133). The liquid is drawn up through a polyethylene uptake tube to a nebuliser which converts the sample into an aerosol. Nebulisers usually operate pneumatically by means of a stream of argon, called the nebuliser gas flow. The aerosol passes into a spray chamber which removes all but the finest droplet size ($<10\mu m$) and this fine fraction (ca 3% of the original) is swept into the centre of the ICP emission source. The plasma consists of ionized argon gas heated inductively to ca 10000K by a load coil. Radio frequency power of ca. 1kW, called the forward power, is coupled into ca. 1ml of the argon. The argon of the plasma is continuously being replenished by a columnar flow of argon emerging from the plasma torch. The aerosol of sample travels up through a vertical tunnel in the centre of the plasma. The sample is heated progressively from the outside to a temperature of about 8000K, causing progressive decomposition to occur. Initially the droplets of sample solution are desolvated and then all molecular bonds are broken in the process of total atomisation. The subsequent degree of ionisation of the atoms varies between elements and can be estimated from the Saha equation (discused in Section 6.4.3).

The plasma is situated within and above the load coil but only a small region of the plasma is viewed for analytical purposes. The observation height is usually specified in mm above the load coil, although this is not definitive and the actual zone of the plasma viewed depends on other parameters, notably the nebuliser gas flow (Koirtyohann et al, 1981). The viewing height used in this work at 14mm is typical of the compromise operating

condition used for multielement analysis (see Section 3.2).

The portion of emitted light is dispersed into its constituent wavelengths in a vacuum spectrometer. For simultaneous analysis a series of photomultiplier tubes (PMTs) are positioned to intercept the intensities of the analyte wavelengths of interest. The response of the PMTs is integrated over a period of time, typically 5s, and gives a measure of the analyte intensity. The average of a number of integrations, taken during one nebulisation, are then calculated by a dedicated computer.

Atomic emission is visible from both neutral atoms (I) and singly charged atoms (II). The exact mechanisms involved in ionisation and emission are not well understood (de Galan 1984). Absolute calibration of the emission intensity for a given concentration of analyte is therefore currently impossible.

The quantitative analysis of samples is achieved by comparing the intensity measured for the sample to that for calibrating solutions, with a range of known analyte concentrations. A calibration equation is then calculated for intensity against concentration, a function that is usually linear over several orders of magnitude (discussed in Chapter 8).

2.4 Sources of Analytical Error in ICPAES

Analytical error can be subdivided into random error (measured as precision) and systematic error (inaccuracy or bias). The precision expresses the reproducibility of an analysis whereas the inaccuracy measures the difference between the analysis and the true concentration of the analyte. All the processes involved in ICPAES probably contribute both types of error at some level. Certain operating parameters, such as forward power, are known to

have a critical effect on analytical performance, (Blades and Horlick, 1981a). However, the identity of the underlying sources of error which dominate the precision and accuracy of the analyte concentration is largely unknown. To identify these sources and assess their relative importance is one object of this study. The descriptive characteristics of these types of errors are known and a discussion of these is a prerequisite to further investigation.

2.4.1 Random Error

The random error associated with an analyte response in ICPAES is normally distributed. This fact, commonly assumed, was confirmed experimentally in Section 4.7.1. Random error can therefore be described using the parameters of the normal distribution i.e. the mean (μ estimated by $\bar{x}$) and the standard deviation (σ estimated by s). The standard deviation of analyte response has been shown to be a function of the analyte concentration as depicted in Figure 2.2a, (Thompson & Howarth, (1976)). The standard deviation of the analyte response tends toward proportionality to the analyte response at high concentrations but as lower concentrations are approached, the standard deviation approaches to an approximately constant value (S_o). This minimum standard deviation of response, is related to what is called the detection limit. This is often defined as the lowest concentration of analyte which can be measured with a 95% confidence limit ($2S_o$).

Precision (P) is more frequently expressed in relative terms as the ratio of the standard deviation over the mean. When converted to a percentage this is also called the coefficient of variation ($CV = 100 * s/\bar{x} = P$). This is also a function of the concentration and is shown in Figure 2.2b. The relationship shows

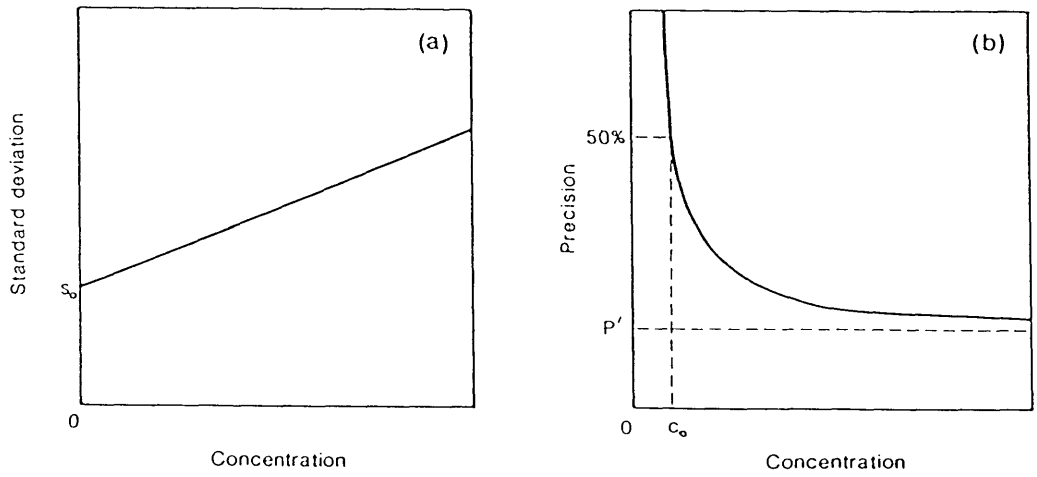


Fig. 2.2
Schematic representation of the variation of precision with analyte concentration when expressed as;
(a) standard deviation; a value s_o is approached at low concentrations,
(b) precision ($100 s_o/x$), a constant value of precision (P') is approached at high concentrations.

that at high concentrations the analyte precision approaches a constant value P', and is not dependent on the analyte concentration. As the detection limit is approached however, the precision rises increasingly, reaching the value of 50% at the detection limit (by definition).

The importance of this relationship for the study of precision is that experimental values of analyte concentration must be well above their detection limit ($> 1000^*$) if the optimum precision (P') is required. It is only these high level precisions which are usefully comparable between different analytes.

2.4.2 **Systematic Error**

There are two general categories of systematic error in ICPAES considered in this work , (i) interference effects and (ii) instrument calibration.

i) Interference effects

The term 'interference effect' is a broad description of an analytical bias associated with the presence of non-analyte elements. There is no mechanism implied in the term and the clarification of the causes of the inaccuracy is an object of this study reported in Chapter 6. An interference effect can be defined as a significant change in the measured concentration of an analyte caused by an element other than the analyte.

Two mathematically distinct types of interference effect can be separated which affect the calibration lines of ICPAES in different ways. **Translational interference** shown in Figure 2.3a consists of constant absolute analyte bias (x) irrespective of the concentration of the analyte. This is also called background interference and is due to a spectral overlap of emissions of

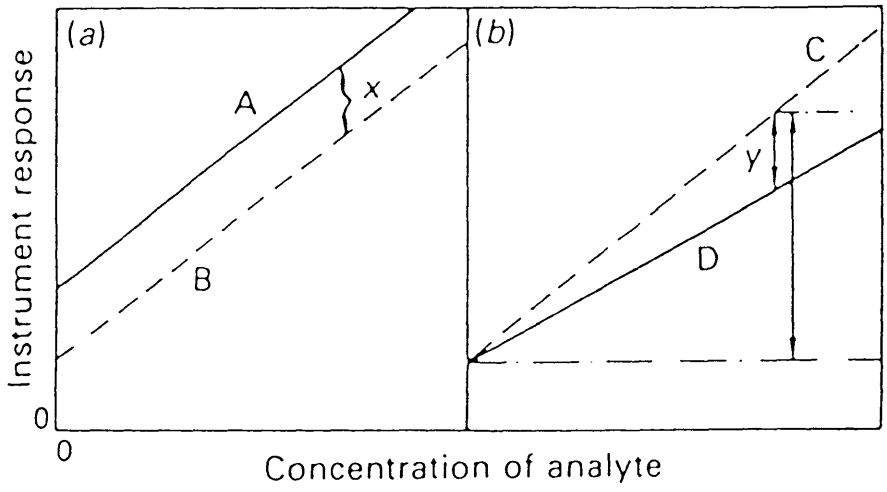


Fig. 2.3
Schematic calibration graphs illustrating the effects of (a) the translational interference: B, no interferent; A, interferent present at concentration c_1; producing a constant bias x; (b) the rotational interference produced by an interfering element of concentration c_1: C, no interferent; D, interferent present at concentration c_1, producing a relative change in sensitivity y.

the interfering element with that of the analyte line. Interference of this type increases predictably with increasing concentration of the interfering element and can be easily corrected on all commercial ICPAES instruments. Significant errors may be introduced by these corrections if the analyte concentration is very low compared with the size of the correction factor (Thompson and Walsh 1983 p126), but in most determinations it is not an major cause of analytical error.

The second type of interference effects are **rotational** in their effects on the calibration line (Figure 2.3b) and are generally known as matrix effects. In this case the absolute size of the analytical bias (y) increases in proportion to the analyte concentration. The bias from a matrix effect can therefore be expressed as a percentage, irrespective of the analyte concentration. The causes of matrix effects will be discussed in detail in Chapter 6. A notable difference between rotational and translational bias is the analyte concentration range at which they are most important. Translational bias is only a significant fraction of the analyte response at low analyte levels, and therefore it can increase the analyte concentration required to give a statistically significant response (i.e. raise the detection limit). A rotational bias of 10% however will not be detectable close to the detection limit where the precision is approaching 50%, but will become increasingly important as the analyte concentration increases and the precision improves towards $\pm$1%.

ii) Calibration

Another potential cause of significant error in ICPAES is the calibration of analyte response versus concentration. The

precision of the analyte response produces a random uncertainty for each calibration point. The size of this error can be estimated for a range of concentration from in Figure 2.2. Uncertainty in the value of the analyte concentration can normally be taken as insignificant unless reference materials are being used for calibration. The second appreciable cause of error is systematic and is due to the fitting of the calibration equation through the experimental points (Thompson (1985)). The error due to curve fitting is sometimes given by the instruments computer software. However even where the inaccuracy of a calibration line is calculated, this only applies to the calibration points. This does not estimate the accuracy to be expected between the points. In the analysis of samples it is probable that most analyte concentrations measured will fall between calibration points and be subject to errors greater than those estimated. There has been no thorough study reported of this source of analytical error in ICPAES.

A separate systematic error originating in calibration procedures is due to instrument drift. Drifts in sensitivity of up to 1% per hour are typical in ICPAES. At the time of calibration the accuracy is known, but in the period before the next calibration the analyte sensitivity will vary and can only be estimated. In this thesis, the characterising of long term drift is combined with that of short term drift, which is perceived as random error (Chapter 4). The real-time estimation of sensitivity using internal standards, is considered as potentially the most cost effective way of reducing inaccuracy due to drift.

2.5 Advantages of ICPAES for Geochemical Analysis

In this section the qualities of ICPAES which have proved useful to geochemical analysis will be discussed for contrast with the shortcomings given in Section 2.6. These characteristics extend beyond the strictly instrumental into the chemical and economical.

ICPAES has proved particularly well suited to the analysis of geochemical samples largely because of the following characteristics.

i) Detection limits are low enough to determine most elements at the concentrations present in geological samples. There are 25 elements for which the average crustal abundance exceeds the detection limit by more than a factor of ten, producing analysis of good precision (Thompson (1986)).

ii) Good precision, usually within 5% for analytes well above their detection limits, which is a big improvement on that from DC-arc AES.

iii) Good accuracy. Chemical interference effects due to the presence of molecules in the excited sample, which are frequently found in AAS, are absent in ICPAES owing to the total atomisation of the sample. Translational interferences are common, but they are well understood and can easily be corrected (see Section 2.4.2). Accuracy within 5% is generally achievable for analytes well above their detection limits at sample concentrations less than 1 gl^{-1}.

iv) Long linear ranges of calibration allow major and trace elements to be determined on the same sample solution, without the dilutions required by AAS.

v) Rapid simultaneous multielement analysis allows higher productivity and hence more cost effective analysis than any other comparable technique. For example the analysis of 250 samples for

25 elements in 8 hours is currently achieved on a routine basis.

vi) The instrument has very flexible equipment options. For example a wide range of methods for sample introduction can be used as alternatives to the nebuliser. These options enable the analyst to implement many types of sample presentation, including enhanced analyte sensitivity (e.g. hydride generation), solid sample introduction (e.g. laser ablation) and partial sample analysis (e.g. fluid inclusion analysis).

All these aspects are discussed in greater detail by Thompson and Walsh (1983). Their relevance to this thesis is in the identification of areas of performance of ICPAES which require improvement.

2.6 Current Limitation of ICPAES for Geochemical Analysis

Many of the assessments of characteristics given above are not absolute but relate to a particular application of the data, or in comparison to another analytical technique. For example precision at $\pm 5\%$ may be 'good' for mineral exploration, or compared with DC-arc data, but in relation to a requirement for $\pm 1\%$ precision, would clearly be described as 'poor'. It is the increasing requirements and expectations of the users of geochemical analysis which therefore 'produce' the perceived limitations of ICPAES.

It was from the following list of constraints that the area of research of this thesis was selected for the reasons given in Section 2.7. The shortcomings of ICPAES have been assessed for applied geochemistry by Thompson (1986) and for geochemistry generally can be summarised as follows:-

i) Sample dissolution problems are caused by the need for a liquid sample to be nebulised. Although the total dissolution of nearly all geological samples is possible with lithium

metaborate fusion, adequate detection limits for many trace elements cannot be achieved by this means. This situation could be improved either by a new chemical dissolution procedure including preconcentration, or else by substantial improvements in instrumental detection limits.

ii) Low abundance of a number of elements of geochemical importance (e.g. U, Mo, W, Cd, Precious Metals, and Rare Earths) still make their direct determination by ICPAES impossible. Chemical separations prior to analysis seems to be the only probable solution for these elements.

iii) Speciation of elements refers to their valency state or to the molecule in which they occur. This cannot be determined directly by ICPAES. Chemical separation of species prior to analysis is the only possible method available.

iv) Cost effectiveness is necessary where geochemical interpretation requires that large numbers of samples be analysed, to good accuracy at reasonable cost. Any method designed to improve technical performance must not seriously impair this factor.

v) Hardware reliability is still a problem in ICPAES, particularly that of the nebuliser. Improved equipment is clearly desirable, but has proved difficult to achieve. The use of computer software to monitor the performance of the instrumentation is probably a more efficient way to improve overall reliability of performance.

vi) Interference effects (described in Section 2.4.2) can cause significant inaccuracy in ICPAES analysis. Spectral effects are well understood and computationally corrected but matrix effects are not understood and only corrected by the 'expedient' of matching the matrix element concentrations of the calibration

solutions to that of the samples. This matching of concentration requires samples of a known and constant composition. This is impossible for batches of geological samples which usually have both unknown and very variable compositions.

Certain analytical tasks in geochemistry require improvements in the accuracy of analysis from ICPAES. 'Whole rock analysis' of silicate rock to produce totals of 100± 1% for example requires an improvement in the accuracy of < 5%, quoted as 'good' in a broader context.

vii) Precision improvement is an equally significant requirement if only as a necessary prerequisite to improved accuracy. It has been argued that for some applications in geochemistry good precision is more important than good accuracy (Rose, Hawkes and Webb, (1979) p65). The achievement of both qualities are clearly the preferable option. Multielement analysis by XRF in particular has increased the expectation for high precision geochemical analysis. With long counting periods XRF can produce precisions in the order of 0.1%, although whether the accuracy achieved matches this figure is debatable.

2.7 The Selection of the Research Objectives

2.7.1 The Feasibility of the Possible Research Objectives

From the foregoing list of limitations of ICPAES in geochemistry it became apparent that two broad strategies emerge for improving analytical performance; the chemical and the instrumental. Some limitations of ICPAES are so fundamental (e.g. detection limits) that excluding a major breakthrough, developments are required in the chemical preparation of the sample before the instrumental analyses. This is the approach adopted by the majority of recent research workers on ICPAES for geochemical analysis, as tabulated by Lawrence (1984, 1985a, 1985b, 1986).

They usually report, novel chemical pretreatments of an increasing range of sample types, for an extending range of elements. A significant breakthrough in purely instrumental performance seems improbable as there have been only secondary improvements in instrumentation over the last ten years. The 'law of diminishing returns' is beginning to apply, in that further improvements to analytical characteristics tend to cost more to develop and produce smaller improvements.

The extra factor to be considered however is the decreasing cost and increasing power of the computer present on all ICPAES systems. Correctly harnessed, this power can enable cost effective improvements in instrument performance to be effected. A second strategy therefore comprises the use of computer software, alone or in combination with hardware to improve some of the performance criteria of ICPAES.

Of the limitations given above, the precision and accuracy seem the most promising items for this style of improvement. Not only is their investigation made simple by new computer spreadsheets but the scope for improved performance seems substantial. In addition there is a clear requirement for such improved data quality.

The assessment of the feasibility of this objective was based on a combination of factors including:-

i) Internal standardisation is established as a powerful method for improving precision in AES but existing modes of application are based on too crude a model to work for multielement ICPAES, (Barnet et al., 1968). There is the potential for improved precision based on the more comprehensive calculations possible with computer processing, if sufficient correlation between element responses is present.

ii) The inaccuracy of ICPAES due to matrix effects is known to be small at low concentrations of sample ($< 1 gl^{-1}$). The pursuit of lower detection limits however, will increasingly require sample concentrations in excess of $10 gl^{-1}$. Under these conditions inaccuracies of up to 30% have been reported (Thompson and Walsh, 1983 p140). The need for rapid and effective means of correcting matrix effects is therefore clear. It is likely to increase with the advent of nebulisers which can reputedly handle sample solutions or slurries at concentrations in excess of 100 gl^{-1}, (Ebdon et al, 1982).

iii) Computer modelling as a means of correcting matrix effects on a purely descriptive basis would currently be an impractical task. This would involve measuring the effects of all possible concentrations of every element on the sensitivity of every intended analyte, followed by studies of the effects of all possible mixtures of elements.

If however the underlying mechanism of matrix effects could be elucidated and the relevant fundamental properties of the matrix element and analyte line identified then a practical correction of matrix effects can be envisaged.

iv) Computing power can permit more complex corrections to be made than were previously possible, and also constitutes a powerful new research tool. For example a wide range of multivariate statistical techniques have never been applied to investigations of ICPAES data, and it seems probable that some new insights would be produced by their judicious use.

2.7.2 The Need for Improved Data Quality in ICPAES

The choice of accuracy and precision as the targets for improved performance was based on a combination of two factors. The scope for improvement appeared substantial, and the need was

clearly required.

In mineral exploration geochemical surveys are designed to locate mineable deposits of abundant metals. For this purpose analysis with precisions of ±5% and accuracies within 10% were adequate and even appropriate. A recent interest in mineral exploration however, has been the modelling of geochemical processes, which requires the accurate measurement of small variations in the composition of rocks, (Govett 1983, p53). The sum of the element composition required for this purpose is 100±1%. The analysis must be accurate enough for this purpose. It must also be fully corrected for intereference effects which can mimic the geochemical associations, an understanding of which is an objective of the geological study.

An example of this would be the correct geological interpretation of small differences between element concentrations in different rock types. A good case would be a traverse across a skarn mineralization where the major element composition of the rocks changes from that of granite to that of limestone. The accuracy of the analysis for the trace metals along the traverse must be independent of the major elements in the rocks. If the apparent change in concentration of the trace element were only due to interference, then an incorrect geochemical interpretation could be made.

A better perception of the real quality of data provides a further motivation for improved data quality in ICPAES. In 1951 there was a famous interlaboratory comparison on the analysis of standard rock by a variety of analytical methods, (Fairbairn et al., 1951). The variability of the results was very large, ranging up to a factor of x 5 for some trace constituents. The surprise which these results created suggests that there was a large

difference between the perceived quality and the real quality of the data being produced routinely at that time. In recent years it has become more common to use a scheme of Analytical Quality Assurance (AQA) to assess the real data quality of analysis by ICPAES. One such system was described by Thompson and Walsh (1983, p119) which led to more realistic estimates being made of accuracy and precision. This has meant that an objective estimation of the real data quality achieved has replaced the intuitive and often optimistic estimates made previously. Now that the accuracy of analysis can be assessed using certified reference materials, the problems of bias are much more clearly exposed. Similarly, the precision measured with samples duplicated, placed at random and analysed 'blind' over the entire period of analysis, reveals realistic precision values. This contrasts with the values measured by repeated analysis of the same solution over a short time period after a long instrument warm-up.

AQA schemes assess the total data quality including sample heterogeneity, and sample preparation as well as the instrumental analysis. When suitably designed the scheme can identify the source of poor data quality and indicate, for example, that a bias may be instrumental in origin. This has clarified the problems that need to be addressed in order to improve data quality.

2.8 Summary

From a consideration of the limitations inherent in analysis by ICPAES, particularly for geochemical analysis, improved accuracy and precision of analysis were identified as the objectives of further study. The need for major element analyses of rocks to within 1% relative precision underlies this approach. The removal of analytical bias is important for two reasons. (i)

For each element, considered individually, an accurate analysis is required. (ii) When multielement behaviour is being used for geochemical interpretation then correlation between element concentrations must not be an artifact of the analytical process. Interference effects can cause correlation between elements which is geologically erroneous.

An increased utilisation of computers in pursuit of this objective was judged to be the most likely way to produce fresh insights into the problems, and cost effective methods for their correction.

CHAPTER 3

GENERAL EXPERIMENTAL DESIGN AND EQUIPMENT

3.1 Introduction

This chapter describes the experimental design and equipment that was used in the various investigations reported in this thesis. In particular those aspects will be discussed which were critical in enabling the measurements to be made with the required accuracy and precision.

3.2 ICPAES Instrumentation

Two inductively coupled plasma atomic emission spectrometer systems (ICPAES) were used in this study. The majority of determinations were carried out on the Applied Research Laboratories ARL 34000C polychromator described in Table 3.1. The operating conditions were generally typical of those used by a wide variety of laboratories for simultaneous determination of a wide range of analytes. They are generally referred to as 'compromise operating conditions' which give the optimum sensitivity and relative freedom from matrix effects over the entire range of analytes. The one operating condition in this study which is atypical, is the solution uptake rate of the nebuliser. A free running (i.e. unpumped) Meinhard concentric glass nebuliser would normally consume 2-3ml min^{-1}. This has been reduced to 1 ml min^{-1} by using an small bore uptake tube (0.5mm i.d. 300mm long). The main objectives of the low uptake rate were to reduce the consumption of sample and increase sensitivity.

Parameter	Instrument*	
	34000C	3520
Determination	Simultaneous	Sequential
Computer	PDP 11/04	PDP 11/23
Forward power/kW	1.25	1.20
Frequency/MHz	27.12	27.12
Viewing height above load coil/mm	14	15
Viewing window square of side/mm	4	4
Torch type	Fassel	Fassel
Gas flow-rates/l min^{-1}:		
Coolant	12	12
Auxiliary	0.4	0.8
Injector (humidified)	1.01	1.00
Spray chamber	Scott Double pass	Conical Single pass
Nebuliser (concentric glass Meinhard)	TR-30-3A	TR-30-3A
Solution uptake rate (unpumped)/ml min^{-1}	1.05	2.40
Uptake tube (polyethylene)/mm	350 × 0.5 i.d.	400 × 0.8 i.d.
Nebuliser tip wash/ml	0.5	0.5
Pre-flush time, number of and time of integrations/s	20, 3 × 5	30, 3 × 3

* Applied Research Laboratories 1-m vacuum spectrometer.

Table 3.1
Description of ICPAES instrumentation and operating conditions.

However, this may also have produced secondary effects in these experiments which cannot be reproduced at higher uptake rates.

A second modification to the commercially available hardware relates to the reduction of memory effects from the nebuliser (Ramsey et al., 1983). This was especially important in studies where elements present at high concentrations of matrix elements were subsequently determined at low concentrations (for example in Chapter 6). Unsuspected memory effects in such cases would produce significant errors in the measured values of relative sensitivity.

The stabilization period or pre-flush is the time from beginning the nebulization of a solution to the beginning of signal integration. The value selected (e.g. 20s) is large enough to give a stable response and prevent memory effects from the previous sample. A constraint on the stabilization time is the need to minimise the total duration of the analysis and hence reduce the effects of instrumental drift.

Optimal and consistant performance of the nebuliser was critical to many of the determinations made in this study. Uptake rates were measured regularly and any deviation of the rate from the maximum value investigated and corrected by the methods described by Thompsom and Walsh (1983, p57).

A second ICPAES system which made determinations sequentially was used for a small number of determinations. This ARL 3520 is also described in Table 3.1. This system was used when the required lines were unavailable on the polychromator system. The only significant difference in the operating conditions of this system was the more typical sample uptake rate of 2.4ml min^{-1}.

3.3 Solution Preparation Techniques

Although the majority of manipulations made in the preparation of analytical solution were standard practices in analytical chemistry, certain aspects are tailored specifically to this study.

3.3.1 Purity of Chemicals

The selection of the appropriate purity of the chemicals used was a necessary compromise between cost and the expected level of the relevant impurities. For example in the study of matrix effects from large concentrations of elements upon a wide range of analytes, a freedom from any detectable trace of these analytes required the use of SpecPure grade chemicals (Johnson Matthey Chemicals Ltd). The inevitable presence of some low level impurities even in SpecPure grade was compensated for in the experimental design discussed below (section 3.4).

The compounds of the elements selected for matrix solutions were chosen on three criteria (i) to enable easy dissolution, (ii) to achieve exact element concentrations and (iii) to introduce minimal inclusion of extra matrix elements from the anions, elements such as nitrogen or sulphur.

The grade of molar hydrochloric acid used was generally AnalaR, except for solutions of SpecPure chemical which were made up in Spectrosol grade (both BDH chemicals). Care was taken to use one batch of acid for the whole preparation and analysis of each experiment to avoid extra sources of variability.

3.3.2 Volumetric Procedures

In investigations into the accuracy and precision of an instrumental technique it was important that no significant error should be introduced by the volumetric procedures that may be misconstrued as instrumental in origin. Great care was taken

therefore that errors in the specification and operation of glassware and automatic-pipettes should be monitored. Economic constraints, however, dictated that the pursuit of the ultimate accuracy should be tempered by a knowledge of the accuracy that would suffice for the intended application. For example relative volumetric error is at a minimum for 1000ml volumetric flasks (Class A Tolerance = $\pm$0.04%). However, 1 litre of a solution containing 10,000 $\mu g\ ml^{-1}$ Ca (Spec Pure) costs about £20. Suites of ten concentrations, for twenty elements clearly restricted the quest for ultimate accuracy in favour of appropriate accuracy. Such decisions are reinforced by the knowledge that only about 1ml of solution from this 1000ml is required for an experiment.

The detailed schemes of volumetric procedure varied for each experiment but certain features were general and are listed below:-

1) The vessel used to make up solutions for final analysis was often a the 15ml polystyrene centrifuge tube with polyethylene cap. This was selected for its negligible trace element contamination, and small volume to minimise the cost of chemicals.

2) The various 'spikes' of multielement solutions were made by calibrated, automatic-pipettes. Precision was usually more important than accuracy. For example, nominal identical calibrating solutions were prepared with replicate aliquots from the same pipette. An explanation of this priority is given in section 3.4. The same approach was used to deliver volumes of matrix elements of high purity at high concentrations. When using an automatic-pipette to dispense 3ml of a matrix element the precision ($\pm$0.2%) was adequate and more important than the bias ($\pm$0.6%).

Furthermore the potential for contamination from an automatic-pipette is smaller than by more traditional means. Care was taken that the disposable tip of the autopipette was kept in position, where maximum precision was required, and discarded when cross contamination was a potential problem.

3) Solutions were not generally 'made up to volume' due to the inaccuracy of the calibrated tubes, but rather 'made up by addition'. This procedure required a running total of all the volumes added to a single tube to be kept and the balance to the final volume calculated. An automatic pipette was then adjusted to dispense the required volume. When pairs of tubes with nominal equal concentrations were required, as in the section (3.4) below, then the additions to both tubes was made without resetting the autopipette calibration.

Justification of these volumetric procedures was sought in the results of various check solutions analysed with the experimental samples. For example, replicate multielement 'spike' solutions were prepared and analysed repeatedly. The volumetric error was not discernable within the analytical uncertainty. For matrix element additions the volumetric precision was apparent from the inspection of the emission intensity of the matrix element. The volumetric precision of the matrix element here was analytically significant but this variation had only a second-order effect on the variability of the analytes intensities. A small proportion of the scatter on Figure 7.1 may be due to this cause and (as stated in Chapter 7) subsequent investigations may warrant a higher degree of volumetric precision.

3.4 The Determination of Relative Sensitivity

Relative sensitivity is a term which is used to express values of sensitivity (S) for given operating conditions in comparison with the sensitivity under standard operating conditions (S_o). The relative sensitivity S_r is S/S_o and can be converted into percentage bias as $(S_r-1) \times 100$. For example if the addition of 10,000 µg ml^{-1} of Ca to a constant concentration of zinc produces a value of S_r of 0.7 this is equivalent to a bias of -30%. Although simple to define, relative sensitivity proved difficult to measure with adequate precision. The experimental design used for its determination was a vital factor in the understanding of matrix effects in ICPAES.

3.4.1 The Experimental Method

In essence the measurement of relative sensitivity depends on the quantification of small changes in the intensity (I) of an analyte 'i', usually due to the addition of a matrix element 'm'. Initially measurements of relative sensitivity were unacceptably variable by drift in the instrument response between the determination of the two values. The key factor in improving the precision of the determination was the design of a complete sub-experiment for each relative sensitivity determination. This sub-experiment comprised the nebulisation of only four solutions over a period of ca. 5 minutes which minimised the effect of drift. The running order of the four solutions was also important. The critical determination of the response change was made between two adjacent solutions. The detailed design for the determination of relative sensitivity was as follows:-

a) Four solutions were prepared.

1) the blank matrix (1M hydrochloric acid)

2) a solution of the analytes in the blank matrix

3) a solution of the matrix element at a specified level in the blank matrix

4) a solution containing both the analytes and the matrix element at the specified levels.

b) Instrumental intensity (I_n) was then measured for the analyte concentration c in the nth solution.

c) The reference net sensitivity is given by $(I_2-I_1)/c$.

d) The net sensitivity in the solution of the matrix element is $(I_4-I_3)/c$.

e) The relative sensitivity S_r in the solution of the matrix element is therefore given by

$$S_r = (I_4-I_3)/(I_2-I_1) \quad \ldots . 3.1.$$

The term (I_4-I_3) allows for the compensation required for possible background enhancements, line overlaps or analyte impurities from the matrix element, which would be identical in solutions (iii) and (iv). For analyte-matrix combinations presenting severe line overlaps or background enhancements, $I_3 \gg (I_4-I_3)$. In this study (e.g. Chapter 6) such combinations were rare and, when encountered, the results were discounted as being subject to unacceptable experimental error.

3.4.2 **The Volumetric Precision**

The absence of a concentration term in equation 3.1 confirms that the accuracy of the multielement 'spike' is not of primary importance. However poor volumetric precision in the addition of this spike between solutions (ii) and (iv) would lead directly to a similar value of precision in the relative

sensitivity. For example if equation 3.1 is simplified for the case where $I_3 \approx I_1 \approx 0$ then

$$S_r \approx I_4/I_3 \quad \ldots\ldots\ldots \quad 3.2$$

A random error in either I_4 or I_3 would therefore produce a random error of 1% in the value of S_r.

The measured precision of the volume dispensed by the autopipette used for the addition of the multielement spike (Gilson Fl000) was $\pm$0.11%. The precision of the final concentration of analyte was also affected by the uncertainty in the final volume of the solution. This was estimated as $\pm$0.1% from the sum of the variances of each volume added in the procedures described in section 3.3.2. This volumetric error then was much smaller than the'random' instrumental error, quantified as $\pm$0.95% (median, 1σ) in Chapter 4. The precision overall σ_{tot} of the determination of relative sensitivity is a sum of the variances of the volumetric manipulations (σ_{vol}^2) and the instrumental measurement (σ_{inst}^2) given by

$$\sigma_{tot} = \sqrt{\sigma_{vol}^2 + \sigma_{inst}^2} \quad \ldots\ldots \quad 3.3$$

The volumetric procedures used in this study therefore contributed an estimated 1% to the overall variance which shows the procedures were appropriate for this application.

The calculations described above could act as guidelines for the design of appropriate volumetric procedures should greater precision be required in future work.

3.5 Computation of Results

All of the experiments described in this thesis produced large data sets which it would have been impossible to process without the aid of a computer. Traditional programming languages, such as FORTRAN which was used in preliminary experimentation, proved too inflexible for this application.

The computer 'language' used for all the calculations in this thesis was the MINITAB computing system (from Pennsylvania State University, Version 1981.1). A full description of MINITAB has been given by Ryan et al. (1976). In appearance to the operator this system looks like a high level language with simple commands in 'English', although at a deeper level unseen by the operator these commands are written in the FORTRAN language. Generically MINITAB can be described at a statistical spreadsheet, where manipulations generally involve columns of results. An example of a list of MINITAB commands can be seen in Appendix B, which were placed together in what is called a macro, rather than a program.

The advantages of such a flexible computing system as MINITAB for this type of investigation can be summarised as follows:-

1) Data sets can be 'investigated' rather than simply processed. For example, when a single analyte is being considered a rapid assessment of the frequency distribution of a data set can help in assessing the suitability of applying other statistical techniques. If the distribution is not 'normal' then the production of a scatter plot against the time of analysis is five seconds work. The correction of any apparent drift by a regression against time followed by applying a correction equation is again rapidly achieved.

In the multielement dimension MINITAB is even more powerful. The complex interelement correlations described in Chapter 4 were only elucidated by interactive investigation of the data. For example producing a correlation matrix, simultaneously with variations in instrumental parameter, multielement drift correction and principal component analysis can all be executed, examined and repeated until meaningful patterns emerge.

Data sets can also be manipulated as matrices. This facility proved useful at a very basic level in transposing data. For example in Chapter 6 data were collected for a range of 18 matrix elements all with responses for 16 analyte elements. This data set could be manipulated in the multimatrix dimension, then easily transposed for multi-analyte studies, and retransposed with equal ease. This feature allowed a degree of flexibility without which the multielement patterns could not have been interpreted or even perceived.

The graphic displays of data produced within the MINITAB system, are evident as a basis for many of the diagrams in this thesis (e.g. Fig. 6.2). Although of low resolution, the rapidity with which plots can be generated allows many speculative unconventional relationships to be rapidly investigated. The labour involved in manual plotting would have left these improbable relationships untested. The identification of Matrix Energy Demand in Chapter 6 is an example of this facility.

CHAPTER 4

SOURCES OF IMPRECISION

4.1 Introduction

The requirement for improved precision in routine analysis, set out in Chapter 2, required a systematic study of 'medium term' precision of ICPAES in the multielement domain.
This chapter describes the investigation of potential sources of imprecision, which utilised a two stage experimental method directed inwards from the two ends of the problem. Firstly a series of measurements here called 'Quasi-Routine Analysis' which represented typical routine multielement analysis over 4.4 hours were examined to characterise the effects of imprecision. It was important to establish whether the apparent "noise" on each separate analyte response is purely random, or whether it was correlated to some extent between the analytes. This investigation of correlation utilized a statistical technique called Principal Components Analysis (PCA). It was expected that PCA would identify the underlying causes of the correlated variation in terms of distinctive multielement 'signatures'.

The second stage of the experimentation was to measure the multielement 'signatures' for ten instrumental operation parameters which might correspond to the "finger prints" identified by the PCA.

This experimental method failed to identify the causes of the imprecision directly, because of inherent limitations of PCA.

However the findings lead, indirectly to the establishment of a simple two-cause model that effectively described 70% of the variance in routine ICPAES. This model facilitated the method described in the next chapter, of substantially improving precision.

4.2 Terminology of Instrumental Precision

The parameters of the normal distribution used to describe random variation were discussed in Chapter 2. However, there is no universally agreed measure of precision in ICPAES. This is because the value of the standard deviation (σ) varies with the time period used for the measurement. The most optimistic and frequently quoted precision can be called the 'short term precision'. This is estimated from a small number of repeated measurements taken contiguously during the continuous nebulization of one solution. A more realistic measure of reproducibility is to determine the precision from separate nebulisations spread over several hours; this is defined here as 'medium term precision'. The most rigorous definition of instrumental precision 'long term precision' would allow for variation between days, weeks, even months of running, and would reflect the effects of changes in hardware, calibration equations and operators. The measurement of such 'long term precision' is prone to errors from solution instability and is rarely reported in the literature.

This work will concentrate on the factors which cause medium term precision to exceed the short term precision, as this is of most practical importance.

Another useful measure of precision is the variance (σ^2). When apportioning origins to various components of random variations, then the additive properties of the variance make it preferable to the standard deviation (σ).

4.3 Established Sources of Imprecision

Any spectroscopic technique can be limited by noise in one of two distinct ways; either 'source limited' where the noise in the source of analytical signal largely determines the precision, or 'detector limited' where the uncertainty in the detection system is larger than that in the analytical signal. In ICPAES, measurement is 'source limited', and from studies of the frequency of the noise Belchamber et al.(1982) established that there are two main causes. Dominant among them are variations caused by the rotation of the plasma at 200-400 H_z and noise generated in the nebuliser at 0-5 H_z. Detector noise, or 'shot noise' is not significant if the ICPAES if correctly adjusted (with voltage to the photomultiplier high enough to measure the background precisely).

Precision measured over longer time periods will also be affected by random errors in calibration measurements. Taking an extreme example, in the absence of calibration drift repeated estimates of an analyte sensitivity, made between each sample determination, will cause the precision to be made worse by a factor of $\sqrt{2}$. In routine analysis however sensitivity estimations are usually made relatively infrequently and it is their accuracy rather than their precision which is potentially the largest source of error.

4.4 Target for Investigation

The short term precision of ICPAES for analytes well above detection limit is generally around 0.5%. This precision would be adequate for most applications if it could be achieved routinely. However, medium term precision is typically 1% and, for some elements such as the alkali metals, up to 2.5%. These precisions

	Wavelength/ nm	Atom/ ion	Order	IP/ eV	EP/ eV	Concentration/ $\mu g\ ml^{-1}$
Ag . .	328.07	I	2	7.57	3.78	1
Al . .	308.22	I	2	5.98	4.02	300
As . .	193.76	I	3	10.5	6.40	—
B	249.68	I	2	8.30	4.96	—
Ba . .	455.40	II	1	5.21	2.72	10
Be . .	313.04	II	2	9.32	3.96	1
Bi . .	223.06	I	2	8.50	5.56	—
Ca . .	317.93	II	2	6.11	7.05	500
Cd . .	226.50	II	2	8.99	9.27	10
Co . .	228.62	II	3	7.86	5.84	10
Cr . .	267.72	II	3	6.76	6.15	10
Cu . .	324.75	I	2	7.72	3.82	10
Fe . .	259.94	II	2	7.90	4.77	500
K	766.49	I	1	4.34	1.62	126
La . .	398.85	II	2	5.61	3.51	10
Li . .	670.78	I	1	5.39	1.85	10
Mg . .	279.08	II	2	7.64	8.86	300
Mn . .	257.61	II	2	7.43	4.81	200
Mo . .	281.62	II	2	7.18	6.07	1
Na . .	588.99	I	1	5.14	2.10	100
Ni . .	231.60	II	2	7.63	6.39	10
P	178.29	I	3	11.00	6.95	100
Pb . .	220.35	II	2	7.41	7.37	10
Rb . .	780.02	I	1	4.18	1.59	—
S	180.73	I	3	10.40	6.86	—
Sb . .	206.84	I	2	8.64	5.99	—
Se . .	196.09	I	2	9.75	6.32	—
Si	288.16	I	2	8.15	5.08	—
Sn . .	189.98	II	3	7.33	6.52?	—
Sr . .	407.77	II	1	5.69	3.04	10
Te . .	214.28	I	3	9.01	5.78	—
Ti . .	337.28	II	2	6.83	3.69	37
V	311.07	II	2	6.74	4.33	10
W . .	239.71	I	3	7.98	5.58	—
Zn . .	202.55	II	2	9.39	6.12	10
Zr . .	349.62	II	2	6.95	3.58	—

Table 4.1
Data for lines used and concentrations in the test solution for quasi-routine analysis.

are too large for applications where an accuracy of better than ±1% is required, such as 'whole rock analysis'. The objective of this investigation was thus to identify the cause of the deterioration from short to medium term precision.

4.5 Experimental Design for Investigation of 'Quasi-Routine Analysis'

The aim of the first half of the investigation was to characterise the precision of routine analysis in the multianalyte domain. However real routine analysis deals with samples of varying composition, which would effectively mask the variations governing the precision. The experiment was designed therefore with only two solutions; one a 'blank' solution containing the acid matrix (1M Hydrochloric acid) and the other containing all of the 24 analyte elements of interest at levels well above their detection limits (>1000*), for the reasons of precision given in section 2.4.1. The overall composition was made generally similar to geological samples; these concentrations are given in Table 4.1 (column 6).

The two solutions were nebulised alternately 75 times each, under the operating conditions given in Table 3.1, over a period of 4.4 hours, after allowing the system to warm up for one hour.

The raw instrument response (in mV) for all the analyte intensities was measured simultaneously with a single 5-s integration and was stored on the dedicated computer. The data set was subsequently transferred to the mainframe computer for statistical analysis.

In this experiment therefore all the variability between the results for the same solution would be due entirely to instrument-based variation.

	Parameter description	Number of settings	Range of settings	Unit	Notes
1	Sample uptake rate	8	0.525–1.369	$\mu g\ ml^{-1}$	Unpumped uptake, varied by length of uptake tubing, 10–80 cm. Measured gravimetrically
2	Forward power	5	1.2–1.3	kW	Reflected power always <5 W
3	Injector gas flow	6	0.94–1.03	$l\ min^{-1}$	Measured at tip of the nebuliser
4	Primary spectrometer slit position	5	−0.007–+0.007*	nm	*First order ± 0.0035 nm in 2nd order ± 0.0023 nm in 3rd order
5	Fume extraction speed	4	0.2–0.5	$m\ s^{-1}$	Measured 40 mm above load coil with no torch gases flowing
6	Primary lens opacity	2	0–35	h	Time after lens cleaning. Opacity by particles from the ICP while running samples
7	Air temperature around spray chamber	4	20–45	°C	Caused by heated air flow.
8	Sample solution temperature	6	5–24	°C	External heating of solution, ambient = 20 ± 1 °C
9	High salt solution nebulisation (to simulate nebuliser - torch salt-up)	5	7–18	min	Nebulisation of 1 and 5% *m/V* Na as NaCl in 1 M HCl
10	ICP warm-up	75	0–264	min	Taken from regression of quasi-routine analysis data

Table 4.2
Instrumental parameters variation scheme.

4.6 Experimental Design to Establish Possible Causes of Imprecision

The second half of the investigation was designed to identify the causes of variations in the 'Quasi-Routine Analysis' data. The results of variation in a number of possible instrumental and environmental factors were examined. The parameters considered were selected on two criteria: (i) those most likely to vary during routine analysis; and (ii) those known, from practical experience, to result in a sensitive change in instrument response. On this basis ten possible causes of variation were examined. Each such parameter was experimentally varied around normal values as described in Table 4.2, while all other parameters were kept constant. The ranges of variation were chosen to be somewhat larger than any expected instrumental or environmental fluctuations so as to give a more precise estimate of coefficients. For the first six parameters listed in Table 4.2 blank integrations were taken at parameter settings identical to those used for the multielement standard solution. For the last four parameters listed, blank integrations under coincident conditions were unobtainable. This necessitated taking readings under conditions as close as was practicable, and using interpolation to calculate comparable blanks where required.

The tenth parameter, 'instrument warm-up', was measured over two time periods. The first period was used 30 minutes from ignition of the ICP, but upon inspecting the data, linear trends convenient for regression were absent. The period used to characterise 'warm-up' was therefore the whole 4.4 hour period used for the 'Quasi-Routine Analysis', during which twice the drift was quite linear. Least-squares linear regression was applied to this

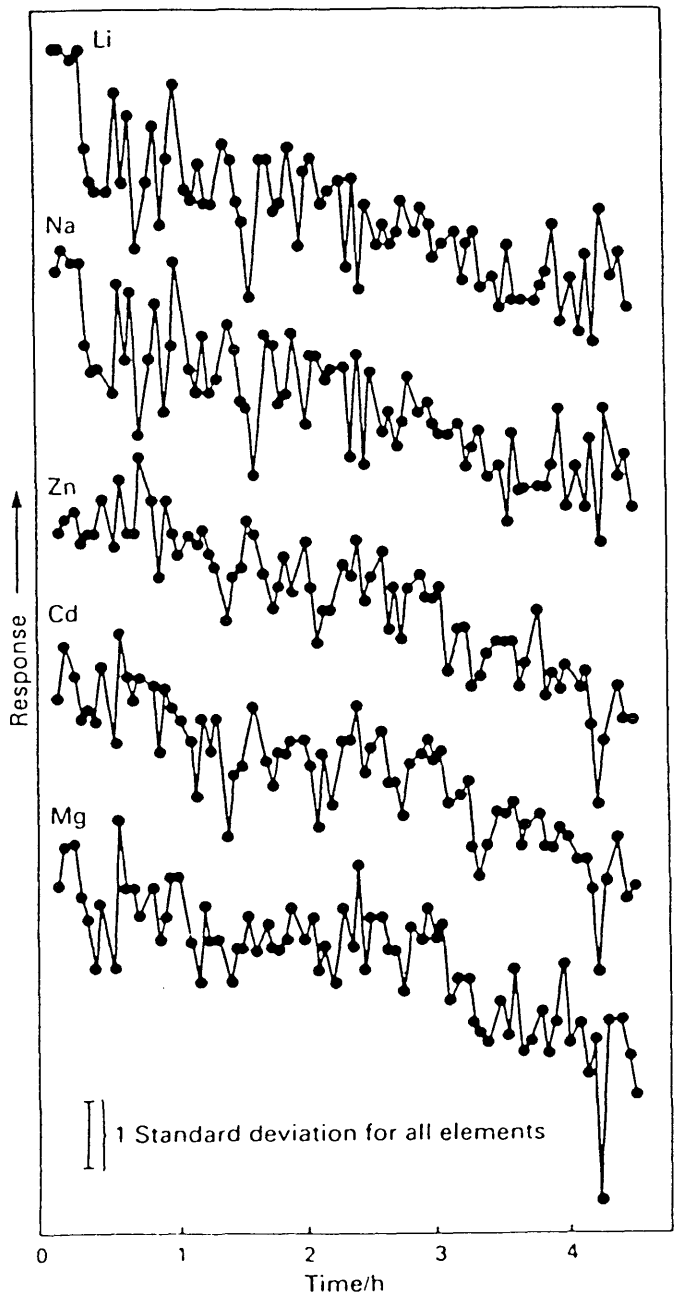


Fig. 4.1
Fluctuations in the response of five elements showing multielement correlation. All responses are scaled to their respective standard deviations.

data and the slope coefficients used to characterise instrument 'warm-up'.

4.7 Results and Discussion

4.7.1 Quasi-Routine Analysis

Initial study of the raw multivolt response given in Appendix A confirmed the difficulty of assessing the similarity between analyte responses by visual inspection. However, some means of intuitive understanding of the data is a necessary prerequisite to the use of multivariate statistical analysis. It enables the selection of appropriate statistical tests and a realistic interpretation of their output. This general observation is exemplified in the treatment of this data set.

Graphical representation of the analyte responses gives some insight into the inter-element relationships present within the data. Figure 4.1 shows the changes of response in the time domain of five elements selected from the 24 measured. Each dot represents one five-second integration. The lithium response shows the medium term fluctuation between integrations (i.e. nebulisations), with an overall downward drift. The sodium response shows a medium-term fluctuation pattern and drift very similar to those of lithium. This similarity suggests a common cause for both variations. The variation in the zinc response, however exhibits no obvious similarity with that of lithium, but many coincidences with that of cadmium. The magnesium pattern displays features in common with those of both lithium and zinc, but has a generally smaller amplitude. From visual inspection therefore, much of the variation in Figure 4.1 appears to be correlated between some of the elements. How many separate causes

	Ag	Al	Ba	Be	Ca	Cd	Co	Cr
Al	0.758							
Ba	0.883	0.941						
Be	0.935	0.740	0.903					
Ca	0.108	0.279	0.244	0.227				
Cd	0.513	0.418	0.504	0.642	0.762			
Co	0.468	0.516	0.550	0.588	0.873	0.904		
Cr	0.711	0.554	0.668	0.811	0.603	0.910	0.833	
Cu	0.828	0.937	0.928	0.790	−0.019	0.285	0.312	0.487
Fe	0.586	0.696	0.717	0.694	0.832	0.877	0.945	0.852
K	0.538	0.800	0.665	0.438	−0.215	−0.030	0.024	0.156
La	0.789	0.891	0.885	0.810	0.410	0.682	0.690	0.776
Li	0.596	0.783	0.694	0.496	−0.324	−0.081	−0.044	0.134
Mg	0.758	0.857	0.866	0.815	0.642	0.802	0.854	0.853
Mn	0.508	0.594	0.632	0.628	0.881	0.845	0.931	0.811
Mo	0.741	0.336	0.554	0.810	0.377	0.751	0.644	0.859
Na	0.545	0.832	0.691	0.451	−0.182	−0.008	0.056	0.169
Ni	0.555	0.399	0.525	0.671	0.737	0.868	0.843	0.857
P	0.116	0.366	0.330	0.204	0.604	0.405	0.523	0.317
Pb	0.238	0.201	0.260	0.354	0.733	0.733	0.752	0.660
Sr	0.731	0.946	0.898	0.743	0.373	0.558	0.615	0.649
Ti	0.754	0.678	0.769	0.794	0.309	0.575	0.580	0.686
V	0.875	0.826	0.905	0.935	0.431	0.768	0.745	0.887
Zn	0.302	0.230	0.306	0.439	0.821	0.825	0.849	0.738

	Cu	Fe	K	La	Li	Mg	Mn	Mo
Fe	0.497							
K	0.862	0.205						
La	0.848	0.806	0.599					
Li	0.890	0.144	0.981	0.577				
Mg	0.727	0.948	0.461	0.927	0.420			
Mn	0.368	0.969	0.070	0.676	0.009	0.875		
Mo	0.358	0.635	−0.009	0.552	0.033	0.640	0.630	
Na	0.884	0.240	0.991	0.644	0.977	0.494	0.101	−0.014
Ni	0.270	0.844	−0.070	0.580	−0.094	0.762	0.853	0.801
P	0.161	0.557	0.064	0.304	0.004	0.466	0.589	0.165
Pb	0.033	0.690	−0.245	0.399	−0.294	0.553	0.730	0.546
Sr	0.880	0.768	0.689	0.958	0.660	0.898	0.635	0.399
Ti	0.669	0.664	0.389	0.732	0.413	0.748	0.601	0.638
V	0.802	0.842	0.481	0.943	0.485	0.939	0.755	0.755
Zn	0.048	0.789	−0.249	0.453	−0.299	0.647	0.809	0.622

	Na	Ni	P	Pb	Sr	Ti	V
Ni	−0.059						
P	0.072	0.447					
Pb	−0.215	0.667	0.412				
Sr	0.731	0.477	0.357	0.316			
Ti	0.410	0.587	0.246	0.360	0.692		
V	0.512	0.720	0.307	0.489	0.877	0.798	
Zn	−0.222	0.805	0.419	0.726	0.365	0.418	0.552

Table 4.3
Correlation matrix for the quasi-routine analysis data after drift correction, showing the generally high level of correlation and particularly strong correlation between certain sets of elements. For example, zinc and cadmium are highly correlated with each other but not with lithium or sodium.

are effective is not evident, but it is abundantly clear that no single factor could cause the behaviour of all these elements. An interesting consequence of this is that no simple internal standard element could mimic this wide range of behaviour.

To facilitate the separation of changes in the sensitivity from those in the background response, the nett sensitivity was calculated by subtraction of the blank intensity. The correlation structure of the background intensity will be discussed in section 4.8. Every reading of the multielement standard solution was corrected individually by subtracting the response for the blank solution nebulised immediately afterwards. In order to separate the correlations in medium term fluctuation of the nett sensitivity from that of the drift (which correlates predominantly with time) the data was drift corrected. This was achieved by least squares linear regression against time, and the rotation of the fitted line parallel to the time axis. The rigorous statistical method used to assess the level of correlation between all pairs of element was the calculation of a correlation matrix. A prerequisite of this calculation is that the variate should be normally distributed, and this was established for all analytes before proceeding. The test used was the linearity of the 'NSCORES' plot calculated within MINITAB. Table 4.3 shows the correlation matrix of the drift corrected data. The time-correlated variance (i.e. the drift) is considered separately, as a parameter in the second part of the experimentation.

The general level of correlation is high, with 107 values greater than 0.7. The similarities of the lithium and sodium responses are confirmed by a large correlation coefficient (.977) as are those for zinc and cadmium (.825). By comparison lithium

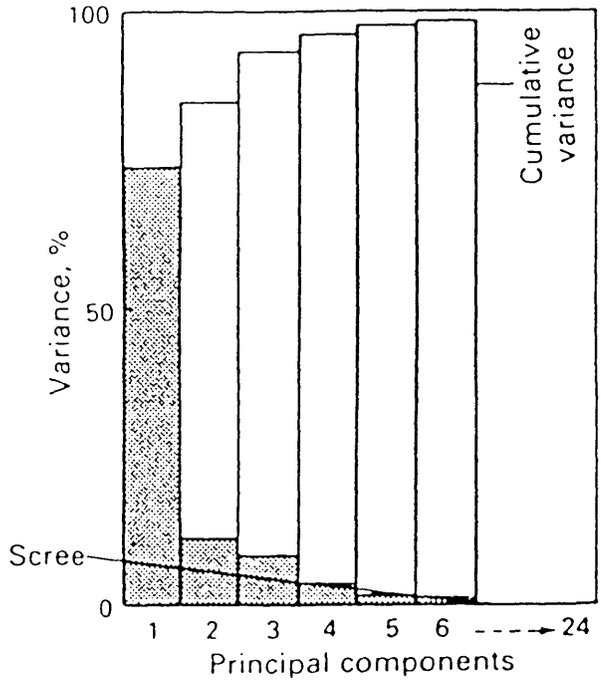


Fig. 4.2
Percentage of the total variance accounted for by the first six principal components in the PCA of the quasi-routine analysis data. The values above the scree line are considered significant and account for 93.4% of the total variance.

and zinc are hardly correlated (-0.299) for 75 readings. (75 degrees of freedom requires a value of r = 0.293 at the 1% level and 0.370 at the 0.1% level). Magnesium is therefore correlated to a highly significant degree with all 23 other elements measured. Phosphorous does not correlate strongly with any other element.

Principle Components Analysis (PCA) was the statistical technique selected for more systematic investigation of the correlation matrix. PCA has become widely used in the applied sciences, and its application to geochemical data interpretation has been explained by Howarth (1983). The work described here is the first known example of the application of PCA to ICPAES analytical variance. The MINITAB MACRO for PCA is given in Appendix B.

PCA was applied to the correlation matrix in order to quantify the amount of variance in the data set that was explained by multielement correlation, and also in an attempt to understand the underlying structure of the correlation matrix. In informal terms, PCA identifies a vector, or 'pseudo element', which has the highest correlation coefficient with all elements and hence accounts for the greatest proportion of the total variance. This vector is called the first principal component (PC1). A second component (PC2) is constructed from the residual variance orthogonal (i.e. uncorrelated) to PC1, and is calculated so as to account for the maximum proportion of the remaining variance. Further principal components, up to the original number of variables (i.e. 24), are calculated in a similar way.

Figure 4.2 illustrates the proportion of variance acounted for in the first six principal components from the analysis of the nett response of the 'Quasi-Routine Analysis' data. This figure

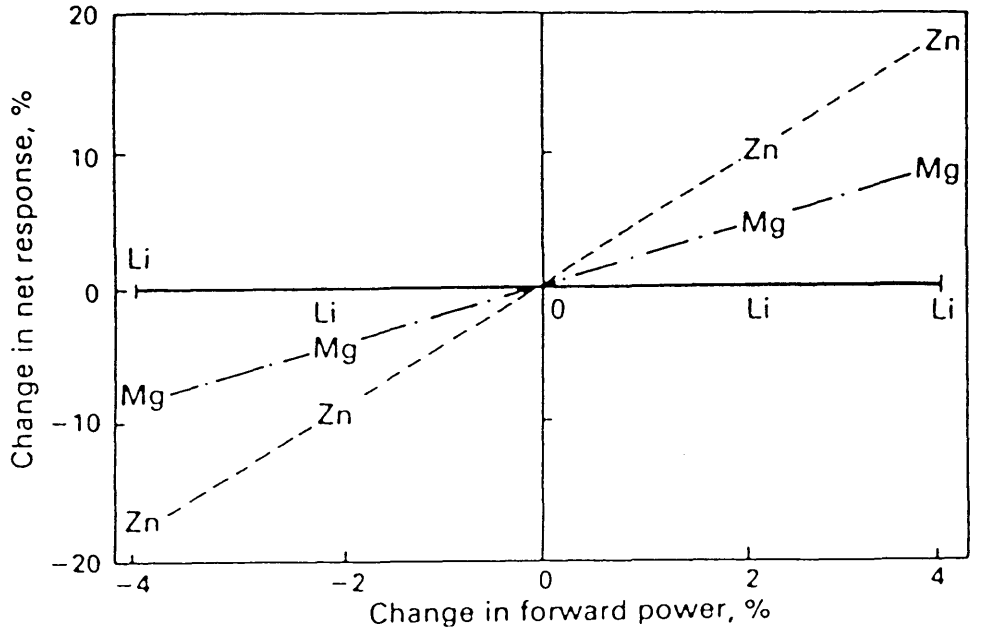


Fig. 4.3
Different effects on the responses of three elements on changing the forward power. Lithium shows no significant change. For regression statistics on all elements see Table 4.5.

	Principal component loadings		
	PCL1	PCL2	PCL3
Ag	−0.821	−0.321	0.389
Al	−0.841	−0.469	−0.238
Ba	−0.893	−0.377	0.027
Be	−0.885	−0.176	0.373
Ca	−0.580	0.675	−0.406
Cd	−0.813	0.478	0.074
Co	−0.835	0.466	−0.152
Cr	−0.893	0.265	0.233
Cu	−0.749	−0.654	0.014
Fe	−0.927	0.291	−0.196
K	−0.444	−0.838	−0.206
La	−0.929	−0.228	−0.051
Li	−0.424	−0.888	−0.077
Mg	−0.986	0.007	−0.123
Mn	−0.856	0.413	−0.199
Mo	−0.728	0.280	0.564
Na	−0.473	−0.830	−0.231
Ni	−0.787	0.485	0.140
P	−0.444	0.273	−0.594
Pb	−0.565	0.619	−0.059
Sr	−0.882	−0.333	−0.207
Ti	−0.945	−0.137	0.204
V	−0.974	−0.104	0.148
Zn	−0.641	0.659	−0.019

Table 4.4
Principal component loadings for the principal components analysis of the quasi-routine analysis data after drift correction. The high values indicate strong correlation between the element and the component.

shows that more than 90% of the total variance is accounted for in the first three principal components. There are no totally objective methods for assessing which components are statistically significant and thus which can be classified as uncorrelated noise (Howarth 1983) but Cattell's Scree test (Cattell 1966) for this data set (shown in Figure 4.2) results in a proportion of less than 10% falling into the latter category.

The loadings of the first three principal components are given in Table 4.4. The numerical values are the correlation coefficients between each element and the stated component. The elements with high loadings in PC1 (e.g. magnesium) would therefore be the best elements to choose as simple internal standard elements, for this particular data set under these analytical conditions. It was expected that the principle component loadings would correspond to some of the possible causes investigated in the second half of the experiment. This was not the case and this failure highlights an inability of PCA to clarify causal relationships under certain circumstances, as will be examined below.

4.7.2 Calculation of Multielement Parameter Signatures (MPS)

In order to facilitate the identification of the causes of the correlated variation under the conditions of routine analysis, and to measure their relative importance, each of the ten instrumental parameters (Table 4.2) was characterised by the relative changes in response of all 24 element channels to changes in that parameter. To illustrate the procedure, the effect of changes in forward power on the nett response for three elements is shown in Figure 4.3. The range of differing susceptibility to

	Sample uptake rate coefficient		Forward power coefficient		Injector gas flow coefficient		Warm-up	
	%/%	*t*-ratio	%/%	*t*-ratio	%/%	*t*-ratio	% in 4.4 h	*t*-ratio
Ag	0.175	9.5	0.795	6.1	−0.605	−2.1*	−1.54	−5.6
Al	0.205	10.6	0.597	6.5	−0.263	−1.1*	−2.32	−7.5
Ba	0.186	8.8	0.266	2.8*	−0.219	−0.9*	1.51	4.7
Be	0.121	6.6	2.780	11.5	−1.483	−5.1	−5.62	−20.7
Ca	−0.003	−0.2*	3.211	19.7	−3.480	−7.7	0.73	2.2*
Cd	0.027	2.0*	3.362	17.4	−3.378	−8.7	−3.29	−13.2
Co	0.048	3.3*	2.806	16.1	−2.788	−8.6	−2.76	−11.6
Cr	0.055	3.4*	2.619	15.7	−2.552	−8.2	−2.04	−9.1
Cu	0.258	12.5	0.148	1.3*	0.311	0.9*	−4.26	−11.4
Fe	0.068	4.3	2.238	15.2	−2.25	−7.7	−1.34	−5.8
K	0.489	22.8	−0.336	−1.3*	1.211	3.9*	−6.41	−10.7
La	0.113	5.5	0.919	14.3	−1.086	−4.4*	−2.20	−8.9
Li	0.557	23.2	−0.718	2.6*	2.290	4.2*	−7.50	−10.9
Mg	0.113	7.0	2.143	20.6	−2.128	−8.0	−2.39	−10.6
Mn	0.058	3.7*	2.269	13.8	−2.335	−7.9	−1.77	−7.4
Mo	0.070	4.2	2.270	12.2	−2.376	−8.2	−2.03	−7.9
Na	0.429	20.0	−0.347	−1.5*	1.241	6.2	−6.47	−11.8
Ni	0.058	4.4	2.859	15.3	−2.862	−8.9	−2.41	−10.3
P	0.115	5.0	2.835	7.6	−2.075	−6.9	−3.50	−4.6
Pb	0.032	2.1*	2.812	16.6	−3.500	−8.0	−1.53	−4.4
Sr	0.147	7.2	0.476	5.9	−0.688	−2.8*	−2.08	−6.9
Ti	0.121	6.1	1.402	11.4	−1.332	−5.1	−2.44	−6.3
V	0.108	5.9	1.707	12.0	−1.596	−6.0	−2.75	−12.1
Zn	−0.016	−1.3*	4.442	20.9	−4.052	−8.3	−4.68	−3.8

	Primary slit setting		Lens opacity, % for ~35 h	High salt neb., % for ~18 min	Air temperature, % for ~+ 25 °C	Solution temperature, % for ~10 °C
	−0.0035 nm, %	+0.0035 nm,† %				
Ag	−1.22	−3.28	−4.00	2.15	−16.59	1.52
Al	−5.48	1.56	−4.50	3.01	−0.44	4.32
Ba	−2.80	−2.78	−2.13	3.10	14.58	5.38
Be	−0.83	−4.46	−4.43	2.37	−11.56	2.10
Ca	−5.16	2.03	−4.14	1.67	−19.7	1.10
Cd	−4.28	−0.63	−13.39	1.47	−19.65	0.97
Co	−3.15	0.33	−12.57	1.55	−17.53	1.05
Cr	−2.92	−0.08	−7.53	1.69	−15.85	1.11
Cu	−5.54	0.78	−3.84	3.15	9.57	5.50
Fe	−3.18	0.51	−8.93	1.91	−9.02	2.34
K	−12.96	3.51	−0.37	3.14	4.79	8.00
La	−6.92	3.08	−1.28	2.22	6.30	3.27
Li	−8.06	1.66	−0.14	4.27	6.50	9.37
Mg	−5.19	0.33	−6.63	2.32	−16.99	2.10
Mn	−1.82	−1.29	−9.63	1.90	−12.14	1.93
Mo	5.48	−6.37	−7.03	1.67	−21.93	−0.21
Na	−13.08	4.56	0.21	—	8.44	8.23
Ni	0.39	−3.32	−13.33	1.68	−18.62	0.78
P	−4.14	2.27	−11.91	1.83	−10.46	5.99
Pb	−1.69	−1.55	−15.42	1.14	−25.28	−0.90
Sr	−8.76	4.87	−2.17	2.88	−17.35	5.91
Ti	−1.05	−1.76	−3.87	2.72	−0.02	3.60
V	−3.46	−0.25	−4.79	2.36	−4.32	3.10
Zn	−3.03	−1.05	−20.86	1.17	−31.26	−1.02

* Values not significant at the 1% level.
† In first order.

Table 4.5
Linear coefficients describing the susceptabilities of 24 elements to nine parameters. All values are % changes in the element response for the various units stated at the top of each column. For example %/% signifies that a 1% increase in forward power will result in a 4.442% increase in the zinc response. t-ratios are given for the parameter coefficients estimated by regression.

forward power variation is evident and forms the basis for the Multielement Parameter Signature (MPS). Each of the elements gave a linear relationship over the measurement range but with a different slope. Least-squares linear regression of the element responses onto the forward power gave the set of slope coefficients shown in Table 4.5. Changes in both measurements were expressed in relative terms before regression. The t-ratios of the regressions are given as a measure of significance. For three degrees of freedom t-values less than 5.8 are not significantly different from zero, at the 1% probability level. Thus the sensitivities of Li,K,Na,Cu and Ba are not significantly affected by forward power over this range of measurement and under the other specified instrumental conditions.

In order to facilitate comparison between the different parameters, the set of coefficients was normalised by dividing by the largest value, that of zinc. The resulting set of values form the Multielement Parameter Signature (MPS) which is quantified in Table 4.6 and illustrated in Figure 4.4, where the elements are arranged in the same descending order of susceptibility to forward power in all cases.

This method of measuring the MPS was used for sample uptake rate and injector gas flow. For all the other instrumental parameters, regression was impractical because of one of the following reasons:- too few measurement points (for lens opacity) imprecision in parameter setting (air and solution temperature, salting), insignificant response variation (fume extract speed) non-linear response (primary slit position). In these cases the MPS was calculated from the ratio of the responses at a disturbed parameter setting to that at the standard operating conditions.

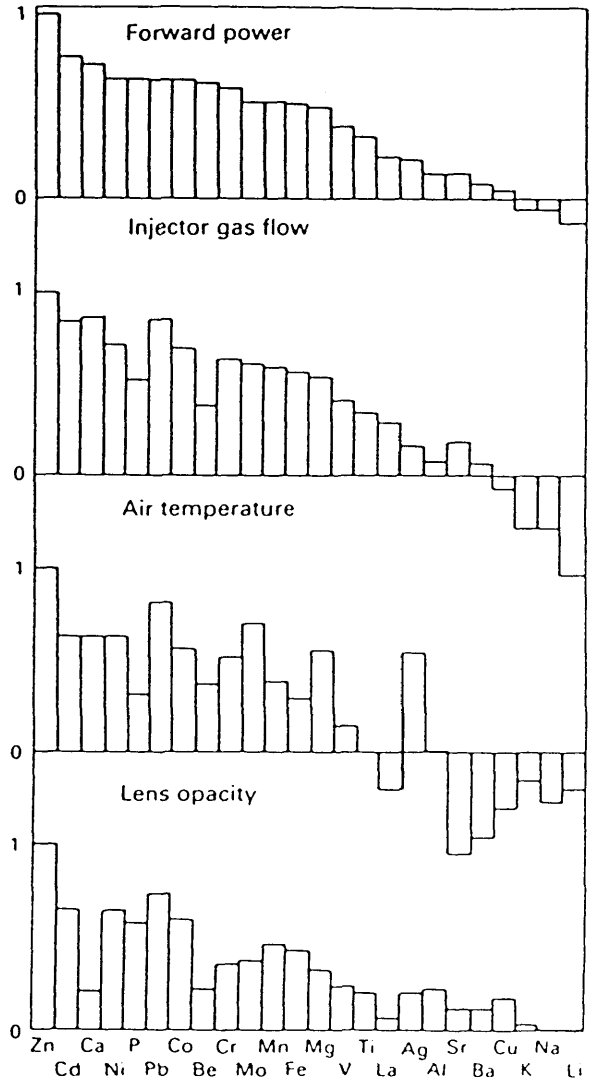


Fig. 4.4
Multielement parameter signatures (MPS) for four instrumental and environmental parameters that correlate strongly with the forward power MPS. The data used are given in Table 4.6 and are arranged in order of descending susceptibility to forward power for all four parameters.

	Forward power	Injector gas flow	Air temperature	Lens opacity
Ag	0.179	0.149	0.531	0.192
Al	0.135	0.065	0.014	0.216
Ba	0.060	0.054	−0.466	0.102
Be	0.626	0.366	0.370	0.212
Ca	0.723	0.859	0.630	0.198
Cd	0.757	0.834	0.629	0.642
Co	0.632	0.688	0.561	0.603
Cr	0.590	0.630	0.507	0.361
Cu	0.033	−0.077	−0.306	0.184
Fe	0.504	0.555	0.288	0.428
K	−0.076	−0.299	−0.153	0.018
La	0.207	0.268	−0.202	0.061
Li	−0.162	−0.565	−0.208	0.007
Mg	0.482	0.525	0.544	0.318
Mn	0.511	0.576	0.388	0.462
Mo	0.511	0.586	0.701	0.337
Na	−0.078	−0.306	−0.270	−0.010
Ni	0.644	0.706	0.596	0.639
P	0.638	0.512	0.335	0.571
Pb	0.633	0.864	0.809	0.739
Sr	0.107	0.170	−0.555	0.104
Ti	0.316	0.329	0.001	0.186
V	0.384	0.394	0.138	0.230
Zn	1.000	1.000	1.000	1.000

Table 4.6
Four multielement parameter signatures, normalised to zinc as the highest value. These data are shown in Fig. 4.4 where the overall similarities to forward power MPS can be discerned.

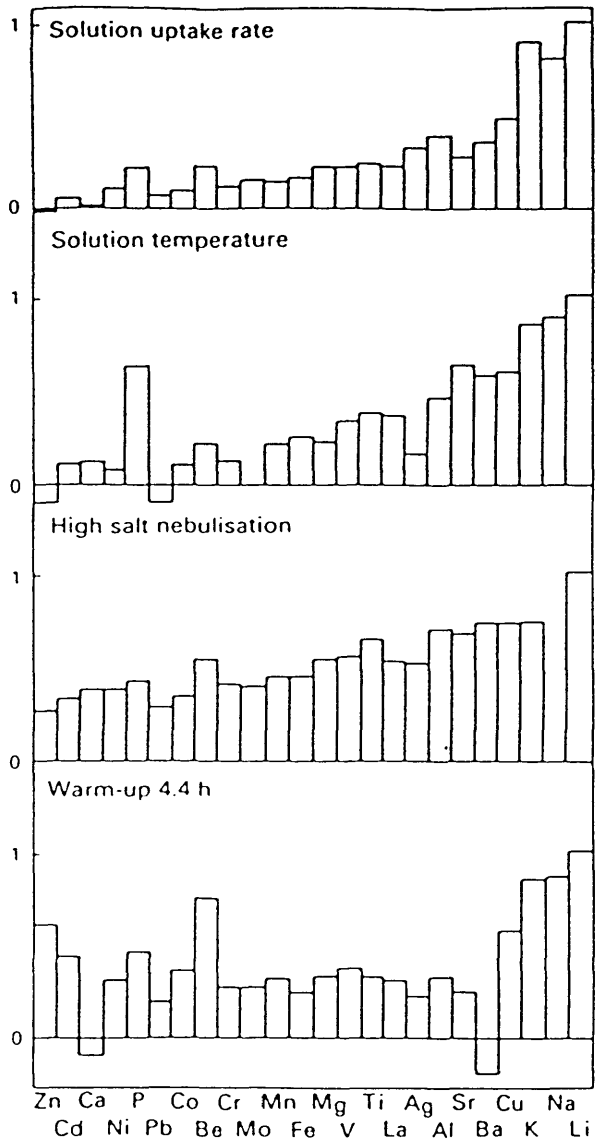


Fig. 4.5
Multielement parameter signatures (MPS) for four instrumental and environmental parameters that correlate strongly with the sample uptake rate MPS. The data used are given in Table 4.7 and are arranged as in Fig. 4.4, that is, in order of descending susceptibility to forward power for all four parameters.

	Sample uptake	Solution temperature	High salt nebulisation	Warm-up 4.4 h
Ag ..	0.315	0.162	0.504	0.206
Al ..	0.367	0.461	0.705	0.309
Ba ..	0.334	0.574	0.726	−0.201
Be ..	0.217	0.224	0.555	0.749
Ca ..	−0.006	0.117	0.391	−0.098
Cd ..	0.049	0.104	0.344	0.439
Co ..	0.087	0.112	0.363	0.368
Cr ..	0.099	0.118	0.396	0.271
Cu ..	0.463	0.587	0.738	0.568
Fe ..	0.121	0.250	0.447	0.178
K ..	0.878	0.854	0.735	0.855
La ..	0.203	0.349	0.520	0.293
Li ..	1.000	1.000	1.000	1.000
Mg ..	0.202	0.224	0.543	0.319
Mn ..	0.104	0.206	0.445	0.235
Mo ..	0.126	−0.022	0.391	0.271
Na ..	0.771	0.878	—	0.863
Ni ..	0.103	0.083	0.393	0.321
P ..	0.206	0.639	0.429	0.466
Pb ..	0.057	−0.096	0.267	0.203
Sr ..	0.263	0.631	0.674	0.278
Ti ..	0.218	0.384	0.637	0.326
V ..	0.194	0.331	0.553	0.366
Zn ..	−0.030	−0.108	0.274	0.624

Table 4.7
Four multielement parameter signatures, normalised to lithium as the highest value. These data are shown in Fig. 4.5 where the overall similarities to the sample uptake rate MPS can be discerned.

	Injector gas flow	Air temperature	Lens opacity
Forward power	−0.957	−0.867	−0.846
	Solution temperature	High salt nebulisation	Warm-up 4.4 h
Sample uptake	0.882	0.651	0.638

Table 4.8
Correlation coefficients between the independently determined MPSs given in Tables 4.6 and 4.7. These values are all highly significant (i.e., >0.61 using P = 0.001).

Ratios were averaged over a number of settings in order to reduce uncertainty.

Figure 4.4 shows a visual comparison of four MPSs. There is a strong similarity between the MPSs for forward power and for injector gas flow. This similarity is even more striking in terms of the raw values in Table 4.5 where the absolute values of the coefficients are also alike. Also, although these instrumental parameters are apparently totally separate, their effects correlate at 0.957. This general pattern appears again in the air temperature MPS although with a greater scatter evident, and also in the lens opacity MPS. All of these four MPSs have been normalised to the zinc coefficient as the highest value.

The MPS bar chart in Figure 4.5, although plotted with exactly the same element order, shows a very different trend. Here the lithium response shows the greatest susceptibility to changes in sample uptake rate, whereas that for zinc gives a non-significant value. Initially it seems counter-intuitive that five elements are not significantly affected by a 2.6 fold increase in uptake rate. The overall pattern of the sample uptake rate MPS is broadly repeated in the MPSs for solution temperature and the effect of high salt. The data plotted in Figure 4.5 is given in Table 4.7. The correlation data given in Table 4.8 substantiates the presence of only two dominant patterns within the effects of these seven parameters.

The MPS of the drift measured over 4.4 hours appears more complex, with high values at both the zinc and lithium ends. This MPS however correlates at 0.85 with an additive mixture of sample uptake rate (decreased by 14.9%) and forward power (decreased by 1.1%). This suggests that multielement drift is not random but

controlled by causes bearing these signatures. Expressed mathematically; if the set of absolute coefficients for each parameter are considered as vectors, '$\underline{U}$' for sample uptake rate and '$\underline{P}$' for foward power. Then the drift '$\underline{D}$' corresponds approximately to the relationship

$$\underline{D} = \underline{U} * 14.9 + \underline{P} * 1.1$$

It must be stressed however that the existence of this relationship does not imply a causal nexus. Any of the parameters bearing the two MPSs quoted, acting alone or in combination, could produce this same drift.

Figure 4.5 shows however that the responses for two elements (calcium and barium) in this particular run did not drift according to this general rule. In a re-run of the Quasi-Routine Analysis experiment barium and calcium did not display this anomalous drift and correlated highly with elements of similar parameter coefficients (e.g. Al, Ti, Sr). The subsequent application of PRISM (Chapter 5) includes these anomalous drifts, even though exclusion would have improved the proportion of variance accounted for.

Two instrumental parameters did not correlate with either the forward power or sample uptake rate MPS. The first was speed of fume extraction, for which no significant effect was detected in the response for any element other than phosphorus (which was enhanced by increased speed). The second was primary slit position, the values for which are given in Table 4.5, but which was considered an unlikely candidate for causing medium term fluctuation.

In order to assess the relative importance of the two MPSs characterised above, within the Quasi-Routine Analysis, PCA alone was clearly inadequate. For example, the first principal component loading (PC1) in Table 4.4, is clearly closely correlated with the elements Mg, V and Ti, which are not extreme in any of the measured multielement parameter signatures (MPS) in Figures 4.4 and 4.5 as would be expected. These elements are distinctive in being at a central position for all MPSs having intermediate values (0.2-0.5). This means that these elements are affected to some extent by variation in all the eight parameters, unlike the 'extreme' elements which are dominantly affected by only one set of four parameters. It was hypothesized, therefore, that PCA had correctly assigned the dominant principal component as being the variation closely correlated with magnesium, even though this was due to two different causes. The fact that the MPS of the two separate causes are negatively correlated contravenes the requirement of PCA that causes should be uncorrelated. This would therefore place constraints on any interpretation of PCA in this case.

The second principal component (PC2) correlates with all of the MPSs being extreme in Li (-.888) and Zn (+.659) but this also was thought to be an artifact of this invalidity.

To test this hypothesis a computer simulation was made of ICP variation, using only the two MPSs from forward power and sample uptake as a model of the dependence, and a random noise generator to simulate the parameter variation. The instrumental parameters were simulated using two independent normal distributions with means and standard deviations selected so as to provide element response distributions similar to those measured in the

Quasi-Routine Analysis. When subjected to PCA the simulated data produced a set of principle component loadings very similar to those of the real data, with magnesium strongly correlated with PC1.

This result strongly supports the hypothesis of the two dominant 'causes' of variation. The recognition that the multielement drift corresponds to the mixture of the two 'causes' also supports the hypothesis.

The final test of the hypothesis was to devise a procedure for correcting the Quasi-Routine Analysis data for all variation, which was based on the MPSs of forward power and sample uptake rate. The percentage of variance removed by the correction would thereby quantify the contribution of any sources of variation conforming to either of these MPSs. The procedure was the parameter related internal standard method (PRISM) described in Chapter 5.

4.7.3 The Significance of the Multielement Parameter Signatures

The persistence of the same sequence of elements in the susceptibilities of seven out of ten parameters investigated, suggests that the pattern reflects a fundamental characteristic of the analyte elements. Knowledge of this characteristic might enable a more general theory to be formulated, which might enable the prediction on the elements susceptibilites under different operational conditions, on various instruments and for any analyte line. The entirely theoretical calculation of the MPS value could be possible if the cause for the variation between analytes is understood.

The work of Blades and Horlick (1981a) suggested that excitation potential (E) is a critical factor in determining the height in the ICP at which the response from atom lines peak, in the region 8-16mm above the load coil (the 'thermal' region). For ion lines the sum of the excitation potential and the first ionization potential ($E + V_1$) is used to calculate the energy required for these emissions. In both cases these are the total excitation potentials (E').

The two fundamental characteristics of the analyte elements investigated for their correlation with MPS values; were therefore the first ionization potential (V_1) of the analyte element and excitation potential (E) of the analyte wavelength used. An extended range of 36 analyte lines given in Table 4.1 was investigated, under the previously described operating conditions. Their MPS's for forward power and sample uptake were determined by a simplified two-parameter setting procedure described in Chapter 5.

The experimental MPS values were therefore divided into those for atom lines and those for ion lines and these values correlated against V_1, E and $E+V_1$ to compare these factors. The results are shown in Table 4.9 and it is clear that the highest correlations come between atom line MPS and their excitation potential, and ion line MPSs and their combined excitation and ionization potentials, confirming Blades and Horlick's findings.

The close relationship of atom line MPSs with their ionization potential is due to an unexpectedly high correlation between the ionization and excitation potentials of the atom lines (0.962). This is obviously a function of the analyte lines chosen, which are usually the most intense emissions from the plasma.

	First Ionization Potential(V_1)	Excitation Potential E	First Ionization + Excitation Potential V_1+E
Atom lines			
Forward Power MPS	.914	.937	.934
Atom lines			
Sample Uptake MPS	-.813	-.886	-.855
Ion lines			
Forward Power MPS	.756	.683	.859
Ion lines			
Sample Uptake MPS	-.533	-.642	-.720

Table 4.9
Correlation coefficients between MPS values and properties of the analyte element and emission line.

Figure 4.6 shows a graph relating the coefficients of the nett response to forward power, against the total excitation potential of the analyte lines. Clearly the atom and ion lines show well-defined separate trends. Both relationships are close to linear and have similar slopes. The regression coefficients and standard deviations for the atom lines are; slope (standard error) 0.549 (0.053), intercept (standard error) -1.31 (0.26); and for ion lines are slope (standard error) 0.501 (0.072); intercept (standard error) -3.85 (0.50).

The separation of the two nearly parallel lines is ~ 5ev of total excitation potential and is clearly due in part to the addition of ionisation potential for the ion lines. However, if relationship to excitation potential alone is plotted for both atom and ion lines, two trends are still apparent although the separation is reduced and the correlation reduced to 0.776.

When considering which analyte lines are most susceptible to variation in forward power therefore, this relationship enables the prediction of ion lines with high total excitation potential.

Figure 4.7 shows the corresponding data for the changes in sample uptake rate. Although the scatter of data is greater here, there are again two distinct linear trends for the atom and ion lines, but in the opposite sense to those for the forward power susceptibility. The total excitation potential value for Mg would seem in some doubt placing Mg clearly away from the general trends in both Figures 4.6 and 4.7. The regression coefficients for the atom lines are slope (standard error) -0.0509 (0.0069); intercept (standard error) 0.518 (0.034) and for the ion lines slope (standard error) -0.0206 (0.0048); intercept (standard error) 0.459 (0.021). For sample uptake therefore the coefficients are generally smaller than those for forward power, an observation

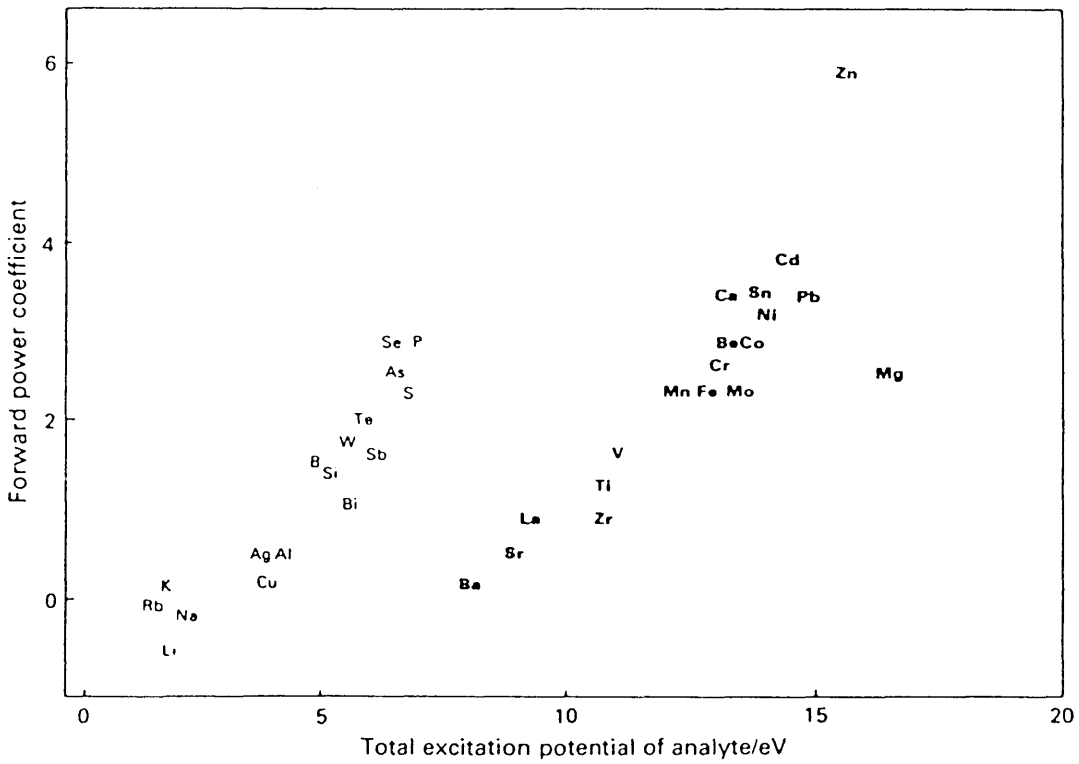


Fig. 4.6
Susceptibility to forward power of 36 elements compared with their excitation potential (E) for atom lines and excitation plus ionisation potential ($E+V_1$) for ion lines (bold type).

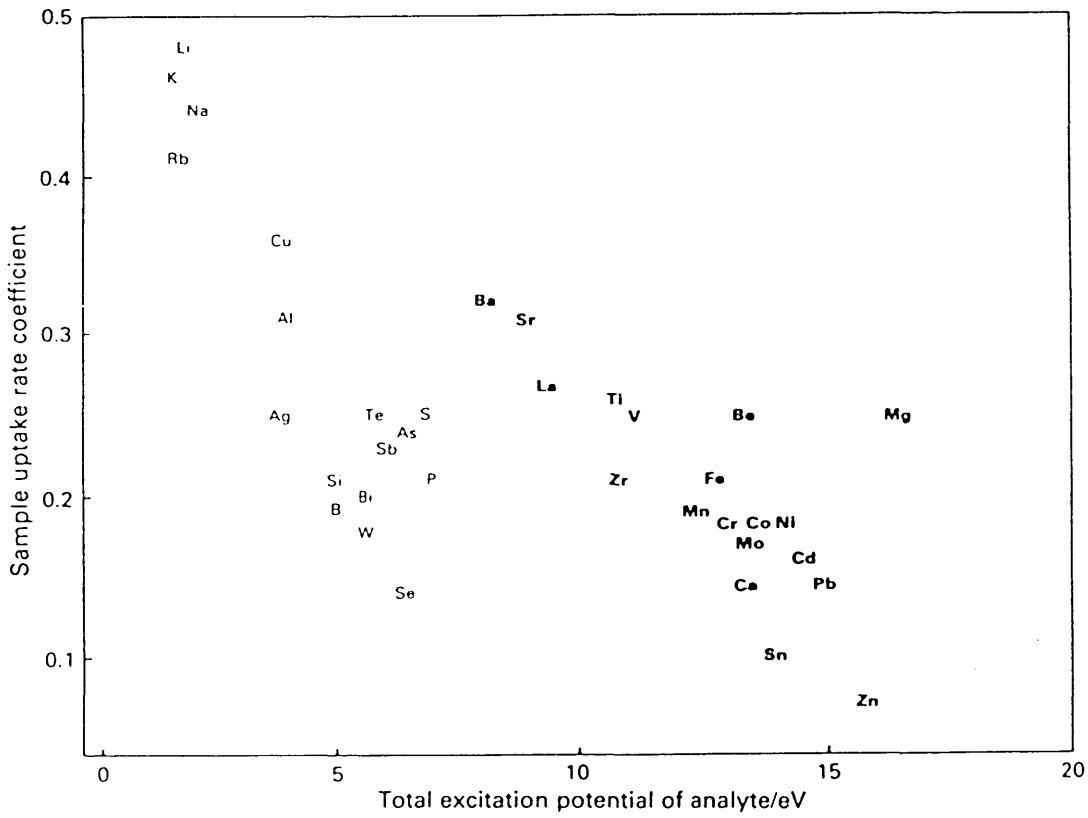


Fig. 4.7
Susceptibility to sample uptake rate of 36 elements compared with their excitation potential (E) for atom lines and excitation plus ionisation potential ($E+V_1$) for ion lines (bold type).

which is not apparent in consideration of the normalized MPS values. Also in this case the intercepts rather than the slopes, are similar for atom and ion lines, and the slopes are different by a factor of 2.5. If excitation potential alone is correlated with the MPS than the value -0.775 is not dissimilar from the separate total excitation potential values in Table 4.9. This indicates a less clear-cut case for the use of total excitation potential than for forward power. High susceptibility to variations in sample uptake is however clearly evident from Figure 4.7 as being greatest in atom lines of low excitation potential.

The relative susceptibilities to forward power described here are consistent with Blades and Horlick's studies of vertical distribution of analyte emission (1981a). At the 14mm observation height used in the study the low EP atom lines are near their peak intensity and relatively insensitive to forward power fluctuations. The high total excitation potential ion lines are a greater distance from their maximum response (e.g. the graphs given in the paper show a peak at 18mm for Zn 202.5nm II) and have much larger susceptibilities to forward power (e.g. Zn 202.5nm II is about nine times more sensitive than Li 670.7nm I). Their results show also that reduced injector gas flow has a similar effect to increased forward power.

The possible mechanism for the relationship between an analyte's susceptibility to forward power variation and the analyte total excitation potential is discussed in Section 6.5.3. No possible 'cause' has yet been proposed for the relationship between the susceptibility to sample uptake rate and the total excitation potential. This interesting area is discussed in Chapter 9 with a tentative causal mechanism suggested for future investigations.

4.8 Correlation Structure of Background Intensities

The study of and improvement of precision of analytical signals well above the detection limit was a primary objective of this study. However, during the experiment design for the 'Quasi-Routine Data' repeated measurements of the 'blank' intensity at the 24 element wavelengths were made. A preliminary analysis of this data by P.C.A. revealed that $\sim 30\%$ of the variance is multielement correlated. The first principle component was dominated by elements with the highest background millivolt values, suggesting that the variation is proportional to the background signal. This conclusion was supported by the readings for several of the parameters given in Table 4.2. Low level precision should therefore be improved by a chemometric correction (similar to PRISM) based on this information, but this interesting possibility was not pursued in this study.

4.9 Summary

Principal Component Analysis (PCA) succeeded in determining that over 90% of the total variance in Quasi-Routine Analysis was not random but multielement correlated. PCA failed to isolate the causes of the variance because they give rise to correlated effects. From ten possible causes of variation in routine ICPAES, only two distinctive multielement parameter signatures (MPS) emerged. Both MPS's are functions of the analyte line total excitation potential but with slopes of opposite signs. The output of the PCA is consistent with the model that the variation in Quasi-Routine Analysis being caused by the compound effect of variations with the two MPSs. It is probable that short-term precision in ICPAES (i.e. between contiguous measurements) is

also limited by similar sources of variation. The various components of the medium-term precision will be analysed further in Chapter 5. The second method of checking the model of two compounded variation, was to devise a correction method based on this model (PRISM). The amount of variance removed would therefore quantify the amount of variance conforming to this model. This parameter related internal standard method (PRISM), described in Chapter 5, also provides a powerful method for improving precision in routine ICPAES.

CHAPTER 5

METHODS OF IMPROVING PRECISION

5.1 Introduction

There are three approaches to improving precision in a source limited technique such as ICPAES:-

(i) The hardware option - to improve the stability of the instrumental hardware;

(ii) The interactive option - to use a feedback loop to continually adjust an instrumental setting to stabilize a physical parameter measurement;

(iii) the software option - to correct the analytical intensity retrospectively.

Since the introduction of the first commercial ICP system the tolerances of various hardware components of the system have been tightened progressively with the realisation of their importance. The coefficients given in Table 4.5 illustrate that relatively small variations in such instrumental parameters as forward power and nebulizer gas flow are often amplified by a factor of up to five in the resultant variation in the analytical response. The first generation of ICPAES instruments frequently had tolerances on forward power of around $\pm$0.5% which is clearly inadequate to achieve analyte measurement precisions of better than 1%. More recently manufacturers have reduced this tolerance to values approaching 0.01%. For nebulizer gas flows the use of mass flow controllers in place of needle valves has achieved similar improvements. A dominant source of signal variation identified as

the rotation of the plasma (Belchamber and Horlick 1982) may well be reduced by the use of a laminar flow rather than tangential flow torch (Davies et al. 1986).

In general however further improvements in hardware will probably result in producing diminishing returns in terms of improved precision. (Even a 'perfect' noise-free instrument would still be limited by the consistency of the samples presented to it). Probably the more cost effective option is to harness relatively cheap computer power to assist in precision improvement. The computer can be utilized in either the interactive or the passive role.

The interactive option uses the computer to monitor a suitable instrument variable and then to adjust an instrumental parameter in order to stabilize the measurement of the variable. Ohls and Koch (1977) for example monitored the RF power in the induction coil ("coil power") and adjusted the forward power from the RF generator to stabilize the coil power reading. In the application of this system by Dorn (1981) the general limitations of the concept became evident. The accurate measurement of the coil power was critical and also the tendency for continual adjustment of the forward power to cause secondary analytical instability. The application of an interactive system for the improvement of accuracy where the efffects are not transient, is discussed in Chapter 7.

The software option or passive use of the computer, is where the analyte signal is corrected retrospectively. This possibility is examined in detail in this study and is considered potentially the most practical method of achieving significant improvements in precision. The technique employed is a generalisation of the internal standard idea.

5.2 Review of Internal Standard Methods for Emission Spectrometry

The first application of internal standardization to Atomic Emission Spectrometry (AES) was by Gerlach in 1925. This innovation allowed AES to evolve from qualitative to quantitative analysis (Ahrens and Taylor 1961). The method utilises the emission intensity of an internal standard element of fixed concentration as a reference to which the intensity of an analyte element is ratiod. In this origin or 'simple' method it was this intensity ratio which was used as a function of analyte concentration for the purpose of calibration and subsequent measurement. Expressed mathematically, if the nett intensity of an internal standard element A is I_A and that of the 'ith' analyte I_i then the concentration of 'i' c_i is expressed by a function φ as

$$c_i = \varphi (I_i/I_A) \quad \ldots\ldots\ldots\ 5.1$$

Since the work of Gerlach, internal standards have been widely applied in emission spectrometry to correct for a wide diversity of spectrochemical and ancillary processes. For example, variations in sample weight, excitation efficiency and volatilization rates in DC arc emission spectrometry have been corrected by this means (Ahrens and Taylor 1961, p95). The success of internal standardisation in improving accuracy and precision has always been critically dependent on the 'matching' of the characteristics of the internal standard line with those of the analyte line. In simultaneous multielement ICPAES the use of internal standards has been particularly problematical because of the virtual impossibility of finding suitable elements which

fulfil the rigorous criteria required for a wide range of analytes. The nine criteria compiled by Barnett et al.(1968) are

1) The internal standard element should have a negligibly low concentration in the sample.

2) The internal standard element should be in a high state of purity for the analyte elements.

3-5) The internal standard element and the analyte element should have similar i) volatilization rate; ii) ionization energy; iii) atomic weight.

6-9) The internal standard line and the analyte line should have similar i) excitation energy; ii) freedom from self-absorption; iii) wavelength; iv) intensity, the latter two particularly for photographic detection methods.

In their experimental studies of ICPAES Barnett et al.(1970) found that even these nine criteria were insufficient to ensure good matching of internal standard with analyte line.

For multielement analysis the use of multiple internal standards is an obvious way of matching a range of analytes with differing characteristics. However with simple division techniques, a near perfect match is still required for each analyte, suggesting one internal standard for each analyte, such a procedure is clearly impracticable for large suites of analytes.

An application of the method to ICPAES analysis of geochemical samples utilising two simple internal standard elements was described by Odegard (1981). Lithium was used as internal standard for alkali elements (Na and K) and yttrium (total excitation potential (E') = 10eV) for all other 18 analytes ranging in total excitation potential from 3.8 eV (Cu 324.7 I) to 14.7eV (Pb 220.3 II). The improvements in precision were combined

with reduction of matrix effects which will be considered in Chapter 7. The methods and time scales of the precision measurements were vague, but the reported precision (1σ) fell substantially from a range of 0.45 - 1.92% (median 0.73) to 0.17 - 1.75% (median 0.39). This implies a 70% reduction in the total variance which is surprising given the mis-matching of some of the line pairs. For example Cu precision was 0.74% and Cu/Y was 0.38%, even though their excitation potentials differ by a factor of three.

Sequential determination of analytes with a monochromator poses extra difficulties for internal standardization. An important advance in these field has been the work of Myers and Tracy (1983). Although the constraints of hardware result in a correction system of limited applicability to polychromators, the investigations of interelement correlation complement those described in Chapter 4. They reported high levels of correlation between all elements only at high level in the plasma, for example, at a viewing height above the load coil of 20mm, compared with 14mm in Chapter 4. The effective viewing height is even higher as they reduce nebulizer gas flow to 0.9 or 0.71 min^{-1} compared with 1.01 min^{-1} used in Chapter 4. The Myers-Tracy system utilises traditional simple division of analyte by internal standard intensity and so depends on using conditions with high correlations and equal amplitudes of variation between the intensities. When these conditions are fulfilled, substantial improvements of precision of over one order of magnitude are reported. Resulting precision values of 0.05% are comparable with the measured values of shot noise (Salin and Horlick 1980). Such precision improvement may be achieved by the particular mechanism of the internal

standard calculation in this case. The division is carried out by real time electronic signal division rather than a software calculation based on integrated signals. The strength of this procedure is the short time interval over which it operates, with a time constant of 0.05s compared with the 5.0s integrations in this study for example. The weakness is the lack of flexibility to perform any calculation other than simple division and especially not individually tailored calculations for different analytes. In terms of practical analysis the necessity of using a high observation height will severely reduce the sensitivity and hence the precision of many analytes and tend to out-weigh the improvements resulting from internal standardization.

As a strategy for simultaneous analysis the choice of choosing operating conditions of generally high signal correlation seems even less practical than for sequential analysis.

The finding of Myers and Tracy that there are two distinct zones of the plasma with different correlation patterns has significance for the theoretical implications of the experimental data given in Chapter 4 and will be discussed in section 9.1.4.3. Variation of background signals are also corrected in the Myers and Tracy system and this will be discussed as a separate problem in section 5.8.

A generalized internal reference method (GIRM) devised by Lorber and Goldbart (1984) and with Eldan (1984) constitutes the ultimate in generalization of the application of mathematics to the use of internal standards. For demonstration purposes GIRM utilizes five internal standards to correct two analyte responses, all seven lines being within a 10nm range of wavelength. The effects of four instrumental parameters on the response ratios for

all of the analyte/reference element pairs were related by quadratic equations. Composite corrections equations solved by numerical analysis improve the precision of the analytes. This approach therefore is not based on a knowledge of the spectrochemical process involved or even on the relative importances of the four instrumental parameters in real variation in routine ICPAES. A more detailed comparison of these methods is given in section 5.7.

5.3 The Parameter Related Internal Standard Method (PRISM)

From the reports of many workers, it was clear that internal standardisation had severe limitations in its application to ICPAES. This was largely due to the impossibility of using a 'matched' internal standard. However, it was also clear that similarities between intensity variations reported in Chapter 4 suggested that the variations of one analyte intensity should provide useful information about the variations in those of other elements. The two mathematical requirements for the simple internal standard calculation (equation 5.1) are that the responses of the analyte and internal element lines should be both highly correlated and have equal amplitudes of variation. The correlation matrix given in Table 4.3 reveals that despite the generally high levels of correlation no element correlates highly ($r > 0.9$) with more than a few other elements. The wide range of coefficient values for analyte variations caused by operating parameters Table 4.5 indicate that equal amplitudes of variations caused by these parameters will occur only exceptionally. A more detailed discussion of the effect of these factors on correction efficiency is given in section 5.4. The successful application of internal standardisation to ICPAES clearly required a method which could

function with both partial correlations and flexible amplitude factors. Abundant computer power made practicable the more sophisticated calculations required by these analyte specific coefficients. The logical progression was therefore to abandon finding 'matched' internal standard lines and substitute a computer model which would in effect simulate how a matched internal standard would behave. One idealistic approach would be to extend a complete computer simulation of the ICP (Mostaghimi et al. 1985) to the level where the relationship between the emissions of all analyte lines would be quantifiable; that would clearly require a very large step forward in the understanding of the plasma. The more pragmatic approach adopted in this study was to find the proximal 'causes' of typical variation in analyte intensity, and then measure the way these causes affected all analytes of interest. If the causes could then be monitored routinely, then the effect on all analytes could be predicted and hence corrected. This is the rationale behind the parameter related internal standard method (PRISM) devised in this study.

The investigations described in Chapter 4 demonstrated the high level of multielement correlation present in routine ICPAES analysis. It also showed that at least seven potential causes of instrumental variation conformed to only two different multielement 'signatures'. The PRISM correction is therefore based on monitoring these two distinct signatures, by means of two internal standards with extreme characteristics, and interpolating the effects of the two signatures on any number of analytes with intermediate characteristics.

For example, under the specified analytical conditions, zinc is significantly affected only by those parameters with the forward

power multielement parameter signature (MPS). Similarly, lithium is affected only by those parameters with the sample uptake MPS. Thus in this case, by declaring zinc and lithium as internal standards, seven potential underlying causes of ICPAES variation can be corrected.

PRISM therefore consists of two distinct operations. The first concerns the measurement of the two MPSs and the second the application of the MPS to the analytical data, in real time, in order to improve precision.

In practical terms a simple PRISM procedure consists of the following:-

1. Specify suitable standard operating conditions for the analysis.

2. Prepare a 'High' solution containing analytes and potential internal standards at concentration levels at least 1000 times their detection limit.

3. Take integrated response measurements of a blank solution and the 'High' solution at the following settings;

   (i) Standard operating conditions

   (ii) With forward power increased by 5% $\pm$ 2%

   (iii) With sample uptake rate decreased by 25% $\pm$ 10% (for example by lengthening the uptake tube for unpumped systems)

   (N.B. The percentage changes in forward power and sample uptake rate do not need to be accurate as it is the relative changes between elements which are required).

4. Calculate the nett intensity (I) for all measurements of the 'High' solution by subtracting the appropriate blank measurement.

5. Select two internal standards (A & B) on the criteria of exclusive response to either forward power or sample uptake. If one internal standard is not totally exclusive then a slight modification to the calculation is required. Non-instrumental criteria for internal standards already stated such as low abundance in samples and non-requirement as an analyte must also be considered. The two elements should preferably not cause or be subject to large spectral interference effects.

6. Calculate the forward power MPS as follows:- If the nett intensity of the internal standard A is I_A generally and I'_A at the standard operating conditions, and if the nett intensity of the 'i'th element is I_i generally and I'_i at the standard operating conditions, then

$$(I_i/I'_i - 1) = f_{iA} \ (I_A/I'_A - 1) \ldots\ldots\ldots \ 5.2$$

where f_{iA} is the function describing the behaviour of the ith element with the internal standard A, upon the change in forward power.

In the model used for PRISM the function is a simple factor k_{iA} given by

$$k_{iA} = (I_i/I'_i - 1) \ / \ (I_A/I_A' - 1) \ldots\ldots \ 5.3$$

When there are n analytes, there will be n values of k_{iA} in the MPS for the internal standard A.

7. In an analogous way, calculate the sample uptake MPS as follows. For each analyte there will also be a value of f_{IB} where generally

$$(I_i/I_i' - 1) = f_{iB} (I_B/I_B' - 1) \quad \ldots\ldots 5.4$$

and in this example

$$K_{iB} = (I_i/I_i' - 1) / (I_B/I_B' - 1) \quad \ldots\ldots 5.5$$

where all nett intensities are measured for a variation of sample uptake rate.

In the more general case a range of settings for each parameter may be used and linear regression employed to estimate the slope coefficient k_{iA} with an enforced zero intercept at the standard operating conditions (Fig. 4.3).

In application to routine analysis PRISM then operates as follows:

8. Add the two internal standard elements to all calibration solutions and samples at a fixed concentration of at least 1000 times their respective detection limits.

9. Measure the nett intensity of both internal standards (I_A^o, I_B^o during the same integrations used for the normal calibration of analyte response I_i^o.

The I_i^o are related to concentration c_i, by a function g

$$c_i = g (I_i^o) \quad \ldots\ldots 5.6$$

The measurement of I_A^o and I_B^o from this integration specifies the internal standard readings and hence the effective operating parameter settings to which subsequent measurements will be 'returned'.

10. For the analysis of a test solution at a particular time after the calibration the nett responses for the internal standards A and B will be I_A and I_B and the response for the ith analyte at unknown concentration c_i will be I_i.

Then the corrected nett response for the ith analyte in the general PRISM procedure, I_{ic} is given by:-

$$I_{ic} = I_i/([1 + k_{iA} (I_A/I_A^{o} - 1)] [1 + k_{iB} (I_B/I_B^{o} - 1)]) \quad 5.7$$

The value of I_{ic} can then be used to calculate concentration in the normal way, substituting for I_i^{o} in with equation 5.6. The blank reading should be added if the calibration function was calculated on gross intensity.

The values of I_A^{o} and I_B^{o} can be updated at calibration adjustments (or 'normalisations') when recalibration is infrequent.

Deviations from linearity in the variation of analyte with internal standard, in the region of the standard conditions, were found to be minimal. Polynomial functions, weighted for experimental variance, may be preferable if large deviations from the standard conditions are to be catered for. In that case the simple factors (k_{iA}, etc) in equation 5.6 are replaced by functions (f_{iA} etc).

For some operating conditions it may prove impossible to select two internal standard elements that are totally mutually exclusive to the two operating parameters. In this case one exclusive element A will suffice, and this element A can be used to correct the non-exclusive element B for the effect of the parameter affecting A and B. The corrected intensity of element B can then be applied in the normal way.

Thus in this case for all analytes and non-exclusive element B the first stage of corrected response gives I_{ic}' where:-

$$I_{ic}' = I_i/[1 + k_{iA} (I_A/I_A^{o} - 1)] \ldots\ldots 5.8$$

and then the second stage for all analytes

$$I_{ic} = I_{ic}'/[1 + k_{iB} (I_B/I_B^{o} - 1)] \ldots\ldots 5.9$$

These two equations then take the place of equation 5.7 in this instance.

There is a close relationship between PRISM and the ordinary internal standard method.

For comparison with equation 5.8, the expression for the correction by the simple ratio internal standard method expressed in an analogous form is:-

$$I_{ic} = I_i/[1 + (I_A/I_A^{o} - 1) \ldots\ldots\ldots 5.10$$

There is a simple relationship between the evaluation functions used to calculate concentrations for both methods. The evaluation function φ is used to calculate the concentraction c_i from the intensity ratio thus:

$$c_i = \varphi (I_i/I_A) \ldots\ldots\ldots 5.11$$

The function g, which was defined using equation 5.6, can be applied to calculate an unknown concentration from the corrected intensity I_{ic}, using:

	Precision as coefficient of variation, %			
	Original	Contiguous	Corrected by PRISM	Accuracy as % bias
Ag	0.74	0.39	0.58	0.71
Al	1.04	0.66	0.51	1.17
Ba	0.91	0.68	1.35	2.36
Be	1.81	0.51	0.56	−1.47
Ca	0.85	0.22	1.29	3.53
Cd	1.17	0.26	0.37	0.19
Co	1.02	0.25	0.38	0.85
Cr	0.82	0.27	0.53	0.48
Cu	1.57	0.80	0.46	−0.37
Fe	0.69	0.34	0.64	1.34
K	2.40	1.16	0.32	0.84
La	0.89	0.50	0.40	1.62
Mg	0.91	0.38	0.47	0.91
Mn	0.79	0.33	0.54	1.67
Mo	0.90	0.26	0.47	−0.01
Na	2.39	1.16	0.47	0.31
Ni	0.95	0.30	0.47	0.62
P	2.17	1.38	1.80	3.87
Pb	0.96	0.28	0.56	0.93
Sr	0.97	0.62	0.53	0.05
Ti	0.83	0.49	0.59	0.19
V	0.99	0.45	0.34	0.02
Median	0.95	0.47	0.52	0.88
Mean	1.17	0.53	0.62	1.07

Table 5.1
Effect of PRISM correction on the precision and accuracy of the quasi-routine analysis data.

$$c_i = g\ (I_{ic}) \ldots\ldots\ldots 5.12$$

Simplification of equation 5.10 shows that

$$I_{ic} = I_i\ I_A^{\,o}/I_A \ldots\ldots 5.13$$

Substituting equation 5.13 into equation 5.12 gives

$$c_i = g\ (I_i\ I_A^{\,o}/I_A) \ldots\ldots 5.14$$

By comparison of equations 5.11 and 5.14 it is evident that if linearity of calibration is assumed, then the two functions φ and g differ only by the constant factor $I_A^{\,o}$, thus

$$\varphi\ (I) = g\ (I)\ I_A^{\,o} \ldots\ldots 5.15$$

5.4 Testing the PRISM Model

The PRISM method of correction described above was applied to the Quasi-Routine Analysis data described in Chapter 4. Zinc was chosen to monitor the parameters with forward power MPS (= A), and lithium to monitor parameters with sample uptake rate MPS (=B). Linear approximation was used for the functional relationships between analytes and internal standards, based on the data described in section 4.6. The values of the coefficients used as k_{iA} and k_{iB} were those given in column 1 of both Tables 4.6 and 4.7. The values of $I_A^{\,o}$ and $I_B^{\,o}$ used throughout were those from the first measurement in the data set, hence the effect of PRISM on drift over 4.4 hours, without any calibration adjustments, was also tested.

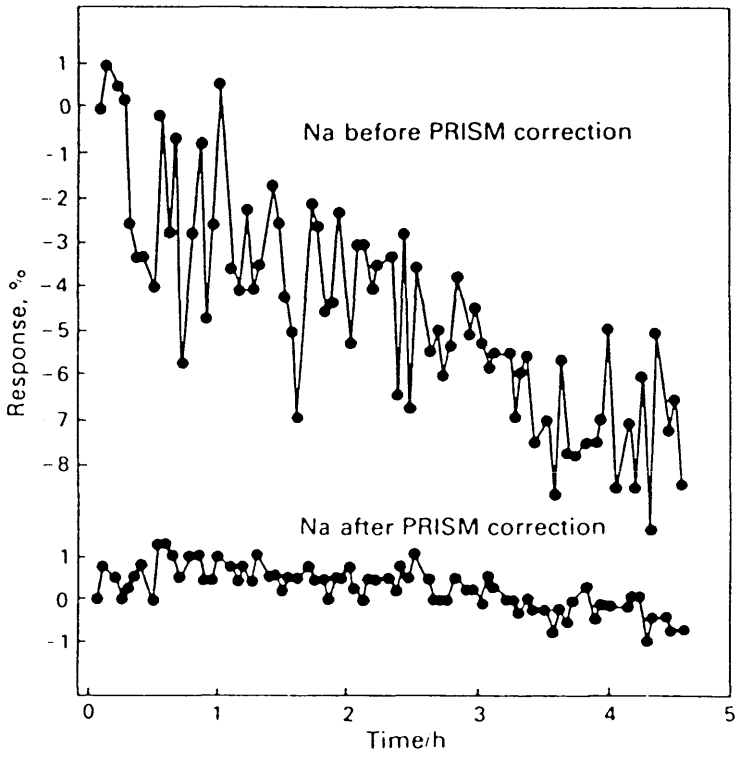


Fig. 5.1
Effect of using PRISM on the variation in response of sodium for discrete integration on a single solution. Both traces are plotted using the same ordinate scale, i.e., the percentage change in response from the initial value. Other elements generally show improvement to a similar degree (see Table 5.1).

	Precision as coefficient of variation, %			
		PRISM with single internal standard		PRISM with
	Original	Zn	Li	Zn and Li
Cd	1.17	0.37	1.08	0.37
V	0.99	0.55	0.64	0.34
K	2.40	2.48	0.31	0.32

Table 5.2
Varying contributions of the two internal standards within the PRISM correction to the precision of three elements.

The precision of the analytes was assessed by considering for each analyte the 75 nett intensity readings as one population and determining the coefficient of variation. The results are given in Table 5.1. The mean values of precision quoted are strongly affected by a few very variable analytes and so median values have been quoted as a more robust measure of the precision over all 22 analyte elements. The original precision in Column 1 is that for the Quasi-Routine Analysis data, and therefore includes time correlated variation (drift) as well as 'random' effects. Column 2 contains typical values for the precision of 'contiguous integration' as defined above.

The precisions resulting after the PRISM correction of the Quasi-Routine Analysis data are given in column 3. The general level of precision has been substantially improved, as measured by the median values given, dropping from 0.95 to 0.52% CV. This signifies a removal of 70% of the total variance in the original data. The median precision achieved closely approaches that for contiguous integrations of 0.47%. A graphical comparison of the response of sodium before and after the use of the PRISM correction is shown in Figure 5.1.

For two elements the precisions are made worse by the use of PRISM. These are barium and calcium which, as shown above, did not drift in the way predicted by the two MPS in PRISM. This may have been due to an instrument malfunction as, on a second set of Quasi-Routine Analysis data, barium and calcium did not drift unpredictably and their variances were reduced by a fraction similar to those of other elements (40%). For this second set of data the median variance was reduced by 75%.

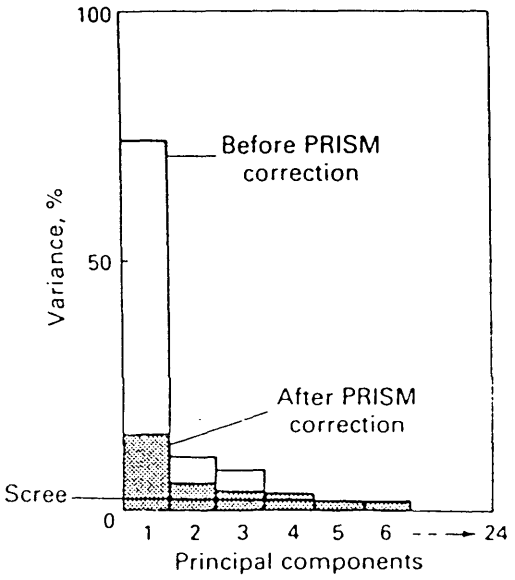


Fig. 5.2
Effect of using PRISM on the variance of the principal components shown in Fig. 4.2. The variance of the PRISM corrected data is expressed as a fraction of the residual variance calculated from the data given in Table 5.1 (i.e. 30%).

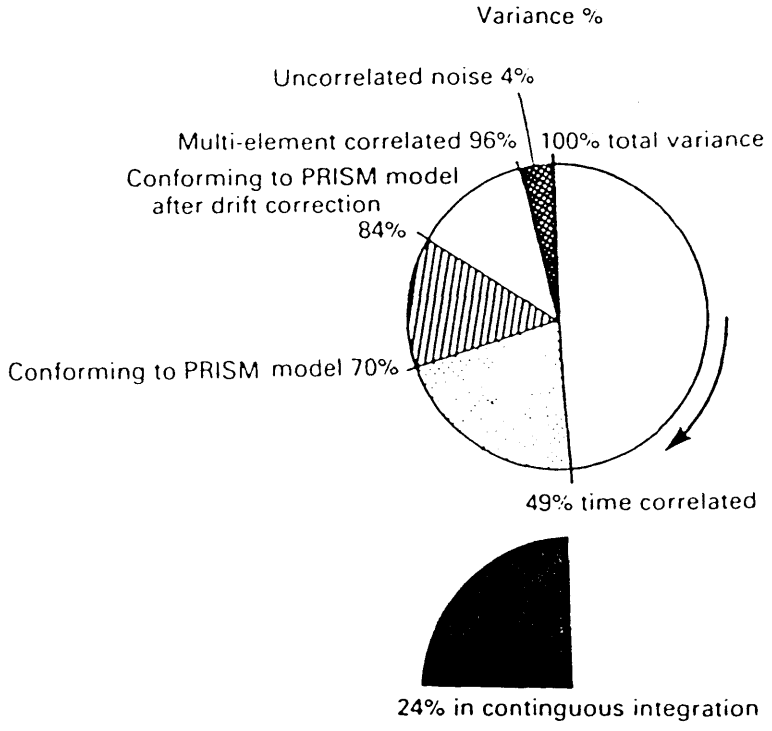


Fig. 5.3
Apportionment of the total variance within the quasi-routine analysis data. The variance typical of contiguous integration is shown for comparison.

The proportion of the corrected variance that arises from each MPS varies from element to element. Treatment of the Quasi-Routine Analysis data with the PRISM equation 5.7 containing only one internal standard, revealed the separate effects of the two MPSs. Three analytes are given as examples in Table 5.2. Cadmium precision is substantially improved only by the correction including the zinc internal standard and hence the forward power MPS. Conversely potassium precision only improves with the lithium internal standard and hence sample uptake rate MPS. The precision of the majority of elements is of an intermediate type, exemplified by vanadium, where both internal standards improve the precision to some extent.

The bias introduced by PRISM correction is given in Table 5.1. It was calculated by using the initial responses for all analyte elements to represent the true concentrations of the analytes, then comparing the mean values of the 74 subsequent replicate determinations, to give the bias. The bias introduced was in the order of 1% for the 22 analytes.

The fraction of the total variance which was purely time-correlated (i.e. drift) was measured as 49%. This was calculated by computing the improvement in the median precision caused by the drift correction described earlier in this paper. Application of PRISM to the drift-corrected data then reduced the variance by a total of 84%.

The 30% variance remaining in the original Quasi-Routine Analysis data after treatment with PRISM was examined by means of PCA. The plot of the variance for the first six principal components is shown in Figure 5.2. The break in slope after PC3

suggests the beginning of the purely random noise. This conclusion is supported by a Scree test. With a cumulative variance at PC3 of 87%, this would suggest that only 4% (i.e. 13% of 30%) of the original total variance is truly random and not multielement correlated. This would further suggest a theoretical minimum median precision of 0.19% over a wide range of elements. This is comparable with the 0.07% minimum precision described by Salin and Horlick (1980). The overall apportionment of variance is shown in the Pie diagram in Figure 5.3.

The reason for 30% of the total variance remaining after PRISM correction may be due to a number of possible causes. Obviously there is a proportion of non-correlated noise, in the region of 4%, which can never be removed by a technique based on multielement correlation. Variation conforming to the PRISM model but which occurs on a time scale within the intergration time could not be corrected by this procedure. This is where the signal processing of the Myers-Tracy (1983) method is clearly advantageous Non-linearity in the analyte/internal standard function may be contributing to incomplete correction. So too may be certain elements such as phosphorous which, as can be seen from Table 5.1, show small improvement in precision, due possible to deviations from the PRISM model. This suggests that causes of variation, not conforming to the two MPS used in PRISM, are significant, if of relatively small extent. It is also possible that the effects of the two type of parameters considered in PRISM are not strictly multiplicative.

The significance of signal correlation and proportionality to the effectiveness of an internal standard method can be expressed mathematically.

Two distinct factors relate variations in response of an analyte (i) and an internal standard element (A), they are the correlation coefficient (r) and the relative amplitude of the variation to a given instrument parameter (j). The possible improvement (R) in signal fluctuation due to internal standardisation by simple division has been given by Myers and Tracy (1983) as;.

$$R \quad [\, 2(1 - r)]^{-0.5} \qquad \ldots\ldots \; 5.16$$

This implies that x20 improvements are possible if r = .999, x7 if r = .990 and only x2 if r = 0.900. Deterioration of precision results if $r < 0.5$. This model however does not apply to this case where the lower correlation to element A is caused by increased condition to element B if the latter can be removed prior to correction. So for example the fact that Table 4.4 shows V/Zn correlation as 0.552 and V/Li as 0.485 does not imply that no improvement is possible. Table 5.1 reveals a clear improvement in the precision of variation by PRISM (average $R \approx 2$). However the poor performance of phosphorus (R = 1.2) in Table 5.1 is clearly traceable to two low correlation in Table 4.4 (P/Zn, r = 0.419; P/Li r = 0.004). Further investigations using computer simulation studies should help to clarify the role of correlation coefficients for two internal standards.

The relationship between the slope factor j and the precision improvement (R) for simple ratio internal standard is given by Myers and Tracy (1983).

$$R = \left| j/(j - 1) \right| \quad \ldots\ldots\ldots 5.17$$

Clearly the insertion of j values in equation 5.7 to allow for its non-unit value allows precision improvement otherwise unattainable. For example without this correction, value of j = 0.8 would produce R = 4; j = 0.7 gives R = 2.3 and values of j less 0.5 would produce deterioration rather than improvements. One further application of equation 5.17 to the PRISM equation is that the effect on precision improvement of errors in the determinations of k_{iA} can be estimated for one internal standard. As a first approximation if a value of k_{iA} is low by 20% then this is equivalent to equation 5.17 where j = 0.8, i.e. the limit of precision of improvement is lowered from ∞ to $\sim$4 times. The % errors in k_{iA} would tend to be greater for higher or lower values of k_{iA} and so precision improvement is progressively more difficult for lower values of k_{iA}.

The long term applicability of the two MPSs was tested by applying the same measured sets (in Tables 5.7 & 5.8) to a second Quasi-Routine Analysis data set produced a year later than the first, under the same operating conditions. The improvement in precision after the use of PRISM, as noted above, was closely similar. However, new MPS coefficients should be measured when ICP operating conditions are changed and, for a constant set of conditions, periodic updating over a period of months should maintain the performance of the correction.

5.5 Some Practical Observations on the Use of PRISM

It must be emphasized that whilst PRISM requires the characterisation of only two operational parameters, the resultant MPSs compensate to a large extent for the variation caused by seven potential sources of variability.

The PRISM equation 5.7 is given in terms of nett response, but initial experimentation suggests that the substitution of concentration values, for both analytes and internal standards, would produce equally good, perhaps better, improvements in precision.

Although a mainframe computer was used off-line for the statistical studies in this work, the computing power required to execute the PRISM correction is very small and could easily be accomplished by the typical micro computer supplied with ICPAES instruments. Computer control of forward power and sample uptake rate, available on some instruments, would also allow the automatic determination of the MPS coefficient determinations.

The application of PRISM to sequential ICPAES determination has not been investigated. While the improvements in precision are not likely to be as good, due to the time delay between the measurement of analytes and internal standard elements, significant reduction in variance would still be expected.

PRISM then offers a practical method of improving medium term precision to the level of contiguous integration precision over a whole wavelength range of ICPAES by the use of only two parameter related internal standards. The correction terms are few in number, straight-forward to quantify, and stable over long periods under consistent operating conditions. The corrections are applied on the basis of mutually independent reference elements, and compensate for changing proportions of the causes of variation within and between batches.

5.6 Comparison of PRISM and the Myers-Tracy Method

The 'signal compensation system' devised by Myers and Tracy (1983) described earlier in this chpater was designed for a dual monochromator ICPAES system. This contrasts with the polychromator system for which PRISM was designed. Dedication of one monochromator to the measurement of an internal standard element matched to the analyte element measured on a second monochromator is feasible (if inefficient). In contrast the equivalent polychormator with 22 internal standard lines fitted to correct 22 analyte lines would be considered hopelessly inefficient.

The relative strength of the Myers-Tracy system is in the high-frequency real-time correction capability originating in the ratioing of raw intensity signals. PRISM cannot match a precision value of 0.02% quoted for the Myers-Tracy method, probably because PRISM is currently limited to data from on integration periods, in this case of 5 seconds. The probability that the variations occurring within that 5 seconds, conform to the PRISM model is considered to be high. The data from Myers and Tracy (e.g. their Figure 2) suggest that elements which correlate, do so consistently over time periods varying from 0.05s. to 10 minutes. A trial of PRISM on analytical signals resolved and stored in the millisecond range is obviously an interesting topic for future.

The mode of signal processing which enables the Myers-Tracy method to achieve good precision is limited to highly correlated analyte/internal standard pairs, unlike PRISM. It is also limited to the use of one internal standard per analyte unlike PRISM where correlations to two internal standards allow for situations where the analyte does not correlate highly with either internal standard. There is also no factor which can allow for the varying

responses of different elements to causes of variation (j) given in Table 4.6 and shown to be critical by equation 5.17 taken from their own paper (Myers and Tracy 1983).

Comparisons of analytical operating conditions to minimize these shortcomings must frequently compromise overall analytical performance. For example, the recommendation of Myers & Tracy is to measure at 20mm observation height where the detection limit is far from optimal. Such compromises are even less practical on a polychromater system.

5.7 Comparison of PRISM and GIRM

It is difficult to compare the effectiveness of PRISM with that of the GIRM procedure of Lorber, Goldbart (1984) and Eldon (1984), because of the very different practical conditions under which they were used. The results quoted for GIRM are very good, for example resulting precision of 0.1 to 0.14% RSD close to he shot noise of 0.07% (Salin and Horlick 1980). However, they were obtained under conditions atypical of routine simultaneous analysis, i.e. continuous nebulisation of a test solution, a run of 30 minutes duration, all wavelengths used within a spectral range of 10nm, and five internal standards used for each of two corrected lines. The corresponding conditions used to test PRISM were:- discrete nebulisation with intercalated blanks, a run of 264 minutes duration, wavelengths spread over a spectral range of about 600nm, and two internal standards used to correct 22 analytes. However the PRISM corrected data closely approached the precision of 'contiguous integrations', and this is probably the limiting value for conditions of routine analysis.

At a conceptual level, PRISM is a special case covered by the most general formulation of GIRM, and the actual methods used are similar. However GIRM relies heavily on a mathematical method applicable to the most general case, rather than on information

specific to ICPAES. By making more use of such specific information PRISM can be formulated and executed in simple mathematical terms. For instance, it is clear from Table IV (in Lorber, Goldbart and Eldon 1984), that the four parameters used in the correction equation are highly correlated in their effects on the line sensitivities, and not almost independent as they are meant to be.

Further investigations into the fundamental properties of the analytes which the MPS values are measuring may allow MPS value to be calculated accurately from such properties. Such values might then not require repeated redetermination, even under new operating conditions. The efficiency, cost effectiveness and robustness of such a system should ultimately be superior on a purely empirical correction such as GIRM.

Regardless of these differences, both GIRM and PRISM are capable of making substantial improvements to the signal stabilities of ICPAES. Thus chemometric methods can be used to improve the precision of simultaneous analysis without resort to costly instrumental improvements.

5.8 Variability in Spectral Background

Although outside the general range of this work, it was noted in Section 4.8 that quite high levels of correlation were observed in the 75 blank readings taken as part of the Quasi-Routine Analysis. Similar findings have been made by Myers & Tracy (1983) and Lorber et al (1984). All have reported a different pattern of correlation to that seen for nett sensitivities, yet a similar chemometric correction is clearly possible. Improved detection limits of up to x20 are reported by Lorber et al (1985), although a practical application has yet to be reported.

5.9 Summary and Discussion

The precision of routine ICPAES can be substantially improved by chemometric means. Difficulties in matching internal standard and analyte lines can be obviated by broadening the concept of internal standardization into monitoring parameters in a model covering the full range of analyte variability. Simple adjustments of instrumental parameters can characterise the model and two suitable internal standards monitor any variations between and within integrations. Operating conditions for optimal analytical performance can be preserved despite lack of correlation between some element responses. This parameter-related internal standard method (PRISM) enables the real-time adjustment of sensitivity and largely obviates the need for the inefficient close interpolation of calibrating solutions for high precision analysis.

Further improvements to PRISM might lie in using higher resolution of the analytical signals in the time domain. Improving the model probably by a better understanding of its theoretical basis should also reduce variance still further. Variations in spectral background are clearly also amenable to chemometric correction and this would form a useful extension to a PRISM package for routine analysis on trace levels to improve detection limits. In the future, when hardware improvements do improve precision, the ability of PRISM to give yet further improvement should prove interesting.

CHAPTER 6

MATRIX EFFECTS AS A SOURCE OF INACCURACY

6.1 Introduction

Matrix effects in ICPAES due to concomitant metallic elements in solution can be a major cause of inaccuracy in trace element analysis (Section 2.7 (ii)). There is however currently no method of predicting the bias to be expected for any combination of analyte and matrix element. This has lead to the general precautionary measure in analysis by ICPAES of always matching the matrix composition of the calibrating solution to that of the sample as a means of eliminating this bias. Such a technique works, but has two main limitations. It cannot cope with batches of samples with variable major element composition or for samples of unknown composition, both of which are typical of geochemical samples. Nor, does this tactic give any quantification of the bias removed and hence any perception of the size of the effects. Such information would enable a deeper understanding of the causes of matrix effects.

This investigation of matrix effects was aimed at answering nine main questions:-

i) what are the probable sizes of inaccuracies from this source?

ii) which analytes are most susceptible to matrix effects?

iii) which matrix elements cause the largest and which the smallest matrix effects?

iv) is there a similarity between the way different matrix elements affect the same range of analytes?

v) can fundamental properties of the matrix elements and analyte lines be used to predict matrix effects either qualitatively or quantitatively?

vi) can the origin of these matrix effects be traced to either the nebuliser or the plasma itself?

vii) can any physical mechanism be hypothesised for the cause of matrix effects?

viii) what is the effect of increasing concentrations of analyte and interfering element?

ix) what implications do these findings have for possible schemes of matrix effect correction?

To achieve these objectives two phases of experimentation were devised. The first phase examined the effect on a range of analytes of one matrix element (calcium) at various concentrations. The second phase extended the study to many matrix elements but only at one, equimolar concentration.

6.2 Previous Work on Matrix Effects

The nature and causes of matrix effects have been widely discussed in the literature. A wide range of effects have been loosely described as 'matrix effects'. The effect on analyte sensitivity of variations in the concentration or nature of the acid medium is well known and is attributed to variations in

viscosity of the test solution (Greenfield et al.1976). This kind of matrix effect is easily managed in practice by standardising the acid concentration in the test solution for both samples and calibration standards.

Matrix effects from metallic elements have been frequently reported but the earlier work is confusing and sometimes inconsistent, owing to the wide range of conditions, often only partially characterised, under which the experiments are carried out. A good summary of the work up to 1981 is given by Blades and Horlick (1981b).

In order to elucidate this situation, several workers have recently carried out spatially resolved studies of matrix effects, by using photodiode arrays to determine the matrix effects at different points in the plasma. (Blades et al.1981b; Kawaguchi et al.1980; Faires et al.1983). In these studies the matrix elements have been restricted to the alkali metals, perhaps because of their earlier widespread use in flame spectrometry as ionisation buffers. The main conclusions of the ICPAES studies are as follows. (i) In the lower part of the plasma analyte channel (i.e., up to 15-20mm above the load coil) enhancements of analyte sensitivity are caused by the alkali metal matrix, for both atom lines and ion lines. This is attributed by Blades and Horlick to increased collisional excitation. (ii) Above a height of about 12mm in the analyte channel the process of ambipolar diffusion becomes increasingly important, leading to a suppression of sensitivity higher than 15-20mm, again for both atom and ion lines. (iii) Ionisation buffering plays only a minor role in the matrix effect. (iv) Analyte lines are affected in a manner related to their excitation potentials.

In relation to practical analysis it is interesting to note that the crossover point from enhancement low in the plasma to suppression at higher levels occurs for many analyte lines in the region usually adopted as a compromise viewing height for simultaneous multielement analysis. For the equipment used in the present study, the choice of viewing height for routine analysis was influenced by the need to minimise matrix effects. Comparative studies of most commercially produced ICPAES instruments running under their respective recommended conditions resulted in matrix effects showing suppression of intensity for the majority of elements.

In the work described information for the calcium matrix is provided, for the operating conditions used in routine analysis. No attempt to obtain spatial resolution of the effects has been made, so the results presented refer to average effects sampled through a moderate sized window (a 4-mm square) at a fixed viewing height in the plasma. Although this tends to produce a blurred picture of the effects, it relates to the situation which practical analysts encounter, but can still be put into the broader perspective by reference to the spatial resolution work of other workers. The use of a polychromator allowed the examination of matrix effects on many lines simultaneously. The use of this extra multielement dimension is a powerful tool in arriving at generalisations about analyte behaviour.

Element	Wavelength/ nm	Atom/Ion I/II	Order	Ionisation potential (IP)/eV	Excitation potential (EP)/eV	Concentration/ $\mu g\,ml^{-1}$
Ba	455.40	II	1	5.21	2.72	5.0
Be	313.04	II	2	9.32	3.96	0.5
Ca	317.93	II	2	6.11	7.05	5.0
Cd	226.50	II	2	8.99	5.47	0.5
Cd	228.62	II	3	7.86	5.84	5.0
Cr	267.72	II	3	6.76	6.15	5.0
Cu	324.75	I	2	7.72	3.82	5.0
La	398.85	II	2	5.61	3.51	5.0
Li	670.78	I	1	5.39	1.85	5.0
Mo	281.62	II	2	7.18	6.07	0.5
Ni	231.60	II	2	7.63	6.39	5.0
Pb	220.35	II	2	7.41	7.37	5.0
Rb	780.02	I	1	4.81	1.59	5.0
Sr	407.77	II	1	5.69	3.04	5.0
V	311.07	II	2	6.74	4.33	5.0
Zn	202.55	II	2	9.39	6.12	5.0

Table 6.1
Information on analyte elements.

6.3 Matrix Effects from Calcium

The selection of calcium for the detailed study of matrix effects was made on the basis of very practical criteria. Limestone, with a calcium concentration ranging from ~ 10 to 40% $^{w}/_{w}$, is a classic example of a variable sample type which cannot be analysed accurately with simple matrix matching. Calcium was known by experience (Thompson and Walsh (1983) p140) to produce ranges of biases of +5 to -30% for different analytes when limestone was dissolved at a concentration suitable for the determination of trace elements ($25gl^{-1}$). This contrasts strongly with the alkali metal which have been extensively studied (Kawaguichi et al.(1980); Faires et al.(1983)) but produced relative small matrix effects at the compromise operating conditions typical of routine multielement analysis. Hitherto the effects of calcium have been incompletely characterised for conditions of routine analysis and their causes were not established (Maessen et al.1982; Schramel 1982).

6.3.1 Experimental Design for the Study of Matrix Effects Due to Calcium

Matrix effects due to calcium were studied by measuring analyte response in solutions containing varying concentrations of calcium.

The instrumentation used for this study was the ARL 34000 polychromator system under routine operating conditions as described in Chapter 3, Table 3.1. When the nebuliser was pumped, an LKB 2132 peristaltic pump was used, fitted with 0.76mm bore poly-vinyl chloride tube. Spectral information relating to the 15 analyte lines used is given in Table 6.1. These elements provided

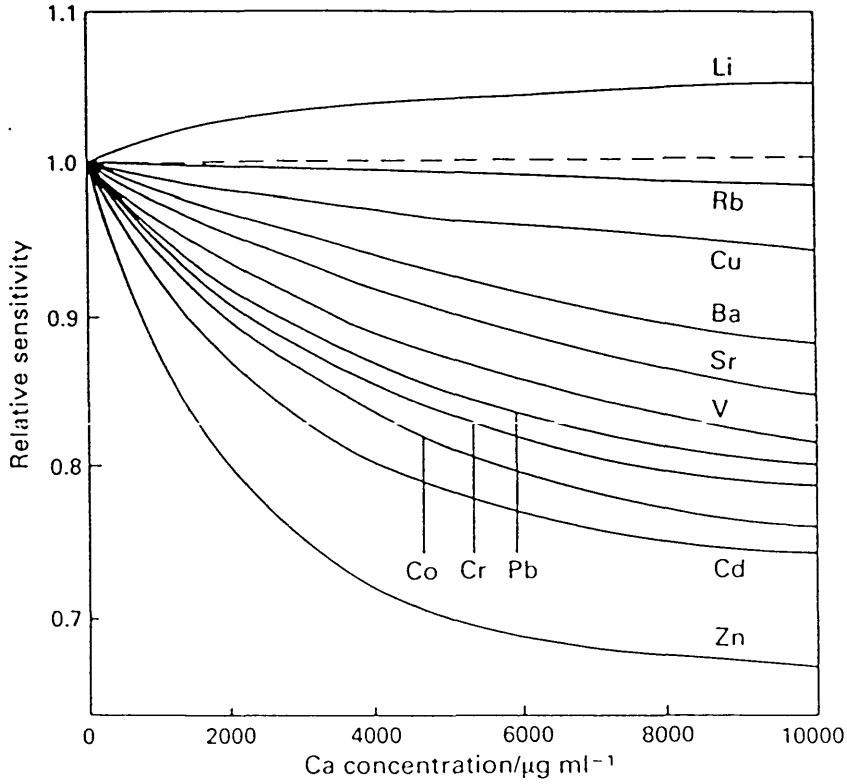


Fig. 6.1
Effect of concomitant calcium concentration on the sensitivity of a selection of analytes.

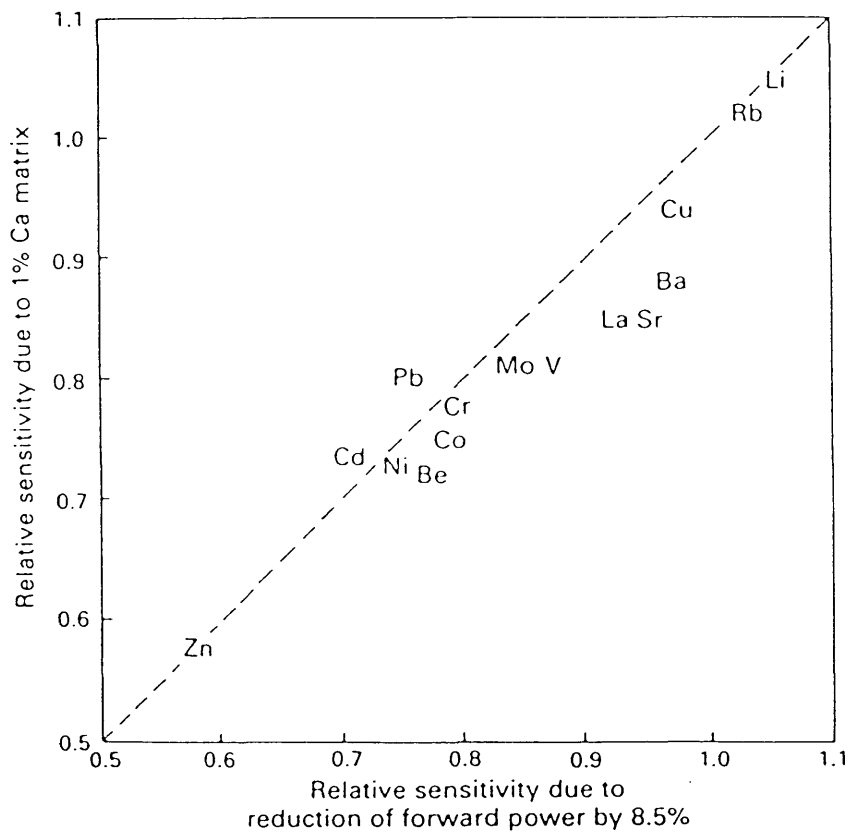


Fig. 6.2
Comparison of the effects of concomitant calcium (at 10000 μg ml^{-1}) and of a reduction in forward power to 91.5% of the normal levels on the relative sensitivities of several analyte lines. The two factors produce very similar effects, suggesting a common mechanism.

lines covering a wide spectral range as well as representing a useful selection of analytes. Calcium concentrations at ten values between zero and 10000 μg ml^{-1} were employed, the latter figure representing the highest value likely to be required in limestone analysis.

The sensitivity at zero calcium concentration was taken as the reference level for each analyte. Each level of calcium studied was regarded as a separate sub-experiment, during which the relative sensitivity was measured by the method described in Chapter 3, (Section 3.4). This consisted of running four test-solutions on the ICPAES instrument under standard conditions but within the briefest possible time-scale. This procedure minimised the effects of any possible drifts in sensitivity or background, although these drifts were in fact very small.

6.3.2 Results for Matrix Effects Due to Calcium Under Standard Operating Conditions

The original response readings were converted into values of relative sensitivities, given in Appendix C. The significance of the results can be seen from Fig. 6.1 ranging from a small enhancement for lithium (+6% at 10000 μg ml^{-1} Ca) to a substantial suppression for zinc (-36% at 10000 μg ml^{-1} Ca). In the multielement domain these results show a striking similarity with the effects on sensitivity of changes in forward power or nebuliser gas flow rate described in Chapter 4. For example in Fig. 6.2 the effect on the analyte sensitivities of 10000 μg ml^{-1} of calcium is compared with the effect of reducing the forward power by 8.5%. The results are very similar. Likewise the effect of calcium on analyte line sensitivities is strongly related to the excitation

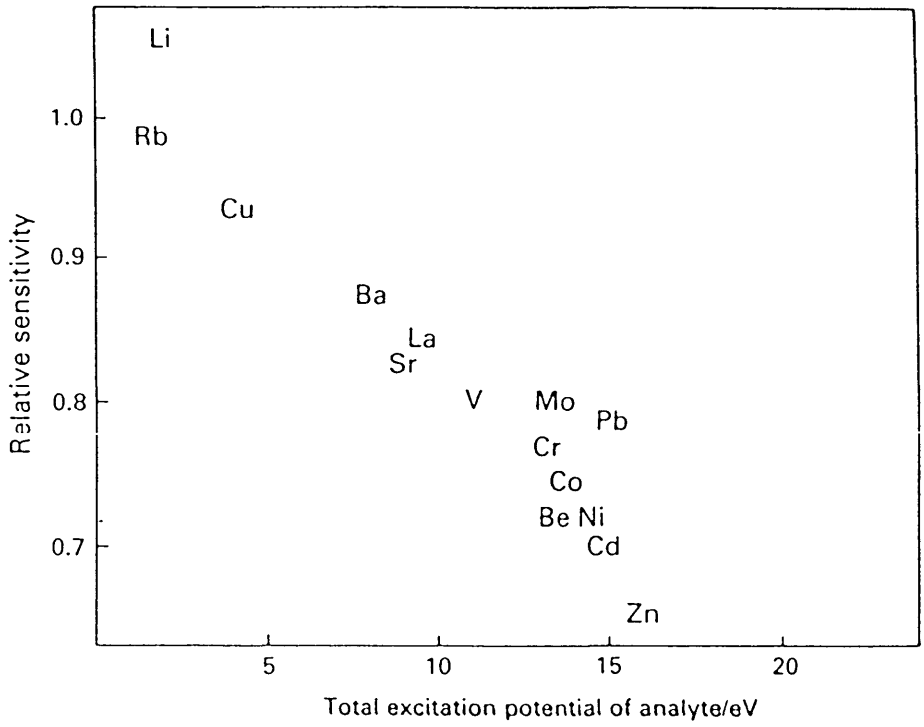


Fig. 6.3
Relationship between the effect of concomitant calcium (at 10000 $\mu g\ ml^{-1}$) on analyte line sensitivities and the excitation potentials of the lines, indicating that the effects are related to a plasma process.

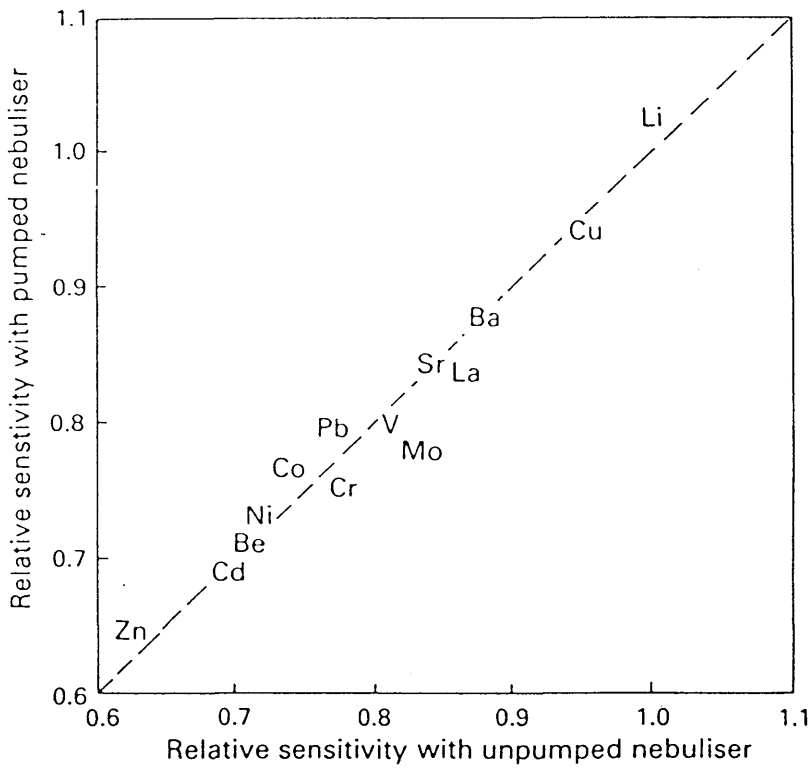


Fig. 6.4
Comparison of the matrix effect of concomitant calcium (at 10000 $\mu g\ ml^{-1}$) on several analyte lines, with pumped and free-uptake nebulisers running under identical flow conditions.

energies of the lines, as shown in Fig. 6.3. These comparisons indicate that the matrix effects observed were due to variations in the efficiency of excitation processes in the plasma rather than the effect of solution viscosity on the nebuliser efficiency.

Clearly there is not a linear relationship between the concentration of calcium present and the change in relative sensitivity of most analytes. It was however confirmed experimentally that the matrix-induced change in sensitivity for a given level of calcium applied to all levels of an analyte, from the detection limit up to at least 10000 times that concentration.

6.3.3 Comparison of Pumped and Free-uptake Nebulisation

In the foregoing experiment the nebuliser was running under conditions of free-uptake, i.e., not fed by a peristaltic pump. For a given hydrostatic head, the efficiency of the nebuliser would be affected by changes in the density, surface tension and viscosity of the solution. Many workers assume that the matrix effects described above are a result of the physical properties of the solutions, and that pumping the solution at a constant rate would reduce or even completely eliminate the effects. In order to test this hypothesis the previous experiment was repeated in the same manner, at a single level of calcium (5000 µg ml^{-1}) but with the nebuliser pumped by means of a low-pulse peristaltic pump. The pump rate was adjusted to be equal to that of the free-uptake nebuliser running on the blank matrix solution (1.0M hydrochloric acid). The uptake rates were measured gravimetrically for best accuracy, and were equalised to within 0.05 ml min^{-1}. The result obtained for all analyte elements was identical to within experimental errors (about 1% change in sensitivity). The results are shown in Fig. 6.4. Thus the matrix effects could not be

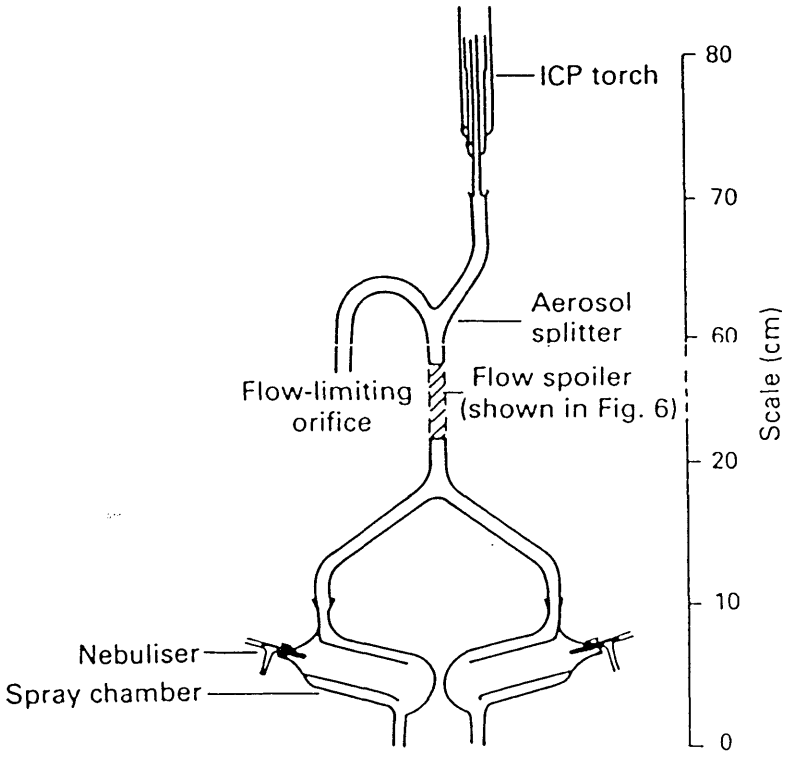


Fig. 6.5
Dual nebuliser equipment for the separate introduction of analyte and interferent solutions into the plasma. The nebulisers were matched, and the mixed aerosol was split equally to obtain realistic conditions.

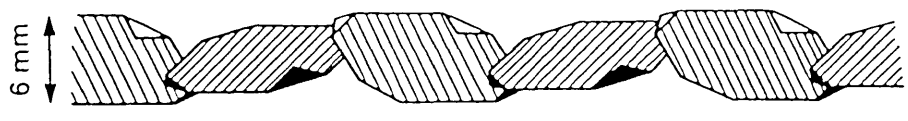


Fig. 6.6
Flow spoiler, constructed from titanium foil, used to mix the aerosol streams from the two nebulisers.

attributed to changes in test solution uptake rate.

6.3.4 Dual Nebulisers for the Separate Introduction of Analytes and Interferent

Confirmation that the nebuliser played a negligible role in causing the matrix effect was sought by the simultaneous introduction of analytes and the calcium interferent into the plasma through separate nebulisers. As the analyte nebuliser could not be affected by the introduction of calcium, any matrix effect observed must be due to plasma mechanisms. Dual nebuliser experiments in ICPAES have been carried out previously by Boumans and deBoer (1976) and by Blades and Horlick (1981b), for the same purpose as in the present work.

The equipment used is shown schematically in Fig. 6.5. The nebulisers were closely matched in performance, and each was run under the conditions given in the Table 3.1. The impedance of the waste outlet to gas flow was matched to that of the plasma torch, so as to produce an equal split of the mixed aerosol. Thus both of the nebulisers and the plasma torch were operated under conditions which were close to normal in respect of injector gas flow. Other operating parameters were as shown in the Experimental section (6.3.1).

The aerosol mixer was constructed from a titanium foil flow spoiler, in the form shown in Fig. 6.6, which was inserted into a 6mm bore glass tube. The total length of the mixer was 300mm.

The multiple swirling and dividing forced upon the two aerosol streams from the nebulisers ensured a good mixing without undue back pressure, and any deposited droplets were able to drain freely down the vertical column. The efficiency of the mixer and

Experiment No.	Solution used	
	Nebuliser 1	Nebuliser 2
1	1 M HCl	1 M HCl
2	Analytes at 10 μg ml^{-1} in 1 M HCl	1 M HCl
3	Ca at 5000 μg ml^{-1} in 1 M HCl	1 M HCl
4	Analytes at 10 μg ml^{-1} + Ca at 5000 μg ml^{-1} in 1 M HCl	1 M HCl
5	Analytes at 10 μg ml^{-1} in 1 M HCl	Ca at 5000 μg ml^{-1} in 1 M HCl

Table 6.2
Experimental design for the comparison of matrix effects with equal calcium concentration added either concomitantly or by separate nebuliser.

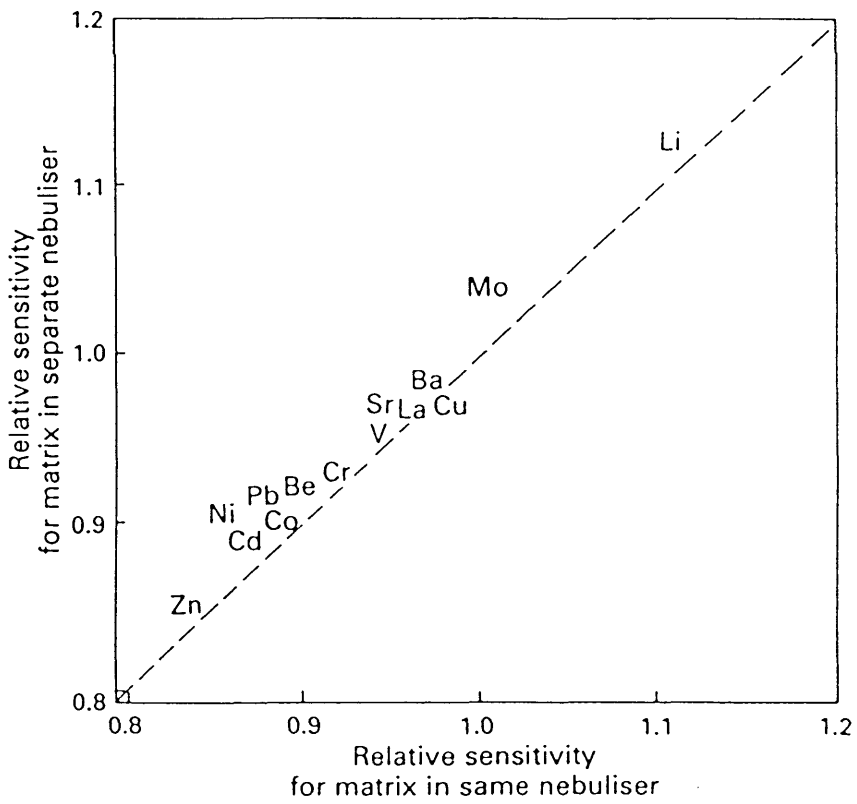


Fig. 6.7
Comparison of the effects of equal calcium concentrations on analyte line sensitivities when the calcium is added either as a concomitant element (i.e., in the same solution) or through a separate nebuliser.

the subsequent splitter was verified by the uptake of solution into each nebuliser combined with the observation of the instantaneous response of the ICPAES on a chart recorder. The system was stable for a period of up to 30 min, after which bulk liquid from condensed aerosol began collecting in the pipework, causing signal instability.

Table 6.2 shows the stages in which the test was conducted. As before, the relative sensitivity of an analyte in the presence of concomitant calcium at a particular level (S_c) was obtained from the formula:

$$S_c = (I_4 - I_3)/(I_2 - I_1) \quad \ldots\ldots\ldots \quad 6.1$$

where the numerical subscript refer to the analyte intensity for the experiment defined in Table 6.2. When the calcium was introduced at the same concentration but through a separate nebuliser, the new relative sensitivity (S_s) was given by:

$$S_s = (I_5 - I_3)/(I_2 - I_1) \quad \ldots\ldots\ldots \quad 6.2$$

Because the efficiency of the two nebulisers was almost identical the rates of introduction of calcium into the plasma were virtually equal in experiments 4 and 5. This was ascertained by recording calcium line intensities during the experiments simultaneously with the analyte line intensities. Thus S_c and S_s can be compared directly.

Fig. 6.7 shows the comparison of the relative sensitivities of the analytes for this level of calcium when it is introduced into the plasma either as a concomitant element (i.e., in the same solution) or when introduced separately by means of a second

nebuliser. The data points fall close to the equality of S_c and S_s. There is a small bias of about 1-2% between the results of the two methods of introducing calcium, which might suggest a small residual nebuliser effect. However the bias is comparable with the experimental error on a single result.

The result of this dual nebuliser study strongly confirmed the hypothesis that the matrix effect under examination arises in the plasma and not as a result of modified nebuliser operation. Any residual nebuliser effect could not have exceeded the experimental error in measuring S_c and S_s, which was of the order of 1% relative for each.

This result is rather more emphatic than those of previous workers. Boumans and deBoer (1976) found nebuliser effects (sensitivity changes) in the range 4-7% compared with plasma effects in the range 21-29%, when ultrasonic nebulisers were used. Blades and Horlick (1981b), studying the enhancement of Mg I 285.3 nm by sodium at a height of 10mm above the load coil, found that 23% of the observed effect was a nebuliser effect, possibly attributable to "aerosol ionic redistribution". Neither of these studies was carried out under operating conditions commonly used in task-related analysis, however, and both studies agree with the present work that the plasma effect greatly predominates over any possible nebuliser effect.

6.3.5 **The Stability of the Matrix Effect**

Under stable conditions of operating the plasma, the matrix effects remain constant and reproducible. When minor changes are introduced into the system, such as those brought about by replacing plasma torches or nebulisers, the broad pattern of

effects remains similar to that described, but with some small variations. Fig. 6.8 shows comparison between the current experiment and a similar experiment conducted 3 years previously, under nominally identical conditions. The greatest differences were observed with elements from the extremes of the range, viz., zinc and lithium. Lithium in particular had changed from a small supression to a small enhancement, and the viewing height used is clearly close to the crossover point for this element.

The differences are probably the combined results of spatial variations in the effect at different parts of the plasma, and in minor variations in viewing height and injector gas flow rate supplied to the plasma.

The viewing height used in this experiment minimises the matrix effect for most elements on our instrument, and is similar to the compromise position widely used for multielement analysis. Similar matrix effects to those detailed above have also been observed on ICPAES instruments from five separate manufacturers, each instrument running under its operating conditions recommended for routine analysis (Thompson, M., personal communication).

6.3.6 Interim Conclusions from Investigation of Matrix Effects from Calcium

The conclusions from this single matrix investigation related to the objectives set out (6.1) can be summarized as follows.

i) The potential inaccuracies from some matrix effects are large (e.g. -36%).

ii) Analyte susceptibility is related to the total excitation potential of the analyte line.

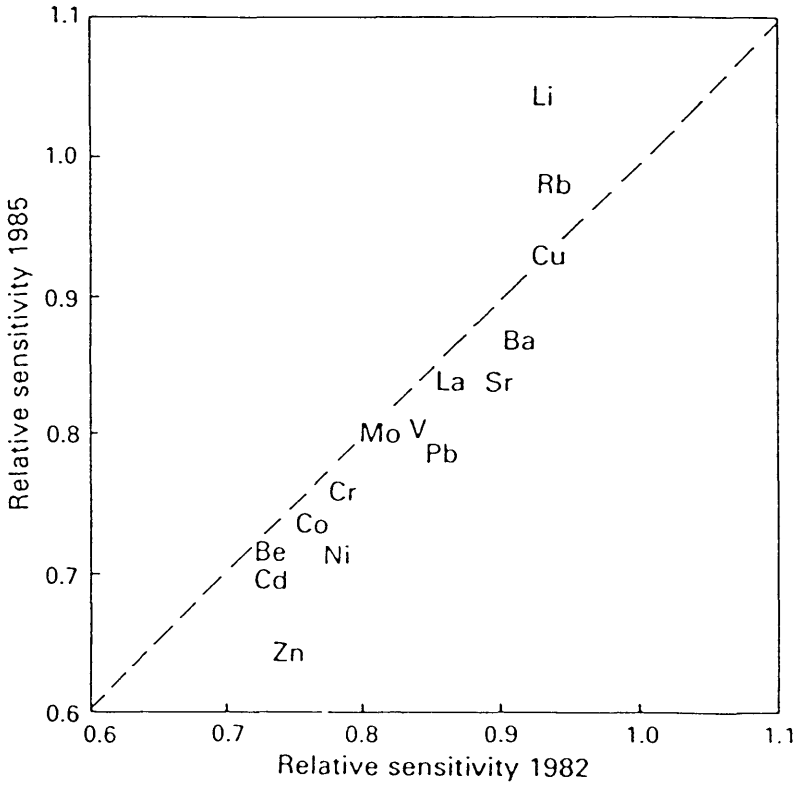


Fig. 6.8
Change in matrix effect in two nominally identical experiments separated in time by about 3 years. The differences are due to small variations in operating conditions (e.g., different plasma torches and nebulisers).

iii) The origin of the matrix effects from calcium has been traced to be almost exclusively in the plasma rather than the nebuliser.

iv) Any theory for cause of matrix effects must predict the relationship with total excitation potential.

v) The effect of increasing concentrations of calcium on the relative sensitivities of analytes is not simply linear. Analyte concentration does not however have any significance on its measured relative sensitivity i.e. the matrix effect.

vi) Alternative strategies to simple matrix matching for overcoming matrix effects are made possible by the stability and partial predictability of the effects.

Of the many options open for extending this work two were considered most pertinent a) to extend the experimental methods devised for calcium to other matrix elements in order to assess the significance of the conclusions drawn from calcium and b) to set up a hypothesis which would explain the occurrence of the relationship between matrix effects and analyte total excitation potential.

Historically these two objectives were not pursued strictly sequentially and generally a) came before b). For clarity of explanation however b) will be taken before a) in section 6.4.

The relationship between calcium concentration and the various analyte relative sensitivities is developed empirically in section 7.4. Options for methods of overcoming matrix effects are described in Chapter 7.

6.4 The Proposed Mechanism of Matrix Effects due to Calcium

6.4.1 The Effect of Temperature on Spectral Intensity

A theoretical mechanism was sought which would account for the experimental data. From the finding that the matrix effect originated in the plasma itself, inspection of the equation describing spectral intensity was an obviously important first step. The selection of temperature as the critical variable in this relationship was initially intuitive but subsequently substantiated.

In the study of the matrix effects from calcium a high correlation was found between the relative sensitivity of the analyte line in the presence of Ca and its total excitation potential (this includes ionisation energy for ion lines). The mechanism underlying this relationship was sought by consideration of the equation describing the net intensity I of the emission from an atom line (Boumans 1966).

$$I = (lAh\upsilon ng/4\pi Z) \exp(-E/kT) \quad \ldots\ldots 6.3$$

where l is the depth of the source, A is the transition probability, h is Planck's consant, υ is the frequency of the transition, n is the number of atoms, g is the statistical weight of the excited state, Z is the partition function, E is the excitation potential of the excited state, k is the Boltzmann constant and T is the atomic excitation temperature.

Assuming initially that only the exponential term varies significantly with small changes of temperature, then equation 6.3,

in its logarithmic form, differentiated with respect to temperature gives

$$\frac{\delta}{\delta T} \ln I = E/kT^2 \quad .....6.4$$

For a relatively small change in temperature ΔT this becomes

$$\ln I = E \Delta T/kT^2 \quad ... 6.5$$

If the intensity of analyte emission is I^o in the blank matrix and I' when calcium is present, then the intensity change caused by the calcium is given by

$$\ln I = \ln I' - \ln I^o = \ln (I'/I^o) = \ln S \quad ... 6.4$$

where S is the relative sensitivity. Equation (3) now becomes

$$\ln S = E \Delta T/kT^2 \quad .... 6.7$$

The implication of this equation is, that if the introduction of calcium to a plasma with excitation temperature T caused a drop in temperature ΔT, then there would be a linear relationship between the relative sensitivities of a range of analytes (ln S) and their corresponding excitation potentials. The relationship would apply equally to ion lines for which it can be derived by an analogous method.

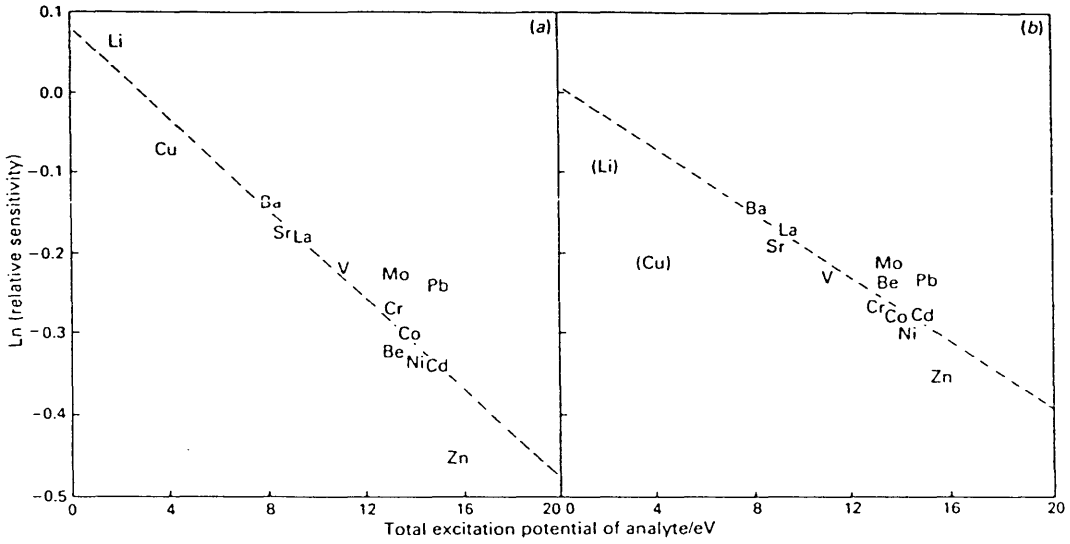


Fig. 6.9
(a) Relative sensitivities of 14 analytes in 10000 μg ml^{-1} calcium plotted against the total excitation potential of each analyte line. These linear relationships are consistent with a fall in excitation temperature in the plasma of 130 ± 14K caused by the calcium. (b) Relative sensitivity data adjusted for the change in the numbers of atoms and ions caused by the change in temperature. The ion lines lie on a linear trend consistent with a fall in excitation temperature in the plasma of 94 ± 17K caused by the calcium. The atom lines, in parentheses, were not used in the regression.

Wavelength/nm	Excitation potential/eV	Relative sensitivity
239.856	5.168	32
272.165	4.555	5
299.496	6.019	50
299.731	6.022	69
422.673	2.933	12 841
504.163	5.168	62
616.644	4.532	26
657.278	1.886	1
732.615	4.625	94

Table 6.3
Nine calcium lines used for the determination of excitation temperature.

Hence a fall in excitation temperature is consistent with the linear relationship between log relative sensitivity and excitation potential shown in Fig. 6.3. The same data are replotted with the logarithm of the relative sensitivity in Fig. 6.9a.

Inspection of equation 6.7 shows that the slope of the regression line shown in Fig. 6.9a can be used to calculate ΔT, the fall in excitation temperature required to produce the observed changes in the analyte sensitivities. The calculation however requires a value for the excitation temperature T, which was determined in a separate experiment.

6.4.2 Determination of Excitation Temperature

The method employed was that described by Boumans(1966, p103), using the intensities of the nine different calcium atom lines listed in Table 6.3. The sequential spectrometer (ARL 3520) described in Chapter 3, Table 3.1 was used to measure the relative intensities I of the nine lines, in their regions of linear response, and the values were corrected for the variations in photomultiplier response. Data for frequency (υ), statistical weight(g) and transition probability (A) were taken from Weise et al (1969) and used to calculate a modified intensity I_n where

$$I_n = I / gA\upsilon \qquad .... 6.8$$

For any pair of atom lines of excitation potentials E_1 and E_2, combining equations 6.3 and 6.8 gives

$$\text{In } (I_1/I_2) = (E_2 - E_1)/kT \qquad ..... 6.9$$

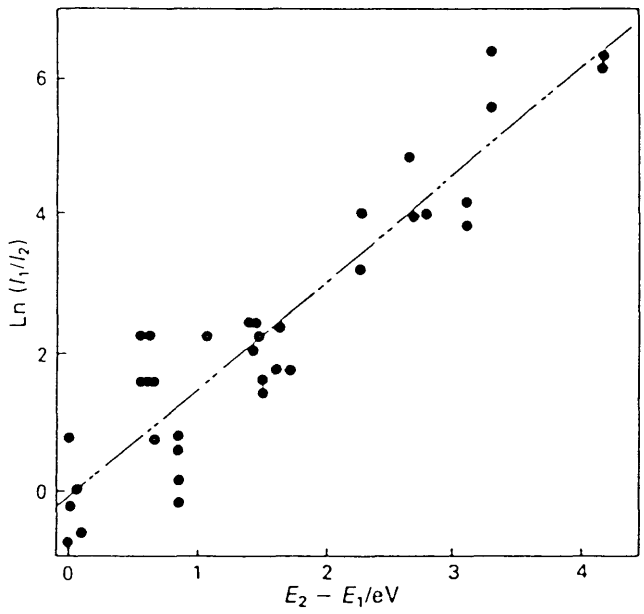


Fig. 6.10
Determination of excitation temperature using pairs of calcium atom lines. The modified intensity ratio varies as a function of the difference in excitation potential with a slope yielding an excitation temperature of 7460 $\pm$ 500K.

Fig. 6.10 shows the values of the modified intensity ratio against difference in excitation potential for the 36 pairs of atom lines measured. The slope of the regression line through the points gave an excitation temperature of 7460K with an approximate standard deviation of 500K. This value agrees well with other values of excitation temperature under similar operation conditions (Alder et al.,1980).

6.4.3 Determination of Change in Excitation Temperature

Using this value of excitation temperature (T), the change in excitation temperature (ΔT) can be calculated from the slope of the regression line shown in Fig. 6.9a, using equation 6.7. The value calculated was -130K with a standard deviation of 14K, for analytes in a 1% m/V calcium solution.

From comparison of this result with the uncertainties in the direct excitation temperature determination ($\pm$500K) it was evident that (i) a direct measurement of T alone could not detect such small changes in excitation temperature, (ii) the value of -130K was dependent to a secondary degree on the uncertainty in the direct measurement T, and therefore slightly less certain than its small standard deviation would suggest.

The initial assumption of a constant number of atoms (n) and ions with temperature, was clearly an over simplification. The Saha equation can be used to calculate the degree of an ionisation α_j of an element j, if local thermodynamic equilibrium (LTE) is assumed. From Boumans (1966) we have a working version of the Saha equation.

$$\log (\alpha_j/1 - \alpha_j) = -\log p_e + 2.5 \log T - 5040\, V_{ij}/T + \log(Z_{ij}/Z_{aj}) - 6.18 \quad \ldots\ldots 6.10$$

where p_e is electron pressure (atm), T the ionisation temperature (K), V_{ij} the ionisation potential (eV), Z_{aj} the partition function for the atom of element j and Z_{ij} for the corresponding ion. Values of V_{ij}, Z_{aj} and Z_{ij} were interpolated from Drawin et al., (1965) except for elements Mn, Be and La where no data for Z were available at 7500K. Extrapolation of data from Boumans (1966, p164) was considered justified as an approximation in these cases.

The ionisation temperature was taken to be equal to the experimentally determined excitation temperature by assuming LTE. Disparities between these temperatures have been reported (Nojiri et al., 1983) and direct measurement of ionisation temperature would clearly be necessary for more accurate estimation of α_j. The value used for electron pressure p_e (2.55×10^{-3} atm) was calculated from the electron density (n_e) reported by Nojiri et al., (1983), measured under similar operating conditions, using the equation

$$p_e = n_e\, kT \quad \ldots\ldots 6.11$$

For each emitting species the ratio was calculated between the number n^o of atoms or ions present at the initial temperature T (7500K) and the number n' at the lower temperature T- T (7370K). Equation 6.7 then becomes

$$\text{In } S - \text{In } (n'/n^o) = E\ T/kT^2 \quad \ldots\ldots 6.12$$

The relative sensitivity data shown in Fig. 6.9a when corrected for n'/n^{o} is replotted in Fig. 6.9b. The ion lines still give a linear trend after this correction, with a slope yielding a fall in excitation temperature of 94 $\pm$ 17K. The scatter of the atom lines Li and Cu after the correction suggests that these simple assumptions do not fully describe the behaviour of atom lines. However, the overall picture remains one of a drop in excitation temperature of ca. 100K being a convincing explanation for the changes in sensitivity of the analytes in a 1% m/V calcium matrix.

To estimate the drop in excitation temperature at various calcium concentrations, a ΔT value was calculated for each analyte at each calcium concentration studied in Section 4.3.1. using equation (6.12). These values, together with an average for each calcium concentration are shown in Fig. 6.11. A small fall in temperature of ca. 20K can be discerned for a calcium concentration as low as 100 $\mu g\ ml^{-1}$. The trend appears to be slightly non linear curving away from the temperature axis.

6.5 The Multi-Matrix Domain

Investigations of matrix elements other than calcium have several aims. The general objective of this chapter is to identify which matrix elements cause large and hence importamt matrix effects and equally to discern which elements do not cause significant effects. A more fundamental objective is to test the general conclusion drawn from investigations into calcium that a drop in excitation temperature is responsible for the symptoms of matrix effects. The ultimate objective was to find a theoretical

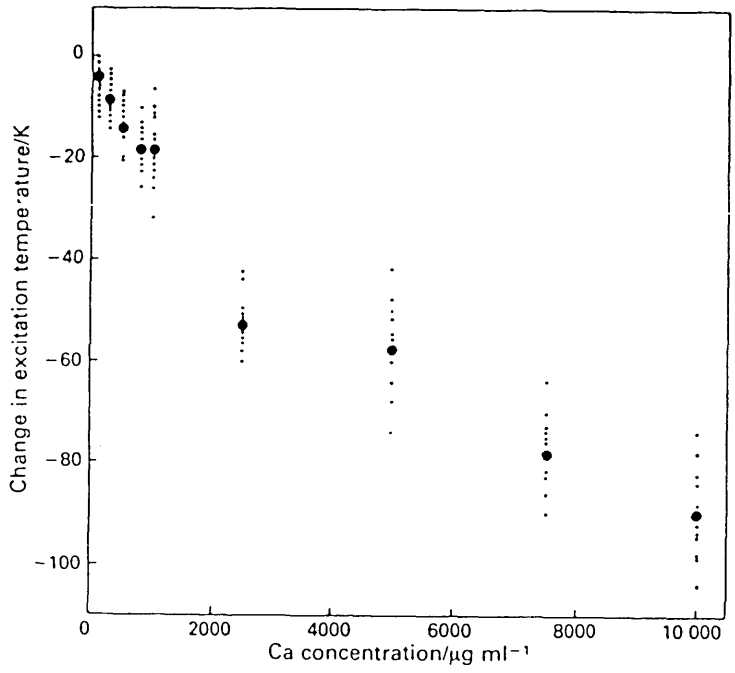


Fig. 6.11
Fall in excitation temperature calculated from relative sensitivity measurements, for a range of analyte in matrices of calcium at various concentrations.

Matrix element	(1) First ionisation potential/eV	(2) Degree of first ionisation/eV	(3) Second ionisation potential/eV	(4) Degree of second ionisation/eV	(5) "Total ionisation energy"/eV	(6) "Dissociation energy"/eV	(7) "Matrix energy demand"/eV	(8) Concentration/ μg ml⁻¹	(9) Relative sensitivity of Zn
Al	5.98	0.9487	18.8	<0.0001	5.67	3.17	8.85	1350	0.955
Ba	5.21	0.9970	10.0	0.0382	5.58	5.84	11.42	6870	0.818
Be	9.32	0.5372	18.2	<0.0001	5.01	3.73	8.73	451	0.916
Ca	6.11	0.9917	11.9	0.0045	6.11	5.17	11.28	2000	0.816
Cu	7.72	0.7320	20.3	<0.0001	5.65	0.69	6.35	3180	—
Fe	7.90	0.8887	16.2	<0.0001	7.02	2.91	9.93	2790	0.876
K	4.34	0.9965	31.8	<0.0001	4.32	2.98	7.30	1960	0.992
La	5.61	0.9948	11.4	0.0243	5.86	8.51	14.37	6950	0.704
Li	5.39	0.9908	75.6	<0.0001	5.34	3.43	8.77	347	0.958
Mg	7.64	0.9370	15.0	<0.0001	7.16	3.24	10.40	1220	0.892
Mn	7.43	0.9352	15.6	<0.0001	6.95	2.97	9.92	2750	0.877
Na	5.14	0.9934	47.3	<0.0001	5.11	2.91	8.02	1150	0.957
Ni	7.63	0.7859	18.2	<0.0001	6.00	2.79	8.78	2940	0.915
Pb	7.41	0.9183	15.0	<0.0001	6.81	0.80	7.60	10360	0.962
Rb	4.18	0.9973	27.5	<0.0001	4.17	2.84	7.01	4270	0.985
Sr	5.69	0.9947	11.0	0.0154	5.83	5.36	11.19	4380	0.844
Ti	6.83	0.9789	13.6	0.0008	6.70	4.58	11.28	2400	0.773
Zr	6.84	0.9700	13.1	0.0005	6.64	6.53	13.17	4560	0.768

Table 6.4
Information on matrix elements.

connection between the effects of all metallic matrix elements which would allow the prediction of their matrix effect on any analyte, i.e. a predictive model.

6.5.1 Experimental Design

A range of 18 metallic elements were chosens as matrices for this study. Non metals were excluded as being outside the scope of the present work. The metals included all the major elements of geological interest (Al, Ca, Fe, K, Mg, Mn, Na) but also elements less commonly encountered practically but with extreme physical properties. (For example Rb and La have extreme first ionization potentials and Cu forms a chloride with a low dissociation energy). The concentration of all matrix element was made equal on a molar basis for maximum comparability. The value of 0.05M was chosen to be the highest practicable for stable nebuliser performance. The actual m/V concentrations used are given in Table 6.4 column 8. Each solution contained only one matrix element.The range of 16 analytes was the same for all matrices and also the same as that in the calcium study, with the addition of sodium. Analyte elements were present at 5 $\mu g\ ml^{-1}$ except for Be, Cd and Mo which were at 0.5 $\mu g\ ml^{-1}$. The lead matrix was an exception with only two analytes Zn and Cd being measured and having an acid matrix of 1.6M nitric acid. All other solutionswere in a 1.0M hydrochloric acid matrix.

The relative sensitivity for each matrix was again measured as described in Section 3.4 to minimize errors from drift.

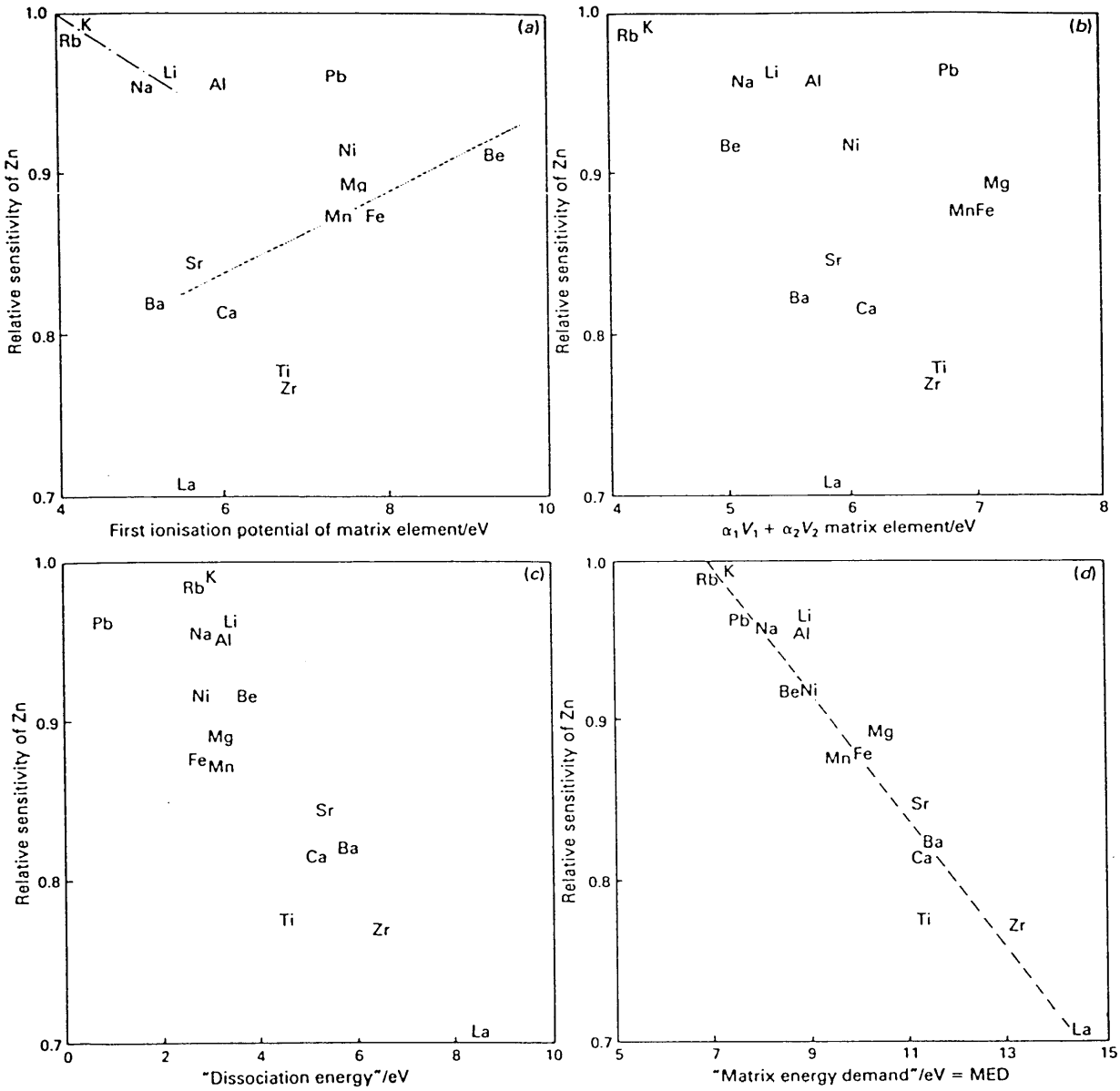


Fig. 6.12
Matrix effect on a single analyte, zinc, expressed as relative sensitivity, for a range of 17 matrix elements at 0.05 M expressed as a function of various properties of the matrix element. (a) First ionisation potential. No overall trend is evident (r = -0.14) although elements from Groups I and II of the Periodic Table lie on their own 'pseudo trends' (broken lines). (b) "Total ionisation energy" including first and second ionisation potentials and degrees of ionisation. Again, no overall trend is evident (r = -0.47). (c) "Dissociation energy" derived from lattice energy without cation ionisation potentials. A discernable trend is evident but with a large amount of variability (r = -0.86). (d) "Matrix energy demand" (MED) as summation of "total ionisation energy" and "dissociation energy" gives a linear relationship with a high degree of correlation (r = -0.97). MED can therefore be used as a predictive property.

6.5.2 **Results**

A significant problem in discussing the results of this study is data presentation. The deductions to be made from the full 'matrix' of 18 matrix elements and 16 analytes (given Appendix D) can be explained initially by reference to one analyte across all the matrix element i.e. in the multi-matrix domain. This approach contrasts with the previous figures and discussion which have been of multiple analytes in one matrix element, i.e., in the multi-analyte domain.

Initially zinc is considered as the single exemplary analyte with its relative sensitivities across the multi-matrix domain given in Table 6.4 column 9. In this context calcium can be seen to cause larger matrix effects than most elements. Some elements, notably lanthanum, titanium and zirconium, produce greater effects than calcium.

A primary objective of this work was to identify which fundamental properties of the matrix elements determined the magnitude of the matrix effect and hence enable useful predictions to be made. A property previously suggested to relate to the matrix effects of elements from Group I of the periodic table is the first ionisation potential of the matrix element (Faires et al., 1983). Fig. 6.12a shows the relative sensitivity data for Zn given in Table 6.4 (column 9) plotted against the first ionisation potential of the matrix element (column 1). (The value for the copper matrix was omitted due to uncertainties caused by a large spectral overlap). No functional relationship is evident (correlation coefficient $r = -0.14$), although points for both Group I and Group II elements fall misleadingly on their own 'trends', but in opposite directions. This illustrates the limitations of

generalisations derived from studies encompassing only a few analytes, particularly when restricted to a single group of the periodic table.

From a consideration of degrees of ionisation (calculated from the Saha equation, and given in columns 2 and 4 of Table 6.4, then it is evident that at 7500K certain matrix elements are only partially first ionised (e.g. Be 54%), while others are significantly second ionised (e.g. Ba 4%). The total "Ionisation Energy" V_{TOT} given in column 5 in Table 6.4 is thus more appropriate than the first ionisation potential, and can be given by

$$V_{TOT} = \alpha_1 V_1 + \alpha_2 V_2 \qquad \ldots\ldots 6.13$$

where V is appropriate ionisation potential and α the corresponding degree of ionisation. Fig. 6.12b shows the same data (Zn relative sensitivity) plotted again this function V_{TOT} for each matrix element. This again proved inadequate as a functional relationship ($r = -0.47$, $p = 0.05$).

Considering the matrix element to cause removal of energy from the plasma a further possible energy requirement was the lattice energy of the species which entered the plasma after desolvation (e.g. $AlCl_3$ in HCl). Lattice energy (U_n), however, is defined in relation to fully ionised products (e.g. Ca^{2+} or Al^{3+}) which is clearly inappropriate in the ICP except for univalent ions. A modified lattice energy with the sum of the ionisation potentials subtracted $U_n - \sum_{i=1}^{n} V_i$ was therefore considered. This "dissociation energy" for each matrice element (column 6 in Table 6.4) is plotted against the Zn relative sensitivity data in Fig. 6.12c. This relationship has a highly significant correlation ($r = -0.86$, $p = <.001$) and showed a discernable trend, with La being

now correctly extreme in both values.

The next logical step was to combine the "dissociation energy" and the "ionisation energy" V_{TOT} in a total "matrix energy demand" (MED) M. This is given by:-

$$M = U_n - \sum_{i=1}^{n} V_i + \alpha_1 V_1 + \alpha_2 V_2 \quad ...6.14$$

where U_n is the lattice energy of the matrix element in the valency state n, as the chloride (e.g., for Al in HCl this would be the lattice energy of $AlCl_3$ expressed in eV). V_i is the ith ionisation potential (in eV) summed to the maximum value n. The values of all these terms are given in column 7 in Table 6.4 for each matrix element.

The values of MED for the matrix elements are plotted against the same Zn relative sensitivity data in Fig. 6.12d. The trend is now clearly linear ($r = -0.97$). Regression statistics are given in Table 6.5. The scatter of points can be attributed to three sources (i) experimental error in the relative sensitivity, estimated as $\pm$ 1%; (ii) uncertainties in the MED data, for example in the value used for ionisation temperature to calculate the degree of ionisation; and (iii) deviation from the model.

Considering now the multi-analyte data, a consistent pattern emerges. The behaviour of the zinc line as an analyte in various matrices was typical of the complete range of analytes studied, although the other analytes were affected, as expected, to a smaller extent, dependent on their total excitation potentials.

Each analyte line tested showed a similar linear relationship to that of zinc against the MED of the matrix element. Regression data are given in Table 6.5. All the standard errors on the slope

Analyte line	Slope/eV^{-1} × 10^2		Intercept	
	Coefficient	Standard error	Coefficient	Standard error
Ba	−1.056	0.284	1.057	0.018
Be	−2.328	0.208	1.129	0.021
Cd	−2.877	0.284	1.176	0.028
Co	−2.437	0.248	1.158	0.024
Cr	−2.504	0.240	1.170	0.024
Cu	+0.428	0.180	0.935	0.018
La	−1.281	0.561	1.052	0.053
Li	+1.064	0.199	0.868	0.020
Mo	−2.456	0.498	1.166	0.049
Na	+0.985	0.197	0.883	0.020
Ni	−2.790	0.315	1.179	0.031
Pb	−1.707	0.331	1.095	0.033
Rb	+1.431	0.245	0.839	0.025
Sr	−1.733	0.347	1.102	0.034
V	−1.874	0.195	1.122	0.019
Zn	−3.996	0.261	1.278	0.026

Table 6.5
Regression coefficients of analyte relative sensitivity against matrix energy demand (MED).

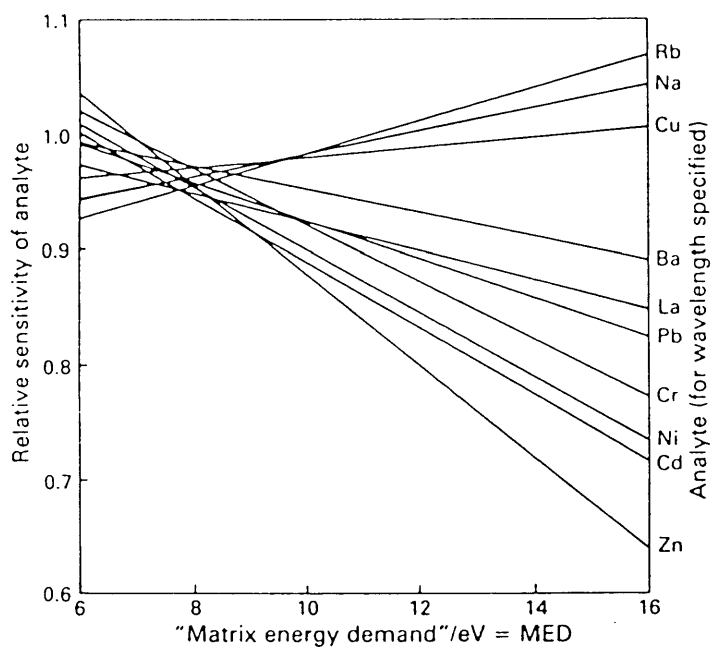


Fig. 6.13
Variation in matrix effects on ten representative analytes as from a range of matrix elements expressed as a function of their MED. Regression coefficients are given in Table 6.5

of the individual regression lines are similar indicating equally small scatter of points about the line (although the slopes of a few are not significantly different from zero e.g. Cu).

The regression lines of 10 representative analytes are shown in Fig. 6.13. Lines for the other analytes were excluded to improve the clarity of the diagram. The atom lines increase in relative sensitivity with increasing MED, in contrast to all the ion lines. This fact qualitatively supports the hypothesis of falling excitation temperature with matrix element addition, as the fraction of the element present as atoms would therefore increase whereas the population of ions should decrease according to the Saha equation. The net change in relative sensitivity is therefore determined by a balance between changing degree of ionisation and changing emission intensity. Matrix elements with values of MED less than 9 eV (e.g. Li, Na, K, Rb, Be, Ni, Cu, Al and Pb) can be seen to produce no matrix effect exceeding $\pm$ 10%, for any analyte, under the operating conditions used.

The relationship between analyte relative sensitivities for one value of MED (i.e. Ca) has already been shown to be a function of the analyte line excitation potential (Fig. 6.3). This "pattern" is clearly seen in Fig. 6.13 extending to other matrix elements with higher values of MED. The pattern becomes obscured at lower values of MED. A more systematic expression of the relationship should be exposed by plotting for each analyte the slope of the regression line (from Table 6.5) against their appropriate excitation potential. This is shown in Fig. 6.14a. There is clearly a single linear trend incorporating both the enhancement of the atom lines and the increasing suppression of the ion lines. (Only the Pb value lies far from the line which may

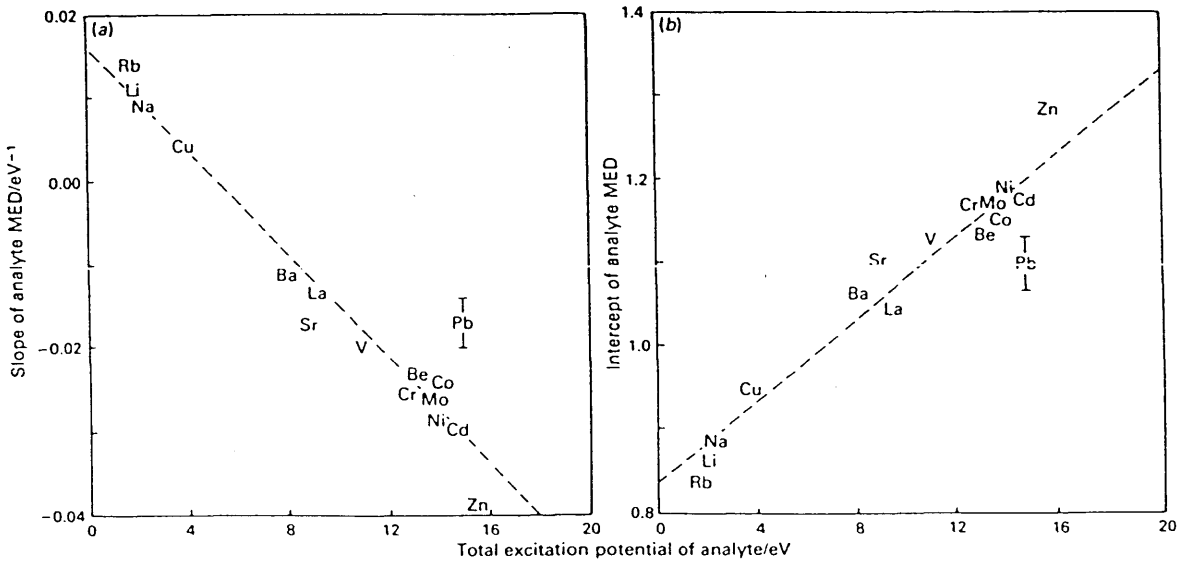


Fig. 6.14
(a) Slopes and (b) intercepts of the regression lines shown in Fig. 6.13 (and listed in Table 6.5) as a function of the total excitation potential of the analyte line. Both trends are linear and enable a predictive model of matrix effects to be considered.

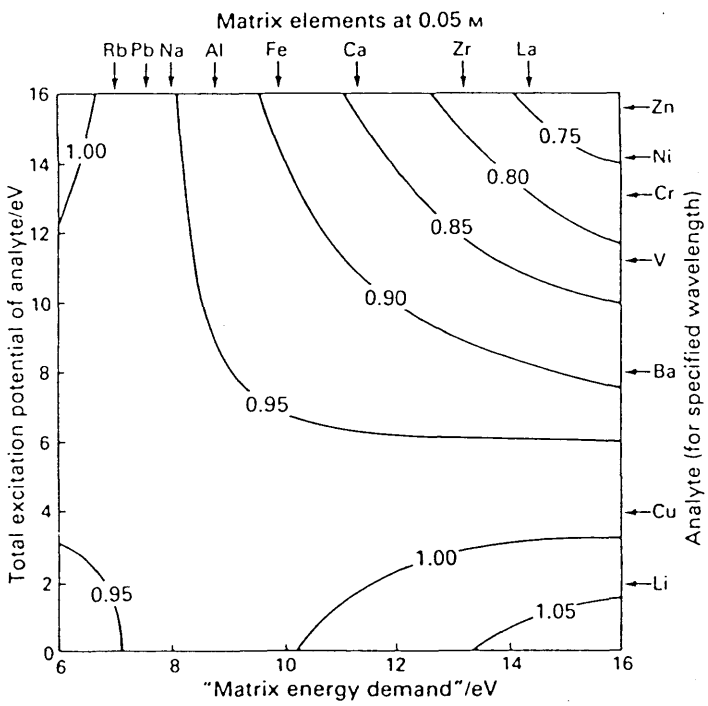


Fig. 6.15
Contour map of predicted matrix effects generated with equation (6.15) annotated with selected analyte and matrix elements. The contour lines are for values of equal relative sensitivity. To predict a relative sensitivity of any analyte - matrix combination, locate the coordinates of the excitation potential of the analyte line and the MED of the matrix element. Biases of > 10% occur only in the top right-hand corner of the diagram.

indicate a suspect excitation potential value). The regression statistics for the line are slope (standard error) -0.00312 (0.00012) and intercept (standard error) 0.0161 (0.0013).

A visual inspection of Fig. 6.13 suggested that there also might be a systematic trend in the intercepts of the regression lines. These are plotted in Fig. 6.14b again, against the analyte line excitation potential. The least squares regression line again gives a significant result: slope (standard error) 0.0244 (0.0013) eV^{-1} and intercept (standard error) 0.0835 (0.014).

The scatter of points however is greater than in Fig. 6.14a as the typical error bars indicated. These two regression equations can be combined to produce a single equation that predicts the relative sensitivity (S_{im}) of any analyte i line of total excitation potential E_i (eV) in any matrix element m of matrix energy demand M_m (eV) at a concentration of 0.05M by

$$S_{im} = M_m (0.0161 - 0.00312 E_i) + 0.0244 E_i + 0.835 \quad ...6.15$$

The implications of this relationship can be best perceived by the graphical representation of equation 6.15 shown in Fig. 6.15. The two axes give the energies associated with the plasma processes, the x-axis showing the 'matrix energy demand' for the matrix, the y-axis showing the excitation potential for the analyte. The contour lines are for constant values of predicted relative sensitivity (i.e. matrix effect) from equation 6.15.

Several general observations can be made from this figure. A large area of the diagram (about 50%) has an expected bias of less than 5%. This confirms the general observation that ICPAES is largely free of serious matrix effects. For example no analyte

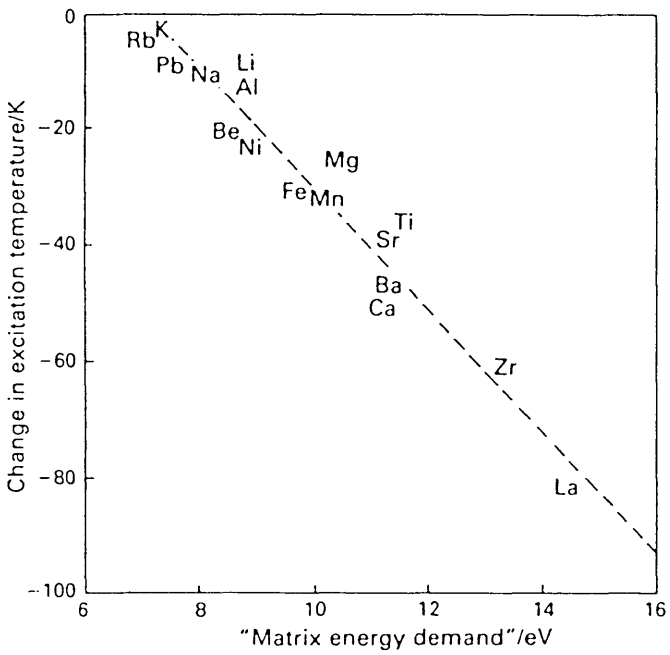


Fig. 6.16
Calculated fall in excitation temperature caused by a range of matrix elements using the zinc analyte as a thermometer. The trend is clearly linear and supports the hypothesis that matrix elements remove energy from the plasma in proportion to their MED.

will be seriously biased by a sodium matrix of 0.05M. Furthermore there is only a relatively small area (ca. 25%) of the figure which predicts large (>10%) matrix effects. These are restricted to analyte lines of high excitation potential (>8eV) in matrices of large MED (>10eV).

A suggested use of this diagram is to identify matrix/analyte combinations which will require matrix matching or some form of bias correction, discussed in Chapter 7. A fully quantitative correction of matrix effect is possible using equation 6.15. However, this is obviously of limited use in applying only to one concentration of matrix element. An investigation of such a scheme is also discussed in Chapter 7. The next stage of this work would be to extend this predictive model by adding on the dimension of changing concentration of matrix element. With this extra dimension it should be possible to predict matrix effects quantitatively from fundamental properties of the analyte and matrix elements over a range of matrix concentration.

6.5.3 **The mechanism of plasma matrix effects**

Equation 6.15 was derived empirically and it is clearly desirable to find the theoretical justification for its existence. The first step is to attempt to extend to the multi-matrix domain the hypothesis that reduced excitation temperature is the mechanism of matrix effects.

For a given matrix element, the matrix energy demand is seemingly associated with a characteristic fall in the excitation temperature ΔT, as determined by equation 6.7. With equimolar matrixes (0.05M) there is a relationship between ΔT and the MED illustrated in Fig. 6.16. The regression line shown in Fig. 6.16

had the coefficients: slope (standard error) 10.46 (0.58) K eV^{-1}; and intercept (standard error) 74.30 (5.80)K.

The standard deviation on the value of ΔT calculated from this equation was estimated by simulation. It is also a function of MED but ranges from 7 to 11 K. The zinc analyte line sensitivity alone was employed to determine ΔT because of the relatively small uncertainties. However, all analytes gave linear relationships between their relative sensitivity and MED of the matrix element, and therefore they would all give linear relationships between ΔT and MED, over this range. The smaller the slope coefficient of the regression however, the greater is the uncertainty in the value of ΔT.

The qualitative interpretation of this relationship is that the higher the MED of the matrix element, the more energy is taken from the plasma and the greater the consequent drop in excitation temperature. The strong similarity between the effects on analyte sensitivities of the addition of calcium and a reduction of forward power, noted in section 6.3.2, lends further support to this hypothesis.

The similarity reported in Chapter 4 between the multi-analyte reponse to variations in forward power, injector gas flow or air temperature can now be extended to include the effect of all matrix elements with MED greater than 10eV. A common mechanism of variation in plasma excitation temperature would seem probable. This would also explain the successful extension of the 'parameter related internal standard method' (PRISM), initially devised for improving precision (Chapter 5) in removing bias due to matrix effects described in Chapter 7.

It is not clear whether the empirical connection between MED and ΔT, which provides a predictive model of matrix effects, can be directly extended into a causal relationship. There seems to be a discrepancy between the values of the power absorbed by the matrix, and that released by the plasma gas in cooling by ΔT. The power absorption associated with the MED can be calculated, given a figure for the efficiency of solution nebulisation and transfer to the plasma. A power of 0.010W is consumed when a 0.05M Ca solution sprayed at 1% efficiency at a rate of 1.05 ml min^{-1} (the Ca MED = 11.28 eV or 1,083 KJ mol^{-1}). The power loss associated with the temperature drop ΔT = 43.7K in 1 l min^{-1} argon is much greater however (at least x50).

A further area of uncertainty is the causal interpretation of the left hand side of Fig. 6.13. In this figure matrix elements with low MED (e.g. Rb) are seen to cause suppression of analytes with the lowest total excitation potential (e.g. Li) and cause slight enhancement to the analytes with high total excitation potential (e.g. Zn). In terms of " ΔT theory" this would imply that they increase excitation temperature, but the suppressions are much bigger than the enhancements which is unexpected. This is perhaps due to increase ionisation which would suppress these atom lines.

This is an inversion of the situation found in matrix elements of high MED. There is some similarity in effect between the addition of Rb (for example) and a lowering of solution uptake rate shown diagrammatically in Fig. 4.5. Both have minimal effects on the sensitivity of high excitation potential analytes such as Zn but both have most effect on the low excitation potential analytes such as Li, Na, K, Cu. There are a number of possible

interpretations of these observations. Experimental error in the data used in Fig. 6.13 was relatively high at the left hand side i.e. at low values of MED. For example, there is only one matrix with a MED value of less than 7 eV (Cu 6.35eV). Perhaps in reality with enough precise data points the lines in Fig. 6.13 would not cross but rather level off. That would made any interpretation of the inverted effect spurious. Inspection of the relative sensitivity data points in Appendix D, however reveals numerous cases of these inversion symptoms. For example, assuming this inversion phenomenon to be a real effect perhaps its mechanism is the same as that for changes in solution uptake rate. Changes in acidity recently examined by Botto (1985) are perhaps in effect changes in low values of MED and hence have the inverted, or 'uptake' multielement parameter signature. Further experimentation is clearly required.

6.6 **Summary**

Taking the objectives set out at the introduction to this chapter, a summary of the conclusions applying to routine operating conditions are:-

i) Matrix effects can cause inaccuracies up to ca. -30% and are thus in need of understanding and correction.

ii) Analyte lines of high total excitation potential are the worst affected.

iii) Matrix elements with high matrix energy demand (MED) values (e.g. >10eV) cause the largest inaccuracies (e.g. >10%). The majority of analyte/matrix combinations are relatively free of marix effects.

iv) All matrix elements with values of MED >10 eV give the same pattern of analyte susceptibility.

v) Fundamental properties of matrix element and analyte lines can be used to predict matrix effects quantitatively, but as yet only at one concentration of matrix element.

vi) Matrix effects due to metallic elements occur dominantly in the plasma rather than the nebuliser.

vii) Reduction in excitation temperature is consistent with the experimental findings as the dominant cause for matrix effects from metallic elements. Large matrix effects (>10%) correspond to reductions in excitation temperature of >30K).

viii) The effect of increasing concentration of calcium on the relative sensitivity of analytes is not a linear function. Further investigations are necessary to clarify the multi-matrix picture. Matrix effects are not significantly affected by changes in analyte concentration.

ix) A deeper understanding of the cause of matrix effects enables us to formulate fresh strategies for their correction. This will be described in Chapter 7.

CHAPTER 7

METHODS OF CORRECTING MATRIX EFFECTS

7.1 Introduction

From the investigations reported in Chapter 6 it is clear that the correction of matrix effects has a key role in obtaining the greatest accuracy by ICPAES analysis. The predictive model that has been developed enables the importance of particular matrix effects to be assessed in relation to the required accuracy of the analysis. This allows a reassessment of the general rule in ICPAES analysis, which is always to match the matrix of calibrating solutions with those of samples as far as is possible. In the absence of knowledge of the occurrence and size of matrix effects this was clearly a wise precaution, but a greater understanding of the mechanism of matrix effects enables a more selective approach to their correction. For analysis of the greatest accuracy in many types of sample there is a requirement for an assessment of suitability of current methods and the development of new methods of matrix effect corection. The ideal qualities of such a method would be that it was:-

A) Effective in removing bias from all analytes to within precision uncertainty (ca $\pm$1%).

B) Flexible - (i) to allow for variability in the concentration of the matrix element, (ii) to allow for mixtures of different matrix elements.

C) Rapid - should not reduce the productivity for sample preparation and analysis by a significant factor (e.g. < 2).

D) Robust and practicable for routine multielement analysis.

E) Capable of being automated, i.e. to run without routine human intervention.

Eleven methods of matrix effect correction are discussed. Three methods, constant matrix matching, simple internal standardisation and simple standard additions are well known. A fourth is a generalisation of the later (GSAM). Seven other novel methods are considered, five with experimental trials, and the relative strengths and weaknesses of all the method will be discussed at the end of the Chapter.

7.2 Current Methods of Correcting Matrix Effects

Matrix effects can be eliminated, and in that sense corrected, by removal of the matrix elements prior to analysis. These non-instrumental methods such as solvent extraction or ion exchange are outside the scope of this discussion , but clearly fail the majority of the criteria listed above.

There are only three current instrumental methods of overcoming matrix effects. The first, simple matrix matching, is the traditional matching of the matrix of the calibrating solution at a fixed level with that of the sample. As discussed earlier this method performs well for samples with predictable and closely similar major element compositions. Impurities in the matrix element used in the calibrating solutions can cause unsuspected errors. This particular problem will become more significant as ICPAES developes and as detection limits become lower. The main limitation of simple matrix matching however, occurs when

sample compositions are not predictable and closely similar. This is typically the case for geological or environmental samples. In this situation, real variations in major elements contents can cause apparent variations in other elements which are totally erroneous. In the worst case a supposed geochemical inter-element correlation may be caused entirely by an analytical matrix effect.

The second current method of eliminating matrix effects is that of standard additions (Kirkbright et al.(1974), p475). In this technique each sample is used as the matrix for its own calibration. A series of additions with a range of analyte concentrations are made to portions of the sample solution. The sensitivity measured for the analyte in the presence of the sample is thus perfectly matrix matched. The intercept of the calibration line through the concentration axis gives an estimate of the analyte concentration in the sample. For accurate results, care must be taken in selecting the analyte concentrations for the standard additions in relation to the concentration of analyte present in the sample. For example an addition of 1 $\mu g\ ml^{-1}$ would be suitable for determining analyte levels at 0.1 $\mu g\ ml^{-1}$, but produce large errors with analyte levels of 100 $\mu g\ ml^{-1}$. In this latter case the estimation of the sensitivity for 1 $\mu g\ ml^{-1}$ would be made very imprecise by the large uncertainty on the response for 100 $\mu g\ ml^{-1}$ typically equivalent to $\pm$ 1 $\mu g\ ml^{-1}$. For single element techniques with large matrix effects such as Graphite Furnace Atomic Absorption Spectrophotometry such a careful application of the standard addition method is a viable proposition. For routine multielement ICPAES however, with the complication of perhaps 30 analytes at widely different concentrations between samples, the basic technique is clearly

impracticable. The standard addition method has the further limitation of not removing translational bias which must be corrected separately.

Improvements to simple standard additions method have been in two directions. The advent of flow injection analysis (FIA) has enabled computer controlled analyte additions of suitable aliquots for a given analyte (Greenfield 1983). Even under the most favourable conditions which minimise manipulative requirements, the method increases the time required for an analysis by several hundred percent for a single analyte.

The generalised standard additions method (GSAM) described by Saxberg et al.(1979) and Kalivas et al.(1981) was designed to be used for multielement analysis, so that a single set of solutions could be used for any matrix. GSAM incorporates a feature which also corrects spectral (translational) interference effects, which are independent of matrix effects and cannot be corrected purely by standard additions in the strict sense. Reported implementations of GSAM to ICPAES have to date, however, been disappointing. For example, Zugatto et al.(1983) describe a GSAM/FIA/ICPAES system for the simultaneous analysis of three analytes. The system requires about 10min for the analysis of each sample, in comparison with the period of about 1min required for a conventional ICPAES analysis for 40 elements. Thus it is not clear at this stage whether GSAM can be satisfactorily applied to task-directed multielement analysis.

Internal standardisation, which was discussed in detail in Chapter 5 as a method of improving precision can also be used to reduce matrix effects. Before the concepts of accuracy and precision were identified as being separate, internal standardisation was reported as a method of generally improving

data quality (Ahrens et al.1961, p90). Improved accuracy has been reported together with improved precision in applications of internal standardisation to ICPAES. Odegard (1981) expressed this improved accuracy crudely by averaging the biases caused by a range of matrix elements at concentrations said to be typical of geological analysis. The use of two simple internal standards reduced the average bias from 4.5% to 2.3% which constituted an improvement in accuracy, if not a total removal of matrix effects. The main limitation of simple internal standardisation, as discussed in Chapter 5, is the selection of a matched pair of lines as internal standard and analyte.

It is clear from the wide variation in matrix effects described in Chapter 6, that no single internal standard, could bring about accurate correction by a process of simple division.

Botto (1985) used simple internal standards with some success to correct matrix effects due to variations in acid concentration . Interestingly the residual errors after this correction were noted by Botto as being related to the total excitation potential of the analytes lines. This suggests a relationship between matrix effects derived from variations in acidity studied by Botto and of metallic elements studied here.

Five new methods of correction for matrix effects in ICPAES were developed in this research to overcome the shortcomings of the available methods and in an attempt to fulfill the criteria set out in Section 7.1. They are (i) a predictive model based on matrix energy demand called the MED-Model, (ii) an empirical model for variable concentrations of matrix element, called the Variable Concentration (VC) Model, (iii) a parameter related internal

standard method (PRISM) (iv) interactive matrix matching (IMM),and (v) interactive power adjustment (IPA).

7.3 The 'MED-Model' Method

In Chapter 6 an equation (6.15) was developed which predicted the relative sensitivity to be expected for any analyte in an aqueous matrix of a single metallic element at 0.05M concentration. The critical properties required are the total excitation potential (E') of the analyte line and the matrix energy demand (MED) of the matrix element. The main limitation of this equation is that it does not predict the variations of matrix effect with the concentration of the matrix element. This excludes its practical use for the correction of matrix effects in geochemical analysis. However, given that extra dimension, it should be possible to use the 'MED Model' as a very general tool to improve accuracy.

In order to make an initial appraisal of the likely performance of such a correction procedure, equation 6.15 was used to generate predicted relative sensitivities for each of the matrix/analyte line combinations previously measured, (listed in Appendix D). A graphical comparison of the predicted and experimental values is shown in Fig. 7.1. Out of an original 265 measurements 14 data points have been omitted where experimental error was high. This was due to either large translational interferences (background or line overlap) or memory effects when an element was measured as an analyte shortly after being run as a matrix element. The regression of experimental upon predicted relative sensitivity gave a slope of 0.98 $\pm$ .03 which is not significantly different from 1.0. This validates overall the

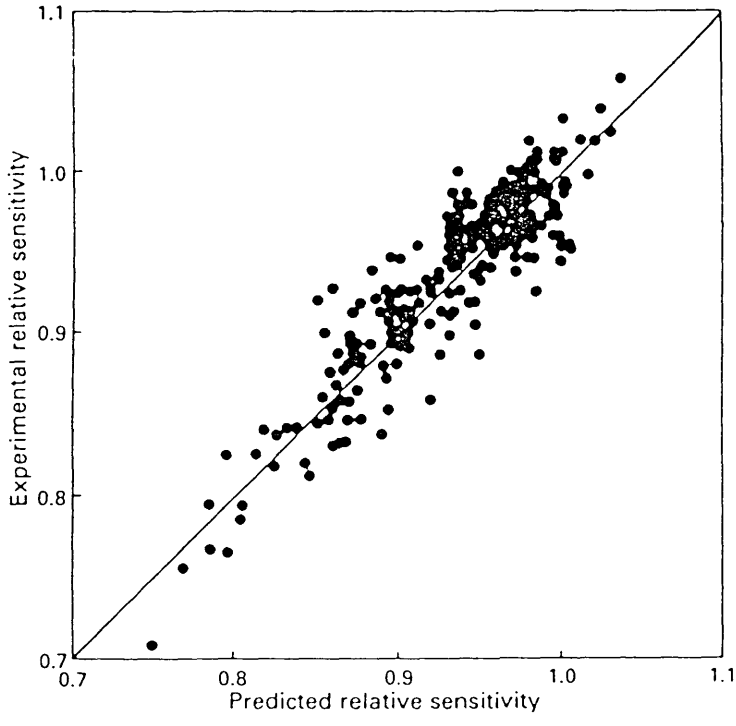


Fig. 7.1
Closeness of fit of the predictive model and the experimental relative sensitivities from which it was generated. A method of matrix effect correction based on the current model would be expected to reduce most matrix effects (-30 to +5%) to within a few per cent.

predictive power of the model represented by equation 6.15. The standard deviation of the residuals was 0.025 which quantifies the average uncertainty of the proposed correction technique. For practical purposes the correction procedure would therefore reduce the bias derived from serious matrix effects to a few per cent. The accuracy of the correction should improve with a more refined model, based on more precise measurements of relative sensitivity and calculation of MED values. For further flexibility the MED-Model should also be extended to allow for mixtures of matrix elements.

The MED-Model method is obviously not yet a practical option for matrix effect removal so that comparison with other methods against the five criteria (listed in 7.1) is tentative, and will be discussed in section 7.8. The accuracy should be comparable or better than in this example. Rapidity should be excellent, requiring only a brief computation after the initial constants have been established. Flexibility will be constrained only by the sophistication of the current model. It would be ideally suited to automation, being entirely software based, given adequate analytical quality assurance.

7.4 The 'Variable Concentration (VC) Model' Method

The main shortcoming of the tested MED model, was the inability to allow for variations in the concentration of the matrix element. Data in this dimension for the calcium matrix are given in Appendix C and have been discussed in Chapter 6. An obvious step was therefore to examine the relationships between the relative sensitivities (S) of the analytes at a range of calcium concentrations (c).

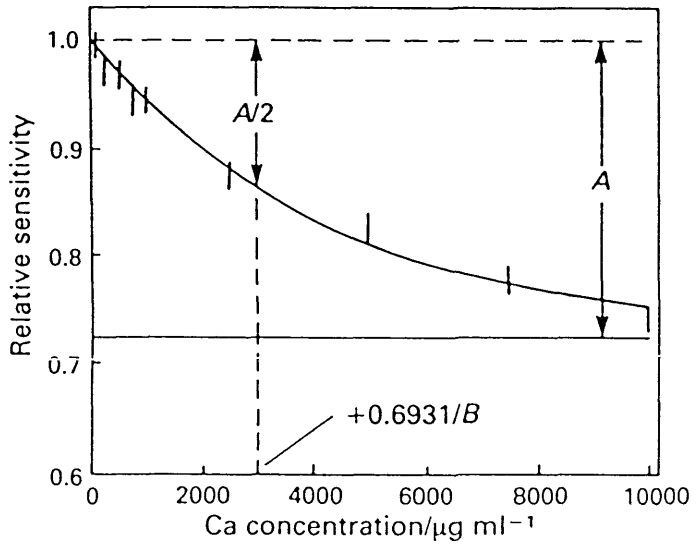


Fig. 7.2
Relative sensitivity of cobalt (S) as a function of calcium concentration (c), with the data points fitted to an exponential decay curve $S = 1 + A(1 - e^{-Bc})$.

Analyte	A	B
Zn	−0.340	4.3×10^{-4}
Cd	−0.279	3.1×10^{-4}
Ni	−0.288	2.8×10^{-4}
Pb	−0.236	2.1×10^{-4}
Co	−0.276	2.3×10^{-4}
Be	−0.269	3.6×10^{-4}
Cr	−0.245	2.3×10^{-4}
Mo	−0.222	2.4×10^{-4}
V	−0.241	1.6×10^{-4}
La	−0.250	9.9×10^{-5}
Sr	−0.260	9.8×10^{-5}
Ba	−0.295	5.8×10^{-5}
Cu	−0.100	1.0×10^{-4}
Li	+0.045	5.2×10^{-4}

Table 7.1
Matrix effect of calcium on various element lines, expressed as parameters of the empirical function $S_r = 1 + A(1 - e^{-Bc})$, where c is the calcium concentration (ug ml^{-1}) and S_r is the analyte sensitivity relative to c = 0.

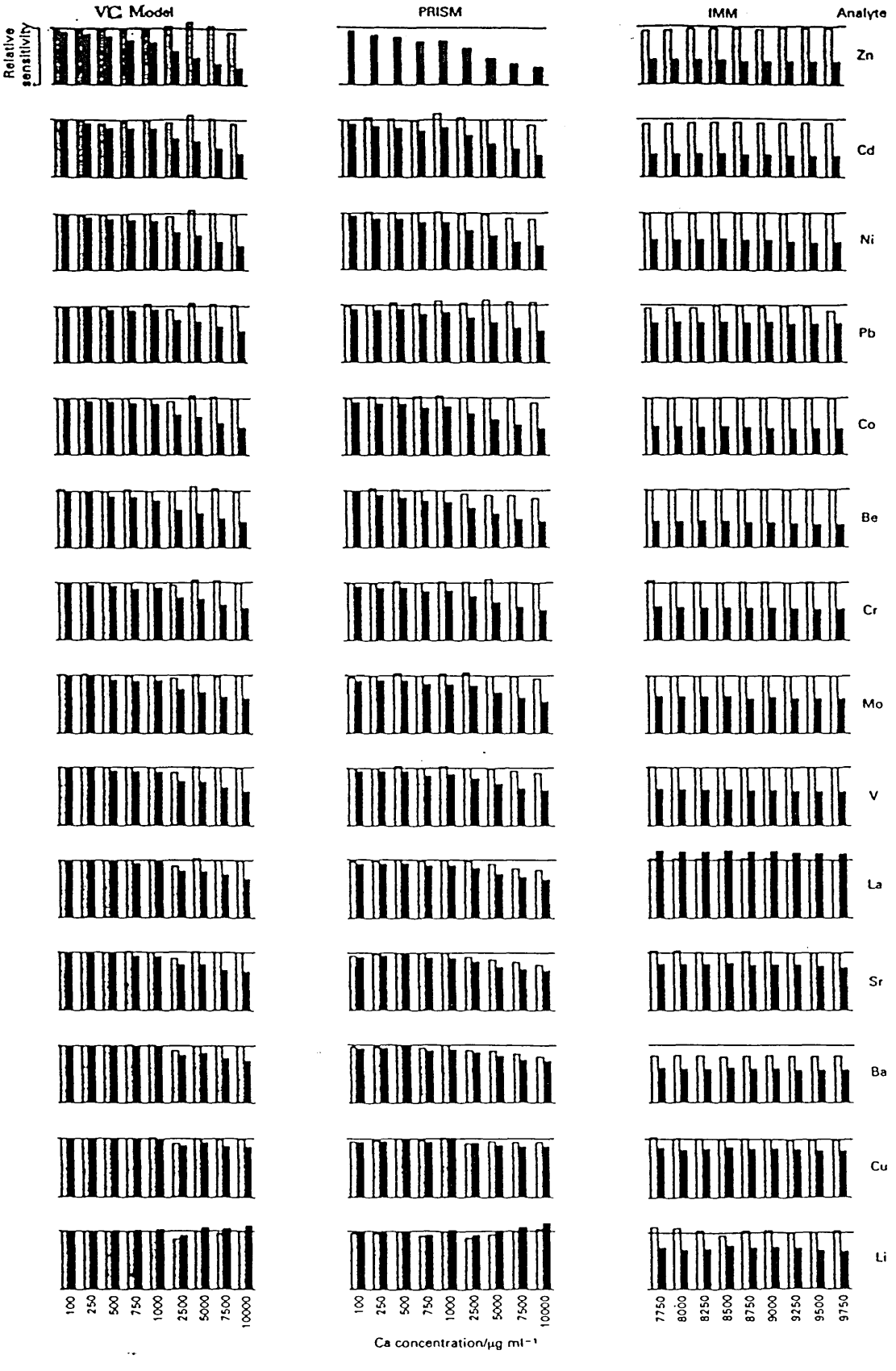


Fig. 7.3
Effectiveness of three methods of correcting the calcium matrix effect: black bars represent raw data; grey bars show the same data corrected by the method designated in the column heading. Relative sensitivities for each analyte are given on a scale from 0.5 to 1.0 in each instance. Zinc is not corrected in the PRISM column as it is used as a parameter-related internal standard. In the IMM column, the raw data contain both matrix effects and spectral interferences, which were corrected simultaneously by IMM. The calcium concentrations given are those for the test solution before analysis. In the IMM technique the solutions are diluted to 4000 μg ml^{-1} during the procedure.

Ca concentration/ $\mu g\,ml^{-1}$	Bias, %					
	Mathematical model		PRISM		IMM	
	Raw	Corr.	Raw	Corr.	Raw	Corr.
100	0.9	0.5	2.7	1.5		
250	2.1	0.9	3.8	0.9		
500	3.5	1.1	3.7	0.8		
750	4.8	1.1	7.1	1.3		
1000	5.0	0.6	6.1	1.3		
2500	13.0	3.4	10.6	2.1		
5000	13.7	1.8	14.8	2.7		
7500*	17.9	0.5	18.6	3.4	18.9	2.3
10000*	20.6	1.3	21.5	4.6	20.9	2.0

* Values for IMM are 7550 and 9750 $\mu g\,ml^{-1}$, respectively.

Table 7.2
Comparison of the improvements in accuracy by three techniques. Values are the average absolute bias of 14 analytes before ("Raw") and after ("Corr") correction (except for PRISM Corr., which is on 13 analytes).

It was found that the experimental data conformed to exponential decay curves of the form

$$S = 1 + A(1 - e^{-Bc}) \qquad \ldots\ldots 7.1$$

where A and B are adjustable parameters, being constants for a particular element.

The non-linear fitting was achieved by means of a numerical method developed by Head (1970). A graphical interpretation of the parameters A and B is shown in Fig. 7.2. The values of the A and B for each analyte are shown in Table 7.1. They were estimated from the data from Appendix C. The curves shown in Fig. 6.1 illustrate these particular values. It is emphasized that the parameters A and B are at this stage regarded as descriptive only.

A correction of the matrix-affected sensitivity can be made if the measured calcium concentration (c) is inserted into the appropriate equation. This 'VC-Model Method' of correction was tested using the data from Appendix C. The results, shown in Fig. 7.3 (column 1), illustrate the ability of this technique to correct all analytes over the full range of calcium concentration, mostly to within 2% of the correct value. This demonstrates the degree of fit of the data to the exponential decay curve. The numerical values before and after correction are listed in Appendix C.

The improvement in accuracy is quantified in Table 7.2. These data were calculated by averaging the absolute bias of the 14 analytes for each concentration of calcium. The sensitivity data for of the 2500 $\mu g\ ml^{-1}$ calcium solution appear to be suspect being systematically lower in many analytes than on previous

experiments. The VC Model still removes 74% of the bias.

Under real conditions the correction would contain extra uncertainty, due to the day-to-day variation in values of parameters A & B and in the determined level of calcium. However, the correction function deals equally well with positive deviations from unit sensitivity (i.e. Li) and the more common negative deviations.

This purely empirical VC-Model contrasts with the MED-Model in the lack of theoretical foundation. For example the values of A and B are both probably related to the total excitation potential of the analyte line, as the studies at both 10,000 µg ml and 2000 µg ml (0.05M) reveal. Comparable investigations to this one for calcium, conducted on a wide range of matrix elements would be an obvious next step in experimentation. Relationships between A and B for each matrix and the corresponding MED and excitation potential may reveal a theoretical basis for A and B. One obvious problem however is that the hypothesis of reduced excitation temperature which underlies the MED Model, simply extended, would imply a linear relationship between the logarithm of relative sensitivity (ln S) and calcium concentration (c). This can be seen from equation 6.12.

$$\ln S - \ln (n'/n^{o}) = E \Delta T/kT^{2} \quad \ldots\ldots\ldots \quad 6.12$$

If there is a direct proportion between the drop in excitation temperature (ΔT) and the concentration of calcium (c) added then, assuming n'/n^{o} is constant (i.e., no change in the number of emitting analyte ions or atoms):-

$$\ln S \propto - c \qquad \ldots\ldots\ldots 7.2$$

The fact that plots of ln S versus c are not linear but curve towards from the concentration axis must therefore be explained in order to extend the MED Model in a more than empirical way. If the calcium atoms, in addition to the ΔT effect had the effect of increasing the proportion of analyte ions to atoms then this would produce the correct qualitative effect.

This is a topic in need of further experimental and theoretical work.

7.5 The Parameter Related Internal Standard Method (PRISM)

7.5.1 Introduction

The development and application of a parameter related internal standard method (PRISM) for the improvement of precision in ICPAES was described in Chapter 4 and 5. It may seem surprising therefore that PRISM has a second application in the removal of bias due to matrix effects. There were indications, however, that this second application might be possible. There was a remarkable similarity in the effects on analyte intensities between the addition of calcium to the solutions, and the reduction of forward power to the plasma. This similarity is illustrated for a 1% $^{w}/_{v}$ Ca solution and an 8.5% reduction in forward power in Fig. 6.2, and has been discussed in Section 6.3.2. The significance of this similarity is that, as PRISM corrects for any variation conforming to the forward power multielement parameter signature (MPS) then it should also correct variation caused by the calcium matrix. The essential difference between them comprises (a) precision improvement involves the correction of 'random' variation with

Element	Wavelength/ nm	Forward power multi-element parameter signature
Ba	455.40	0.149
Be	313.04	0.660
Ca	317.93	—
Cd	226.50	0.757
Cd	228.62	0.662
Cr	267.72	0.620
Cu	324.75	0.111
La	398.85	0.279
Li	670.78	−0.127
Mo	281.62	0.521
Ni	231.60	0.671
Pb	220.35	0.657
Rb	780.02	−0.029
Sr	407.77	0.204
V	311.07	0.454
Zn	202.55	1.000

Table 7.3
Forward power multielement parameter signature used for PRISM correction of matrix effects shown in Figure 7.3

time; whereas (b) the accuracy improvement involves the correction of a systematic variation produced by a given matrix. This difference which is only apparent in the time domain should not affect the effectiveness of the correction. Moreover any 'random' variations superimposed on systematic bias, where both conform to the same MPS, should also be corrected. Thus precision and accuracy should be improved simultaneously.

7.5.2 The Application

The capability of PRISM to correct the matrix effect due to calcium is shown in Fig. 7.3 (column 2). A data set given in Appendix E and replicating that used to produce Fig. 6.1 (Appendix C) was corrected by PRISM, using the multielement parameter signature (coefficient vector) for forward power determined close in time to the matrix experiment, and shown in Table 7.3 Fig. 7.3 shows corrected and uncorrected data at several calcium concentration levels for a range of analytes. The line Zn II 202.55 was used as an internal standard, and the correction took the form similar to that used for precision improvement in equation 5.14.

$$I_{i,\,corr} = I_i/[1 + k_{i,Zn}\,(I_{Zn}/I^{o}_{Zn} - 1)] \quad ...7.3$$

where I_i is the net intensity for the ith analyte, which is corrected by PRISM to give $I_{i,corr}$. I_{Zn} is the net intensity of the zinc line for the test solution, and I^{o}_{Zn} is that when no interferent is present. The coefficient $k_{i,Zn}$ takes a value for each line which expresses its sensitivity to a reduction in forward power relative to that of zinc. This is only a half-PRISM correction selected because only the forward power MPS appears to

be reflected in matrix effects. Thus no allowance is being made for the sample uptake MPS via a second internal standard.

Data corrected by PRISM fall mostly within a few per cent of the correct value for all but two analytes, representing a substantial improvement in accuracy. The deviation of strontium and barium from this pattern is discussed in the next section. Table 7.2 lists the bias remaining after PRISM correction (averaged over all analytes) in relation to calcium concentration. Only at the highest calcium concentrations is the correction incomplete.

7.5.3 Discussion

An alternative explanation for the ability of PRISM to improve both precision and accuracy can be made on the basis of the hypothesis of reduced excitation temperature. If the addition of calcium does reduce excitation temperature as described in Section 6.4.3, and reduction of forward power does similarly, then this application of half-PRISM in reality corrects all analyte intensities back to a fixed excitation temperature.

An important implication of this explanation is that zinc is acting as an excitation temperature indicator or thermometer in this half-PRISM method, and would allow for the application of half-PRISM to the effects of other matrix elements. In fact all of the 18 matrix elements studied in Chapter 6 conformed to the reduced excitation temperature hypothesis. It would seem probable therefore that half-PRISM would correct all their effects similarly to that of calcium. Even mixtures of different matrix elements, if they cause no other effects than a fall in excitation temperature, should be corrected by PRISM.

7.5.4 **Limitations**

Complications in this simple picture, noted in Chapter 6, are evident in these results. In Fig. 6.2 comparing the effects of added calcium and reduced forward power to the plasma, the elements Ba, Sr and La are clearly much more affected by calcium than power. In their curve shapes with changing Ca concentration these three elements have significantly lower values of B parameter than other elements. Comparison of the half-PRISM equation 7.3 with that of the exponential curve shape equation reveals that half-PRISM cannot fully correct a matrix effect unless the B parameter values of the analyte and the internal standard are the same. The effect of this is evident in Fig. 7.3 where Ba in particular is under corrected.

The reason for the divergent behaviour of these elements is not known, but one possibility is that it is due to sample uptake effects. In the full PRISM correction described in Section 5.3 there are two internal standards. The high excitation potential in line (e.g. Zn II 202.55nm) corrects, it now appears, for variations in excitation temperature. The low excitation potential atom line (e.g. Li I 670.78nm) was used to monitor any variability with a multielement parameter signature (MPS) similar to that of sample uptake rate. The second MPS has yet to be conclusively explained by a theoretical mechanism. Inspection of this 'Uptake MPS' in Table 4.7 reveals that Ba, Sr and La have values among the highest. It is possible to advance a theory to the effect that changes in forward power do produce only changes in excitation temperature. Calcium however, in addition to the ΔT effect, also produces a slight increase in the Uptake-MPS. Hence the enhancement of lithium and the more linear curve shapes for Ba, Sr and La. It

would then follow that a full PRISM including the Uptake-MPS might be more effective for matrix correction. Extending the application of PRISM to the (viscosity based) matrix effects from acid concentration would be an interesting exercise to test this theory.

Another suggestion for these anomalous results could be that the calcium is affecting the degree of ionization and hence the number of emitting species of the analyte over and above the ΔT effect. This would imply that Ba, Sr and La are in some way more susceptible perhaps because of their significant degree of second ionization given in (Table 6.4). Studies of a wider range of analytes in other matrix elements at variable concentration might enable the validity of this theory to be tested.

7.6 Interactive Matrix Matching (IMM)

7.6.1 Introduction

Normal 'simple matrix matching', discussed in Section 7.2, 'removes' matrix effects very accurately but only if the concentration of the matrix element does not vary between samples beyond a narrow tolerance. For geological samples this is rarely the case. A simple technique suffices when the matrix effect is due effectively to one element. The requirement is therefore to dilute all samples until the concentration of the matrix element matches that in the calibrating solution. To achieve this manually is tedious, involving one analysis for the matrix element, a calculation, a variable dilution and then a second analysis for the analytes. IMM carries out this entire proceudre in one automated operation.

The practicability of this idea was tested in relation to the problem of the multielement analysis of limestones discussed in Section 6.3. The software used was designed for this particular

application. For example the range of matching was limited to the 75% to 100% calcium carbonate typical in limestone. This enabled a fine matching tolerance to be achieved, but limited the range of limestones which could be analysed. With an alternative design it would have been possible to increase the range to 30-100% calcium carbonate. This improved flexibility would be obtained at the expense of matching accuracy.

7.6.2 General Operation of IMM

The interactive matrix matcher (IMM) is essentially a variable diluter under computer control. Fig. 7.4 shows a schematic diagram of the IMM system. The solution sample is combined with diluent, mixed, and a portion taken to the nebuliser for analysis, the balance going to waste. One fixed speed peristaltic pump supplies sample to the mixer and also feeds the nebuliser. A second variable-speed peristaltic pump supplies the adjustable proportion of diluent to the mixer as directed by the computer. By means of specially written software the computer monitors the concentration of the matrix element in the diluted sample and adjusts the diluent flow until the concentration reaches a target or reference level. All calibrating solution are prepared with the matrix element at this reference level. Once diluted to the reference level therefore, the multielement analysis can proceed in the normal way without any matrix effects. Translational (or background) interferences (Section 2.4.2) are also matched by IMM, and this eliminates the need for separate quantification and correction of these effects.

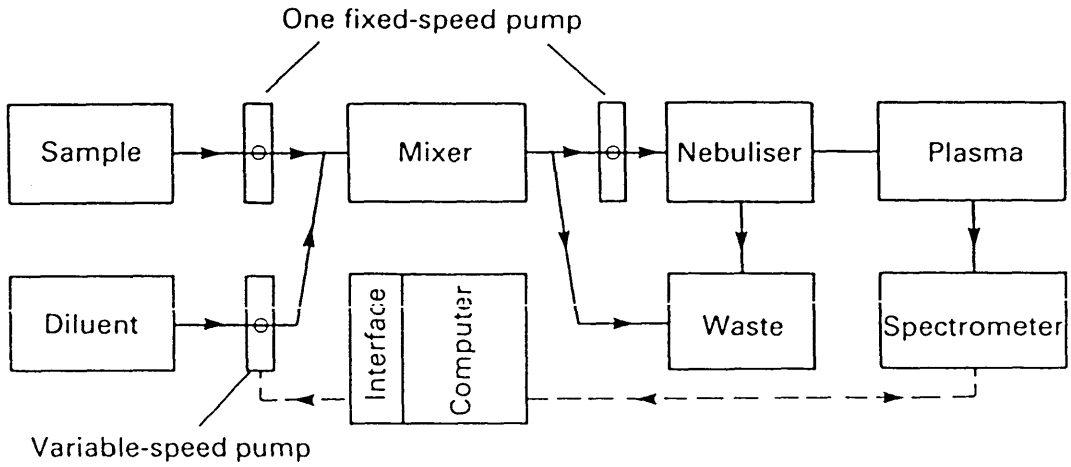


Fig. 7.4
Schematic diagram of the interactive matrix matching (IMM) system. The variable-speed pump (and thence the dilution of the test solution) are controlled by the computer, in response to the initial determination of the matrix element. The dilution of the test solution is adjusted so that the matrix element concentration moves to a reference level used in the calibration solutions.

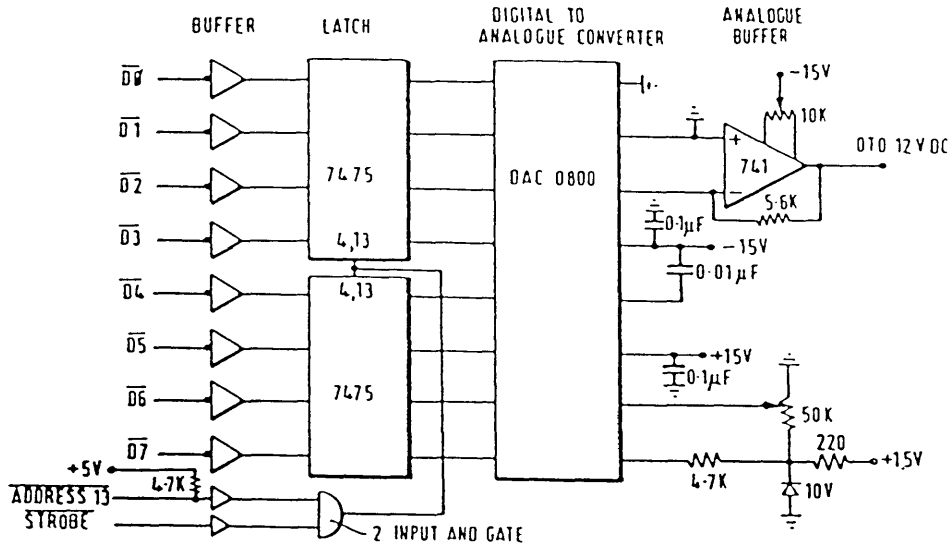


Fig. 7.5
Circuit diagram of electronic interface between ICP and IMM.

Table 7.4 Equipment and Instrumental Conditions used in IMM Experiment

IMM	Fixed Speed Pump: Nebuliser feed	Watson Marlow ML/RE/200rpm max Speed 69rpm (setting 346) Number of rollers 3 Pulse rate $\sim 3.5 sec^{-1}$ Tubing Silicone 0.5mm i.d. Flow rate $\sim 1.25 ml\ min^{-1}$
	Variable Speed Pump:	Watson Marlow 501U/100rpm max + 501AA pump head/20rpm max. Speed 12-20rpm (s = 158-252) Number of rollers 6 Pulse Rate 1.1 - 1.8 sec^{-1} Tubing PVC 0.76mm i.d. Flow rate 1-1.6ml min^{-1} External control 0-12V
	Mixer:	Silicone rubber tubing 70mm x 0.8mm i.d. Filament 56mm x 0.8mm Nylon (from N2000 mesh) with 3mm long 140^{o} zig-zags.
	Stream divider/ combiner	Glass 'h' 30mm long, i.d. 0.8mm
	Connecting tubing	Polyethylene 0.5mm i.d.
	Tolerance on contiguous measuring precision	<1% (relative)
	Tolerance on matrix matching	<2% (relative)
ICPAES	Preflush	30s
	Integrations	5s (x3)

7.6.3 Hardware

A description of the IMM hardware used is given in Table 7.4. The selection of the equipment should be made on the grounds of criteria discussed below, but was in practice, tempered by financial consideration. The pumps ideally should maintain the desired flow rates with minimal drift with time, minimal pulsing, and with a high degree of reproducibility when speeds are adjusted or tubing reclamped. The variable speed pump, in addition, should be externally controllable with high resolution and repeatibility. High pump speeds and fine bore pump tubing were used to increase the number of pulses occurring within the integration time, thus reducing random noise. They were used also to reduce the dead volume of the whole system with a consequent reduction in sample transport time. Low dead volume in connecting tubing and the mixer was similarly of primary importance. The mixer operates by causing turbulence in the liquid stream whilst creating minimal back pressure. The design was adapted from that used for atomic absorption by Ramsey et al.(1982) and consisted of one filament from a nylon mesh sieve inserted into a piece of silicone rubber tubing. Experimentation to establish the mixing efficiency utilized the mixing of sodium hydroxide containing phenolphthalein indicator and hydrochloric acid. Total mixing, indicated by the decolourising of the mixture, occurred within the initial 30mm of the mixer under the flow rates used in IMM. This procedure also allowed the pulsation of mixing at the frequency of diluent pump to be studied.

The electronic interface between the dedicated computer of the ICP and the variable speed peristaltic pump enabled software commands to produce specified diluent flow rates. The interface

circuit, shown in Fig. 7.5 converted the software CALL (1,13,0,s) in which the software pump rate setting s was 0 to 255, into a proportional voltage in the range 0-12 volts DC. The WM 50IU pump motor then rotated at a speed from 0-100rpm proportional to this signal voltage. Experimental work established a non-linear relationship between s and the diluent pump flow rate (d). The software was designed to allow for this non-linearity. The printed circuit board containing the interface circuit was situated in the main card rack of the ICP. The deficiencies of all the hardware and its possible improvement will be discussed in Section 7.6.6.

7.6.4 Software

The software was written for the specific application of IMM to the analysis of limestones rather than for general applications. The routines were located within the analysis programmes provided with the instrument and were written in the language ARL EXTENDED BASIC. This enabled the various stages of IMM to be implemented at the appropriate stages in the normal analytical process. A listing of the IMM software is given in Appendix F as inserts into two ARL programmes, the setting up ($AASC) and the analysis ($ASC1).

The programmes were designed to be flexible tools for the development of the IMM technique rather than efficient for routine analysis. It was known that the hardware was not ideal in terms of stability or linearity and the programme therefore made minimal assumptions about the capabilities of the hardware. Diagnostic readings are frequently printed and options for changing tolerances were inserted for development purposes.

The general flow chart in Fig. 7.6 shows the broad sequence of events in the operation of IMM. The detailed description of the operation is given in Appendix G.

Table 7.5 Calibration Scheme for IMM Experiment

(CARB 1) Blank space indicates concentration not used

Solution	1	2	3	4	5	6
Ag	0	1				
Al	0	10	40	100	200	
As	0					20
Ba	0	10	100	50	20	
Be	0	1				
Ca*	4000	4000	4000	4000	4000	4000
Cd	0	1				
Co	0	10				
Cr	0	10				
Cu	0	10				
Fe	0	10	40	100	200	
K	0	10	50	100	20	
La	0	10				
Li	0	10				
Mg	0	10	200	100	40	
Mn	0	10				
Mo	0	1				
Na	0	10	20	100	50	
Ni	0	10				
P	0				20	
Pb	0	10				
Rb	0	10				
S	0				20	
Sr	0	10	100	50	20	
V	0	10				
Zn	0	10				

*Ca values not used for calibration.

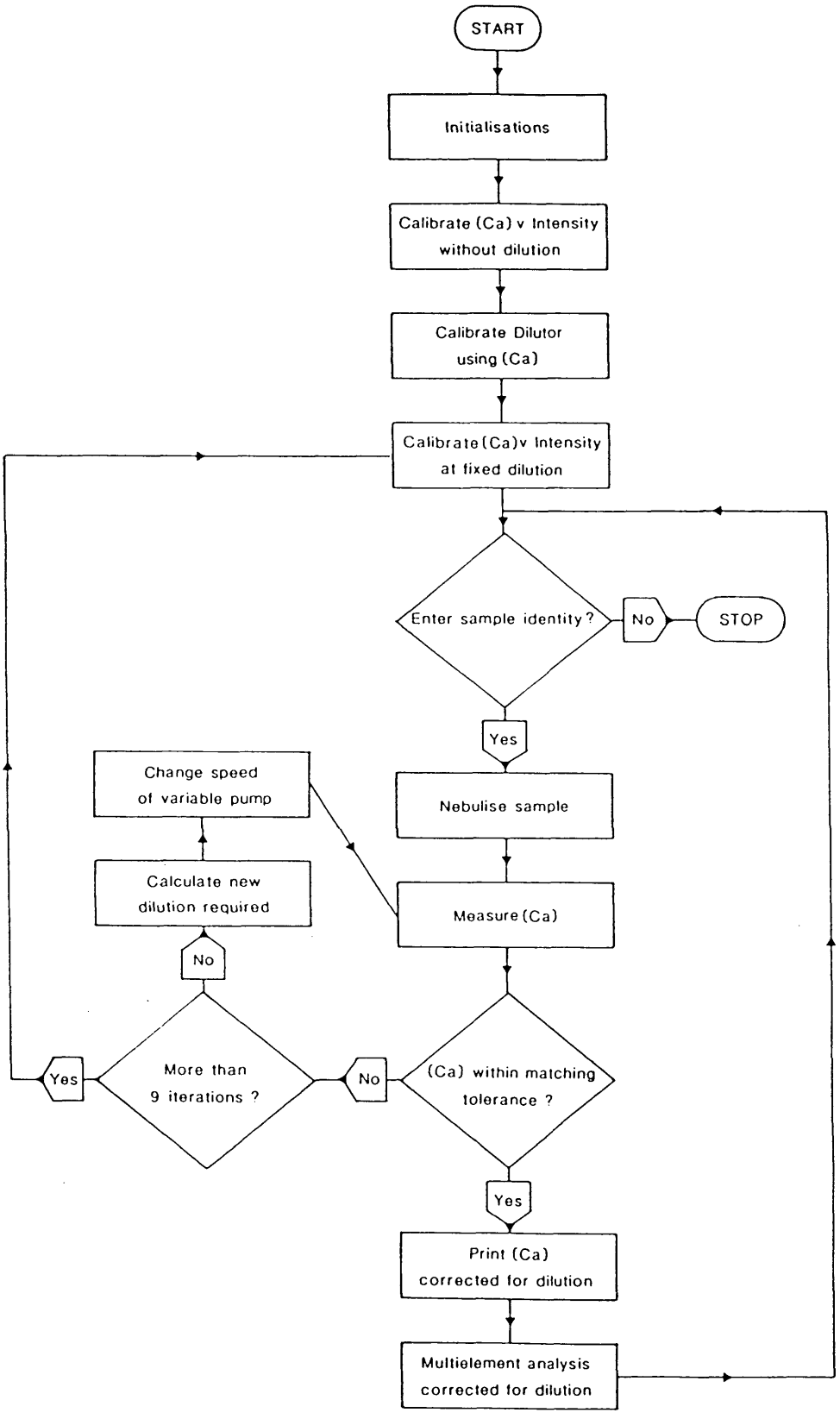


Fig. 7.6
Simplified Flow Chart for Interactive Matrix Matching (IMM).

Once the matrix is matched by IMM the rest of the analysis proceeds normally. The multielement analysis utilised standard ARL software with the calibration scheme given in Table 7.5. All six calibrating solutions are in a matrix of 4000 µg ml Ca. The calibration ranges of the analyte elements cover the concentrations typically found in limestones according to Wedepohl (1969). The higher level minor elements are distributed amongst the solutions so as to maintain an approximately constant total dissolved solid content. The calibration of the analytes was performed without IMM but using the same nebuliser, and the calibration normalised prior to any IMM run. Trace element drift was not corrected for in this experimentation due to its short duration.

7.6.5 The Experimental Trial of IMM

Nine test solutions were prepared to simulate the analysis of limestones with the composition 75-100% calcium carbonate, dissolved at $25gl^{-1}$. Their calcium concentration are given in Figure 7.3 as are the list of 14 analytes present in all solution at 10 µg ml^{-1} except for Cd, Be and Mo at 1 µg ml^{-1}. The acid matrix used for all solutions including the diluent, was 1M hydrochloric acid. The operating conditions of the ICP are generally those given in Table 3.1 except where respecified in Table 7.4. The peristaltic pumps of the IMM were warmed up at typical flow rates for 2 hours before the analysis, to minimize drift during analysis.

To illustrate the effect of using IMM the same nine solutions were analysed by a non matrix-matched routine ICP calibration called GEN3. The detailed calibration scheme for GEN3 is given by Thompson & Walsh (1984 in their Table 5.4) and included the routine mathematical correction of translational interference from calcium.

Table 7.6 Calcium concentration determined by IMM compared with actual values

Calcium Concentration % w/w		
Measured	Actual	Bias
31.06	31.00	0.06
32.64	32.00	0.64
33.26	33.00	0.26
34.57	34.00	0.57
35.50	35.00	0.50
36.06	36.00	0.06
37.45	37.00	0.45
38.24	38.00	0.24
39.63	39.00	0.63

A compraison of the two techniques is shown in Figure 7.3 (column 3) and the numerical values given in Appendix H. The unmatched calibration (GEN3) produced inaccuracies in analyte concentration of up to -30% as discussed earlier. Interactive matrix matching reduced this bias to within 2% in most cases. The effect on lanthanum is noteworthy in that a signal enhancement due to background enhancement outweighs the sensitivity suppression, giving a net positive interference in the raw data. IMM's ability to correction simultaneously for background and matrix effects is clearly evident for this analyte. Barium results shows the largest residual bias after IMM averaging -9.1%, however the high precision of the corrected bias ($\pm$0.5%) suggests that calibration drift is responsible rather than a deficiency in IMM. Corrected cadmium results show a similar but smaller bias (3.3$\pm$0.4%). An analyte sensitivity normalization within IMM software would probably improve the overall accuracy of correction. Averaged over all 14 analytes Table 7.2 shows that IMM reduces the bias tenfold from around 20% to 2% in this application. A small component of this improvement however is due to a pure dilution effect rather than to the action of IMM. The average bias of 20% was measured from solutions nebulized at 10,000 $\mu g\ ml^{-1}$ Ca, which would only have had an average bias of around 12%. The full potential of IMM could be judged more directly if samples were prepared with 25,000 $\mu g\ ml^{-1}$ Ca.

A second benefit of analysis using IMM is the high accuracy of the major element analysis produced. Table 7.6 lists the calcium concentration found in the nine (experimental) solutions compared with the actual concentration. The average bias at 0.38 $\pm$ 0.23% (absolute), 1.0 $\pm$ 0.7% (relative) is small and shows IMM to be a powerful technique for high accuracy analysis. The bias is

however significantly greater than zero, suggesting a small systematic bias in the calibration which may be removed. The relative precision of the calcium determination at 0.7% is similar to the value measured for contiguous integrations (Table 5.1) and probably cannot be improved upon due to this limiting factor. The calcium concentration is determined at one single reference level after matrix matching and therefore no errors should occur due to the curve fitting of the calibration.

The extra time for analysis caused by IMM in this implementation is approximately two minutes per sample. After the initialization period of 30 minutes each solution took on average 4.5 minutes for matrix matching and multielement analysis. The accurate removal of matrix effects by IMM therefore has the disadvantage of reduced sample throughput, although improved hardware and software should reduce this disadvantage.

7.6.6 Possible Improvements to IMM

The hardware used in this trial of IMM was known to be unsuitable. Drifts in pump flow rates were measured and found to be up to 3% per hour even after a warm up period. This obviously puts a very large demand on the software to keep updating the calibration equations. The lack of linearity in the control of the diluent pump also was undesirable because of the extra complexity generated in the calibration procedure. Pumps with predictable, stable and linear flow rate would enable a significant shortening of the initialization period and a much more robust routine operation. An initial survey of possible alternatives to the current peristaltic pumps for IMM suggest that the LKB 2132 the

most promising for future developments. The mixing chamber was a potential source of instability in IMM, not because of the incomplete mixing originally feared, but rather as an extra cause of drift in pump flow rates. In the balance of priorities between low dead volume and increased back pressure, the former may have been over stressed. Further experimentation on mixer design is clearly desirable. Generally the routine application of IMM requires a second generation of more robust hardware. This would enable us to use simplified software which would provide substantially better performance than the prototype.

Extending the applicability of IMM beyond the single matrix element described here could be achieved by two approaches. Where two interfering matrix elements vary reciprocally from sample to sample, as do calcium and magnesium in dolomitic limestone samples, then one element could be present in the diluent solution, so as to bring the ratio of the two elements to a standard level in the mixture before determination of the trace analytes. A more general extension of IMM that would in principle allow any mixture of matrix elements to be corrected, would be to add an internal standard element to both the sample and diluent channels. At any mixture of sample and diluent, therefore, the concentration of the internal standard element would be constant. However, the measured intensity of the internal standard element would depend on the level of matrix effects from whatever source. If the response of the internal standard element in the calibration solutions were taken as the target, and all samples diluted to give this target response then the matrix effects on all analytes should be similarly matched. This assumes that all matrix effects have a common mechanism, and for a large range of elements this would seem

to be justified by the results given in Chapter 6. A study of the extension of this technique to matrix effects such as those of oils would be very interesting. The addition of the internal standard element could be achieved automatically by adding one further channel to the fixed speed pump, combining its flow with the nebuliser feed, but this would necessitate using a second mixing chamber.

7.7 Other Methods of Correction

There are two further possible methods for correcting matrix effects which will be considered.

7.7.1 Matrix Swamping

The technique of matrix swamping or buffering is commonly used to reduce interference in atomic absorption spectrophotometry (Kirkbright et al.(1974) p523). The exponential curve shape shown in Figure 6.1 indicates that in ICPAES at sufficiently high concentration of calcium the matrix effect will closely approach an asymptotic sensitivity. In terms of the Variable Concentration Model described in section 7.4 this asymptote has the value 1+A. Thus above a certain calcium concentration, the sensitivity will become constant. Potentially, therefore, addition of this level of calcium to all test solutions and the standard solutions should ensure freedom from matrix effects. The level at which this stabilisation takes place can be calculated from the decay parameter B. For example the level at which the sensitivity falls to 1+0.95A is given by -ln 0.05/B (see Figure 7.2).

There are several considerations, however, which mitigate against this potentially useful method. (i) No calcium determination could be carried out simultaneously with the trace

Table 7.7 Correction of Matrix Effects for 8000 μg ml^{-1} Ca by Interactive Power Adjustment (IPA)

	Relative Sensitivity	
	Raw	Corrected
Ba	0.867	0.898
Be	0.606	0.764
Cd	0.737	0.971
Co	0.767	0.968
Cr	0.792	0.974
Cu	0.945	0.963
La	0.853	0.933
Li	0.984	1.040
Mo	0.799	0.979
Ni	0.740	0.951
Pb	0.803	1.031
Sr	0.850	0.891
V	0.819	0.947
Zn	0.675	0.996

analytes. (ii) Translational (spectral) interference would be increased by this method, possibly to a level which would seriously degrade detection limits for trace analytes. (iii) Some analyte sensitivities do not stabilise sufficiently (according to the exponential decay function) until high concentrations of calcium are reached, levels which may give rise to problems of nebuliser blockage. (iv) It is not known whether the exponential functions can be extrapolated validly beyond 10000 $\mu g\ ml^{-1}$ of calcium.

An alternative approach which could be envisaged might consist of the addition of a second matrix element to act as an excitation buffer. From the multi-matrix results of Chapter 6 it seems clear that no element would have a high enough MED to swamp the effects of changing calcium concentration for example. Minor matrix effects from elements with MED less than 10eV could conceivable be swapped by elements such as lanthanum but limitations (i) and (ii) above would still apply.

7.7.2 Interactive Power Adjustment (IPA)

The similarity between the multianalyte effects of matrix element of high MED and reduction in forward power to the plasma was discussed in connection with PRISM section 7.5. An alternative strategy to a chemometric correction however is to increase forward power automatically to offset the matrix effect, interactive power adjustment (IPA). In terms of the excitation temperature model, therefore if calcium reduces the temperature by ΔT then the forward power can be adjusted to increase the excitation temperature by the same ΔT. Tentative experimentation with manual adjustment of forward power, using Zn II 202.55nm as the thermometer, suggested that IPA will remove the majority of the matrix effects from a

8,000 µg ml calcium solution. Table 7.7 lists the relative sensitivities as defined in Section 3.4, without adjustment (Raw) and those with power adjustment (Corrected). The latter were calculated as the nett analyte sensitivity in the presence of calcium at the increased forward power divided by the nett sensitivity in acid blank at the normal forward power setting. The need to monitor the changes in background intensity with changes in forward power (achieved here by running 8000 µg ml^{-1} Ca alone) could be problematical for routine application of IPA. Either an off-peak background measurement would have to be made at each new forward power setting or else a chemometric correction could be made for such predictable variations. The results in Table 7.7 show full removal of 33% bias for Zn sensitivity as this was the target of the power adjustment. Ten of the analytes are correction to within 5% of their reference sensitivity although four elements Be, La, Sr, Ba are outside this limit. These are also the elements which responsed poorly to matrix effect correction by PRISM probably for similar reasons as suggested in section 7.5. The under correction of around 4% could clearly be lessened by using a reference line of intermediate total excitation potential such as Co or Cd. More detailed investigation of IPA is required before the full potential of the technique can be established. However, such an interventionist strategy to stabilize the excitation temperature of the plasma is relatively cheap to construct and well suited to for automated operation.

7.8 Comparison Between Methods for Correcting Matrix Effects

As set out initially in this chapter there are six criteria by which a method for correcting matrix effects in ICPAES can be judged. Where new methods have been only partially investigated, a rigorous comparison with existing methods is impossible. However, all techniques have relative strengths and weaknesses and Table 7.8 identifies these. Each method is given one of five classifications for each of the six criteria, with symbols ranging from very poor to very good. At present there are no bench mark tests which would enable fully objective scoring. The scores are therefore based, in varying proportions, on the experimental results discussed in this chapter, and reports in the literature. Table 7.8 should enable the selection of the most appropriate method for a given circumstance. For example where samples have variable multiple matrix elements, accuracy is paramount and speed no limitation then the only method of analysis currently available is by standard additions. If however a method is required for development which has the potential to reduce all matrix effects from all metallic elements in any concentration to within 2% without causing any loss in productivity then extension of the MED model is a likely choice. The conclusion for the IPA method implied by Table 7.8 is that it performs well against all six criteria, as judged by initial experimentation.

In general the fastest methods are likely to be entirely software-based (e.g. MED-Model) rather than those with machine intervention such as IMM, IPA or GSAM. The design of the IMM configuration for limestone illustrates the generality that a highly accurate correction is achieved at the expense of a relatively narrow concentation range. A general MED-Model would

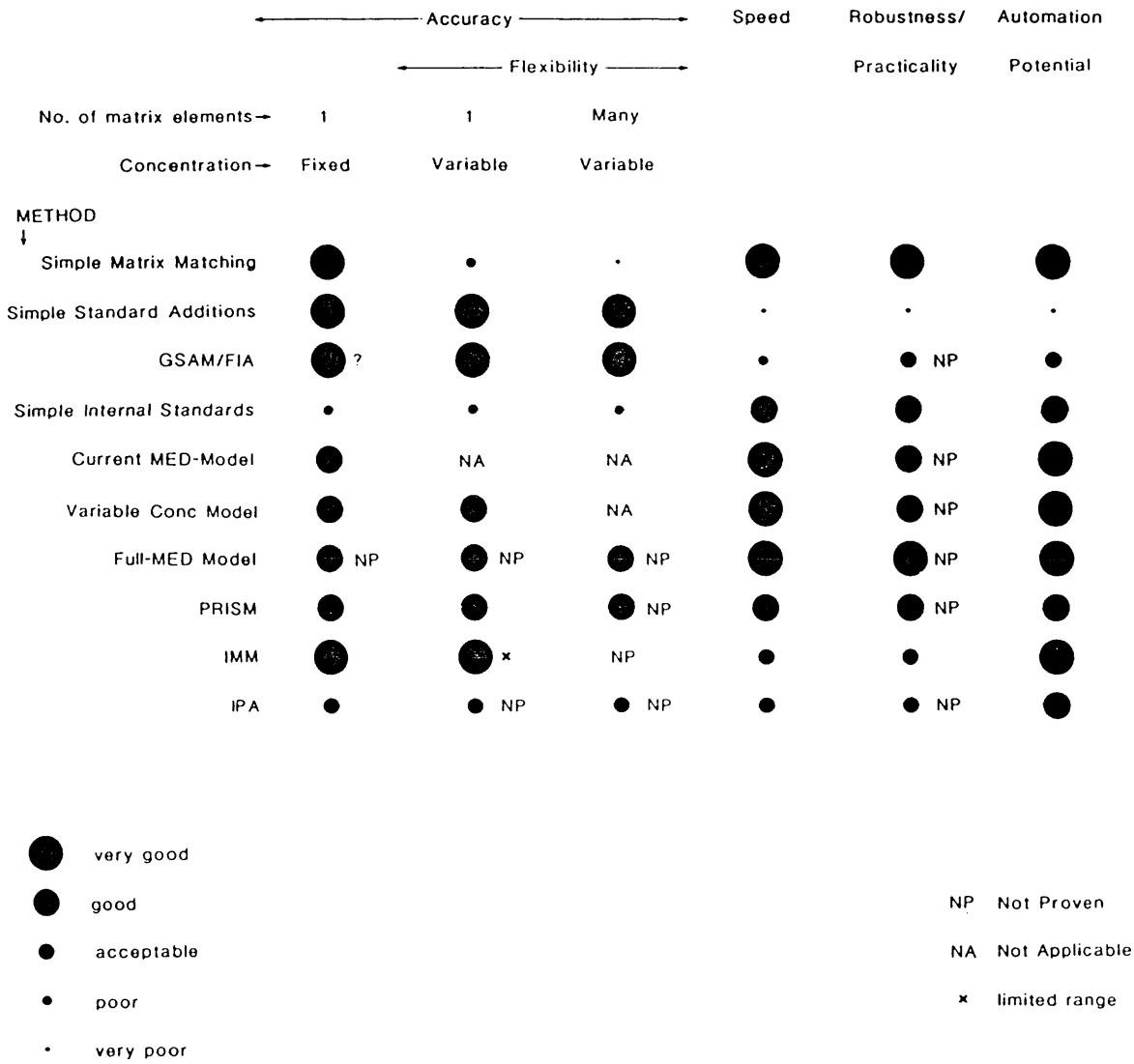


Table 7.8
Comparison of ten methods of correcting bias due to matrix effects.

therefore be unlikely to provide as high a level of accuracy for a particular matrix as constant matrix matching could provide.

The comparison of the accuracies of three methods in Table 7.2 shows this effect, although the performance of IMM was impaired by the lack of sensitivity adjustment. The quality of correction from the variable concentration (VC) - Model in this table would possibly be impaired in routine operation by the variability of the fitted parameters, making IMM generally the most accurate of the automated methods.

The problems posed by mixtures of different matrix elements has not been addressed in this study nor has the ability of the various methods to correct for their effects. A study of mixed matrix effects from four matrix elements by Maessen et al (1982) showed that the effects of two relatively high MED element (Ca and Mg) were approximately additive, but not so mixtures including the two low MED element (Na and K). The third column of Table 7.8 estimates the probable performance of the existing and new methods with mixed matrix effects. Standard additions is the only technique known to correct for variations in sensitivity in this instance. If all matrix elements act only by reducing excitation temperature then PRISM should behave just as for the example calcium alone as should IPA. The ability of the full MED model depends on a deeper understanding of the way single elements 'withdraw' power from the plasma and thence how two elements interact.

The robustness of a method for correcting matrix effects is harder to quantify than speed or accuracy yet it is just as critical for routine use. An obvious factor is that software-based corrections have no extra hardware to cause problems. Errors from

software-based corrections would therefore not prevent analysis proceeding but must be assessed by the rigorous Analytical Quality Assessment (see section 2.7.2), that must accompany the use of any of these methods. PRISM, once the MPS values are established, only requires the addition of one or two internal standards, which could be automated with a high quality peristaltic pump. IMM however is much more dependent on reliable, high-specification equipment and specific programs. Reliability is much less easily achieved under these conditions, but may eventually yield the most accurate correction of any automated method. IPA appears initially to have less intricate hardware and software demands than IMM but less promising accuracy of correction.

When all these methods are fully characterised, and even extended, for example to attempt the correction of the effects of variable acid concentration, it seems probable that no single 'best' method will emerge. The ICP will simply utilize the method of bias removal most appropriate to the samples and the required data quality.

CHAPTER 8

SELF-MATRIX EFFECTS AS A CAUSE OF CALIBRATION CURVATURE

8.1 Introduction

The long linear calibration range of ICPAES is one of its advantageous qualities which was listed in Chapter 2. Curvature in the response-to-concentration calibration is however well known, although poorly quantified in the literature. Deviations from linearity are widely reported at concentrations of the analyte from 10^4 to 10^6 times the analyte detection limit (Thompson and Walsh (1983) p24).

In the absence of a definitive study on linear ranges of ICPAES calibration ranges, two alternative 'rules-of-thumb' have been used by practical spectroscopists. One such maintains that there is a constant "orders-of-magnitude" linear range above the detection limit for all lines of a particular element. This implies that the selection of a less sensitive line would automatically provide linearity to higher concentrations. The second assumption is that curvature of all lines of one analyte occurs at approximately the same concentration irrespective of sensitivity, giving greatest linear range to the most sensitive lines. Neither assumption has been systematically investigated.

Several mechanisms have been suggested as causes for the deviation from linearity but no model exists which can predict either the linear range a given line will exhibit or what shape the calibration curve will be. Such a model, if ever formulated, would help both in line selection, and in producing

an appropriate curve-fitting equation that is fundamentally rooted in spectrochemical theory.

In this chapter a new cause of curvature will be postulated and compared with established causes to assess its validity and relative importance. The new mechanism is based on a 'self-matrix effect'. In Chapter 7 matrix effects produced by a range of matrix elements acting on a range of analyte lines have been described. The theory of a reduced excitation temperature was used to describe these effects. A logical extension of these findings is that a matrix element should thus affect the sensitivity of its own emission lines. If increasing concentrations of a matrix element such as calcium reduces the excitation temperature, then the sensitivity of emitted calcium radiation should decrease in an analogous way to that of other analyte lines. This self-matrix effect will be evident as a curvature of the response-to-concentration calibration curve.

Verification of this cause of curvature depends on distinguishing self-matrix effects from other reasons for calibration curvature. Three criteria were proposed to identify curvature due to self-matrix effects, based upon the previous findings for matrix effects on other elements.

i) A linear relationship between the log of relative sensitivity of various emission lines of an element at one concentration and their total excitation potentials.

ii) The slope of line in (i) should imply the same drop in excitation temperature as measured from lines of other elements.

iii) The shape of the response-concentration calibration curve should correspond to that measured for other elements at the same concentrations of matrix element. An appreciation of the

characteristics of other causes of line curvature is clearly a prerequisite to experimental design and interpretation of results.

8.2 Established Causes of Calibration Curvature in ICPAES

There has been no definitive exposition of the causes of curvature in the intensity versus concentration calibration of ICPAES. In the established spectrochemical literature there are descriptions of nine factors which cause the broadening of emission lines and hence potentially reduce the linear relationship between the peak height response and the analyte concentration. They are called natural, Doppler, Lorentz, Holtzmark, Stark, Zeeman, quenching, self-absorption and hyperfire structure broadening. Kirkbright and Sargent (1974) give a clear description of these effects as applied to atomic absorption spectrophotometry. For ICPAES it is generally accepted that the most significant of these causes of non-linearity is self-absorption.

Self-absorption occurs when analyte species in one region of the plasma absorb the radiation emitted by analyte species in another region. Human and Scott (1976) reported that self-absorption effects are at their greatest high in the plasma (25mm above the load coil) where emissions from a hot centre core are absorbed by a cooler outer ring. In contrast self-absorption was reported as small, low in the plasma (ca. 10mm) where, due to external heating, emissions came primarily from the hotter outer skin of the plasma. Self-absorption is important only for lines that have their lower energy level at or near the ground state so that self-absorption within this source is easily induced (Kirkbright et al.(1974) p40). The large effect of self-absorption in comparison with other causes of line broadening is due to the

fact that it is the centre of the line which has the greatest proportion of the effect. As peak height is effectively the parameter of the line measured, the depression of the centre is most evident.

Exact calculation of the extent self-absorption is not possible but Human & Scott (1976) give a relationship for absorbance where

$$\text{Absorbance} = \text{const.} * N.f./ \Delta\upsilon_D \quad .....8.1$$

where N is the number of ground state atoms, f is the oscillator strength of the absorption line and $\Delta\upsilon_D$ is the Doppler half width. For various emission lines of one element at a fixed concentration, the degree of self-absorption will be proportional to $f/ \Delta\upsilon_D$. The doppler half width is the result of doppler broadening where thermal motion of the emitting species changes the frequency of the emitted light. The relative atomic mass (M) of the analyte, the temperature (T) and the frequency of the emitted light (υ_o in cm^{-1}) give a value for the doppler half width (Kirkbright et al. 1974 p37).

$$\Delta\upsilon_D = 7.162 * 10^{-7} \quad \upsilon_o \sqrt{T/M} \qquad 8.2$$

Thus, if line curvature is due primarily to self-absorption then for a given analyte concentration by combining equations 8.1 and 8.2 the curvature of an analyte line of wavelength λ should be proportional to $f\lambda$.

A second recognised cause of curvature in calibrations is ionisation self-interference. This is not related to line

broadening but is due to changes in the concentration of the emitting species. This mechanism occurs when the increasing concentration of the analyte suppresses its own degree of ionisation, and this increases the ratio of atoms to ions. For atom lines therefore, ionisation self-interference produces curvature away from the concentration axis, the opposite of any other mechanism. For ion lines the curvature produced is towards the concentration axis. This effect will be greatest for elements with low ionisation potentials, for example 'upward' curvature was reported for lithium by Boumans et al (1973). It is interesting that lithium has a low "matrix energy demand" (8.77eV) and therefore would be predicted not to produce strong self-matrix effects to cancel out this curvature. Human and Scott (1976) report that ionisation self-interference is most pronounced high in the plasma (ca. 25mm) but is still discernable lower down (ca. 10mm) for a line with a small excitation potential (e.g. 1.6eV), for an element of moderate ionisation potential (e.g. Ca = 6.11eV).

For a particular element at a given concentration the degree of ionisation will be constant and cannot therefore affect the curvature of various emission lines differently, excepting the distinction between atom and ion lines.

Other possible causes of curvature in calibration lines noted by Human and Scott (1976) are nebuliser efficiency, sample transport in the plasma and spectrally unresolved stray light. The former two causes could not give differential effects between emissions from lines of the same element. Stray light would not be expected to produce curvature related to the properties of the underlying emission lines.

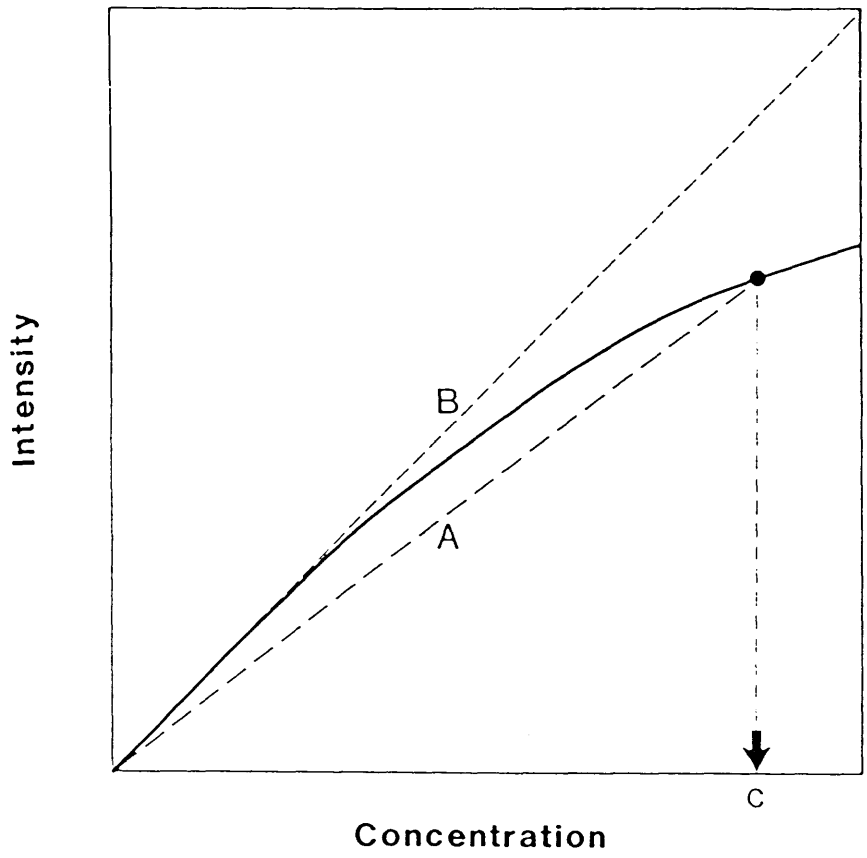


Fig. 8.1
A schematic calibration graph. The relative sensitivity at concentration c is the slope of the cord A divided by the slope of the tangent at zero concentration B (i.e. the reference sensitivity).

To summarise, therefore, self-matrix effects as a cause of curvature in calibration should be uniquely identified if a linear relationship is observed between the degree of curvature and the excitation potential of the emission line. The slope of this line should correspond to a fall in excitation temperature, measured independently.

8.3 Initial Investigations

Verification of the hypothesis that self-matrix effects were responsible for the curvature of response-concentration calibration curves in ICPAES was sought initially in data sets produced for other purposes. During the experimentation described in Chapter 6 on the matrix effects of various calcium concentrations on a range of analytes given in Appendix C, the responses on CaII 317.93nm were measured but not used. When plotted as a calibration curve this data (given in Table 8.1) produced a typical curve shape, initially linear and gradually curving towards the concentration axis.

The objective was to compare this curvature with that predicted by the fall in excitation temperature measured from the analyte relative sensitivity (Section 6.4.3). As the fall in excitation temperature was hypothesised as the only cause of curvature then, at any given excitation temperature, the calibration should be straight. The sensitivity of the calcium emission at a given concentration (c) can therefore be calculated from the slope between that point to the zero concentration point (i.e. the cord (A)) shown diagrammatically in Fig. 8.1. The relative sensitivity at the calcium concentration is the ratio of the slope of the cord to the tangent at zero calcium concentration

Table 8.1 A comparison of self-matrix effect and matrix effect on other elements. The calibration data for calcium for calcium (II 317.93 nm) is expressed as relative sensitivity shows similarity to the relative sensitivity of concomitant cadmium and berylium.

(1)	(2)	(3)	(4)	(5)	(6)
Calcium Concentra-	Calciumm Response	Sensiti- vity at each concentra- tion	'Relative Sensiti- vity to 100	Relative Sensiti- vity' of Cd	Relative Sensiti- vity off Be
$\mu g\ ml^{-1}$	mV	$mV/\mu g\ ml^{-1}$	$\mu g\ ml^{-1}$ Ca		
0	0.01				
100	47.79	0.4778	1.000	.990	.989
250	113.7	0.4548	.952	.968	.973
500	231.5	0.4630	.969	.931	.947
750	339.4	0.4525	.947	.924	.931
1000	445.9	0.4459	.933	.924	.906
2500	1025	0.4100	.858	.829	.825
5000	1896	0.3792	.794	.811	.797
7500	2614	0.3485	.729	.751	.752
10000	3234	0.3234	.677	.716	.723

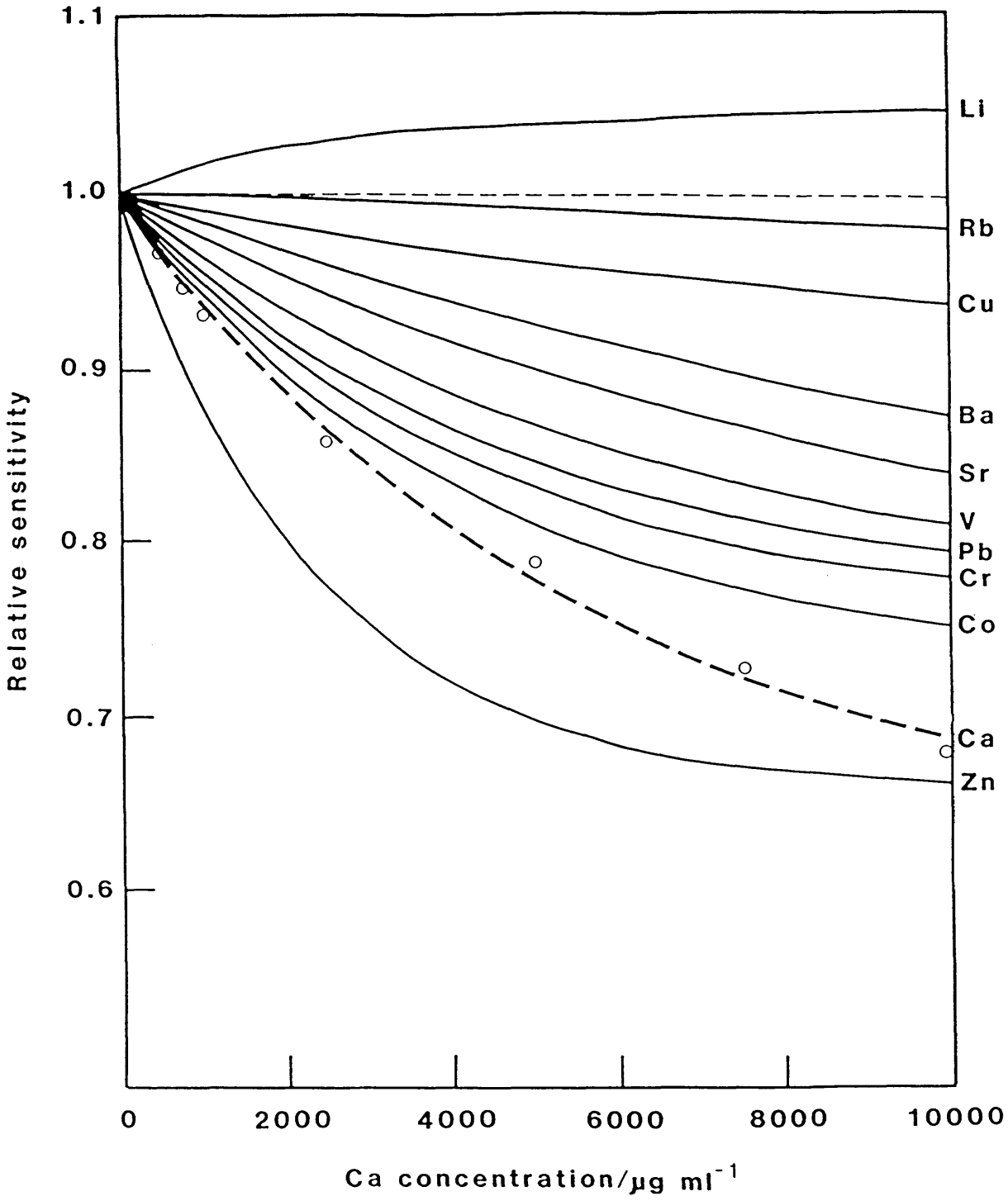


Fig. 8.2
The effect of increasing calcium concentration on (i) the relative sensitivities of concomitant analytes and (ii) the Ca II 317.9nm emission line. The similarity in curve shape suggests a common cause.

(B). The latter 'reference sensitivity' can be estimated from values of the sensitivity at low calcium concentration. For this data set the reference sensitivity was measured at 100 μg ml^{-1} Ca, and the calculated sensitivity and 'relative sensitivities' are given in Columns 3 and 4 of Table 8.1. For comparison the relative sensitivity of the concomitant cadmium and beryllium are repeated in Columns 5 and 6. The general similarity is noteworthy and initiated the further investigation described.

A further comparison is shown in Figure 8.2, in which the calcium relative sensitivity points are superimposed on the data for other elements from Figure 6.1. The curve shape of the calcium data shows marked similarity to that of barium and strontium. When the relative sensitivity data for calcium is fitted using the same empirical equation used for the analyte data (7.1) then the fitting parameters are: A = 0.387, B = 1.7E-4. A comparison of these values with those for the other elements given in Table 7.1 quantifies the similarity in curve shape. The A value is comparable with that of Zn II 202.55nm, and the B value intermediate between that of Be and those of Sr and Ba. The relatively large value of A is indicative of the low relative sensitivity at 10,000 μg ml Ca (0.677) which when plotted against the total excitation potential of this calcium line (13.16eV) places it on the same trend as for the analyte lines in both Figures 6.3 and 6.9a.

The drop in excitation temperature for 10,000 μg ml Ca implied by this relative sensitivity using equation 6.7 is -144K, which is comparable with the value measured from the multi-analyte data which was -130K.

These findings therefore strongly suggest that the curvature of this calcium calibration line is consistent with the single mechanism of a self-matrix effect. To test the more general applicability of this hypothesis further experiments were required.

8.4 Experimental Design

An experiment was designed to enable the most unambiguous identification of the role of self-matrix effects in line curvature to be made. The study was restricted to one element to preclude differences between elements (for example degrees of ionisation). Fourteen calcium lines described in Table 8.2 were selected to include both atom and ion lines and span a wide range of excitation potentials, wavelengths and detection limits. Fifteen test solutions were prepared with calcium concentrations ranging from 0.1 to 10,000 µg ml^{-1} listed in Table 8.5, in hydrochloric acid (1M). Volumetric error was monitored to prevent sequential dilution error being misconstrued as non-linear response. Sequential determination of the 14 calcium lines was performed using the ARL 3520 ICPAES under the operating condition given in Table 3.1.

A comparison was made between the matrix effects from calcium on other elements and self-matrix effects under similar operating conditions. Four solutions were used in the measurement of analyte relative sensitivities of the other elements as described in Section 3.4. The calcium concentration was chosen as 10,000 µg ml^{-1} and 13 other elements at concentrations of 5 µg ml^{-1} and 0.5 µg ml^{-1} (Be, Cd and Mo). The wavelengths measured were those in Table 6.1.

(1)	(2)	(3)	(4)	(5)	(6)	(7)
Line Number	Wavelength λ	Order	Atom/ Ion	Total Excitation Potential	Oscillator Strength	$f\lambda$
	nm			eV	f	
1	239.856	2	I	5.17	0.043	10.0
2	272.165	2	I	4.56	0.001	0.20
3	299.496	2	I	6.02	0.148	44.0
4	299.731	2	I	6.02	0.054	16.0
5	315.887	2	II	13.16	0.910	290.0
6	317.933	2	II	13.16	0.820	260.0
7	370.603	2	II	12.58	0.173	64.0
8	373.690	2	II	12.58	0.173	65.0
9	393.366	2	II	9.26	0.690	270.0
10	422.673	1	I	2.93	1.750	740.0
11	504.163	1	I	5.17	0.076	38.0
12	616.644	1	I	4.53	0.042	26.0
13	657.278	1	I	1.89	5×10^{-5}	0.03
14	732.615	1	I	4.63	-	-

Table 8.2 - Description of 14 calcium lines studied

8.5 A New Curve Fitting Equation

In order to provide an objective description of the parameters of the intensity of the calcium lines with concentration a new curve fitting algorithm was evolved. The form of the equation was based on the self-matrix mechanism of curvature and so the goodness of fit of this model was also an indication of the validity of the mechanism.

The most widely used equation for curve fitting in ICPAES is the splined polynomial. This utilises a series of overlapping polynomial equations, usually of the second order in the form:-

$$c = B(0) + B(1)\,I + B(2)I^2 \quad \ldots\ldots\ldots 8.3$$

where the concentration (c) is calculated from the intensity (I) using three coefficients B(0), B(1) and B(2). The fitting of this equation is problematical in a number of respects. The equation is purely empirical and has no foundations in spectrochemical theory. This leads to useful information being ignored, such as the essentially linear nature of most calibration graphs. Secondly equation 8.3 has concentration explicity as the dependent variable whereas it is truely the independent variable. This 'transposed' fitting produces more realistic curvature but misplaces the experimental error on the wrong axis of the regression, a feature, in itself, likely to cause inaccurate fitting. Systematic studies of the errors produced by the splined polynomial have not been reported in the literature but personal experience suggests that great care is required in the selection of the number and concentrations of standards in order to minimize the inaccuracy between points and line.

What is clearly desirable is a calibration equation based on a knowledge of the causes of curvature. The starting point for the new equation developed here however was the empirical equation (7.1) used to fit the matrix effects from calcium on a range of analytes.

$$S_r = 1 + A(1 - e^{-Bc}) \qquad \ldots\ldots\ldots 7.1$$

where S_r is the relative sensitivity, c is the concentration of calcium (in $\mu g\ ml^{-1}$) and A and B are constants for a given analyte. If calibration line curvature is caused by 'self-matrix' effects then the manipulation of this equation to describe the intensity (I) at a concentration (c) should produce a single calibration line which accurately describes the progressive deviation from linearity typical of calibration graphs for ICPAES.

Replacing the relative sensitivity (S_r) in 7.1 by the sensitivity at a given concentration $^{dI}/_{dc}$ and the sensitivity at low concentration (the reference sensitivity) by So we get

$$dI/dc = S_o (1 + A(1 - e^{-Bc})) \qquad \ldots\ldots 8.4$$

integrating we get

$$I = S_o (\kappa + c + Ac + (A/B)e^{-Bc}) \qquad \ldots\ldots 8.5$$

where κ is the integration constant.

When c = O then I = I_o, rearranging we get

$$I/S_o = \kappa + A/B = I_o/S_o \quad .... \ 8.6$$

hence

$$\kappa = I_o/S_o - A/B \quad ..... \ 8.7$$

substituting 8.7 into 8.5 we have

$$I/S_o = I_o/S_o + c + A_c + (A/B)e^{-Bc} - A/B \quad ..... \ 8.8$$

giving the final calibration equation as

$$I = I_o + (1 + A)\ S_o\ c - (AS_o/B)\ (1 - e^{-Bc}) \quad .... \ 8.9$$

Although the initial equation (7.1) was empirical in its description of matrix effects, this response-concentration equation (8.9) should provide a single calibration for the six orders of magnitude, directly related to the proposed mechanism of curvature. By comparison a commercial splind polynomial package (ARLAB) required four equations to fit the same range of calibration.

The fitting of equation 8.9 was performed using a numerical method developed by Head (1970).

8.6 **Results and Discussion**

Calibration graphs for the fourteen lines studied are shown in Figure 8.3. Lines are plotted with their true relative intensities, i.e. the most sensitive line is number 9 at the top.

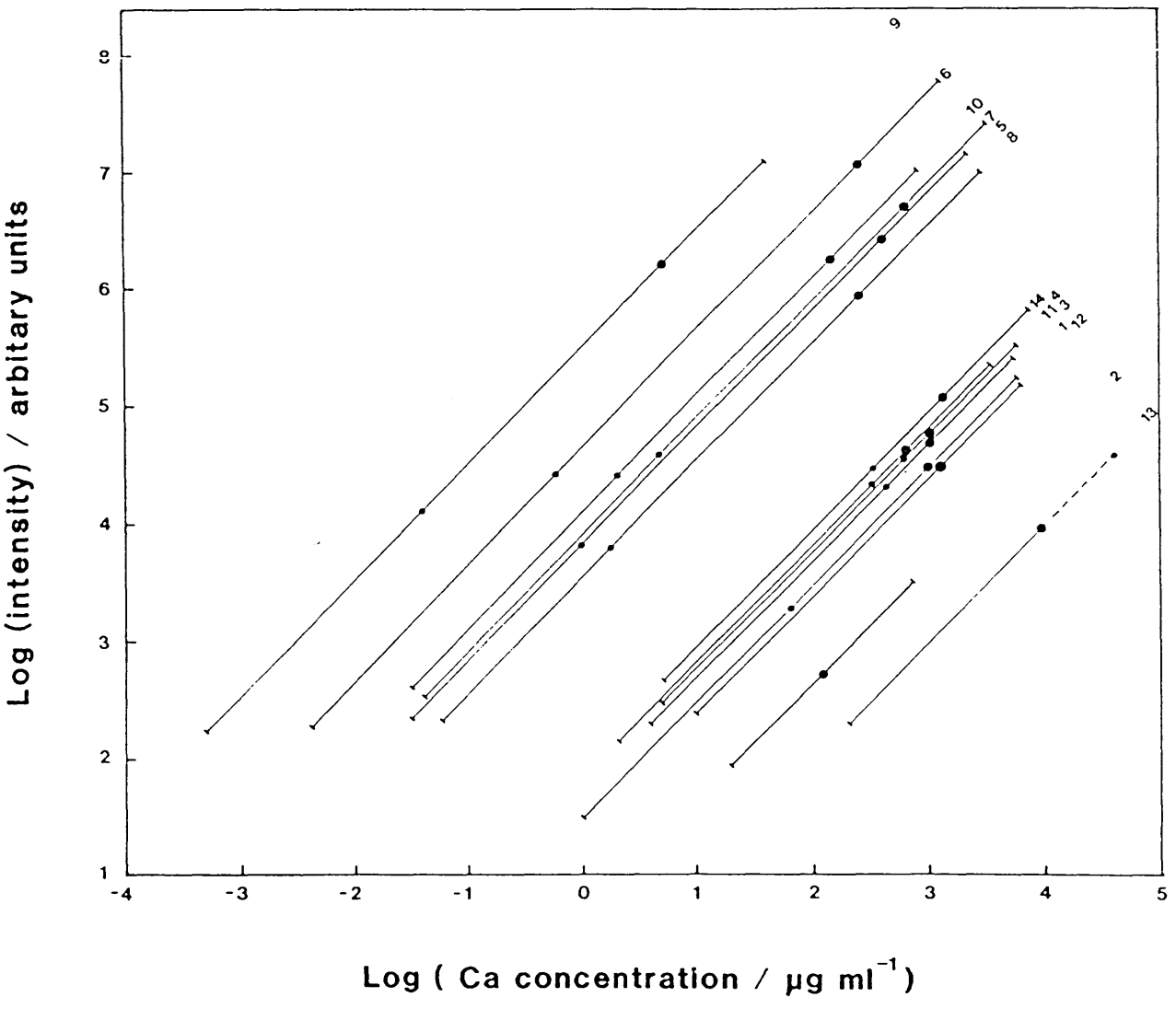


Fig. 8.3
The calibration graphs of the fourteen calcium lines between their detection limit and concentration at which 5% curvature occurs. Also marked are background equivalent, concentration (•), and concentration at which 1% curvature (•) is apparent. Non linearity is not apparent on the log/log scale.

Ca Conc $\mu g\ ml^{-1}$	Intensity Experimental/mV	Intensity Fitted/mV	Residual /mV	Scaled Residual
0	3.99	4.05	-0.06	-1.91
0.1	4.16	4.12	0.04	1.15
1	4.95	4.87	0.08	1.90
10	12.33	12.40	-0.07	-0.74
25	24.68	24.89	-0.21	-1.05
50	45.78	45.73	0.05	0.15
75	66.86	66.55	0.31	0.58
100	86.93	87.36	-0.43	-0.61
250	211.53	211.81	-0.28	-0.17
500	417.97	418.05	-0.08	-0.02
750	628.87	622.75	6.11	1.22
1000	830.40	825.89	4.51	0.68
2500	2001.00	2012.86	-11.86	-0.74
5000	3845.00	3870.95	-25.95	-0.84
7500	5649.33	5582.12	67.21	1.49
10000	7102.76	7149.97	-47.30	-0.83

Table 8.3 - Example of goodness of fit between experimental data from CaI 370.6nm and equation 8.9. The scaling factor for the residuals was 0.008 of the gross intensity

(1)	(2)	(3)	(4)	(5)	(6)
Line Number	Wavelength nm	Ic mV	Equation Fitting Parameters So mV/µgml	A	B x10 ^{4}
1	239.856	15.37	0.2505	-0.3584	0.5333
2	272.165	147.70	0.0595	-0.2862	5.9280
3	299.496	174.07	0.4078	-0.3977	0.5243
4	299.731	178.94	0.5669	-1.2538	0.2561
5	315.887	0.96	1.0031	-0.7532	0.6411
6	317.933	2.95	5.0560	-1.3526	0.5770
7	370.603	4.05	0.8342	-2.9471	0.1006
8	373.690	4.38	1.0863	-0.6508	0.5697
9	393.366	3.54	90.0660	-0.4228	95.3300
10	422.673	4.50	2.2775	-0.2296	6.0899
11	504.163	392.10	0.6148	-0.1986	1.0661
12	616.644	258.73	0.2090	-0.6799	0.2456
13	657.278	551.00	0.0144	-	-
14	732.615	149.00	0.4402	-0.5241	0.2843

Table 8.4
Parameters for equation 7 fitted to the calibration data of the calcium lines.

Each line is plotted from its detection limit to the point where deviation from linearity equals 5% of the intensity. Deviations from linearity are visually imperceptible on this diagram.

8.6.1 Estimation of Relative Sensitivity

The primary objective of the data manipulations was to calculate the 'relative sensitivity' for all 14 calcium lines at a single calcium concentration, which could then be compared with the total excitation potentials of the lines. However the average response values measured (listed in Appendix I), gave no single concentration where all the lines gave significant signals. A calcium concentration of 5000 $\mu g\ ml^{-1}$ was chosen as the best value for the comparison of curvatures between the lines, although two ion lines (#6 = 317.9nm, #9 = 393.4nm) had already saturated at lower concentrations (2500,and 100 $\mu g\ ml^{-1}$ respectively).

All of the calibration lines were fitted to equation 8.9, and exhibit a close fit over the entire range of concentration. A typical example is given in Table 8.3, and for all lines in Appendix I. The fit was assessed by scaling the residuals to an estimate of the between-nebulisations precision, taken as 0.8% of the intensity for this case. The scaled residuals have a mean of 0.02 and a standard deviation of 1.07 which indicates that the equation has no lack of fit but only deviations due to random error. The fitted parameters I_o, S_o, A and B for all of the fourteen calcium lines are listed in Table 8.4. This excellent goodness of fit of this single form of equation extended over lines spanning a wide range of properties.

One exception however was line #13 (CaI 657.3nm) where the deviation from linearity was so slight as to make significant

Table 5 Curvature data for the calcium lines

(1) Line Number	(2) Wavelength nm	(3) Sensitivity related to line 13($\log_{10}$)	(4) Relative Sensitivity at 5000μgml^{-1} Ca	(5) Concentration at which 5% curvature occurs ($C_{5\%}$) μgml^{-1} Ca	(6) Detection limit (2σ) (C_L) μgml^{-1}	(7) "Linear range" Orders of magnitude log ($C_{5\%}/C_L$)
1	239.856	1.50	.952	5800	1.0	3.8
2	272.165	.65	.816	700	20.0	1.5
3	299.496	1.70	.946	5200	4.0	3.1
4	299.731	1.84	.903	3200	2.0	3.2
5	315.887	3.86	.886	2200	0.03	4.9
6	317.933	4.67	.822	1300	0.004	5.5
7	370.603	3.91	.918	3200	0.04	4.9
8	373.690	3.57	.908	2900	0.06	4.7
9	393.366	5.52	-	40	0.0005	4.9
10	422.673	4.11	.840	800	0.03	4.4
11	504.163	1.79	.934	5700	5.0	3.1
12	616.644	1.41	.943	6300	10.0	2.8
13	657.278	0.00	1.000	> 10000	200.0	> 1.7
14	732.615	1.97	.949	7200	5.0	3.2

Table 8.5
Curvature data for the calcium lines.

fitting of equation 8.9 impossible. In this case a 'relative sensitivity' value of unity at 5000 μg ml^{-1} Ca was assumed to be the most realistic within experimental error.

For all the other lines the 'relative sensitivity' (S_r) at 5000 μg ml^{-1} Ca was calculated from equation 8.10 where I_e is the experimental intensity, c is the concentration and the values of I_o and S_o are the fitted values given in Table 8.3.

$$S_r = (I_e - I_o)/S_o c \qquad \ldots\ldots 8.10$$

In the instance of CaII 317.9nm a short extrapolation of the fitted equation was used to produce the fitted response in place of an experimental response. For line CaII 393.4nm a fifty-fold extrapolation giving a relative sensitivity value of 0.586 was considered unreliable but a value well in excess of that at the last experimental point (0.850) seemed probable. The computed values of 'relative sensitivity' at 5000 μg ml Ca are listed in Column 4 of Table 8.5.

The logarithms of the relative sensitivities are plotted as a function of their total excitation potentials in Figure 8.4(a). The regression line through eleven of these points has the coefficients:- slope (standard error) -0.0095 (0.0024), intercept (standard error) -0.007 (0.021).

The t-ratio for this slope is -3.96 indicating a slope significantly greater than zero ($p < 0.005$). Equation 6.7 gives a drop in excitation temperature of -46 $\pm$12K. The intercept is not significantly different from zero ($t = 0.3$, $p = > 0.1$) which implies

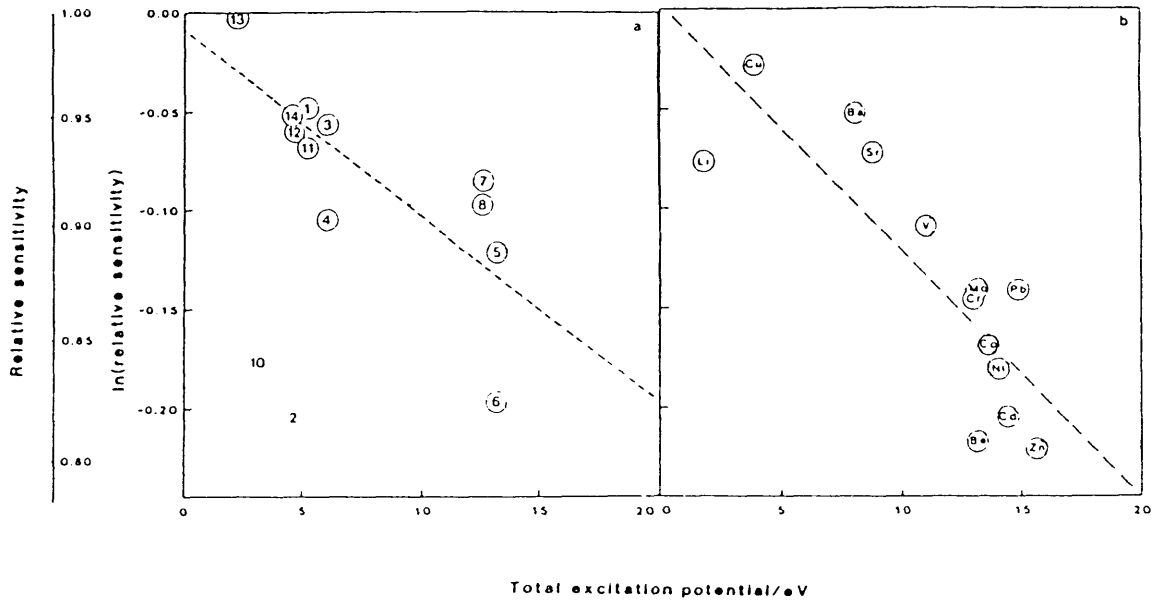


Fig. 8.4
(a) Relative sensitivities of calcium lines at 5000 μg ml Ca plotted against total excitation potential, with the regression line. Points 2 and 10 are not included in the regression. (b) Relative sensitivities of lines of other elements in 5000 μg ml^{-1} Ca with regression line. The overall trends of the two data sets are indistinguishable by regression, suggesting the common origin of reduced excitation temperature. Deviations of individual points from the regressions, where greater than the experimental error (ca 1%), are presumably due to factors affecting specific lines.

complete linearity being approached by lines of low excitation potential. (For example line #13 Ca I 657.3nm).

8.6.2 Lines showing anomalous curvature

Three of the relative sensitivity value are clearly well below the general trend of the eleven values. This implies that these three calcium lines are more curved than can be accounted for by self-matrix effects alone. From the data in Table 8.2 it is clear that line #10 (CaI 422.7) has an extremely high value of $f\lambda$ (740) and as a resonance line would therefore be the line most susceptible to self-absorption effects.

The second line which gives 'anomalous' curvature is line #9 (CaII 393.4nm). This line, with a sensitivity ten times greater than any other (column 3 of Table 8.2), saturated at 100 $\mu g\ ml^{-1}$ Ca with a relative sensitivity value of 0.850. With a total excitation potential of 9.26eV the relative sensitivity predicted at 5000 $\mu g\ ml^{-1}$ Ca by the regression line through the eleven points, would be 0.804. Clearly the curvature of this line does not conform to the self-matrix effect model. The value of $f\lambda$ for this line although relatively high (270) is less than line # 5 which conforms well to the model, and therefore self-absorption should not be greater for this line according to equation 8.1. However Human and Scott (1976) studied the wavelength profile of this line (CaII 393.4) and reported self-absorption at an observation heights as low as 10mm. It would appear therefore that despite the predictions of equation 8.1, self-absorption seems to be the most probable cause of the 'anomalous' curvature of this line.

The third line to deviate substantially from the model is

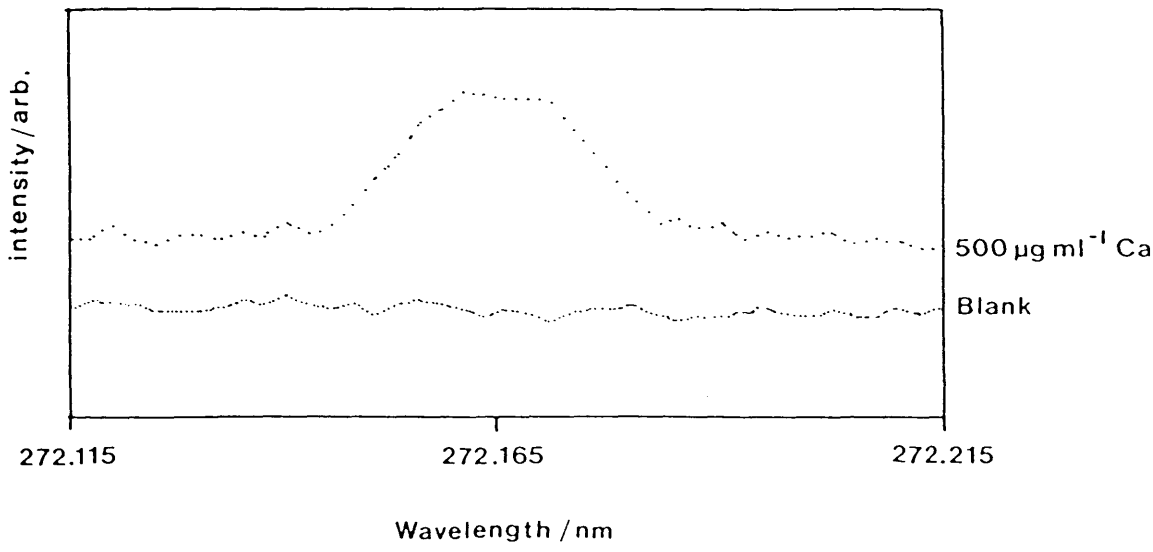


Fig. 8.5
Wavelength scan of Ca line #2 (Ca I 272.2 nm) showing suggestion of a complex structure.

line #2 (CaI 272.2nm). Having very low values of excitation potential, $f\lambda$, and sensitivity the reason for this anomalous curvature was suspected to be hyperfine structure. A wavelength scan of this line using the ARL3520, shown in Figure 8.5 reveals the possibility of two component peaks ca. 0.01nm apart, symmetrically about the quoted wavelength which would be expected to affect the linearity of the calibration of this line adversely.

The overall picture from the curvature of the calcium lines shown in Figure 8.4, once the 'anomalous' behaviour of the three lines has been explained, is that the significant regression against the excitation potential is compatible with the self-matrix hypothesis.

8.6.3 Comparison of Self-matrix Effects with Matrix Effects on Other Elements

Further corroboration of this conclusion was sought by comparing this regression, and hence implied drop in excitation temperature, with the regression line fitted to the matrix effects on other elements at the same concentration of calcium (5000 μg ml^{-1}). Unfortunately the experimental determination of matrix effects was carried out at 10000 μg ml Ca, however, the very reproducible nature of these effects suggest that these data could be normalized to estimate the relative sensitivity at 5000 μg ml^{-1} Ca. This normalization was achieved by calculating the ratio of the bias ($1-S_r$) at 10000 μg ml^{-1} Ca to that at 5000 μg ml Ca in the data set in Appendix C. The experimental bias at 10,000 μg ml Ca for all elements was then multiplied by this ratio to give the predicted bias at 5000 μg ml Ca.

This predicted bias was converted into the logarithm of the relative sensitivity and was plotted against the total excitation potentials of the emission lines in Figure 8.4(b). This gives a visual comparison of the relative sensitivities from these elements and those from the calcium lines in Figure 8.4a; they are clearly very similar. The regression line for these elements has slope (standard error) -0.0124 (0.0024), and intercept (standard error) 0.004 (0.028). This slope is not significantly different from that through the calcium lines (-0.0095 $\pm$0.0024) and implies a similar drop in excitation temperature (-60 $\pm$ 12K c.f. -46 $\pm$12K). The effectively zero intercept, again implied no matrix effects for lines of zero excitation potential. These two regression lines are therefore statistically indistinguishable and this strongly supports the hypothesis that both effects are due to the same mechanism i.e. a fall in excitation temperature.

The relative importance of any other causes of calcium line curvature is further diminished by this finding. For example ionisation self-interference which would have reduced equally the curvature of all the atom lines would have prevented the coincidence with the analyte line data. A small component of other causes of curvature may be the cause of scatter within the data on the calcium lines but self-matrix effects must be dominant to result in the similar implied excitation temperature.

8.6.4 Conventional Views of ICPAES Calibration Curvature Refuted

This data set can also be used to check the applicability of the two traditional assumptions on the linear ranges of analytical calibrations in ICPAES. The assumption that all lines of the same element curve at one concentration is clearly refuted by the

variability of curvature at 5000 μg ml^{-1} Ca (column 4 of Table 8.5). The second assumption that of a constant concentration ratio between the detection limit and the onset of curvature was tested from the data given in Table 8.5, columns 5 and 6. The concentration at which the relative sensitivity fell to 0.950, (that is a line curvature of 5%,) was calculated from the fitted equations. The detection limit was quantified as the concentration equivalent to two standard deviations of the blank response. The concentration ranges from the detection limit to 5% curvature, given in Table 8.5 column 7, are very far from being constant, varying from 5.5 orders of magnitude for line # 6 (CaII 317.9nm) to 2.8 for line # 12 (CaI 616.6nm).

A tentative observation from these limited data is that lines of high excitation potential, although most susceptible to self-matrix effects, have generally the longest linear range due to proportionately lower detection limits. A much broader study would be required to substantiate this conclusion.

8.7 Conclusions and Recommendations for Future Work

This investigation into the causes of the curvature of calibration graphs in ICPAES, although limited in its scope, has found evidence for a new mechanism producing non-linearity. The proposed mechanism consists of a progressive lowering of the excitation temperature of the plasma by an increasing concentration of the analyte. The experimental results suggest that this 'self-matrix effect' is the dominant cause of curvature for the majority of the emission lines studied rather than self-absorption as previously suggested. This conclusion applies to the operating condition typical of routine analysis used in this study, but at

high plasma viewing heights increased self-absorption and ionisation self-interference would be expected to play an increasing role in causing curvature.

Further investigations are clearly required spanning a range of analytes, as well as a range of lines for each analyte. Such a study could conclude more firmly the significance of self-matrix effects in general. Extrapolating the multi-matrix/multi-analyte study of matrix effects in Chapter 6 several predictions could be made which may help with designing such an experiment. Because calcium has a relatively high matrix energy demand (MED) the size of its self-matrix effects will be larger than those for the majority of elements. In the extreme case of lithium for example, the low MED value may give minimal drops in temperature whereas the low ionisation potential will tend to produce relatively large ionisation self-interference, as reported by Boumans et al (1973). Quantifying the self-matrix effect may well prove dependent on accounting for other causes of curvature. To this end a useful ability would be to predict self absorption effects accurately and to model the curve shape they would be expected to produce.

The new curve fitting equation developed for this study has potential for the improved calibration of ICPAES emission. While being modelled on the self-matrix effect it provided a good fit for all but the most linear of the 14 lines studied. The equation fitted equally well the two lines which were curved due to putative self-absorption effects. Deeper understanding of matrix effects may improve on the existing empirical equation, for example with total excitation potential as the exponential term. This in turn should provide an improved intensity-concentration equation. The algorithm used to fit the equation devised here requires initial

estimates of the parameters. The further investigation described above might enable such values to be estimated from the MED of the analyte element and the total excitation potential of the analyte line. Increased computer power is needed both to run the algorithm used to fit the equation and to solve it for concentration, which requires a numerical method. The computer power required will probably not prove to be a limiting factor when set against the improvements in speed and accuracy of calibration. Further research is required in the assessment and implementation of better curve fitting equations for ICPAES.

Many of the methods of correcting matrix-effects could be applied to linearise calibration that are curved due to self-matrix effects. A PRISM-style correction would in theory, linearise CaII 317.9nm for example, which should extend the useful working range, and should enable a more accurate curve fitting with fewer calibrating points.

A preliminary investigation of this hypothesis is shown in Figure 8.5. The calibration data for calcium used was that given in Table 8.1. A half-PRISM correction was applied (equation 5.14) using the intensity of Zn II 202.55 nm measured simultaneously and given in Appendix C. The value of k_{iA} used was 0.723 taken from Table 4.6. The concentration at which 5% curvature occurs is increased from ca. 250 µg ml^{-1} to ca. 7500 µg ml^{-1}, extending the 'linear range' by 1.5 orders of magnitude. The fact that PRISM does not remove all curvature, particularly at high calcium concentrations, may be due to two causes. Differences in the curve shape shown in Figure 8.2 have been discussed previously and would lead to incomplete correction. Alternatively it is possible that a

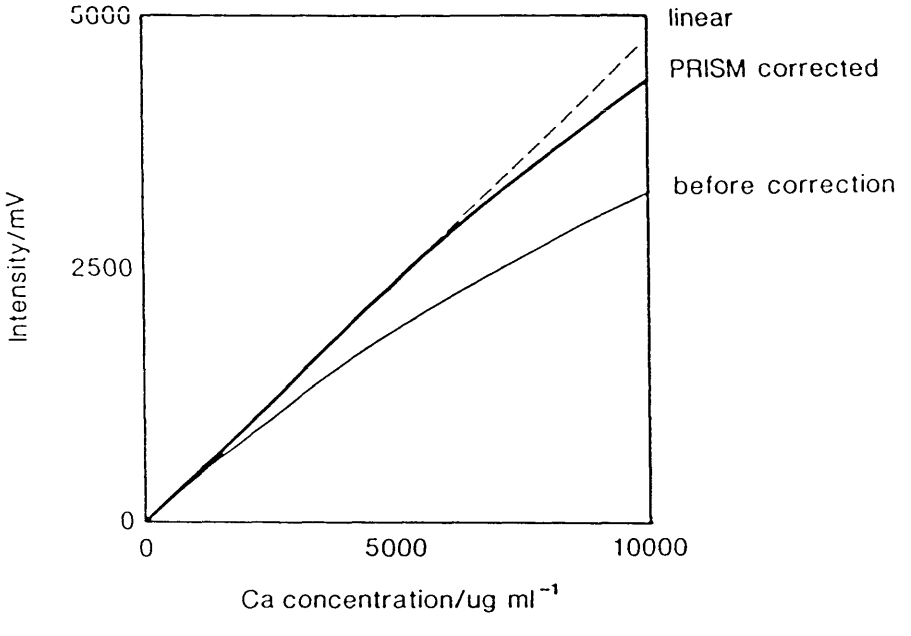


Fig. 8.6
An example of the reduction of calibration curvature using the PRISM correction (e.g. Ca II 317.93nm).

second cause of curvature becomes more significant at high calcium concentrations, for example self-absorption. The general practicality of this technique of linearising calibrations must await more detailed investigation. The addition of a fixed large concentration of an element with a large MED, when an analyte of lower MED is being calibrated should also linearise a calibration curve by this mechanism.

One final conclusion from this chapter is that neither of the current 'rules-of-thumb' for predicting the concentration at which curvature begins is correct. Significant deviations from linearity do not occur at concentrations which are at a constant ratio to the detection limits nor at one fixed concentration for all lines of one analyte. Rather, for one analyte, it is the total excitation potential which determines the onset of perceptible non-linearity, in the majority of cases. More fundamentally the self-matrix effect theory suggests that no ICPAES calibration curve is ever truely linear but only appears to be so over a limited range within the precision of measurement.

CHAPTER 9

CONCLUSIONS AND RECOMMENDATIONS FOR FUTURE WORK

The most significant findings from the previous chapters will be recapitulated, and the broad conclusions discussed in the context of the objectives given in Chapter 1. The scope for further investigations will be suggested in the appropriate section.

9.1 The Precision of ICPAES

9.1.1 Identification of the Problem

The real precision of analysis produced by ICPAES is poorly perceived by analysts. This is a limiting factor in assessing any need for improvements. If the precision is measured with contiguous integrations during one sample nebulisation then a very optimistic value of ca 0.5% is obtained. A true precision at that level is adequate for most geochemical analysis, and so no problem is perceived from this view point.

Analytical quality assurance (AQA) provides a much truer appreciation of precision. Duplicated sample dissolutions are often used to estimate precision (Howarth and Thompson 1976) giving typical values for ICP in the range 2-5%. This procedure measures the total analytical precision rather than the instrumental precision alone. However when standard solutions are run repeatedly over the duration of the analysis the precision measured is purely instrumental in origin. The precision values measured by this means are typically 1-2%, a level that is not adequate for all geochemical analysis. The discrepancy between

this value and that for contiguous precision arises from the definition of precision without reference to the time period of the measurement. The classification of two different measurements of precision as 'contiguous' and 'medium-term' was a simple but necessary step.

The objective therefore was to reduce the medium-term precision to ca. 0.5%. This would enable large batches of geochemical samples to be analysed with the required reproducibility.

9.1.2 The Structure of Multielement Variations

The next factor which impeded progress was the designation 'random' to describe variations in analytical intensity. When plotted against time the variation of intensity of a line of an element such as sodium in Figure 4.1 appears random, with long-term drift superimposed. The word 'random' implies that there is no pattern, and the variations are therefore uncorrectable. A crucial factor in the investigation of precision in Chapter 4 was the use of the multielement dimension. A multi-variate statistical technique, principal component analysis (PCA) showed that over 90% of the variance was correlated between the elements rather than purely random variations restricted to a single element. This discovery suggested that substantial improvements in the precision could be made if the underlying pattern of the multielement variation could be identified and subsequently monitored.

The multielement dimension was also used in the investigation of the possible causes of the multielement variation. It was surprising to find that, from the ten instrumental and environmental parameters investigated, only two patterns of multielement behaviour emerged. One pattern, typified

by the effect of variations in forward power to the ICP ('Power') showed increasing susceptibility with higher total excitation potential E' of the emission line used for intensity measurement (Figure 4.6). This behaviour was shown to correspond well with that predicted for variations in the excitation temperature of the plasma. The second pattern, typified by the effect of variation sample uptake rate to the nebuliser ('Uptake'), shows an opposite trend with greatest sensitivity the lowest value of E' (Figure 4.7).

9.1.3 The Improvement of Precision

It was originally hoped that ten different multielement parameter signatures (MPS) would have diagnostic uses. To that end, the fact that only two non-specific MPS were found was a disappointment. This simple two-MPS system was, however, much easier to develop into a method for improving precision than ten different MPSs would have been. Such a system, called the parameter-related internal standard method 'PRISM', was described in Chapter 5. The ability of PRISM to remove a large proportion of the variance (ca. 70%) showed that the variations in routine ICPAES analysis largely conformed to the two MPSs identified from the investigations of operating parameters.

The Internal Standard Method (ISM) has been used for 60 years for improving the quality of analysis for AES but has been problematical in application to ICPAES. It required identical behaviour of the analyte and internal standard line. One of the problems in applying ISM was explained by the experimental result showing the variable susceptibilities of analyte intensities to all the parameters examined. Element emission lines respond to variation in parameters such as forward power with different

amplitudes depending on E'. It is impossible therefore by simple division to predict directly the size of variations in many other elements. Once a separate correction factor for each element for an internal standard is calculated then this limitation is overcome.

The second limitation of ISM is that it assumes perfect correlation between variations in the analyte emission and the internal standard element emission. Even if there is only one cause of the variation in both emission lines then they will not be perfectly correlated because of the truly random variations. It is clear from this investigation however that at least two sources of non-random variation are acting upon all element emissions, and so perfect correlations will not be expected for any pair of elements. What is required therefore is that both of the separate causes of variation must be monitored independently and each analyte element corrected for the effects due to both causes. These are the two respects in which PRISM improves upon ISM.

PRISM uses an emission line with a high value of E' (e.g. Zn II 202.55nm) to monitor variation in the excitation temperature of the plasma. The 'Power' MPS can then be used to calculate the correction for all other element lines. An emission line with a low value of E' (e.g. Li I 670.78nm) is used to monitor variations confirming to the 'Uptake' MPS and a second correction can be made for each element line from this cause.

PRISM improved the precision over a period of 4 hours by a factor of two. The resultant precision was very similar to that measured from contiguous integrations (0.5%). In addition to the improvement in precision, PRISM also removed long term drift and

hence enabled the operator to obtain improved accuracy. In effect PRISM provides a real-time estimation of sensitivity which obviates the need for repeated calibrations throughout the analytical run. PRISM therefore can also improve productivity, especially for high precision analysis when frequent repetition of calibration is usually required.

9.1.4 Future Work on Precision Improvement

This work could be extended in any of three directions, 1) a deeper understanding; 2) an improved correction; 3) a broader application.

9.1.4.1 Fundamental studies

A deeper understanding would involve identification of the underlying causes. If the 'Power' MPS can be proved to be caused by variations in excitation temperature (ΔT) then an explanation for the difference in behaviour between atom and ion lines is required. A cause of the 'Uptake' MPS could also be pursued. One tentative mechanism which qualitatively fits the data is that uptake variation results in the superimposition of two effects; analyte concentration (Δn) and excitation temperature (ΔT). For example if the sample uptake rate increases by 10% the analyte concentration in the plasma would also be expected to increase by 10%. The fact that Li intensity increases by 5.6% and Zn intensity not at all, may be due a cooling of the plasma caused by the increased amount of water introduced to the plasma. The predicted effect of this fall in excitation temperature would be, as found experimentally, that Zn is affected most, and Li least. The fact that Li emission is increased by 5.6% and not 10% may be aerosol ionic redistribution (Borowiec et al., 1980). There are problems with this theory however. Boumans and de Boer (1976)

estimated that the water entering the ICP consumed 20% of the total power input which would support a fall in temperature due to the water. However Alder et al.(1980) reported that increased water vapour increased the excitation and ionization temperatures. It would be possible to design an experiment to test this proposed hypothesis for 'Uptake' effects.

If all short term analytical variations could be expressed in terms of ΔT and Δn then perhaps a simpler form of PRISM could be derived from fundamental constants.

Certain elements, notably phosphorus were not significantly improved by the use of PRISM. This suggests that there may be a third cause of variation. Extending the methodology used in this study to other elements, particularly those with low wavelength lines (P = 178nm) may reveal a multielement pattern which could identify this third cause.

9.1.4.2 **Improved methods of precision correction**

In this study PRISM was applied retrospectively to complete data sets. The correction of data in real-time would be an advantage, but only if the program could run quickly (not more than 5 seconds per sample). This should be achievable with the current generation of computers present on ICP systems. On-line addition of internal standard elements to sample solutions is also desirable, but this would be expensive to achieve the volumetric precision required.

The low precision value (0.02%) achieved by the Myers-Tracy method (1983) suggest that high resolution of time for intensity correction may be advantageous. In their study, correction was achieved by division of the analogue signals, which would be undesirable for PRISM due to its mathematical inflexibility. A

relatively simple experiment to test the likely performance of a high resolution PRISM could be based on three elements Zn, Mg, Li. If their simultaneous signals could be digitised every 0.05s, then the improvement in precision of Mg could be studied as the time constant varied.

A comparative study of the performance of PRISM and GIRM for the same routine data set would also be a worthwhile undertaking to assess possible methods improvement. The extension of PRISM to correct for variations in background intensities is also worth investigation. In the Section 4.8, 30% of the variance on background emission was classified as multielement correlated. This would imply that given the correct model for the variation, then improvements in detection limits should be possible by a method analogous to PRISM. However Meyers-Tracy (1983) using signal division failed to achieve improved detection limits, despite high levels of correlations found across the spectral background.

9.1.4.3 Broader application of PRISM for precision improvement

The first step is to apply PRISM to other ICPAES instruments under similar operating conditions. If the theory for the cause of uptake variations is correct, then the independence of Zn (II 202.55nm) from variations in uptake may have been specific to one uptake rate. Assuming that the virtual independence of Li (I 670.78nm) to changes in forward power can be reproduced on other machines, then the two stage PRISM correction (equations 5.14 and 5.15) should be more generally applicable.

Investigation of PRISM under substantially different operating condition would be informative. At high observation

heights the generally high levels of correlation suggest the improvements from PRISM would still be substantial.

The application of PRISM-like corrections to other multielement analytical systems would be interesting. ICP-Mass Spectrometry for example has worse problems of data quality than ICPAES (Munro et al., 1986). If multielement correlation is shown to be high using PCA then potentially a similar correction might be possible, if the causes of variation could be monitored independently.

9.2 Inaccuracy caused by Matrix Effects

9.2.1 The Investigation and Modelling of Matrix Effects

Matrix effects were established as a potential source of significant inaccuracy in geochemical analysis by ICPAES. In the analysis of limestone as an extreme example, the bias of analyte concentration caused by calcium can vary from +10 to -36%, depending on the particular analyte. The source of this interference effect was located dominantly within the plasma rather than in the nebuliser.

A predictive model was constructed for the bias produced by any matrix element on the intensity of any analyte emission. The susceptibility of the analytes was found to be a linear function of the total excitaiton potential (E') of the particular emission line measured. The property of the matrix element which was found to be a linear determinant of the bias produced on analytes was called matrix energy demand (MED). The MEDs were calculated from fundamental properties of the elements and measured the energy required to convert the matrix element into on a gaseous ion with an appropriate degree of ionisation. This MED-model was based qualitatively on the hypothesis that all plasma matrix effects are

due to the reduction of excitation temperature of the plasma caused by the addition of the matrix element. Typical values of falls in excitation temperature were in the region 0-100K. The model was limited to one concentration of matrix element (0.05M). The effect on analyte sensitivity of changing concentration of one matrix element was found to be non-linear and accurately described by a two parameter, exponential equation.

An important use of the model in its current form is a prediction of the combinations of matrix element and analyte line that will produce significant analytical bias. For example biases of $>10\%$ are to be expected only for analyte lines with high values of excitation potential (>8eV) in matrices with values of MED greater than ca.10eV. For the wavelengths studied, this would mean large biases for the analyses of Be, Cd, Co, Cr, La, Mo, Ni, Pb, V and Zn in samples containing large concentration of Ba, Ca, Fe, La, Mg, Mn, Sr, Ti or Zr. In these instances, some method of correction for matrix effects is required if an accuracy better than 10% is to be achieved. Conversely a large proportion of matrix/analyte combinations studied gave no bias greater than 5% and this confirms the general perception of ICPAES being largely free of matrix effects. These conclusions pertain specifically to the operating conditions used for this investigation, which are typical of those used generally for routine analysis.

9.2.2 Methods of Correcting Matrix Effects

The methods currently used for the correction of inaccuracy due to matrix effects were found to be poorly suited to routine geochemical analysis. Either they relied on batches of samples having constant and predictable major elemental composition or else they were considered so slow as to be impracticable.

Seven new methods of correction were proposed and developed to various extents in order to assess their potential strengths and weaknesses. Six of the methods utilised computers either in purely a passive role to compute corrections (4 methods) or else in an interactive role (2 methods). In the interactive mode the computer can intervene in the analytical process by the control of instrumental parameters, or test sample composition.

A comparison of ten methods of correction is given in Table 7.8 but the conclusions can be summarised. The greatest accuracy of correction was achieved by Interactive Matrix Matching (IMM) but at the expense of a limited range of sample composition and a two fold drop in productivity. IMM is currently restricted to the correction of the effects of a single matrix element. This limitation however enables the advantage of simultaneous correction for background interference effects.

The second interactive method devised was Interactive Power Adjustment (IPA). This method depends on the similarity in effect between the addition of a matrix element and the reduction of the forward power to the plasma. Initial experimentation suggested that the accuracy of correction was comparatively poor due to discrepancies between the two effects. The method was further complicated by different variations in background response from the two effects. The potential strengths of IPA are its flexibility and automation potential.

The most flexible of the methods in terms of the range of matrix elements corrected was the MED-model. Although currently limited to one concentration of the matrix element, all effects from 18 matrix elements on 16 analyte lines were corrected to within a few percent. A purely chemometric correction of the

effects from a range of concentrations for one matrix element (VC-model) were successful for a large range of analytes. The full potential of chemometric correction will only be evident from a combination of these two models, but the main strengths will probably be speed and flexibility rather than accuracy.

The ability of the parameter-related internal standard method (PRISM) to correct matrix effects was initially unexpected. PRISM was originally devised for the improvement of precision. The correction is effective for the entire range of matrix element concentration and is predicted to work for any matrix element with a high MED value. The accuracy for the correction of the effects from calcium is acceptable for all but a few analytes (e.g. Sr, Ba and La). A particular advantage of the PRISM method is that improvement in accuracy is accompanied by a simultaneous improvement in the precision. Furthermore inaccuracy due to long term drift will be removed in addition to that due to matrix effects.

In summary, when the best of these techniques are fully developed, the removal of analytical bias due to matrix effects in ICPAES should become feasible on a routine basis. The productivity of the analysis will probably be inversely related to the accuracy of correction required.

9.2.3 **The Theory of Matrix Effect Correction**

The rationale for the use of PRISM for improving accuracy lies in the mechanism causing matrix effects. Essentially, the action of Zn (II 202.55nm) as a line of high total excitation potential is to monitor excitation temperature. In precision improvement the zinc thermometer corrects for short term fluctuations in the excitation temperature. In accuracy

improvement, it is the systematic cooling of the plasma brought about by the matrix element which is monitored by zinc. Once the change in temperature is quantified the individual effect on each analyte can be predicted and corrected. Because these matrix effects originate dominantly in the plasma then the monitoring of the 'Uptake' related variation was negligible and left uncorrected. It is probable however that matrix effects caused by the variable viscosity of samples (e.g. oils) would require this 'second-half' of the PRISM correction to remove matrix effect. Investigation of this conjecture would be worthwhile.

The concept of normalising the excitation temperature can be extended to all the correction methods considered. The normalisation is either chemometric (as in MED-Models, VC-Model and PRISM) or else achieved in reality by the interactive methods (IMM and IPA).

9.2.4 Future Work on Imrpoving Accuracy

Although accuracy and precision have been treated as separate objectives in this thesis it has been shown repeatedly that the factors limiting both analytical qualities have many similarities.

9.2.4.1 Plasma investigations

A deeper understanding of the effect of temporal fluctuations of the temperature of the plasma would enable better correction of both its random and systematic variations. The current model of matrix effects is based on the excitation temperature of the plasma but this is known to be an over simplification. A first attempt at allowing for variation in the degree of ionisation expected to accompany a fall in temperature, produced poor agreement with the experimental intensities. This

was particularly true for the atom lines. This may be due to the lack of local thermodynamic equilibrium (LTE), frequently reported in the plasma (Alder et al., 1980), which implies that the ionisation and excitation temperature need not be equal. The more accurate prediction of the behaviour of the atom lines is particularly important, as they are also the lines most affected by the sample 'Uptake' variations. This would therefore enable better elucidation of the 'Uptake' effects.

9.2.4.2 **Nebuliser based matrix effects**

In the condition of constant viscosity used in this study, the nebuliser was found not to contribute appreciably to matrix effects. An extension of the study of matrix effects to changes in viscosity should reveal the role of the nebuliser and 'Uptake' effects more clearly. Botto (1985) in his study of the effects of variable acid concentration noted the importance of the total excitation potential of the analyte lines, but was unable to correct his results for this effect. With the knowledge of the role of excitation temperature from this work, the pure 'Uptake' effect should become evident. The theory of increased cooling by greater uptake of solvent could also be tested by this means.

9.2.4.3 **Variable concentrations of matrix element**

The premise of a fall in excitation temperature to explain matrix effects predicts a linear fall in analyte sensitivity (ln S_r) with increasing concentration of matrix element. This was found not to be the case for the calcium matrix. An investigation of this non-linearity is a basic prerequisite for a better correction of matrix effects. Also there is the problem that the energy 'required' by the MED of the matrix element is not matched by the energy implied by the cooling of the argon in the plasma.

These two problems may be interrelated. The non-linearity may be improved by correction for variable ionisation of the matrix and analyte elements. Also there may be some slight component of changing the analyte concentration in the aerosol fraction reaching the plasma. Furthermore, the reduced water content of a solution containing 1% Ca would be expected not to cool the plasma as much as would be predicted from a calculation based solely on the increased calcium content. Computer modelling of this situation should prove helpful in calculating the expected non-linearity to be expected from these causes. A systematic study of the effect of changing concentrations of a range of matrix elements would be desirable to ascertain the general picture of the curve shapes produced, for a range of analytes.

9.2.4.4 **The effects of multiple matrix elements**

The studies in this thesis were restricted to the effects of single matrix elements. Real samples often have several elements at levels which could cause significant inaccuracy. It would be desirable to extend the theories developed here to this more general case. If matrix effects were caused only by the reduction of excitation temperature then it would be predicted that mixtures of elements would produce additive effects. In a study by Maessen et al (1982) approximately additive effects were found for Ca and Mg but not for mixtures including the alkali metals. In the current study the alkali metals were found to give very small effects. This might suggest that a careful consideration of errors would play a large factor in refuting the additive hypothesis. Comparison between the studies are made difficult because the operating condition of Maessen's work was significantly different from this work, producing larger effects

from alkali metals. An improved understanding of the effects of uptake changes and cooling by water content would be a necessary prerequisite of interpreting multiple-matrix data.

9.2.4.5 **The spatial dimension**

Much study in recent years has been on a spatial resolution of the plasma, (Blades et al (1981a)). It was hoped that a better understanding of plasma processes would be gained than is possible in studies limited to one observation height. Spatial studies have improved our understanding but the mass of data produced has perhaps obscured simple mechanisms such as that of variable excitation temperature. What is now required is an integration of the spatial dimension and the multielement dimension used in this study. Perhaps the fall in excitation temperature caused by calcium as perceived at 14mm may simply reflect an upward movement of the plasma. In that case perhaps minute adjustments of observation height or plasma support gas could be used to compensate. The careful combination of patterns in both dimensions will undoubtedly prove rewarding. In particular it would allow the assessment of the applicability of many findings of this thesis to other operating conditions.

9.2.4.6 **Improved methods for the correction of bias**

A clearer understanding of the processes involved in matrix effects should enable more accurate chemometric corrections to be made over a wider range of matrix elements, at various concentrations, and with any combination of elements.

This should also apply to techniques based on internal standard or 'monitor' elements such as PRISM and IPA. If the currently anomalous behaviour of Ba and Sr for example, are due to ionisation temperature effects then suitable refinements to the

model should improve the accuracy of their correction.

The most urgent requirement for the IMM technique is better hardware, in the form of reproducible flow rates and mixing characteristics, to achieve reliable operation. The extension of IMM to correct for matrix effects from any element would require matching to a monitor element. This would be expected to re-introduce the problems of anomalous behaviour for some elements. Also the matching would require the addition of some matrix element with a high MED value but which should not cause problems of background interference.

9.3.1 Self-matrix Effects and Calibration Curvature

A new mechanism for curvature in the calibration of ICPAES was identified. The self-matrix effect is a logical extension of the matrix effect, to the case where the lines affected are those of the matrix element itself. The curvature of eleven out of the fourteen calcium lines investigated conformed to that predicted by the MED-Model of matrix effects. A different cause of curvature, self absorbance, was suspected of being the dominant cause for two lines with high values of $f\lambda$ (oscillator strength * wavelength).

These conclusions were limited to the typical observation height used (14mm) and self-matrix effects would be expected to be of lesser importance at higher observation heights.

A new curve fitting equation was developed which was considered superior to currently available equations in several respects. The new equation was derived from the observed shape of analyte matrix effects and therefore conformed well to the inherent shape of calibration curves. This contrasts with the splined-polynomial normally used, which is not based on spectrochemical information. This form of equation usually

requires four segments to span the five orders of magnitude typical of ICPAES calibrations. The new form of equation can span this range with one equation from 0.1 to 10,000 µg ml^{-1} with excellent goodness of fit over the whole range. The increased computational requirement of the new equation should not prove a limiting factor.

9.3.2 Future Work on Self-Matrix Effects

The current study was limited to calcium and the general importance of self-matrix effects will only be known from similar studies on a wide range of elements. A better characterisation of other causes of curvature, notably self-absorbance, is required to effectively separate the two effects.

A fuller understanding of the matrix effects should result in better prediction of line curvature from fundamental properties of the element and the particular emission line.

Methods of correcting matrix effects should be investigated for their ability to linearise calibration curves. This should enable an extension of their useful range of calibration.

9.4 General Conclusions

A new insight has been achieved into the factors controlling variations in analyte intensity in routine analysis, and hence data quality in ICPAES.

There are common factors which limit both accuracy and precision in analysis by ICPAES. The two primary causes have been identified. Very similar mechanisms are responsible for limiting both components of data quality but the effects differ mainly in being either random or systematic, in the time domain. The causes have been identified tentatively as i) variations in the excitation temperature of the plasma and ii) the concentration of analyte entering the plasma.

Random variations in excitation temperature, for whatever reason, result in variation in analyte intensities which becomes apparent as imprecision. A **systematic** drop in excitation temperature caused by the addition of a matrix element produces a change in sensitivity which results in inaccuracy. The bias produced is greatest for elements with a high value of matrix energy demand (MED). In both random and systematic variations the analytes are affected in proportion to the total excitation potential of the line measured.

Random variation in the amount of analyte reaching the plasma have been tentatively identified in the effects of parameter related to sample uptake. Systematic variations in the amount of analyte were not found to be an important component of the matrix effects studied here. They may become significant at very high concentrations of sample or matrix acid.

Significant improvements in both precision and accuracy have been achieved either by keeping excitation temperature and analyte concentration constant, or by the retrospective correction of the data to these conditions. Precision has been improved by a factor of two, to ca. 0.5%. The accuracy have been improved by up to a factor of ten to ca. 2%. The methods employed have the potential for further improvements in performance.

Both the investigation of the effects and their subsequent correction have been made practicable by the appropriate use of computers. The multielement dimension was developed as a new tool for the investigation of variation in ICPAES. This tool relies on flexible, high level software. Techniques developed for the improvement of data quality used multielement data maniputlations which were both evolved and executed, using the same tools. Other

techniques utilised computers as part of a system to intervene in the process of analysis in order to achieve the same objectives. This interactive solution is a new approach to problem solving in analytical chemistry.

It was the particular problems and requirements of geochemical analysis which directed and motivated this study. The findings and methods of corrections from this work however have general applicability to all analysis by ICPAES. High precision and accuracy is equally important for example in the analysis of precious metal alloys. Even where high data quality is not required, the prediction of what the expected quality for a new analyte/matrix combination is a new and useful ability.

9.5 Priorities for Future Work

Throughout this chapter recommendations have been made for new research suggested by particular findings. In this section the broader objectives will be identified.

An extension of the experimental techniques developed here to a broader range of analytical conditions is required. This would enable a verification of these findings and a deeper understanding of the fundamental processes limiting analytical variability.

A more sophisticated computer model of the factor effecting analyte intensity would be a useful objective and research tool.

The developing of the correction techniques into robust, practicable methods is required before they can be applied to routine analysis.

Comparisons under more realistic conditions are required between the methods of correction developed here and other methods. It will be particularly interesting to resolve one

fundamental question; viz is a correction method based on spectrochemical knowledge (e.g. PRISM) any better than a method which is purely descriptive (e.g. GIRM).

The development of improved hardware, not covered in this work, is now more evident as a limiting factor. The laminar flow torch, already being developed by Davies et al.(1986), and a less 'noisy' nebuliser should provide further improvements in precision.

The same methodology used in this study could be applied to investigate and improve accuracy and precision in other multielement analytical techniques, for example ICP-mass spectrometry.

Further utilisation of computer power is an obvious progression from this work. In the interactive mode the devices already described could be used more generally. The interactive matrix matching (IMM) equipment for example could be used to prepare a range of multielement calibrating solutions. Alternatively by adjusting the sample uptake, IMM could compensate for variations of the 'Uptake' parameters (described in Section 4.7.2). Computer control of all the instrumental operation parameter would enable multiple interactive adjustments to be investigated.

An expert system for analysis by ICPAES is a further use of computer power to improve performance which is likely to appear in the near future. As the correction methods, such as those described here, become more complex it will become impractical for every user of an instrument to understand its operation and place confidence in its results.

The expert system can be envisaged with the following characteristics. The comparison of the data quality required and that produced will be a crucial factor for the expert system. The user will specify the quality of data required and the system will use its knowledge-base to design the analytical procedure which should produce analysis of that quality. The predictive models produced in this thesis would be ideal for such a knowledge base. A suitable scheme of analytical quality assurance would then be specified by the system, and the quality assessed continuously as the analysis proceeds. The accuracy and precision achieved in practice could then be used to further modify the methods being employed to control the data quality.

Such a knowledge-base would not only provide a systematic framework for the findings of this research but also reveal the gaps in our knowledge which require future research.

The constraint of cost-effectiveness would ideally be included in the system to produce a realistic compromise between the quality and the speed of the analysis. The expert system should therefore be able to tell the user, for the given analytical problem, what accuracy and precision could be achieved at what speed, and at what cost. The ultimate requirement would therefore become that the geochemist should ascertain just what quality of analysis is really required for the correct interpretation of a given geochemical problem.

This requirement has never been scientifically investigated, although it underpins the objectives of this thesis. A systematic study is needed to quantify the analytical data quality that is required so that it will not significantly affect the geochemical interpretation. Only then can a realistic target be placed on the accuracy and precision required for geochemical analysis by methods such as ICPAES.

REFERENCES

AHRENS, L.H. AND TAYLOR, S.R. (1961). "Spectrochemical Analysis" Pergamon Press, Oxford, pp88-104.

ALDER, J.F., BOMBELKA, R.M. AND KIRKBRIGHT, G.F. (1980). Spectrochim Acta 35B, 163-175.

BARNETT, W.B., FASSEL, V.A. AND KNISELEY, R.N. (1968). Spectrochim Acta 23B, 643-664.

BARNETT, W.B., FASSEL, V.A. AND KNISELEY, R.N. (1970). Spectrochim. Acta. 25B, 139.

BELCHAMBER, R.M. AND HORLICK, G. (1982). Spectrochim. Acta 37B, 17.

BLADES, M.W. AND HORLICK, G. (1981a). Spectrochim. Acta 36B, 861.

BLADES, M.W. AND HORLICK, G. (1981b). Spectrochim. Acta 36B, 881.

BOROWIEC, J.A., BOORN, A.W., PILLARD, J.H., CRESSER, M.S. AND BROWNER, R.F. (1980). Anal. Chem. 52, 1054.

BOTTO, R.I. (1985). Spectrochim. Acta. 40B, 397.

BOUMANS, P.W.J.M. (1966). "Theory of Spectrochemical Excitation" Hilger & Watts Ltd., London.

BOUMANS, P.W.J.M. AND de BOER, F.J. (1976). Spectrochim. Acta. 31B, 335.

BOUMANS, P.W.J.M., WAGENAAR, H. AND de BOER, F.J. (1973). XVII Colloquium Spectrosc. Int., Florence Reprints, Vol. 1, p114.

CATTELL, R.B. (1966). "Handbook of Multivariate Experimental Psychology". Rand McNally, Chicago Il. U.S.A. pp174-243.

DAVIES, J. AND SNOOK, R.D. (1986). J. Anal. At. Spectrom. 1, 195.

DORN, G. (1981). in "Developments in Atomic Plasma Spectrochemical Analysis" Barnes, R.M. (ed.), Heyden, Philadelphia, P.A., U.S.A, pp369-382.

DRAWIN, H.W. AND FELENBOK, P. (1965). "Data for Plasma in Local Thermodynamic Equilibrium". Gauthier-Villars, Paris.

EBDON, L. AND CAVE, M.R. (1982). Analyst, 107, 172-178.

FAIRBAIRN, H.W., ET AL. (1951).
U.S. Geol. Surv. Bull. 980, 42.
FAIRES, L.M., APEL, C.T. AND NIEMCZYK, T.M. (1983).
Appl. Spectrosc. 37, 558.
de GALAN, L. (1984).
Spectrochim. Acta. 39B, 537.
GERLACH, W. (1925).
Z. Anorg. Chem., 142, 383.
GOVETT, G.J.S. (1983).
in "Handbook of Exploration
Geochemistry". Ed. Govett, G.J.S. Elsevier, Amsterdam.
GREENFIELD, S. (1983).
Spectrochim Acta. 38B, 93.
GREENFIELD, S., JONES, I.L. AND BERRY, C.T. (1964).
Analyst, 89, 713.
GREENFIELD, S., McGEACHIN, H. McD. AND SMITH, P.B. (1976).
Anal. Chem. Acta 84, 67.
HEAD, J.H. (1970).
U.S. Air Force Acad. Techn. Rep., No. 70-5, pp49.
HOWARTH, R.J. (1983).
"Statistics in Data Analysis in Geochemical Prospecting",
Elseview, Amsterdam, pp238.
HUMAN, H.G.C. AND SCOTT, R.H. (1976).
Spectrochim. Acta. 31B, 459.
KALIVAS, A.H. AND KOWALSKI, B.R. (1981).
Spectrometry. Anal. Chem. 53, 2207.
KAWAGUCHI, H., ITO, T., OTA, K. AND MIZUIKE, A. (1980).
Spectrochim Acta, 35B, 199.
KIRKBRIGHT, G.F. AND SARGENT, M. (1974). "Atomic Absorption and
Fluorescence Spectroscopy". Academic Press, London.
KOIRTYOHANN, S.R., JONES, J.S., JESTER, C.P. AND YATES, D.A.
(1981).
Spectrochim. Acta. 36B, 49.
LAWRENCE, D.M. (1984).
At Spectrosc. 5, 156.
LAWRENCE, D.M. (1985a).
At Spectrosc., 6, 23.

LAWRENCE, D.M. (1985b).
At Spectrosc., 6, 94.
LAWRENCE, D.M. (1986).
At Spectrosc., 7, 14.
LORBER, A., ELDAN, M. AND GOLDBART, Z. (1985).
Anal. Chem. 57, 851.
LORBER, A. AND GOLDBART, Z. (1984).
Anal. Chem. 56, 37.
LORBER, A., GOLDBART, Z. AND ELDAN, M. (1984).
Anal Chem. 56, 43.
MAESSEN, F.J., BALKE, J., AND de BOER, J.L. (1982).
Spectrochim Acta. 37B, 517.
MOSTAGHIMI, J., PROULX, P. AND BOULAS, M.I. (1985).
Spectrochim Acta. 40B, 153-166.
MUNRO, S., EBDON, L. AND McWEENY, D.J. (1986).
J. Anal. Atom. Spectrom. 1, 211.
MYERS, S.A. AND TRACY, D.H. (1983).
Spectrochim Acta. 38B, 1227.
NOJIRI, Y., TANABE, K., UCHIDA, H., HARAGUCI, H., FUWA, K.,
AND WINEFORDNER, J.D. (1983).
Spectrochim. Acta 38B, 61-74.
ODEGARD, M. (1981).
J. of Geochem. Exp. 14, 119.
OHLS, K. AND KOCH, K.H. (1977).
ICP Inf. Newsl., 5, 192.
RAMSEY, M.H. AND THOMPSON, M. (1982).
Analyst 107, 232.
RAMSEY, M.H., THOMPSON, M. AND COLES, B.J. (1983).
Anal. Chem. 54, 1626.
ROSE, A.W., HAWKES, H.H. AND WEBB, J.S. (1979).
"Geochemistry in Mineral Exploration". Academic Press,
London.
RYAN, T.A., JOINER, B.L. AND RYAN, B.F. (1976).
"Minitab Student Handbook". Duxbury Press, North Scituate,
Mass. U.S.A.
SALIN, E.D. AND HORLICK, G.A. (1980).
Anal. Chem. 52, 1578.

SAXBERG, B.E.H. AND KOWALSKI, B.R. (1979).
Anal. Chem. 51, 1031.
SCHRAMEL, P. (1982).
ICP Inf. Newsl., 7, 429.
THOMPSON, M. (1985).
Analyst 101, 443.
THOMPSON, M. (1986).
"Applied Geochemistry in the 1980s" ed. I. Thornton
and R.J. Howarth. Graham and Trotman, London, p191-211.
THOMPSON, M. AND HOWARTH, R.J. (1976).
Analyst 101, 690.
THOMPSON, M. AND WALSH, J.N. (1983).
"A Handbook of Inductively Coupled
Plasma Spectrometry". Blackie, Glasgow and London.
WEDEPOHL, K.H. (1969).
Ed. "Handbook of Geochemistry", Springer-Verlag, Berlin.
WENDT, R.H. AND FASSEL, V.A. (1965).
Anal. Chem. 37, 920.
WIESE, W.L., SMITH, M.N. AND MILES, B.M. (1969).
"Atomic Transition Probabilities". Vol. II Sodium through
Calcium U.S. Dept.of Commerce, National Standards Reference
Data System NSRPS-NBS-22.
ZAGATTO, E.A.B., JACINTHO, A.O., KRUG, F.J., REIS, B.F.,
BRUNS, R.E. AND ARAVJO, M.C.U. (1983).
Anal. Chem. Acta, 145, 169.

COLUMN COUNT ROW	ZN 75	SR 75	PB 75	CD 75	BA 75	NI 75	MN 75	FE 75
1	100.570	637.650	75.8100	504.040	594.700	116.490	467.210	305.110
2	100.890	637.460	76.4300	509.030	594.360	116.830	469.760	306.080
3	101.030	637.100	76.7600	506.280	597.110	116.970	470.590	306.210
4	100.270	634.050	75.6400	501.880	597.460	116.050	468.380	304.310
5	100.510	627.410	75.9600	503.720	590.440	116.340	469.220	304.500
6	100.570	622.820	76.1900	502.410	582.850	115.860	466.290	303.410
7	101.180	627.960	76.4300	507.040	587.970	117.210	471.180	305.700
8	100.190	618.350	76.4000	500.610	583.870	116.340	468.060	303.190
9	101.800	638.280	77.7200	509.700	598.480	116.940	475.560	308.690
10	100.590	633.150	77.5900	505.850	591.460	116.050	472.390	306.610
11	100.560	632.960	76.8900	504.730	593.410	115.950	471.910	306.390
12	102.180	623.140	77.1600	506.280	586.250	117.490	472.810	306.230
13	101.180	631.420	77.2600	505.740	592.110	116.790	472.980	306.900
14	99.570	630.320	76.3300	499.700	589.540	115.350	468.590	304.520
15	101.190	627.670	77.7400	505.820	590.010	116.920	473.080	306.490
16	100.410	630.990	76.9800	503.870	597.110	116.880	473.790	306.970
17	100.080	636.950	76.2700	502.000	598.660	115.620	471.760	306.610
18	100.470	624.700	76.5300	500.390	586.070	115.810	469.480	304.790
19	100.220	623.660	75.7400	496.010	585.940	114.950	466.980	303.000
20	100.410	629.980	76.6900	502.230	593.320	116.350	471.870	306.100
21	100.210	626.290	77.0700	499.690	591.970	115.370	470.910	305.200
22	99.660	628.330	76.9600	502.130	589.460	115.700	470.280	305.510
23	98.610	626.760	75.4700	492.580	589.210	114.420	465.590	302.620
24	99.430	627.770	75.8400	497.830	592.790	115.410	468.480	304.120
25	99.850	625.700	75.9200	498.690	592.700	115.870	469.620	304.630
26	100.760	624.540	76.9300	501.530	591.410	116.710	472.080	306.110
27	100.370	622.160	77.6200	503.960	585.970	116.520	471.690	305.810
28	99.400	629.770	75.8800	498.440	594.960	115.800	470.000	305.710
29	98.870	629.830	75.9200	496.700	596.010	115.190	468.380	304.490
30	99.300	626.210	76.7500	499.820	592.500	116.000	470.220	305.100
31	99.880	625.980	76.3900	499.670	595.910	116.440	471.280	305.620
32	99.180	633.360	75.9100	501.010	600.000	116.210	471.490	306.410
33	100.240	629.690	77.1600	500.320	592.470	115.880	470.080	305.790
34	99.240	630.580	76.3300	498.990	600.040	115.930	471.280	306.200
35	98.080	625.560	75.3000	492.860	597.760	114.730	466.990	303.320
36	98.890	626.940	76.2200	499.550	593.830	115.570	468.720	304.990
37	98.760	626.990	75.8400	494.880	593.080	114.460	466.100	303.530
38	99.810	632.550	76.0900	501.110	601.770	116.090	471.790	306.900
39	99.710	626.200	77.1400	500.780	596.110	115.250	470.500	305.820
40	100.230	635.380	76.5500	503.750	605.800	116.870	474.310	308.600
41	99.060	626.420	76.8400	498.310	594.560	115.880	469.000	305.300
42	99.340	631.160	76.2700	500.020	596.480	115.640	469.890	306.510
43	100.110	627.540	76.6100	501.910	598.200	116.180	471.300	306.510
44	98.280	628.250	76.1800	497.070	602.360	115.660	469.200	305.080
45	99.180	626.630	76.2900	496.630	599.550	115.510	469.820	305.400
46	98.120	622.320	75.8400	493.910	595.380	114.840	466.190	303.600
47	99.350	632.110	75.8100	498.510	602.610	115.490	469.900	306.290
48	99.610	627.660	77.1800	499.450	599.780	115.510	469.790	305.800
49	99.090	632.360	77.2800	500.760	606.450	116.510	472.290	307.400
50	99.080	627.680	77.1800	498.590	603.370	115.540	470.300	306.000
51	99.220	631.080	77.2200	500.220	600.080	115.640	470.790	306.900
52	97.430	622.690	75.1100	495.260	594.290	114.710	465.680	303.420
53	98.300	624.830	76.7600	496.540	598.750	115.110	467.260	304.120
54	98.420	624.050	76.5000	496.610	598.830	115.580	468.970	305.020
55	97.210	620.690	75.6700	491.170	595.570	114.410	464.180	302.090
56	97.160	622.580	75.9100	488.700	595.760	114.140	463.170	301.900
57	97.690	620.290	75.6600	491.110	594.070	114.190	463.690	301.880
58	98.090	624.260	75.6500	494.740	600.520	114.770	467.190	303.980
59	97.980	616.380	76.2300	493.920	595.590	115.020	465.990	302.990
60	97.910	624.650	75.7800	495.550	602.970	115.010	467.920	304.640
61	97.020	617.450	75.5000	491.260	595.480	113.690	463.410	301.630
62	97.480	620.270	74.6100	492.870	593.980	114.210	464.480	302.600
63	98.690	622.760	76.1100	494.510	595.960	114.730	466.070	303.790
64	96.670	616.880	75.7400	491.510	593.460	114.190	462.760	301.300
65	97.370	619.230	75.4600	491.660	597.260	114.510	464.970	302.910
66	97.010	628.790	76.1500	493.060	607.340	114.760	467.500	304.610
67	97.670	619.390	75.9700	492.710	597.410	114.650	464.770	302.710
68	97.050	619.950	75.2500	490.670	598.180	114.170	464.620	302.610
69	97.420	615.010	76.1400	490.770	590.320	113.940	462.480	301.380
70	96.390	623.620	75.6000	488.280	600.340	113.870	462.500	301.690
71	94.230	603.590	73.8500	480.270	583.520	111.680	453.190	295.500
72	95.770	623.440	75.4300	488.950	604.020	113.630	463.560	302.310
73	97.190	622.570	76.8400	492.120	602.950	114.810	465.680	303.390
74	96.370	620.440	75.0900	486.840	601.660	114.020	462.890	301.690
75	96.290	615.470	75.2700	487.740	595.490	113.280	461.070	300.310

Appendix A Quasi-routine analysis data set

COLUMN	F	MG	MO	NA	AL	V	BE	CA
COUNT	75	75	75	75	75	75	75	75
ROW								
1	625.890	199.630	173.620	252.890	226.010	349.000	697.600	227.130
2	636.310	200.600	172.670	254.970	226.580	349.830	696.040	229.390
3	650.610	200.500	173.510	253.670	226.980	349.870	696.720	229.300
4	620.570	199.250	172.120	253.470	226.370	348.120	695.260	226.810
5	626.030	198.630	172.690	246.480	223.800	347.000	691.220	229.700
6	633.630	197.370	170.520	244.580	221.580	343.710	681.270	229.210
7	633.270	198.910	172.020	244.350	223.050	346.450	687.220	231.810
8	629.250	197.120	172.020	242.930	221.170	343.420	683.110	229.210
9	659.980	201.200	173.320	252.190	227.450	350.320	694.070	233.400
10	615.710	199.420	171.500	245.830	224.480	347.110	685.120	232.580
11	633.680	199.600	171.580	251.220	225.690	347.410	686.050	231.970
12	646.670	198.630	172.760	238.740	221.540	345.210	684.080	235.080
13	651.370	199.510	171.860	245.530	224.560	347.050	685.170	233.890
14	647.660	198.140	169.280	250.290	224.690	344.390	678.730	231.400
15	646.940	198.700	172.430	241.180	222.960	345.850	682.950	234.210
16	648.700	199.790	172.490	246.330	225.810	347.390	687.070	233.320
17	643.670	199.860	170.330	253.800	227.700	347.110	683.520	232.540
18	652.800	198.000	169.860	244.290	222.650	343.310	674.640	233.100
19	628.060	196.980	169.260	242.840	222.210	341.610	673.380	231.090
20	653.220	198.950	171.250	247.000	224.520	345.210	680.950	233.420
21	641.040	198.100	170.930	242.570	223.250	344.240	679.420	232.690
22	643.440	198.100	170.640	243.830	223.300	343.720	674.390	233.820
23	633.800	197.080	168.510	247.920	223.690	341.320	670.370	230.370
24	637.270	197.780	169.410	246.230	224.200	343.140	675.080	231.530
25	647.590	197.650	170.210	242.130	223.170	343.180	676.840	232.310
26	640.210	198.540	172.100	240.640	222.580	344.000	678.900	234.210
27	644.030	197.750	171.640	235.620	220.500	342.680	671.740	235.810
28	655.160	198.370	169.350	247.480	224.840	343.980	674.140	233.200
29	649.780	197.800	169.520	246.530	224.660	343.140	674.180	231.690
30	644.320	197.820	170.840	241.950	223.050	343.100	673.410	233.670
31	655.690	198.190	171.580	242.370	223.480	343.790	677.310	233.510
32	644.640	199.050	170.440	247.180	225.780	345.240	678.310	233.790
33	639.790	198.060	169.220	240.220	223.010	343.240	670.550	234.710
34	651.360	198.730	170.760	245.320	225.070	344.500	676.900	233.390
35	644.900	197.120	169.360	245.400	224.300	342.000	672.920	230.620
36	652.430	197.700	169.350	243.120	223.170	342.380	669.840	233.620
37	639.400	196.800	168.240	244.300	222.980	341.010	666.630	231.900
38	627.070	199.070	171.050	244.760	225.260	345.050	676.620	234.510
39	642.460	197.680	170.330	237.120	222.250	342.830	672.500	234.380
40	650.000	200.030	172.170	245.550	226.360	347.000	680.160	236.000
41	651.770	197.290	169.840	236.370	221.980	342.220	668.960	234.510
42	634.810	198.670	169.760	244.270	224.170	343.240	668.650	235.390
43	635.690	198.550	171.000	239.370	223.280	343.610	671.700	235.480
44	633.740	197.660	170.150	240.300	223.770	343.300	673.220	232.920
45	634.930	197.730	170.800	238.440	222.970	342.820	671.640	233.900
46	628.130	196.520	168.980	240.200	222.080	340.550	665.050	232.500
47	633.920	198.430	170.540	243.680	224.820	344.020	670.600	234.410
48	642.240	198.050	170.330	240.360	223.550	343.280	669.790	234.590
49	647.220	199.050	171.510	241.560	225.050	345.350	676.020	235.460
50	637.240	198.030	170.950	240.250	223.910	343.700	672.100	234.110
51	641.030	198.450	170.620	238.890	223.430	344.040	667.540	236.400
52	637.800	196.370	169.120	239.260	221.510	340.120	660.060	233.430
53	641.180	196.980	169.840	239.480	222.410	341.300	664.300	233.400
54	644.930	197.070	170.830	236.150	221.690	341.940	665.520	234.600
55	637.500	195.630	168.890	238.460	221.290	338.960	658.550	232.020
56	623.290	195.460	168.110	239.390	221.390	338.860	656.920	231.570
57	639.950	195.240	168.220	234.950	219.970	338.560	658.080	232.100
58	654.400	196.460	170.360	235.990	221.770	341.440	663.990	233.310
59	627.510	195.450	170.570	231.890	219.530	339.410	660.910	233.310
60	633.480	197.150	170.380	238.780	222.870	342.180	665.440	233.600
61	636.220	194.870	169.130	233.880	219.650	338.210	657.560	231.630
62	624.190	195.230	168.480	234.350	219.690	338.810	656.370	233.290
63	627.250	196.070	169.260	234.470	220.420	340.250	657.810	234.290
64	611.540	194.890	168.640	234.710	219.540	337.860	655.060	231.920
65	616.240	195.630	169.640	235.770	220.400	339.430	658.050	232.920
66	619.150	197.280	169.990	240.510	223.940	343.100	665.980	233.200
67	615.410	195.290	169.950	232.210	219.720	339.450	657.810	232.910
68	604.720	195.640	169.160	235.870	220.490	339.280	656.890	232.800
69	609.490	194.510	169.220	232.350	218.180	337.110	649.720	233.420
70	622.600	195.280	168.790	238.280	221.470	339.260	654.890	231.700
71	589.520	190.800	165.350	229.920	215.240	331.200	639.360	227.420
72	627.620	195.670	168.580	240.750	222.400	339.700	658.360	231.310
73	626.310	195.870	170.160	235.490	221.320	340.740	659.180	233.210
74	599.050	194.880	168.750	236.870	220.810	338.810	655.770	231.110
75	625.900	193.750	168.050	232.370	218.400	336.930	651.090	231.190

APPENDIX A (continued)

COLUMN	CU	AG	LI	TI	CO	K	LA	CR
COUNT	75	75	75	75	75	75	75	75
ROW								
1	230.240	117.310	311.360	38.8100	73.9800	553.310	178.650	340.470
2	230.370	117.000	311.940	38.7500	74.5200	557.480	179.390	342.430
3	230.660	117.570	310.830	38.8000	74.3800	554.600	179.450	342.170
4	230.470	117.310	311.860	38.7000	73.7700	554.980	178.170	339.400
5	226.600	116.460	299.930	38.6000	74.2400	536.620	177.710	340.120
6	223.340	114.550	296.160	38.0400	73.7300	532.450	175.850	337.280
7	224.710	115.330	294.750	38.3400	74.2400	532.020	177.200	341.140
8	222.590	115.220	295.050	38.1000	73.7300	531.030	175.030	337.700
9	229.460	116.630	306.020	38.8600	74.9900	549.920	179.760	344.250
10	225.580	115.380	295.420	38.4000	74.4200	532.670	178.280	339.990
11	227.100	115.810	304.330	38.4600	74.3900	549.010	178.220	339.540
12	221.840	115.270	287.060	38.3400	74.5800	518.370	176.180	340.850
13	225.490	115.740	296.100	38.4200	74.4200	534.180	177.980	340.470
14	225.830	114.820	302.850	38.1600	73.8300	546.090	176.940	337.250
15	223.340	115.610	290.290	38.4800	74.5800	525.640	176.790	340.270
16	226.720	116.610	298.800	38.6100	74.4300	537.820	177.600	341.030
17	228.780	116.000	308.380	38.6100	74.1800	553.030	178.390	338.420
18	222.630	114.340	294.160	38.0200	74.0300	531.890	175.970	337.130
19	222.410	114.370	292.620	38.0000	73.5100	527.620	175.400	335.120
20	225.030	115.390	298.900	38.3400	74.1100	541.200	176.670	338.680
21	223.540	114.970	293.000	38.2500	73.8400	527.100	176.130	337.620
22	222.930	114.880	293.000	38.1800	73.8800	531.360	176.630	338.260
23	223.920	114.760	300.230	37.9900	73.0900	541.000	175.780	333.640
24	224.220	115.190	298.130	38.1900	73.5700	537.510	176.010	336.440
25	223.160	115.000	292.750	38.1500	73.5400	526.980	175.880	336.810
26	222.190	115.600	289.930	38.4000	74.2300	524.910	175.900	338.200
27	218.780	114.110	281.460	38.0800	74.2900	512.300	175.430	338.590
28	224.710	114.750	299.090	38.3300	73.9100	540.090	176.850	336.540
29	224.980	115.030	298.690	38.2500	73.3600	537.490	176.610	335.980
30	222.190	114.960	291.530	38.1000	73.8200	529.110	175.980	338.480
31	223.180	115.350	293.750	38.3800	73.6600	530.760	175.810	338.890
32	225.710	115.830	299.250	38.4200	73.9100	539.270	177.550	337.850
33	221.850	114.390	287.530	38.1100	73.9500	522.480	176.580	337.350
34	224.720	116.020	297.580	38.4900	73.8800	536.680	176.790	338.150
35	224.140	115.320	298.650	38.1600	73.1800	536.050	175.520	334.590
36	222.570	114.350	292.810	38.1300	73.5200	530.150	176.050	335.980
37	222.500	113.670	295.130	37.9500	73.4400	534.590	175.500	334.910
38	224.790	116.250	295.900	38.5200	73.8800	534.660	177.540	338.720
39	220.990	114.990	284.940	38.2600	73.8100	516.840	175.880	338.310
40	225.900	116.430	296.470	38.6800	74.3800	535.740	178.410	341.320
41	220.970	114.470	282.480	38.1700	73.6400	511.640	176.270	336.290
42	222.720	115.280	293.470	38.2400	74.0000	533.950	177.140	338.550
43	222.160	115.800	287.800	38.3100	74.0500	521.770	176.710	338.670
44	223.580	115.670	290.720	38.4500	73.5000	524.000	176.150	337.260
45	221.920	115.390	287.930	38.3000	73.7500	518.990	175.860	336.640
46	221.250	114.460	289.650	38.0300	73.3100	524.010	175.240	335.190
47	223.940	115.540	293.780	38.4200	73.8300	531.120	177.270	337.120
48	222.290	115.550	289.490	38.2500	73.7400	524.450	176.480	338.080
49	224.430	116.100	291.710	38.6700	74.1800	526.970	177.490	338.550
50	222.820	115.400	290.420	38.5500	73.6400	523.780	176.380	338.270
51	221.930	115.310	286.050	38.3600	74.0800	521.510	177.280	338.930
52	219.920	114.300	287.650	37.9900	73.2100	522.520	175.230	334.790
53	221.240	115.340	289.150	38.2100	73.3000	522.530	175.540	335.430
54	220.030	115.010	283.710	38.2300	73.4200	514.660	175.530	337.580
55	219.680	114.200	287.560	37.8200	72.7000	519.970	174.620	334.050
56	220.020	113.950	288.610	37.8200	72.5500	522.940	174.770	333.780
57	218.380	113.730	282.410	37.8600	72.6700	511.900	174.230	333.270
58	220.470	115.170	284.210	38.1200	73.0900	514.410	175.510	336.490
59	217.710	114.620	279.170	37.9800	72.8800	506.150	173.970	334.760
60	221.480	115.320	288.320	38.2100	73.0400	521.760	175.930	337.090
61	218.060	114.190	281.540	37.9100	72.6900	510.140	173.700	332.960
62	217.560	113.470	280.450	37.8600	72.7400	510.870	174.380	334.070
63	218.330	114.380	280.430	37.9800	72.9600	510.990	175.290	335.620
64	217.560	114.210	282.340	37.7700	72.2900	512.520	173.570	333.850
65	218.600	114.620	283.930	38.0500	72.7500	516.020	174.280	335.390
66	222.990	116.170	290.730	38.4400	73.0300	523.560	176.400	336.530
67	217.920	114.770	278.480	38.0800	72.6200	503.870	174.360	334.890
68	218.820	114.540	283.770	37.9800	72.8200	514.620	174.470	334.530
69	215.530	113.390	277.250	37.6900	72.6100	506.960	173.520	334.130
70	220.540	115.040	286.840	37.9600	72.1900	520.050	175.180	333.370
71	213.230	112.100	276.070	37.0000	70.9500	502.100	170.690	327.420
72	221.420	114.940	292.010	38.0700	72.1500	528.260	175.000	333.790
73	219.860	114.980	283.790	38.2600	72.9400	513.160	175.110	335.940
74	219.710	114.460	286.560	37.9400	72.0400	517.230	174.230	333.660
75	216.380	114.010	279.630	37.6100	72.1300	507.020	172.900	332.070

APPENDIX A (continued)

```
NOTE    MINITAB MACRO FOR PRINCIPAL COMPONENT ANALYSIS
NOTE
NOTE  FOR SET OF 24 VARIABLES
RETRIEVE
COUNT C1 K1
CORR C1-C24 M1
EIGEN M1 C25 M2
NOTE CORRELATION MATRIX
LET C26 = 100 * C25/24
PARSUM C26 C27
NAME C25'EIGVAL' C26'CUMEV' C27'CUMPCT'
PRINT C25 C26 C27
LET C29 = SQRT(C25)
LET C30 = 1/C29
DIAG C29 M3
DIAG C30 M4
MULT M2 M3 M5
NOTE PRINCIPLE COMPONENT LOADING
PRINT M5
MULT M2 M4 M6
NOTE PRINCIPLE COMPONENT COEFFICIENTS
PRINT M6
LET C1=(C1-AVER(C1))/STAN(C1)
LET C2=(C2-AVER(C2))/STAN(C2)
LET C3=(C3-AVER(C3))/STAN(C3)
LET C4=(C4-AVER(C4))/STAN(C4)
LET C5=(C5-AVER(C5))/STAN(C5)
LET C6=(C6-AVER(C6))/STAN(C6)
LET C7=(C7-AVER(C7))/STAN(C7)
LET C8=(C8-AVER(C8))/STAN(C8)
LET C9=(C9-AVER(C9))/STAN(C9)
LET C10=(C10-AVER(C10))/STAN(C10)
LET C11=(C11-AVER(C11))/STAN(C11)
LET C12=(C12-AVER(C12))/STAN(C12)
LET C13=(C13-AVER(C13))/STAN(C13)
LET C14=(C14-AVER(C14))/STAN(C14)
LET C15=(C15-AVER(C15))/STAN(C15)
LET C16=(C16-AVER(C16))/STAN(C16)
LET C17=(C17-AVER(C17))/STAN(C17)
LET C18=(C18-AVER(C18))/STAN(C18)
LET C19=(C19-AVER(C19))/STAN(C19)
LET C20=(C20-AVER(C20))/STAN(C20)
LET C21=(C21-AVER(C21))/STAN(C21)
LET C22=(C22-AVER(C22))/STAN(C22)
LET C23=(C23-AVER(C23))/STAN(C23)
LET C24=(C24-AVER(C24))/STAN(C24)
COPY C1-C24 M7
MULT M7 M6 M8
COPY M8 C1-C24
NAME C1'PC1' C2'PC2' C3'PC3' C4'PC4' C5'PC5' C6'PC6'
NAME C7'PC7' C8'PC8' C9'PC9' C10'PC10' C11'PC11' C12'PC12'
NAME C13'PC13' C14'PC14' C15'PC15' C16'PC16' C17'PC17' C18'PC18'
NAME C19='PC19' C20'PC20' C21'PC21' C22'PC22' C23'PC23' C24'PC24'
NOTE    PRINCIPLE COMPONENT SCORES
PRINT C1-C24
```

Appendix B MINITAB macro for Principal Component Analysis

APPENDIX C - Matrix effects from calcium on 14 analytes - Set 1, used for VC model correction. (Source E1273)

Calcium concentration/ µg ml^{-1}

Analyte		100	250	500	750	1000	2500	5000	7500	10,000
Zn	Corr.	**.973**	**.980**	**.985**	**.986**	**.990**	**1.005**	**1.041**	**1.008**	**.96**
	Raw	.959	.944	.920	.894	.872	.780	.729	.679	.640
Cd	Corr.	**.998**	**.989**	**.969**	**.980**	**.997**	**.975**	**1.039**	**1.004**	**.975**
	Raw	.990	.968	.931	.924	.924	.829	.811	.751	.716
Ni	Corr.	**.991**	**.982**	**.987**	**.989**	**.992**	**.969**	**1.025**	**1.000**	**.983**
	Raw	.983	.962	.950	.935	.923	.829	.803	.742	.717
Pb	Corr.	**.995**	**.988**	**.977**	**.986**	**1.006**	**.963**	**1.010**	**.999**	**.993**
	Raw	.991	.977	.955	.952	.961	.871	.856	.812	.787
Co	Corr.	**.993**	**.985**	**.990**	**.984**	**.994**	**.961**	**1.022**	**1.001**	**.985**
	Raw	.987	.970	.961	.941	.938	.845	.829	.774	.740
Be	Corr.	**.998**	**.996**	**.990**	**.995**	**.986**	**.982**	**1.028**	**1.004**	**.978**
	Raw	.989	.973	.947	.931	.906	.825	.797	.752	.723
Cr	Corr.	**1.000**	**.986**	**.990**	**.984**	**.997**	**.967**	**1.020**	**1.007**	**.983**
	Raw	.994	.973	.963	.946	.946	.863	.850	.805	.767
Mo	Corr.	**1.005**	**1.004**	**.985**	**.983**	**1.003**	**.977**	**1.009**	**.989**	**1.000**
	Raw	1.000	.991	.960	.947	.955	.879	.853	.806	.798
V	Corr.	**.998**	**.991**	**.993**	**.984**	**.997**	**.958**	**1.012**	**1.000**	**.991**
	Raw	.994	.983	.975	.958	.961	.882	.877	.831	.801
La	Corr.	**1.001**	**.997**	**.996**	**.989**	**1.003**	**.957**	**1.007**	**1.000**	**.995**
	Raw	.999	.991	.984	.971	.979	.904	.908	.869	.839
Sr	Corr.	**.992**	**.992**	**.994**	**1.011**	**1.002**	**.956**	**1.011**	**.995**	**.998**
	Raw	.991	.986	.982	.971	.978	.902	.909	.861	.836
Ba	Corr.	**.997**	**.997**	**1.001**	**1.005**	**1.006**	**.955**	**.992**	**.994**	**1.001**
	Raw	.995	.993	.991	.982	.989	.917	.933	.891	.871
Cu	Corr.	**.999**	**1.006**	**1.010**	**1.004**	**1.019**	**.964**	**1.014**	**.994**	**.996**
	Raw	1.000	1.004	1.005	.997	1.010	.943	.975	.942	.933
Li	Corr.	**.996**	**1.003**	**.996**	**1.000**	**1.008**	**.940**	**1.000**	**.987**	**1.011**
	Raw	.998	1.009	1.006	1.014	1.026	.971	1.041	1.030	1.057

MATRIX→ ANALYTE↓	NA-PRS	NA-ERS	K-PRS	K-ERS	AL-PRS	AL-ERS	FE-PRS	FE-ERS
CD	.955266	.962956	.976002	.98042	.931287	.952411	.899865	.882497
CO	.955751	.975737	.974792	.99354	.933731	.968035	.904877	.914993
CR	.956255	.983074	.973535	1.00030	.936271	.969423	.910085	.923759
MO	.956038	.980670	.974076	.99841	.935178		.907844	.926398
NI	.955547	.970961	.975302	.98505	.932702	.960272	.902767	.902374
V	.957428	.983146	.970606	.99665	.942188	.965723	.922218	.937377
ZN	.954597	.957288	.977673	.99171	.927911	.955078	.892942	.876170
RB	.963472	.964795	.955517	.95859	.972670	.962900	.984724	.925164
CU	.962050	.981951	.959067	.98918	.965500	.981196	.970021	.966126
PB	.955062	.980846	.976511	.99236	.930258	.955979	.897756	.900234
LI	.963306	.977940	.955931	.95252	.971834	.965898	.983010	.943588
LA	.958671	.988539	.967502	.99988	.948458	.885316	.935075	.950105
BA	.959430	.985874	.965608	.99373	.952284	.964399	.942921	.959079
SR	.958920	.978492	.966882	.98410	.949712	.919920	.937646	.952849
BE	.956019	.950876	.974124	.95683	.935082		.907646	.914632
NA	.963147		.956329	.96658	.971030	.962103	.981362	.946711

MATRIX→ ANALYTE↓	MN-PRS	MN-ERS	MG-PRS	MG-ERS	CA-PRS	CA-ERS	SR-PRS	SR-ERS
CD	.900191	.893001	.886141	.916822	.860669	.851961	.863397	.861730
CO	.905175	.916031	.892274	.929611	.868883	.882496	.871388	.896618
CR	.910357	.919320	.898648	.946649	.877421	.884687	.879694	.893927
MO	.908127		.895905	.944635	.873746	.901007	.876119	.921932
NI	.903077	.900422	.889692	.916395	.865424	.867755	.868023	.882785
V	.922424	.934442	.913495	.955206	.897306	.904179	.899040	.910165
ZN	.893304	.877096	.877669	.891963	.849321	.815937	.852357	.843915
RB	.984599	.964366	.989989	.986092	.999760	.994229	.998714	.991030
CU	.969974	.972362	.971995	.981117	.975660	.972404	.975267	.977825
PB	.898092	.926036	.883559	.940677	.857211	.898693	.860032	.926264
LI	.982894	.968172	.987891	.989796	.996950	.983089	.995980	.956924
LA	.935214	.945988	.929230	.970779	.918381	.925242	.919542	.926249
BA	.943018	.961611	.938832	.980124	.931241	.947310	.932054	.947601
SR	.937771	.948053	.932377	.970353	.922596	.930704	.923643	
BE	.907930	.907952	.895663	.919192	.873422	.866961	.875804	.880172
NA	.981254	.970869	.985874	.986215	.994249	.982346	.993352	.973210

MATRIX→ ANALYTE↓	BA-PRS	BA-ERS	BE-PRS	BE-ERS	TI-PRS	TI-ERS	NI-PRS	NI-ERS
CD	.85662	.86092	.934522	.925691	.860684		.933134	.926101
CO	.86517	.88702	.936701	.950622	.868896	.83561	.935427	.939199
CR	.87405	.88782	.938967	.947769	.877433	.84790	.937810	.953349
MO	.87023	.91124	.937992	.957956	.873759		.936785	.973117
NI	.86157	.87541	.935784	.949341	.865438	.83291	.934462	
V	.89473	.91287	.944244	.955934	.897316	.89103	.943362	.961085
ZN	.84482	.81772	.931511	.916317	.849338		.929967	.915158
RB	1.00131	1.01310	.971430	.991997	.999755	1.03050	.971962	.940512
CU	.97624	1.00093	.965035	.991935	.975658	.97949	.965234	.954527
PB	.85303	.91676	.933604	.963942	.857226	.84680	.932169	.900617
LI	.99839	.99162	.970684	.993265	.996945	1.00697	.971177	.954800
LA	.91666	.93396	.949836	.934270	.918387	.85948	.949245	.966015
BA	.93004		.953248		.931246	.91596	.952835	.958824
SR	.92104		.950954	.936867	.922601	.88432	.950421	.959328
BE	.86989	.86218	.937906		.873435	.84589	.936694	.946971
NA	.99558	1.00816	.969967	.979148	.994244	1.01620	.970423	.943731

MATRIX→ ANALYTE↓	LA-PRS	LA-ERS	LI-PRS	LI-ERS	ZR-PRS	ZR-ERS	RB-PRS	RB-ERS
CD	.77121	.75303	.933549	.95473	.80590	.78952	.984668	.98572
CO	.78673	.79060	.935808	.97849	.81859	.83920	.982751	.99986
CR	.80287	.79524	.938156	.98409	.83178	.83760	.980757	1.00574
MO	.79592	.82654	.937145	1.00121	.82610	.84160	.981615	1.02135
NI	.78019		.934857	.96869	.81324	.82465	.983558	.98964
V	.84045	.83828	.943625	.98322	.86250		.976114	.99885
ZN	.74976	.70379	.930428	.95838	.78837	.76801	.987318	.98520
RB	1.03408	1.06159	.971803	.97291	1.02077	1.02147	.952193	
CU	.98853	.99233	.965175	.96696	.98354	1.00363	.957820	.94137
PB	.76467		.932598	.98505	.80056		.985476	1.01554
LI	1.02877	1.02976	.971030		1.01643	1.00103	.952849	.93719
LA	.88028		.949421		.89505	.85280	.971194	.98504
BA	.90458	.89164	.952958	.96487	.91492	.90395	.968191	.99008
SR	.88824	.84136	.950580	.96788	.90156	.89878	.970210	.98575
BE	.79531	.76404	.937056	.94061	.82560	.81781	.981691	.95692
NA	1.02366	1.03948	.970287	.98159	1.01226	1.01796	.953480	.97190

MATRIX→ ANALYTE↓	CU-PRS	CU-ERS	PB-PRS	PB-ERS
CD	1.00383	.954440	.967305	.962200
CO	1.00035	.962679	.966806	
CR	.99673	.972494	.966287	
MO	.99828	.989594	.966510	
NI	1.00181	.949240	.967016	
V	.98829	.969135	.965079	
ZN	1.00864		.967994	.961971
RB	.94484	.917620	.958854	
CU	.95506		.960318	
PB	1.00530	.950950	.967515	
LI	.94603	.908010	.959024	
LA	.97935	.959788	.963798	
BA	.97390	.944349	.963017	

Appendix D Matrix Effects of 18 Elements on 16 Analytes

APPENDIX E - Matrix effects of calcium on 14 analytes - Set 2 used for PRISM corrections. (Source E1324)

Calcium Concentration $\mu g\ ml^{-1}$

Analyte		100	250	500	750	1000	2500	5000	7500	10,000
Zn	Corr.	**1.000**	**1.000**	**1.000**	**1.000**	**1.000**	**1.000**	**1.000**	**1.000**	**1.000**
	Raw	.970	.924	.909	.865	.864	.804	.727	.673	.634
Cd	Corr.	**.996**	**1.007**	**1.005**	**.995**	**1.044**	**1.007**	**.996**	**.990**	**.956**
	Raw	.973	.949	.936	.894	.936	.858	.790	.745	.691
Ni	Corr.	**.989**	**1.004**	**1.007**	**1.000**	**1.007**	**.976**	**.977**	**.952**	**.941**
	Raw	.969	.953	.946	.910	.915	.848	.798	.744	.710
Pb	Corr.	**.994**	**1.003**	**1.024**	**1.016**	**1.028**	**1.011**	**1.042**	**1.018**	**1.016**
	Raw	.974	.952	.963	.926	.936	.881	.855	.799	.771
Co	Corr.	**.991**	**1.007**	**1.012**	**1.007**	**1.018**	**.996**	**.993**	**.973**	**.965**
	Raw	.971	.956	.951	.916	.926	.867	.814	.763	.731
Be	Corr.	**1.005**	**1.015**	**1.006**	**.996**	**.987**	**.968**	**.956**	**.960**	**.951**
	Raw	.985	.963	.945	.908	.898	.842	.783	.753	.721
Cr	Corr.	**.989**	**1.003**	**1.013**	**1.006**	**1.014**	**1.005**	**1.004**	**.995**	**.986**
	Raw	.971	.956	.956	.922	.928	.883	.834	.793	.762
Mo	Corr.	**.975**	**.994**	**1.009**	**1.000**	**1.005**	**1.015**	**1.004**	**.978**	**.961**
	Raw	.959	.954	.961	.930	.933	.912	.860	.812	.777
V	Corr.	**.989**	**1.002**	**1.010**	**.994**	**1.006**	**.988**	**.978**	**.964**	**.954**
	Raw	.976	.967	.968	.933	.944	.900	.857	.821	.796
La	Corr.	**.979**	**.991**	**1.002**	**.986**	**.997**	**.983**	**.962**	**.946**	**.932**
	Raw	.970	.970	.977	.949	.959	.929	.889	.859	.837
Sr	Corr.	**.970**	**.986**	**.995**	**.972**	**.988**	**.958**	**.934**	**.917**	**.902**
	Raw	.964	.971	.976	.945	.960	.919	.882	.856	.834
Ba	Corr.	**.980**	**.986**	**.999**	**.976**	**.990**	**.957**	**.947**	**.920**	**.921**
	Raw	.975	.975	.985	.956	.969	.929	.907	.876	.870
Cu	Corr.	**.980**	**.992**	**1.011**	**.986**	**1.009**	**.984**	**.981**	**.977**	**.979**
	Raw	.977	.984	1.000	.971	.994	.963	.951	.941	.939
Li	Corr.	**.985**	**.979**	**1.000**	**.959**	**.999**	**.953**	**.980**	**1.002**	**1.034**
	Raw	.989	.988	1.011	.975	1.017	.976	1.014	1.043	1.082

```
1 ENTRY ** $AASC(IMM)--(CHAINS $ASC1)** VER23.3.83


1967 REM
1989 REM
1990 REM        PROGRAMMING FOR IMM 1990-4540 MHR 31.8.82
1991 REM
2000 PRINT:PRINT"SETTING UP OF IMM-<CR> WHEN READY":WAIT
2010 DIM G0(30):  REM SOFTWARE PUMP RATE (SPR)
2020 DIM G1(20):  REM REPLICATE  MILLIVOLTS
2030 DIM G2(30):  REM ITERATIVE DILUTION FACTORS
2040 DIM G3(30):  REM ITERATIVE DILUENT PUMP RATES
2050 DIMC2(30):REM [CA] IN ITERATIONS
2060 PRINT "DILUENT PUMP ON FULL"
2061 LET J=0:LET G0(J)=255
2062 GOSUB 4500:REM DIL PUMP ON FULL
2063 PRINT"MEASURE & INPUT DILUENT PUMP UPTAKE";:INPUT G7
2064 PRINT:PRINT"SET SAMPLE UPTAKE TO APPROX=";:USE6.2:PRINT G7*.98/1.5
2100 PRINT "INPUT MEASURED SAMPLE PUMP RATE";:INPUT S0
2120 PRINT "INPUT MAXIMUM CV ON CALCIUM MV'S";:INPUT C0
2130 PRINT"INPUT MATCHING TOLERANCE IN %";:INPUT T0
2135 PRINT"SETTING SPR TO GIVE 0.4 DILUTION FACTOR":LET G9=255*1.5*S0/G7
2139 LET J=0
2140 LET G0(0)=G9:GOSUB 4500:REM INITIAL SPR
2150 CALL(0,0,0,0,0,0):REM RESET INSTUMENT
2160 PRINT"ENTER IMM:-PRE-FLUSH,INTEGRATION TIME, NO OF INTEGRATINS";:INPUTP0,I0,N0
2170 REM
2180 PRINT:PRINT"TWO CHANNEL CA CALIB":PRINT
2190 PRINT"PUMP 4000 MG/L CA UP BOTH CHANNELS THEN<CR>":WAIT
2200 GOSUB 3500 :REM MEASUREMENT
2210 LET Q7=Q4
2220 PRINT"PUMP 3000 MG/L CA UP BOTH CHANNELS,THEN<CR>":WAIT
2230 GOSUB 3500:REM MEASUREMENT
2240 LET Q8=Q4
2250 LET B1=1000/(Q7-Q8)
2260 LET B0=4000-B1*Q7
2270 PRINT"CA CALIBRATION  -SLOPE="B1"INTERCEPT="B0
2280 REM
2290 PRINT:PRINT"CALIBRATION OF DILUTOR"
2300 LET C1=10000:LET J=0
2305 LET G0(0)=G9:REM PUMP TO INITIAL SPR
2310 PRINT:PRINT"PUMP 10,000 MG/L CA AS SAMPLE,THEN <CR>":WAIT
2320 GOSUB 4100:REM PUMP ITERATION
2330 LET G5=J:REM ADDRESS OF BALANCE CONDITIONS
2335 PRINT"INPUT SPR GUESS FACTOR FOR 7500(.583 FOR LINEAR)";:INPUT G8
2340 LET C1=7500:LET J=10:LET G0(10)=G0(G5)*G8:REM GUESS FOR SPR FOR CA 7500-4000
2350 PRINT"PUMP 7500 MG/L CA AS SAMPLE THEN <CR>":WAIT
2360 GOSUB 4100:REM PUMP ITERATION
2370 LET G6=J:REM BALANCE ADDRESS
2380 REM PUMP CALIBRATION
2390 LET B3=(G0(G5)-G0(G6))/(G3(G5)-G3(G6))
2400 LET B2=G0(G5)-B3*G3(G5)
2410 PRINT"SPR V P CALIB:-SLOPE="B3,"INTERCEPT="B2
2414 LET C6=G0(G5)/G3(G5):LET C7=G0(G6)/G3(G6)
2415 PRINT"SPR/DPR AT 10K & 7K5="C6,C7
2416 LET E6=(C6-C7)/(G3(G5)-G3(G6))
2417 LET E7=C6-E6*G3(G5)
2418 PRINT"Y V X, (SPR/DPR) V DPR;- SLOPE="E6,"INTERCEPT="E7
2420 REM
2430 PRINT:PRINT:PRINT"READY FOR SAMPLES"
2440 CHAIN$ASC1,0
3500 ENTRY SINGLE SOLUTION MEASUREMENT
3510 FOR I=1 TO N0:REM  FOR EACH INTEGRATION
```

Appendix F Program listing for Interactive Matrix Matching (IMM)

```
3530 IF I=1 THEN GOSUB4000:GOTO 3560: REM FULL PRE-FLUSH &READ
3550 GOSUB 4040:REM READ ONLY
3560 LET G1(I)=Q1-Q0:NEXT I:REM NETT MV
3570 GOSUB 4060:REM TIP WASH
3580 REM STATS ON MV'S
3590 LETQ2=0:LETQ3=0
3600 FOR I=1 TO N0
3610 LET Q2=Q2+G1(I)
3620 LET Q3=Q3+G1(I)*G1(I)
3630 NEXT I
3640 LET Q4=Q2/N0
3645 IF N0=1 THEN 3690:REM  NO SD FOR 1 INTEGRATION
3650 LET Q5=SQR((Q3-Q2*Q4)/(N0-1))
3660 LET Q6=Q5*100/Q4
3670 PRINT:PRINT"CA MV=";:USE 8.2 :PRINTQ4"CV=";:USE 6.2:PRINT Q6
3680 IF Q6>C0 THEN PRINT"OUTSIDE SPEC -REPEATING":GOTO 3510
3690 RETURN
4000 ENTRY TO PRE-FLUSH,OFFSET,INTEGRATE,READ & RETURN MV
4010 CALL(1,6,3,4):REM PRE FLUSH LIGHT
4020 LET P1=P0*50:IF INT(P1)>1 THEN DELAY P1:REM PRE FLUSH
4030 CALL(5,0,0):CALL(7,Q0,24):REM READ CA OFFSET=Q0
4040 CALL(5,I0,0):CALL(7,Q1,24):REM READ CA MV=Q1
4050 CALL(0,0,0,0,0,0):RETURN: REM RESET INSTRUMENT
4060 CALL(16,4,1):DELAY 2:CALL(16,4,0):RETURN:REM TIP WASH
4099 REM
4100 ENTRY PUMP ITERATION FOR PUMP CALIB
4101 REM
4107 GOSUB 4500:REM INITIAL SPR
4110 GOSUB 3500:REM MEASUREMENT
4120 LET C2(J)=Q4*B1+B0:REM  [CA]
4130 LET G2(J)=C2(J)/C1:REM DILUTION FACTOR
4140 LET G3(J)=(1/G2(J)-1)*S0:REM DILUENT PUMP RATE DPR
4142 LET J3=J
4144 IF C1=7500 THEN LET J3=J-10:REM ITERATION COUNTER
4146 PRINT:PRINT"THIS WAS ITERATION NUMBER ";:USE3:PRINT J3
4148 PRINT "THE SPR WAS";:USE4:PRINTG0(J)
4160 PRINT"MEASURED [CA]=";:USE9.2:PRINT C2(J)
4170 PRINT"MEASURED DILUTION FACTOR=";:USE7.4:PRINTG2(J)
4180 PRINT"CALCULATED DILUENT PUMP RATE(DPR)=";:USE6.3:PRINTG3(J)
4185 PRINT"SPR/DPR=";:USE6.1:PRINT G0(J)/G3(J)
4187 LET B6=(C2(J)/4000-1)*100:REM % OF TARGET
4189 PRINT"OFF TARGET BY";:USE 6.2:PRINT B6;"%"
4191 IF ABS(B6)<T0 THEN 4260
4195 IF J=9 THEN PRINT"NO BALANCE AFTER 9 ITERATIONS ":GOTO 2290
4197 PRINT"OUT OF SPEC -ITERATING"
4200 LET J=J+1
4210 LET G4=(C1/4000-1)*S0
4220 LET G0(J)=G0(J-1)*G4/G3(J-1):REM BETTER SPR
4230 GOSUB 4500:REM     SET NEW SPR
4250 GOTO 4110:REM GO ROUND FOR NEXT MEASUREMENT
4260 PRINT"BALANCED WITHIN SPEC"
4270 RETURN
4500 ENTRY ROUTINE FOR SETTING NEW SPR
4505 LETG0(J)=INT(G0(J)+0.5)
4510 IF G0(J)<256 THEN IF G0(J)>0 THEN 4530
4514 IF J=0 THEN 4520
4515 LET G0(J)=G0(J-1):REM USE LAST SPR FOR FUTURE GUESSES IF NEW OUT OF RANGE
4520 PRINT"SPR OUT OF 0-255 RANGE-WILL REMEASURE AT LAST SPR":GOTO 4540
4530 CALL(1,13,0,G0(J))
4535 PRINT"NEW SPR="G0(J)
4540 RETURN
6000ENTRY SLIT ROUTINES
```

Appendix F (continued) Program listing for Interactive Matrix Matching (IMM)

```
1 ENTRY **$ASC1(IMM+QUTE)**  VER 23.3.83


3090 REM        PROGRAMMING FOR IMM 3090-4540  MHR 1.9.82
3095 LET U1=0:REM ZERO RECAL COUNTER
3100 PRINT' CALCIUM RECALIBRATION -USE S.P. SOLUTIONS-ON SAMPLE LINE ONLY':PRINT:PRINT
3102 PRINT'DO YOU WANT TO CHANGE MATCHING TOLERANCE';:INPUT@05
3104 IF @05='Y' THEN INPUT TO
3110 PRINT'DO YOU WANT TO CHANGE IMM PRE FLUSH OR NUMBER OF INTEGRATIONS';:INPUT@04
3112 IF @04='Y' THEN PRINT'NEW PREFLUSH,NUMBER OF INTEGRATIONS';:INPUT PO,NO
3120 LETJ=G5
3130 GOSUB4500:REM SETSPR AT 0.4D EXPERIMENTAL
3140 PRINT'PUMP 10000 MG/L S.P. CA AS SAMPLE, THEN<CR>':WAIT
3150 GOSUB 3500:REM MEASUREMENT
3160 LET Q7=Q4
3170 PRINT'PUMP  7500 MG/L S.P. CA AS SAMPLE, THEN<CR>':WAIT
3180 GOSUB 3500:REM MEASUREMENT
3190 LET Q8=Q4
3192 IF U1=0 THEN 3200:REM FIRST RECAL
3194 PRINT' % CHANGE IN10000 CA='((Q7*B5+B4)/1E4-1)*100
3195 PRINT' % CHANGE IN 7500 CA='((Q8*B5+B4)/7500-1)*100
3196PRINT'DO YOU WANT THIS (N)EW ,(O)LD CALIB OR TRY (A)GAIN ';:INPUT@03
3197IF@03='A'THEN3100
3198IF@03='O'THEN3220
3199IF@03<>'N'THEN3196
3200 LET B5=2500/(Q7-Q8)
3210LET B4=10000-B5*Q7
3220 PRINT'CALIBRATION OF [CA] IN SAMPLE:-SLOPE='B5'INTERCEPT='B4
3222 LET U1=U1+1:REM INCREMENT RECAL COUNTER
3230 GOTO1529:REM GO FOR SAMPLE TITLE ETC.
3250 ENTRY BALANCE CA FOR EACH SAMPLE
3255 LET J=20:REM ARRAY ADDRESS
3260 LET G2(J)=G2(G5):LET G3(J)=G3(G5):LET G0(J)=G0(G5):REM 10000 BALANCE CONDITITONS
3265 GOSUB 4500:REM SET SPR FOR 100%CACO3
3270 PRINT'PUMP SAMPLE,THEN<CR>':WAIT
3280 GOSUB 3500:REM MEASUREMENT
3290 LET C2(J)=Q4*B5+B4:REM [CA]
3300IFJ>20THEN3322:REM SKIP [CA] W/W PRINT
3310 PRINT'% CALCIUM IN SAMPLE='C2(J)*D*1E-4:REM DIRECT [CA]
3320 REM ADJUSTING MATRIX TO 10000 [CA] APPARENT IN SAMPLE
3322 LET B6=(C2(J)/1E4-1)*100:REM %OFF TARGET
3324 PRINT'OFF TARGET BY ';:USE6.2:PRINT B6
3330 PRINT'[CA] IN SOLUTION WAS ='C2(J)
3332 PRINT'SPR WAS ='G0(J)
3334 PRINT'DILUTION FACTOR WAS ='G2(J)
3336 PRINT'CALCULATED DPR WAS ='G3(J)
3338 IF ABS(B6)<TO THEN 3430
3340 PRINT'OUT OF SPEC -ITERATING'
3360 IF J=25 THEN PRINT'NO BALANCE AFTER 5 ITERATIONS SO RECAL':GOTO3100
3370 LET J=J+1
3380 LET G2(J)=G2(J-1)*10000/C2(J-1):REM IMPROVED D
3390 LET G3(J)=(1/G2(J)-1)*S0
3400 LET G0(J)=G3(J)*B3+B2: REM HENCE NEW SPR
3404 PRINT'NEW SPR FROM SPR V DPR ='G0(J)
3405 LET E8=(G3(J)*E6+E7)*G3(J)
3406 PRINT'IF SPR/DPR V DPR CALIB USED THEN NEW SPR WOULD HAVE BEEN='E8
3410 GOSUB 4500:REM SET SPR
3420 GOTO 3280:REM GO ROUND AGAIN
3430 USE3:PRINT J-20' ITERATIONS GAVE BALANCE WITHIN SPEC'
3440 LET D=D*(1/G2(J)):REM  MODIFY ORIGIONAL DILUTION FACTOR D
3450 PRINT 'CAX INDIRECT='C2(J)*G2(20)*D*1E-4
3460 RETURN
3500 ENTRY SINGLE SOLUTION MEASUREMENT
3510 FOR I=1 TO NO:REM  FOR EACH INTEGRATION
3530 IF I=1 THEN GOSUB 4000:GOTO 3560:REM FULL PRE-FLUSH&READ
3550 GOSUB 4040:REM READ ONLY
3560 LET G1(I)=Q1-Q0:NEXT I:REM NETT MV
3570 GOSUB 4060:REM TIP WASH
3580 REM STATS ON MV'S
3590 LETQ2=0:LETQ3=0
3600 FOR I=1 TO NO
3610 LET Q2=Q2+G1(I)
3620 LET Q3=Q3+G1(I)*G1(I)
3630 NEXT I
3640 LET Q4=Q2/NO
3645 IF NO=1 THEN 3690:REM  NO SD FOR 1 INTEGRATION
3650 LET Q5=SQR((Q3-Q2*Q4)/(NO-1))
3660 LET Q6=Q5*100/Q4
3670 PRINT:PRINT'CA MV=';:USE 8.2 :PRINTQ4'CV=';:USE 6.2:PRINT Q6
3680 IF Q6>C0 THEN PRINT'CV OUTSIDE SPEC -REPEATING':GOTO 3510
3690 RETURN
4000 ENTRY TO PRE-FLUSH,OFFSET,INTEGRATE,READ & RETURN MV
4010 CALL(1,6,3,4):REM PRE FLUSH LIGHT
4020 LET P1=P0*50:IF INT(P1)>1 THEN DELAY P1:REM PRE FLUSH
4030 CALL(5,0,0):CALL(7,Q0,24):REM READ CA OFFSET=Q0
4040 CALL(5,I0,0):CALL(7,Q1,24):REM READ CA MV=Q1
4050 CALL(0,0,0,0,0,0):RETURN: REM RESET INSTRUMENT
4060 CALL(16,4,1):DELAY 2:CALL(16,4,0):RETURN:REM TIP WASH
4099 REM
4500 ENTRY ROUTINE FOR SETTING NEW SPR
4505 LETG0(J)=INT(G0(J)+0.5)
4510 IF G0(J)<256 THEN IF G0(J)>0 THEN 4530
4513 IF J=10 THEN 4520:REM FIRST VALUE
4514 IF J=20 THEN 4520:REM FIRST VALUE
4515 LET G0(J)=G0(J-1):REM USE LAST SPR WHEN NEW ONE OUTSIDE SPEC
4520 PRINT'SPR OUT OF 0-256 RANGE-WILL REMEASURE AT LAST SPR':GOTO 4540
4530 CALL(1,13,0,G0(J))
4535 PRINT'NEW SPR='G0(J)
4540 RETURN
```

Appendix F (continued) Program listing for Interactive Matrix Matching (IMM)

APPENDIX G - OPERATING PROCEDURE FOR INTERACTIVE MATRIX MATCHING (IMM)

1. Initialisation

Figure 7.6 gives the simplified flow chart for IMM and Appendix F the program listing. This appendix explains the processes described in the flow chart so that the program can be understood. The initialisation commences with the keyboard input of approximate pump flow rates to improve iteration performance. Tolerances for contiguous precision intensity measurement (e.g. 1%) are entered to ensure that stable conditions have been achieved after adjustment. The selection of the tolerance on the matching of matrix concentration (e.g. 2%) is a compromise between a maximum reduction of the matrix effects and the need to avoid 'hunting' of the system.

2. Initial Calibration of Calcium versus Intensity

The initial calibration of the matrix element, in this case calcium, does not involve dilution, and is included to allow the calibration of the diluter. Two calcium solution (3000, 4000 $\mu g\ ml^{-1}$ Ca) corresponding to the range in the samples (75%-100% $CaCO_3$) are pumped through both sample and diluent channels. A linear calibration of response (mV) versus concentration is made between the two points. This linearity was verified independently.

3. Calibration of the diluter

The diluter is calibrated so that for any required dilution factor (d) the required software pump rate setting (s) can be calculated. The data from the initialisation, on the measured sample pump rate (p_s) and diluent pump rate (p_d) was used as a starting point. The reference concentration of calcium was fixed as 4000 $\mu g\ ml^{-1}$. The range of dilution factors required for this application range from 0.4 (for the dilution of 10,000 to 4,000 $\mu g\ ml^{-1}$ Ca) to 0.533 (for 7,500 to 4000 $\mu g\ ml^{-1}$ Ca). Using the approxmate data from the initialisation on sample pump rate (ρ^{o}_{s}) and diluent pump rate ρ^{o}_{d}) then if

$$d = p_s/(p_s + p_d) \quad \ldots\ldots\ldots \text{G.1}$$

then

$$p_d = p_s(1/d - 1) \quad \ldots\ldots\ldots \text{G.2}$$

To calculate p_d required for the dilution factor 0.4, we have

$$p_d = 1.5\ p_s \quad \ldots\ldots \text{G.3}$$

In the initial value of s was set by the computer at 255 = s^o. Using the first approximation that diluent pump rate (p_d) is proportional to the software pump rate setting (s) we have

$$s = 255\ p_d/p_d^{\,o} \quad \ldots\ldots\ldots \text{G.4}$$

combining with G.3 we get $s = 255 * 1.5\ p_s/p_d^{\,o}$ G.5

This estimate of the value of s to achieve a dilution factor of 0.4 is then tested while using 10,000 µg ml Ca as a sample. An iteration procedure (discussed below) is then used until the response equivalent to 4000 µg ml Ca is achieved. The software pump rate setting at that stage is then a calibration point $s_{o.4}$. The other calibration point is $s_{o.53}$ and this is determined by analogous means, but using $s_{o.4} * 0.583$ as the initial guess, which assumes linearity. The two point calibration of the dilutor can now be made in the form.

$$s = B(o) + B(1)\ p_d \quad \ldots\ldots\ldots \text{G.6}$$

This calibration is not affected by errors in the initial estimates of flow rates.

The setting up of the IMM is now complete, and the repetitive operations are carried out in program $ASC1.

4. Recalibration of Calcium versus Intensity at a fixed dilution For greatest accuracy in calcium determination and matching, the calibration of calcium response against

concentration is now repeated. In this calibration however the calcium solutions are presented only through the sample line. A two point calcium calibration is used at 10,000 and 7500 $\mu g\ ml^{-1}$ Ca expressed as the calcium in the original sample solution not that which is nebulised.

During calibration the IMM is set at dilution factor 0.4 (i.e. $s_{o.4}$).

5. The Analysis of the Sample for Calcium

Sample analysis commences, at the same dilution factor ($s_{o.4}$). The measured calcium concentration (Ca_2), calculated from the most recent calibration, is compared with reference level (Ca_1 = 10,000 $\mu g\ ml^{-1}$ on this calibration). If it is within the tolerance then multielement analysis proceeds via the normal ARL software. If the calcium is not matched, a new dilution factor d_2 is calculated from the last dilution factor d_1 from the relationship

$$d_2 = d_1 \ Ca_1/Ca_2 \qquad \ldots\ldots\ldots \text{G.7}$$

For example if d_1 was 0.4 and Ca_2 was 7500 $\mu g\ ml^{-1}$ then d_2 the required dilution factor is 0.5333.

The required diluent pump rate is then calculated from equation G.2, and the software pump rate setting from equation G.6. On this new setting, the calcium is measured again. Occasionally the calcium is still outside the matching tolerance and the iteration is repeated. The calcium concentration in the diluted solution is matched to within the tolerance interval around the reference level. The calcium concentration in the sample is then calculated from the current dilution factory. This factor is also used for the calculation of multielement analysis which follows. This process of iteration, described for samples, is essentially the same as that used in the initial pump calibration.

APPENDIX H - Matrix effects of calcium on 14 analytes - set 3, used for IMM correction. (Source E467 Raw, E490 Corr).

Calcium Concentration µg ml^{-1}

Analyte		7750	8000	8250	8500	8750	9000	9250	9500	9750
Zn	Corr.	**.968**	**.972**	**.981**	**.986**	**.980**	**.976**	**.981**	**.980**	**.981**
	Raw	.712	.709	.706	.705	.694	.694	.687	.692	.694
Cd	Corr.	**.964**	**.963**	**.967**	**.973**	**.971**	**.965**	**.967**	**.970**	**.965**
	Raw	.703	.700	.696	.695	.685	.686	.678	.680	.676
Ni	Corr.	**.985**	**.988**	**.987**	**.987**	**.985**	**.985**	**.988**	**.986**	**.990**
	Raw	.772	.767	.763	.764	.756	.756	.745	.747	.744
Pb	Corr.	**.979**	**.975**	**.979**	**.986**	**.985**	**.979**	**.983**	**.981**	**.947**
	Raw	.853	.853	.851	.851	.843	.847	.834	.839	.839
Co	Corr.	**.988**	**.989**	**.992**	**.991**	**.993**	**.991**	**.992**	**.991**	**.991**
	Raw	.749	.744	.741	.743	.733	.734	.725	.726	.724
Be	Corr.	**.989**	**.996**	**.993**	**.984**	**.989**	**.992**	**.990**	**.985**	**.985**
	Raw	.733	.726	.720	.724	.714	.712	.701	.699	.697
Cr	Corr.	**1.000**	**.993**	**.992**	**.992**	**.993**	**.994**	**.995**	**.994**	**.994**
	Raw	.779	.776	.771	.773	.764	.764	.754	.756	.755
Mo	Corr.	**.983**	**.982**	**.986**	**.992**	**.992**	**.982**	**.986**	**.989**	**.987**
	Raw	.813	.808	.805	.808	.798	.799	.789	.791	.791
V	Corr.	**1.000**	**.998**	**.997**	**.994**	**.999**	**.996**	**.994**	**.993**	**.996**
	Raw	.812	.805	.802	.808	.796	.797	.789	.786	.784
La	Corr.	**1.008**	**1.006**	**1.004**	**1.000**	**1.009**	**1.005**	**1.001**	**1.001**	**1.001**
	Raw	1.085	1.072	1.072	1.086	1.068	1.073	1.063	1.057	1.053
Sr	Corr.	**1.014**	**1.008**	**1.004**	**1.000**	**1.012**	**1.006**	**.997**	**.999**	**.991**
	Raw	.906	.894	.897	.910	.891	.897	.891	.881	.873
Ba	Corr.	**.912**	**.912**	**.907**	**.897**	**.911**	**.913**	**.908**	**.907**	**.910**
	Raw	.800	.792	.794	.809	.799	.803	.795	.790	.788
Cu	Corr.	**1.025**	**1.017**	**1.007**	**.990**	**1.011**	**1.008**	**.997**	**.995**	**.996**
	Raw	.930	.915	.919	.941	.923	.929	.919	.908	.906
Li	Corr.	**1.049**	**1.038**	**1.018**	**.978**	**1.019**	**1.021**	**1.004**	**.995**	**1.018**
	Raw	.878	.857	.862	.890	.870	.876	.865	.854	.852

line #1

P1	P2	P3	P4
15.37488	.250485	-.3584299	5.333817E-05

X-value	Y-value	Y-calcd	Residual	Scaled resid
0	15.16	15.37488	-.214879	-.3939265
10	17.82	17.87956	-5.956269E-02	-.1076129
25	21.64	21.63544	4.564286E-03	8.079525E-03
50	27.98	27.89328	8.671761E-02	.1485043
75	34.4	34.14792	.2520867	.4179155
100	40.39	40.39955	-9.544372E-03	-1.536516E-02
250	77.89	77.84711	4.289246E-02	5.846288E-02
500	139.63	140.0241	-.3940582	-.4288416
750	202.17	201.9096	.2604523	.2353818
1000	263.9	263.5074	.3925781	.3039236
2500	627.27	627.2662	3.845215E-03	1.614409E-03
5000	1208	1212.925	-4.925049	-1.194241
7500	1783.33	1775.626	7.703736	1.31688
10000	2313.67	2318.236	-4.566407	-.613681

line #2

P1	P2	P3	P4
147.695	5.946058E-02	-.2862171	5.928031E-04

X-value	Y-value	Y-calcd	Residual	Scaled resid
10	148.13	148.2891	-.1590881	-8.029483E-02
50	151.7	150.6555	1.044464	.5178305
100	153.73	153.5916	.138382	.0679242
250	162.47	162.2599	.2101135	9.889091E-02
500	176	176.2801	-.2800903	-.1239338
750	190.53	189.8306	.6993713	.2907626
1000	202.6	202.9762	-.3761902	-.1489272
2500	275.1	275.9865	-.8865051	-.2726869
5000	390.3	387.1318	3.168213	.7195578
7500	499.67	494.3817	5.2883	.9620863
10000	599.87	600.7467	-.876709	-.1349053

line #3

P1	P2	P3	P4
174.068	.4078256	-.397732	5.243201E-05

X-value	Y-value	Y-calcd	Residual	Scaled resid
0	171.17	174.068	-2.898026	-1.561562
1	174.63	174.4759	.1541138	8.227519E-02
10	178.03	178.1456	-.1156159	-6.116756E-02
25	184.3	184.261	3.903198E-02	2.031329E-02
50	195.5	194.4486	1.051422	.5316926
75	205.43	204.631	.7989655	.3941324
100	215.17	214.8083	.3616943	.1742391
250	276.93	275.7599	1.170136	.4906949
500	377.07	376.9271	.1428833	4.952027E-02
750	479.27	477.5762	1.693817	.4987169
1000	578.07	577.7145	.3555298	9.138761E-02
2500	1161.33	1168.179	-6.848755	-1.006186
5000	2103.67	2115.599	-11.92847	-1.035606
7500	3048.67	3022.063	26.60718	1.638035
10000	3868.67	3892.603	-23.93311	-1.176459

line #4

P1	P2	P3	P4
178.9359	.5669439	-1.253761	2.56099E-05

X-value	Y-value	Y-calcd	Residual	Scaled resid
0	174.43	178.9359	-4.50589	-2.007704
1	178.33	179.5034	-1.17337	-.5138924
10	183.17	184.6059	-1.435928	-.615829
25	192.27	193.1052	-.8352356	-.3447541
50	209.23	207.258	1.971954	.7606968
75	223.97	221.4059	2.564133	.9359174
100	238.17	235.5405	2.629501	.9124827
250	325.5	320.1033	5.396729	1.437211
500	464.93	460.1408	4.789246	.9300771
750	605.27	599.0566	6.21344	.9482259
1000	738.57	736.8557	1.714294	.2173928
2500	1509.67	1540.602	-30.93213	-1.983248
5000	2739.67	2795.516	-55.84644	-2.001901
7500	3967.33	3950.296	17.03467	.4240296
10000	5049.33	5011.152	38.17871	.7487005

P1=Io, P2=So, P3=A, P4=B, X=(Ca), Y=I

Appendix I Calibration and Fitting Data for 14 Calcium Emission Lines

line #5

P1	P2	P3	P4
.9570033	1.005085	-.7532387	6.411315E-05

X-value	Y-value	Y-calcd	Residual	Scaled resid
0	.98	.9570033	2.299672E-02	4.554709E-02
1	1.95	1.960342	-1.034141E-02	-2.028721E-02
10	10.9	10.98547	-8.546829E-02	-.1541358
25	25.77	26.01868	-.2486801	-.3954522
50	51.05	51.05086	-8.583069E-04	-1.136454E-03
75	76.68	76.05283	.6271744	.7099551
100	101.14	101.0239	.1161041	.1154461
250	249.83	250.2223	-.3923035	-.2242824
500	494.77	496.5093	-1.739319	-.5848711
750	745.83	739.8623	5.967713	1.41109
1000	982	980.3311	1.668945	.3084927
2500	2345.67	2365.066	-19.39551	-1.58611
5000	4446.33	4470.698	-24.36817	-1.071993
7500	6442	6356.136	85.86377	2.625001
10000	8008.67	8053.99	-45.31983	-1.117812

line #6

P1	P2	P3	P4
2.948741	5.056222	-1.352607	5.76988E-05

X-value	Y-value	Y-calcd	Residual	Scaled resid
0	3	2.948741	.0512588	9.953166E-02
1	8.17	8.004786	.1652145	.305472
10	52.84	53.49505	-.6550484	-.8571688
25	128.53	129.2297	-.6997376	-.6123813
50	256.33	255.2705	1.059464	.594653
75	384.47	381.064	3.405975	1.406063
100	507.67	506.5962	1.073883	.3534428
250	1253.33	1254.73	-1.400269	-.2069368
500	2458.33	2482.208	-23.87818	-1.8667
750	3692.67	3685.707	6.962891	.3671762
1000	4874.33	4865.603	8.727051	.3508835
2500	11473.3	11467.57	5.727539	.0989785

line #8

P1	P2	P3	P4
4.381243	1.086254	-.6507744	5.69736E-05

X-value	Y-value	Y-calcd	Residual	Scaled resid
0	4.3	4.381243	-8.124256E-02	-.2596439
1	5.44	5.467602	-2.760124E-02	-8.725734E-02
10	15.15	15.24261	-.0926075	-.2680779
25	31.31	31.52541	-.2154083	-.5468188
50	58.71	58.64443	6.557465E-02	.1377243
75	86.2	85.73683	.4631653	.8291537
100	113.13	112.8048	.3251801	.5085786
250	274.97	274.6914	.278595	.2476598
500	542	542.5211	-.5211182	-.2705702
750	813.97	807.9028	6.067139	2.212742
1000	1074.33	1070.875	3.455444	.9808272
2500	2572.33	2599.924	-27.59375	-3.441909
5000	4933	4976.797	-43.79688	-2.900648
7500	7228	7164.027	63.97315	2.909987

line #9

P1	P2	P3	P4
3.536911	90.06613	-.4227609	9.533146E-03

X-value	Y-value	Y-calcd	Residual	Scaled resid
0	3.17	3.536911	-.3669105	-.7112736
.1	12.71	12.54187	.1681356	.2983509
1	94.31	93.42195	.8880462	.9140511
10	885.2	886.6121	-1.412048	-.2866521
25	2143	2150.255	-7.255371	-.6469346
50	4126.33	4117.368	8.962402	.4241223
100	7652.33	7657.042	-4.711914	-.1215612

Appendix I (continued) Calibration and Fitting Data for 14 Calcium Emission Lines

line #10

P1	P2	P3	P4
4.502423	2.277508	-.2295675	6.089878E-04

X-value	Y-value	Y-calcd	Residual	Scaled resid
0	4.44	4.502423	-6.242228E-02	-.1195371
1	6.8	6.779771	2.022934E-02	3.788266E-02
10	26.95	27.26158	-.3115788	-.4908685
25	61.43	61.34111	8.889389E-02	.1101331
50	118.3	117.9839	.3161469	.2896444
75	174.23	174.4335	-.2034607	-.1483869
100	232.7	230.6931	2.006912	1.20644
250	566.67	564.4157	2.254273	.6762785
500	1099.33	1107.206	-7.875977	-1.313396
750	1631.33	1635.292	-3.961548	-.4576306
1000	2142.67	2150.749	-8.079102	-.7204896
2500	5100.33	5062.401	37.92969	1.458742
5000	9571.67	9595.51	-23.83985	-.492983

line #11

P1	P2	P3	P4
392.0963	.6148348	-.1986181	1.066121E-04

X-value	Y-value	Y-calcd	Residual	Scaled resid
0	388.1	392.0963	-3.996277	-.6795234
1	393.73	392.7111	1.018951	.1716187
10	397.33	398.244	-.9139709	-.1530094
25	407.13	407.4631	-.3330994	-5.486459E-02
50	425.13	422.8218	2.308228	.3692396
75	438.83	438.1723	.6577149	.1029562
100	453.07	453.5149	-.4448853	-6.812215E-02
250	546	545.4018	.5982666	.0801966
1000	1005.67	1000.647	5.023255	.4166359
500	698.33	697.9148	.4152222	4.622156E-02
750	852.7	849.6564	3.04364	.289127
2500	1892.33	1891.884	.4456787	2.130059E-02
5000	3264.33	3328.97	-64.64014	-1.865877
7500	4790.33	4718.025	72.30518	1.448906
10000	6046.67	6070.285	-23.61524	-.3780452

line #12

P1	P2	P3	P4
258.7273	.2089594	-.6798834	2.455655E-05

X-value	Y-value	Y-calcd	Residual	Scaled resid
.1	257	258.7485	-1.748505	-.4897772
1	259	258.9363	6.375122E-02	.017758
10	260.9	260.8166	8.337403E-02	.0231017
25	263.97	263.9501	.0199585	5.483555E-03
50	269.67	269.171	.4990235	.1349916
100	278.87	279.606	-.7359925	-.1942599
250	311.47	310.8583	.6116943	.1486608
500	363.33	362.7731	.5568848	.1201918
750	416.27	414.4717	1.798309	.3483273
1000	467.17	465.9561	1.213898	.2140271
2500	772.57	770.4434	2.126648	.2437223
5000	1244.33	1261.647	-17.31677	-1.288134
7500	1747	1733.559	13.44116	.7277295
10000	2188	2187.329	.6708985	2.932249E-02

line #14

P1	P2	P3	P4
149.0066	.4402272	-.5240661	2.842893E-05

X-value	Y-value	Y-calcd	Residual	Scaled resid
.1	147.87	149.0508	-1.180771	-.952734
1	149.53	149.4464	8.364868E-02	.067045
10	153.2	153.4086	-.2085724	-.1647491
25	159.63	160.0104	-.3803558	-.2929984
50	171.47	171.0093	.4607239	.3394289
75	182.23	182.0053	.2246857	.1592217
100	192.8	192.9965	-.1964874	-.1342127
250	259.67	258.859	.8110352	.4509885
500	370.47	368.3041	2.165924	.9207491
750	479.73	477.3458	2.384247	.822537
1000	587.23	585.9851	1.244934	.362305
2500	1224.7	1229.555	-4.854981	-.7329933
5000	2238	2271.908	-33.90796	-2.900596
7500	3314	3278.685	35.31543	2.068859
10000	4251.7	4252.327	-.6264649	-2.879173E-02

Appendix I (continued) Calibration and Fitting Data for 14 Calcium Emission Lines

APPENDIX J - SYMBOLS AND ABBREVIATIONS

A	transition probability
AAS	atomic absorption spectrophotometry
AES	atomic emission spectrometry
AQA	analytical quality assurance
ARL	Applied Research Laboratories
CV	coefficient of variation
c	concentration
c_o	detection limit
$\underline{D}$	vector of instrumental drift
DC	direct current
d	dilution factor
E	excitation potential
E'	total excitation potential (including first ionisation potential for ion lines)
f	a function
GIRM	generalised internal reference method
GSAM	generalised standard additions method
g	statistical weight
h	Planck's constant
I	intensity
ICPAES	inductively coupled plasma atomic emission spectrometry
IMM	interactive matrix matching
IPA	interactive power adjustment
ISM	internal standard method
i	i'th analyte

j	relative slope factor
K	absolute temperature
k	Boltzmann's constant
K_{iA}	inter-element correction factor
LTE	local thermodynamic equilibrium
M	relative atomic mass
M_m	matrix energy demand of matrix element m
MED	matrix energy demand
MPS	multielement parameter signature
m	matrix element
NAA	neutron activation analysis
n	number of (e.g. atoms)
n_e	electron density
P	precision
$\underline{P}$	vector of forward power to the plasma
p	probability
PCA	principal component analysis
PCn	'n'th principal component
PMT	photomultiplier tube
PRISM	parameter related internal standard method
P	flow rate of diluent pump
p_e	electron pressure
R	possible improvement in precision
r	correlation coefficient
S	sensitivity
S_o	reference sensitivity
S_r	relative sensitivity

s	software pump rate setting
s	estimate of standard deviation
T	atomic excitation temperature
t	statistic of normal distribution
$\underline{U}$	vector of sample uptake rate
U_n	lattice energy in valancy state n
V_n	ionisation energy for removal of nth electron
V_{TOT}	total ionisation energy
VC	variable concentration
$w/_w$	ratio by weight
XRF	X-ray fluorescence
$\bar{x}$	estimate of mean
z	partition coefficient
α	degree of ionisation
κ	integration constant
λ	wavelength
μ	mean
υ	frequency
$\Delta\upsilon_D$	Doppler half width
σ	standard deviation
I	atom line
II	ion line

APPENDIX K - LIST OF PUBLICATIONS

1. Interactive Matrix Matching: A New Method of Correcting Interference Effects in Inductively Coupled Plasma Atomic Emission Spectrometry.
   Thompson, M., Ramsey, M.H. and Coles, B.J.
   Analyst, 1982, 107, 1286.

2. Improved Precision in Inductively Coupled Plasma Atomic Emission Spectrometry by a Parameter-related Internal Standard Method.
   Ramsey, M.H. and Thompson, M.
   Analyst, 1984, 109, 1625.

3. Correlated Variance in Inductively Coupled Plasma Atomic Emission Spectrometry: Its Causes and Correction by a Parameter-related Internal Standard Method.
   Ramsey, M.H. and Thompson, M.
   Analyst, 1985, 110, 519.

4. Matrix Effects Due to Calcium in Inductively Coupled Plasma. Atomic Emission Spectrometry; Their Nature, Source and Remedy.
   Thompson, M. and Ramsey, M.H.
   Analyst, 1985, 110, 1413.

5. A Predictive Model of Plasma Matrix Effects in Inductively Coupled Plasma Atomic Emission Spectrometry.
   Ramsey, M.H. and Thompson, M.
   Journal of Analytical Atomic Spectroscopy, 1986, 1, 185.

6. Self-Matrix Effects as a Cause of Calibration Curvature in Inductively Coupled Plasma Atomic Emission Spectrometry.
   Ramsey, M.H. and Thompson, M.
   Submitted for publication.